

**The German-Russian Project on Siberian
River Run-off (SIRRO): Scientific Cruise Report
of the Kara-Sea Expedition "SIRRO 2000"
of RV "Akademik Boris Petrov" and first results**

**Edited by
Ruediger Stein and Oleg Stepanets
with contributions of the participants**

**Ber. Polarforsch. Meeresforsch. 393 (2001)
ISSN 0176 - 5027**

The German-Russian Project on Siberian River Run-off (SIRRO): Scientific Cruise Report of the Kara-Sea Expedition "SIRRO 2000" of RV "Akademik Boris Petrov" and first results

Das deutsch-russische Verbundprojekt "Siberian River Run-off (SIRRO)": Wissenschaftlicher Fahrtbericht über die Karasee-Expedition "SIRRO 2000" mit FS "Akademik Boris Petrov" und erste Ergebnisse

Ruediger Stein
Alfred Wegener Institute for Polar and Marine Research Columbusstraße,
Bremerhaven, Germany
e-mail: rstein@awi-bremerhaven.de

Oleg Stepanets
Vernadsky Institute of Geochemistry and Analytical Chemistry
Kosygin Street, Moscow, Russia
e-mail: stepanet@geokhi.ru

Table of Content

1. Introduction	1
(O. Stepanets, R. Stein)	
2. Itinerary	3
(R. Stein, O. Stepanets)	
3. Physical and Chemical Oceanography	6
(L. Stephantsev, H. Köhler, L.A. Kodina, B. Shmelkov, J. Simstich, V.J. Sukhoruk, V.G. Tokarev, L.N. Vlasova)	
3.1. Some peculiarities of the hydrological structure on a meridional section Kara Sea - Yenisei Estuary - Yenisei River (L.Stephantsev, B.Shmelkov)	6
3.2. Distribution of surface-water salinity (H. Köhler, J. Simstich)	15
3.3. Is water from the Rosette Sampler a suitable proxy for bottom water? - Comparison of salinity in Rosette and Multi Corer (J. Simstich)	18
3.4. Nutrient distribution along the Yenisei River - Kara Sea transect in September 2000. (V.J.Sukhoruk, V.G.Tokarev, L.N.Vlasova, L.A.Kodina)	21
4. Sediment trap investigations in the Kara Sea	29
(D. Unger, S. Schayen, B. Gaye)	
5. Marine Biology	34
(C. Eckert, I. Fetzer, V.V. Larionov., P. Lubin, P.R. Makarevich, I. Suck)	
5.1. Taxonomic composition and productivity of the microalgal communities of the Ob Bay and Yenisei Bay in the summer 1999. (P.R. Makarevich, V.V. Larionov)	34
5.2. The taxonomic and ecological descriptions of the phytoplankton assemblages from the Yenisei Bay and adjacent waters of the Kara Sea in September 2000. (V.V. Larionov, P.R. Makarevich)	48
5.3. The role of zooplankton for the turn-over of organic matter in the Kara Sea - First results and basic facts (I. Suck)	63
5.4. Distribution of meroplankton and juveniles along a transect in the eastern Kara Sea (I. Fetzer)	68
5.5. Macrobenthos of the Yenisei and inner Kara Sea (P. Lubin, C. Eckert)	71

6. Marine Geology	76
(R. Stein, K. Dittmers, E. Ivanova, M. Kraus, S. Krivanek, M. Levitan, J. Matthiessen, F. Schoster, J. Simstich, T. Steinke)	
6.1. Sediment sampling program (F. Schoster, K. Dittmers, E. Ivanova, S. Kriwanek, M. Levitan, J. Simstich, R. Stein, T. Steinke)	79
6.2. GeoChirp and ELAC sediment echograph profiling (K. Dittmers, R. Stein)	83
6.3. Core Logging: Magnetic susceptibility (K. Dittmers, R. Stein, T. Steinke)	89
6.4. Facies variability of surface sediments along the Yenisei transect based on grain-size composition, heavy and light mineral data (M. Levitan)	92
6.5. Distribution of aquatic palynomorph along the salinity gradient in the Kara Sea (J. Matthiessen, M. Kraus)	107
6.6. Grain-size and sediment composition of sediment cores based on lithological core description and smear-slide estimates (R. Stein, M. Levitan)	110
6.7. Lithostratigraphy of gravity cores and correlation with sediment echograph profiles („Akademik Boris Petrov“ Kara Sea expeditions 1999 and 2000) (R. Stein)	120
6.8. Benthic foraminifera in sediments from the southern Kara Sea: Preliminary results (E. Ivanova)	141
7. Geochemistry	151
(O. Stepanets, B. Beeskow, M.P. Bogacheva, A. Borisov, K. Fahl, E. Galimov, B. Hollmann, L. Kodina, H. Köhler, V. Komarevsky, G.S. Korobeinik, A. Ligaev, S.V. Ljutsarev, K. Neumann, T.N. Pribylova, S. Prijmak, S. Schayen, F. Schoster, E. Sedjich, E. Sisov, G. Solovjeva, N. Starshinova, R. Stein, V.J. Sukhoruk, V.G. Tokarev, D. Unger, L.N. Vlasova, T.I. Waisman)	
7.1. Geochemistry of dissolved organic matter (DOM) (H. Köhler, K. Neumann)	151
7.2. The influence of dissolved organic matter on the behavior of several radionuclides in sea and fresh water: Preliminary results. (O. Stepanets, A. Ligaev, A. Borisov, G. Solovjeva, L. Kodina, A. Spitzzy, H. Köhler)	155
7.3. The carbon isotope composition of phytoplankton along the Ob–Kara Sea transect in August–September 1999. (L.A. Kodina)	157
7.4. Particulate organic carbon in river and sea waters: Concentration and stable isotope ratio (M.P. Bogacheva, S.V. Ljutsarev, L.A. Kodina)	161

7.5.	Geochemistry of carbon and silica: water column and sediment sampling. Material, methods and first results (D. Unger, S. Schayen, B. Gaye)	164
7.6.	Geochemistry of particulate organic matter in the water column and sediments of the Yenisei River and inner Kara Sea (K. Fahl, B. Hollmann, R. Stein)	175
7.7.	Preliminary results of geochemical investigations of sediment cores along the Yenisei Profile (Acoustic Units I - II) (L.A.Kodina, V.G.Tokarev, V.J.Sukhoruk, L.N.Vlasova, T.N.Pribylova)	179
7.8.	Methane and other hydrocarbons in sediment cores along the Yenisei-Kara Sea profile. (G.S.Korobeinik, V.G.Tokarev, L.A.Kodina, T.I. Waisman)	185
7.9.	Carbonate minerals ikaite and glendonite and carbonate nodules in Holocene Kara Sea sediments: Geochemical and isotopic evidences. (L.A.Kodona, V.G.Tokarev, L.N.Vlasova, T.N.Pribylova)	189
7.10.	Radioecological research in the Yenisei and Ob rivers and adjacent Kara Sea shelf. (O.Stepanets, A.Borisov, V.Komarevsky, A.Ligaev, E. Sisov, G.Solovjeva)	197
7.11.	The investigation of sedimentation rate of the Kara Sea modern sediments using radioactive tracers. (O.Stepanets, A Borisov, A.Ligaev, E.Galimov)	205
7.12.	The identification of chemical elements in bottom sediments using X-Ray fluorescence analysis. (E.Sizov, O.Stepanets, V.Komarevsky, I.Roschina)	213
7.13.	The determination of heavy metals in water samples using sorption method for preconcentration of elements. (O. Stepanets, G.Solovjeva, S.Prijmak, N.Starshinova, E.Sedjich)	217
7.14.	Major and minor elements in suspended matter and sediments from the Yenisei River and the southern Kara Sea (F. Schoster, B. Beeskow)	220
8.	References	227
9.	Annex	236
9.1.	Station list	237
9.2.	Lithological core description	247
9.3.	Summary table of planned investigations by participating institutes	284
9.4.	List of participants	286

1 Introduction

O.V. Stepanets¹ and R. Stein²

¹Vernadsky Institute of Geochemistry and Analytical Chemistry, RAS, Moscow

²Alfred Wegener Institute for Polar and Marine Research, Bremerhaven

Within the framework of the joint Russian - German project on “The Nature of Continental Run-Off from the Siberian Rivers and its Behavior in the Adjacent Arctic Basin (Siberian River Run-off - SIRRO)” and based on the results of the first two Kara Sea expeditions in 1997 and 1999 (Matthiessen and Stepanets, 1998; Stein and Stepanets, 2000), a third expedition with RV “Akademik Boris Petrov” was carried out in the Ob and Yenisei estuaries and adjacent inner Kara Sea in August-September 2000 (Fig. 1-1). This year, we concentrated the work on a south-north transect from the Yenisei River toward the open Kara Sea between 70°N and 77°N (Fig. 1-1). The participating Russian and German scientists intended to study biological, geochemical and geological processes relevant for the understanding of the freshwater and sediment input by the Siberian rivers Ob and Yenisei and the impact on the environments of the inner Kara Sea. During the expedition, an extensive sampling program was carried out on a total of 40 stations (Fig. 2-1).

The scientific program of the project covered a wide range of objectives:

- (1) to characterize the supply of the rivers Ob and Yenisei with respect to their dissolved and suspension load, to identify processes modifying the river supply in the estuaries and the inner shelf sea, and finally to analyse the dispersal and deposition of the river supply in the Kara Sea;
- (2) to study the response of the planktic and benthic biota on variations in the river supply along the salinity gradient from the estuaries to the inner shelf;
- (3) to study the geochemistry of dissolved and particulate organic matter and hydrocarbon gases in the water column and the sediments;
- (4) to study the dispersal and distribution pattern of contaminants;
- (5) to reconstruct temporal and spatial changes in the late Weichselian and Holocene paleoenvironment along transects from the estuaries of the rivers Ob and Yenisei towards the open Kara Sea; and
- (6) to calculate (Holocene) total sediment and organic carbon budgets for the Ob and Yenisei estuaries and the inner Kara Sea.

The research institutes involved in this expedition are from the Russian side the Vernadsky Institute of Geochemistry and Analytical Chemistry (GEOKHI) Moscow, the Shirshov Institute of Oceanology (IORAS) Moscow, and the Murmansk Marine Biological Institute (MMBI), and from the German side the Alfred Wegener Institute for Polar and Marine Research (AWI) Bremerhaven, the Research Center for Marine Geosciences (GEOMAR) Kiel, and the Institute for Biogeochemistry and Marine Chemistry (IFBM) Hamburg.

This report presents the scientific program and initial results of the expedition and outlines future research to be performed on the material obtained during the expedition. In addition, some results from studies of the 1997 and 1999 material are also presented. In this context, we would like to mention that results obtained within the joint Russian-German Siberian River Run-off Project have also already been submitted to international journals (e.g., Opsahl et al., 1999; Shevchenko et al., 1999; Matthiessen et al., 2000; Schoster et al., 2000; Stein, 2000; Head et al., subm.; Matthiessen and Kraus, subm.).

The success of our expedition is mainly based on the excellent cooperation between crew and scientists. We would like to thank captain Igor Vtorov and his crew for their untiring and able support during work onboard RV "Akademik Boris Petrov".

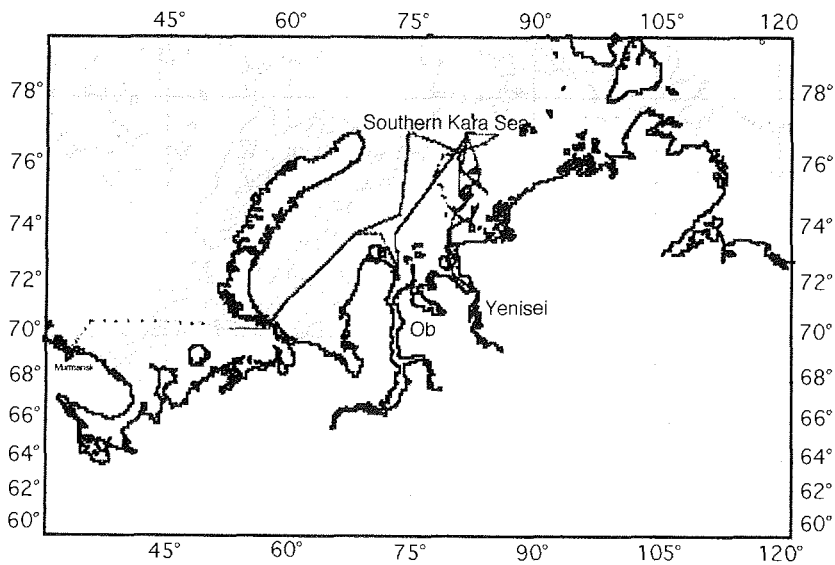


Fig. 1-1: Cruise track of the Kara Sea Expedition 2000 with RV "Akademik Boris Petrov"

2 Itinerary

R. Stein¹ and O.V. Stepanets²

¹Alfred Wegener Institute for Polar and Marine Research, Bremerhaven

²Vernadsky Institute of Geochemistry and Analytical Chemistry, RAS, Moscow

RV “Akademik Boris Petrov” left Murmansk early in the morning of August 31, 2000, onboard 37 crew members and 34 Russian and German scientists. In the afternoon of September 03, we reached our study area in the southern Kara Sea (Fig. 2-1).

During the expedition, an extensive sampling program was carried out on a total of 40 stations (Fig. 2-1). The stations for sediment sampling were carefully selected based on profiling results by means of a ELAC Sediment Profiler and a 3.5 kHz Sediment Profiler. Furthermore, the profiling results give detailed information about the seafloor topography and the thickness and structure of the youngest (Holocene?) sediment cover. In addition, one sediment trap was deployed north of the Yenisei Estuary (Fig. 2-1) to obtain data on the seasonal variation of particle flux during one year.

The following sampling equipment was used:

- 1) water column: CTD/Rosette, Large Volume Sampler “Batomat” (200l), Water Bucket, and Plankton Nets;
- 2) sediments and biota: Large Box Corer, Multicorer, Large Gravity Corer (with 5 m and 8 m core barrel), Benthos Dredge, and Epibenthos Sledge.

During the first two days, we carried out a biological, geochemical, and geological sampling program in the western part of the study area. During transit, the 3.5 kHz Sediment Profiler was tested on the S-N transect between stations BP00-01 and BP00-03. Bad weather conditions with strong easterly winds and high waves prevented to finish our work at Station BP00-03, and we decided to steam towards the southwest. In the wind shadow of the “Islands of Arctic Institute”, a detailed sampling program for all disciplines could be completed between 76°30'N and 74° 30'N at 81°E (Stations BP00-04 to BP00-07; Fig. 2-1). At Station BP00-07 carefully selected based on a 3.5 kHz sediment profiling survey, the first long sediment cores with lengths of 6.3 to 7.3 m were obtained. In the morning of September 08, we had the first ice contact at 74° 39.6'N, 82° 38.6'E. Due to too strong packice conditions, we had to stop our course towards the northeast. After having finished a short station directly at the ice edge (Fig. 2-1; BP00-09; 74° 50'N, 83° 26'E), we headed towards the southwest. At station BP00-12, parts of the mooring system deployed during the BP-1999 expedition, could be recovered (acoustic releaser and floating spheres; the sediment trap itself was broken off). During the next six days (September 09 to 14), an extensive sampling program was carried out in the River Yenisei between 73° 30'N and about 70°N. On September 12, we reached our southernmost station BP00-19 (69° 58.9'N, 83° 27.2'E) where the Yenisei freshwater endmember could be sampled successfully. On September 14 we left the Yenisei, heading towards the north. In the afternoon, we deployed a sediment trap at 74° 0.3'N, 80° 0.5'E (Fig. 2-1; Station BP00-24). In the early morning of September 15, a major packice field was ahead of us at about 74° 45'N, 81° E. Thus, we changed the course towards the northwest. During the following two days, station work was carried

out in the northern to northeastern part of our study area. In the early morning of September 17, we had to leave this area due to a strong westerly storm. In the wind shadow of the island “Izvestii Zik”, a successful biological, geo-chemical and geological sampling could be performed. At this station BP00-30 (75°59'N, 83° 02'E), one of the longest gravity cores of this expedition could be obtained.

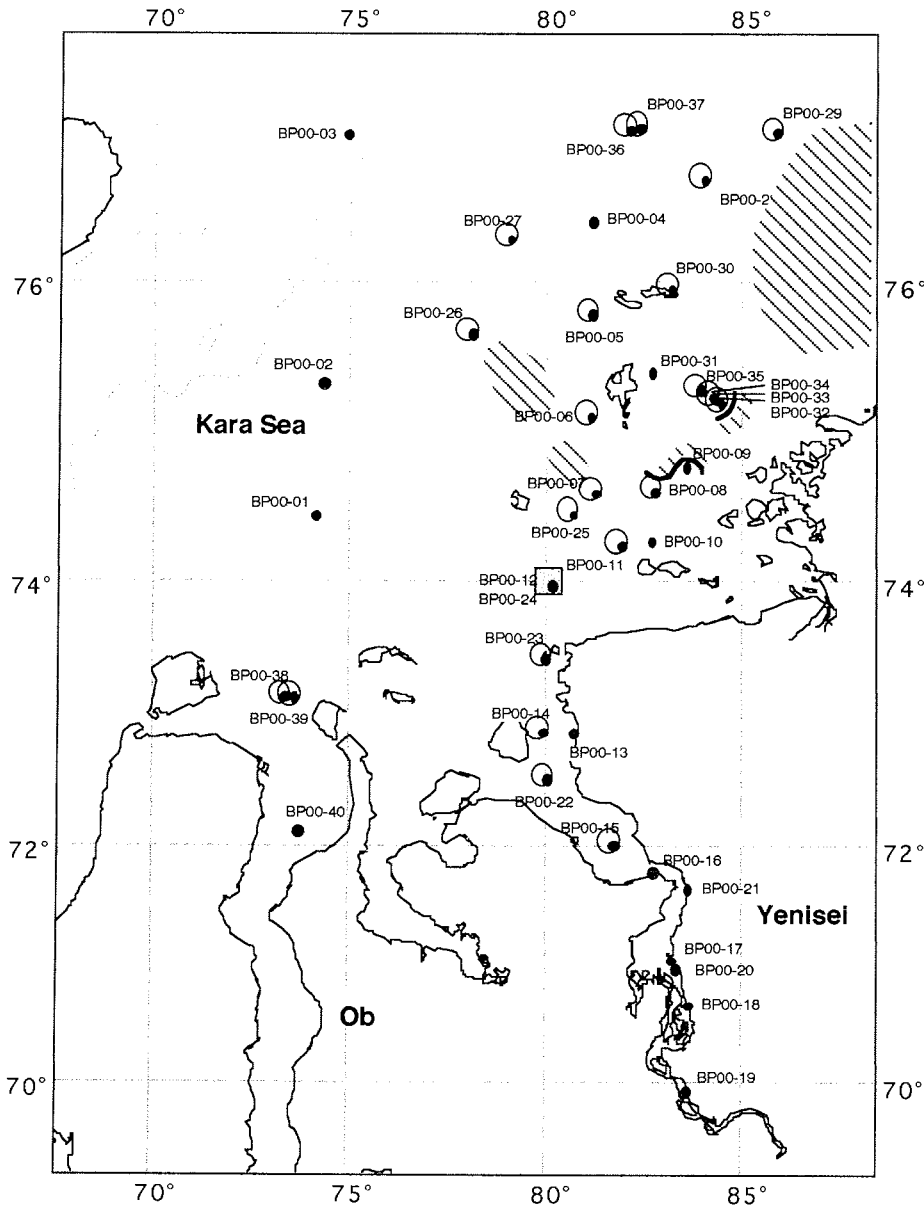


Fig. 2-1: Location of sampling stations during the “Akademik Boris Petrov” Expedition 2000. The large open square marks the station where the sediment traps was deployed. Hatched area marks occurrence of sea/pack ice during the expedition.

Due to the westerly storm, the packice has been pressed towards the east, and we were able to reach the area east of the "Islands of Arctic institute". On September 18, we carried out a sediment echograph survey and a geological sampling program across an (?) "end-morain structure" (Stations BP00-32 to BP00-35). During the night September 18/19 we headed again towards the north. On September 19, we had the last main station at $76^{\circ} 57.7'N$, $81^{\circ} 57.8'E$ (Station BP00-36), where all sampling gears were used.

In the afternoon of September 19, we were on transit to the Ob Bay area. In northern Ob Bay, two gravity cores were obtained at stations BP00-38 and BP00-39 (Fig. 2-1). We finished our station work at $72^{\circ} 10'N$, $73^{\circ} 33'E$, where a large-volume water sampling was carried out (Station BP00-40).

On September 21, 01.00h ship time (= Moscow time) we have finished our station program in the study area and started steaming towards the west. On September 24, we arrived at Murmansk. "Akademik Boris Petrov" left Murmansk on September 30 and arrived in Bremerhaven on October 06, 2000.

3.1 Some peculiarities of the hydrological structure on a meridional section Kara Sea - Yenisei Estuary - Yenisei River

L. Stephantsev and B. Shmelkov

Vernadsky Institute of Geochemistry and Analytical Chemistry, RAS, Moscow, Russia

Introduction

The hydrography of the Arctic Ocean is influenced by strongly variable geographical and hydrological boundary conditions. At first, the ocean is an almost enclosed basin, surrounded by the American and Eurasian continents, which has a variable bottom relief. Secondly, the Arctic Ocean is divided into smaller areas by many islands that cover a surface area about 3.5 times larger than all islands of the Atlantic Ocean. And, at last, the Arctic basin differs from all other major oceans of the world by a strong continental discharge. The annual quantity would make up, compared to the area of the ocean, a fresh water layer with a thickness of 35.5 m. Of all Arctic seas, the Kara Sea is the one that is most influenced by continental discharge and, for this reason, it is most interesting to examine the nature of continental run-off from the Siberian rivers and its behavior in the adjacent Arctic basin. The basic purpose of our investigation is to study the temporal and spatial structure and distribution of salinity and temperature which are important for the interpretation of the results of the geochemical and geological studies.

Working program

The hydrological survey was conducted in the area between 77° and 70° N and 71.5° and 86° E. To obtain vertical salinity and temperature profiles of the water column and for subsequent sampling of selected depths we used a rosette sampler (24 bathometers, volume 1.7) including STD-probe "MARK - 3B" of the company EG&G OCEAN PRODUCTS to measure electrical conductivity, temperature and pressure up to depths of 6000 m. Precision of measurements of temperature in the range from -32°C up to +32°C is $\pm 0.005^\circ\text{C}$, electrical conductivity in the range from 1 up to 65 mmho is ± 0.005 mmho, and pressure in the range from 0 up to 320 db is ± 0.1 db. The instruments were calibrated in August 2000 by the company "GENERAL OCEANICS INC." MIAMI. The salinity and the temperature values were verified at some stations by means of the portable hand-held conductivity meter WTW-LF330.

The hydrological survey could be performed at a total of 24 stations. The stations are shown in Figure 3-1. On each station one to five soundings were conducted. Simultaneously with measurements of profiles of temperature and salinity the spot sampling of water was conducted. The horizons for sampling were selected based on previous profiles and absolute values of temperature and salinity from the same station. The sampling was conducted in the period from September 4 to 20, 2000.

Results and discussion

Our hydrological survey was not detailed enough to perform a detailed analysis of the time-space structure of fields of salinity and temperature. However, some features of the hydrological structure of the water column in the investigated area could be revealed. In

particular, we were able to fix the southern border of penetration of high saline waters of the Kara Sea into the Yenisei Estuary. So, when considering vertical profiles of salinity from stations 17, 18, 19 and 20 (Fig.3-2) it is possible to state that the bottom layer of high saline waters of the Kara Sea penetrates to 71° N into the estuary. Profiles of salinity from stations 17 and 20 show a thickness on the order of 5 m of the high saline waters having values of about 18 ppt. On profiles from stations 18 and 19 this layer is not observed any more. This is apparently caused by the geometry of a channel of the Yenisei which has a double meander at 71°N that restricts further distribution of high saline waters at the bottom to the south.

It is possible to outline the geographical distribution of three reference groups of vertical profiles of temperature and salinity: naturally river profiles (st.18,19), estuary profiles (st.13-17,20-22) and marine profiles (all remaining). Representative profiles of each of group are shown in Fig. 3-3 (st.19 - river, st.22 - estuary, st.8 - marine). The river profiles are characterized by almost complete homogeneity of the water column both of salinity and of temperature (temperature, e.g., differences < 0.5°C down to 20 m depth). Average values of temperature and salinity are about 11°C and 0.05 ppt, respectively. Estuarine profiles have a more or less one-step structure with a homogeneous upper layer of 5 up to 18 meters thickness. Both salinity and temperature monotonically change from the thermocline to the bottom (salinity incremented from 0.05-7.0 ppt up to 17.0-30.0 ppt and temperature decreased from 2-10°C up to -0.5-8°C). Average values of salinity and temperature in the upper homogeneous layer vary between 0.05 up 7.0 ppt and from 5.3 up to 10.5°C, respectively. The marine profiles have much more variable structures with presence of inverse temperatures and salinities. The profiles of temperature have a higher small-scale variability because at low temperatures the variability of density of seawater in basic is determined by salinity. Alternating layers of temperature differences of about 1°C are marked having a thickness of about several meters. At stations 27 and 28 a surface layer with low temperature about 0°C was observed that apparently is linked to the presence of ice-reinforced fields in the north-east part of the polygon.

Quasi-meridional sections of the spatial distribution of temperature and salinity are shown in Figure 3-4. The sections were plotted from north to south, and on the lower horizontal and upper horizontal axes the distance in nautical miles and the number of the stations are given, respectively. Both the salinity and the temperature profiles show a pronounced frontal zone at latitude 73°N (st. 22, 23) with a horizontal temperature and salinity gradient of about 0.5°C/km and 0.2ppt/km, respectively. The extent of the frontal zone is about 50 miles. The location of the frontal zone practically coincides with results obtained during the expedition in 1999. However, the calculated horizontal gradients of temperature and salinity are much higher in 2000. Apparently, in 1999 measurements were conducted during the maximum of an offset of fresh water, and in 2000 in the more late period of time. In the northern part of the sections local anomalies of salinity and temperature are marked, that are caused by the unstable character of the spatial distribution of hydrological parameters in the open part of the polygon.

The spatial distribution of temperature and salinity are shown in Figures 3-5 and 3-6. The distribution pattern can be considered only as schematic description because the number of measurements is too low and the stations are too irregularly distributed and were not measured synoptically.

When looking at the maps it is evident that temperature and salinity are much more variable on the horizon of 2 meters than on the horizon of 25 meters. This suggests that the effect of river run-off is not obvious at greater depths. Notably lower temperatures are found in the eastern part, linked to the proximity of the shore and presence of ice-reinforced fields in the north-east part of the study area. At the surface, there are lenses with negative temperature. In the distribution of surface salinity, local lenses of fresh water are seen, that also supports our view of an unstable character of the spatial distribution of hydrological parameters in the open part of the polygon.

On the whole, our measurements correspond quite well to the data from the literature and results from the previous four expeditions of RV "Akademik Boris Petrov" into the Kara Sea.

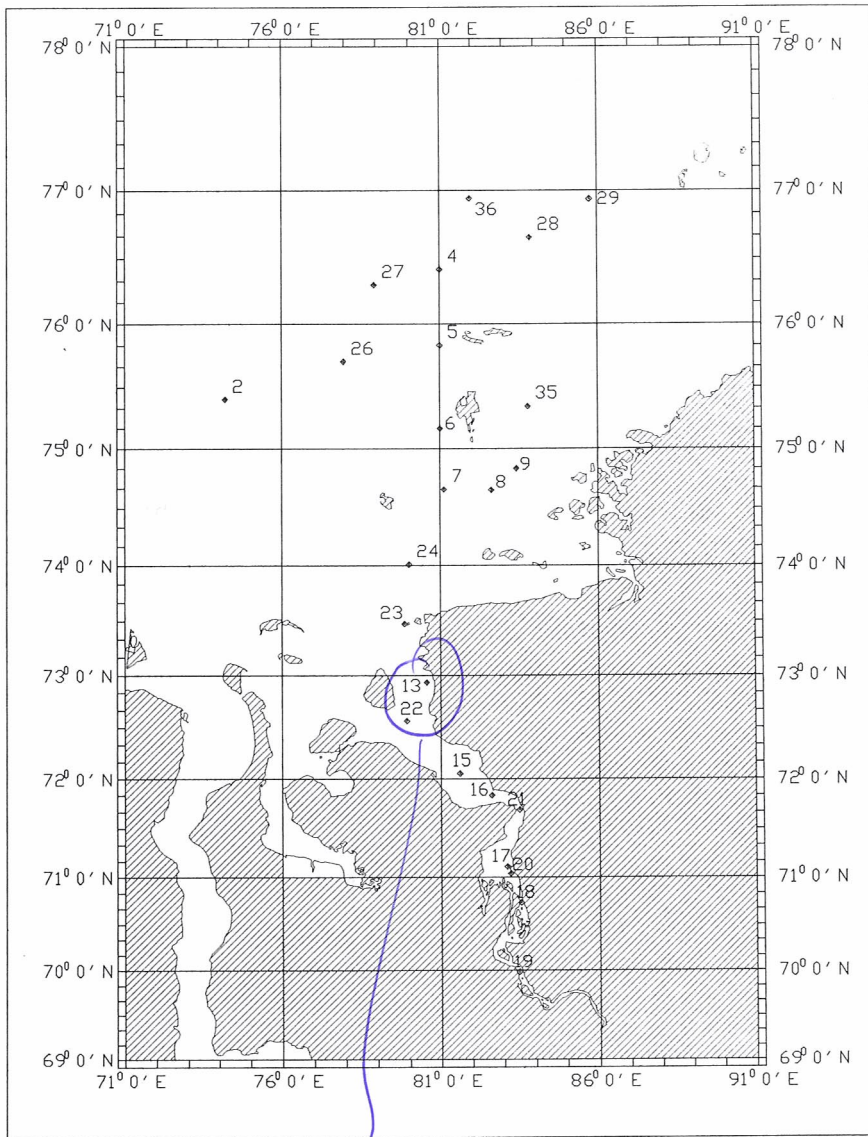
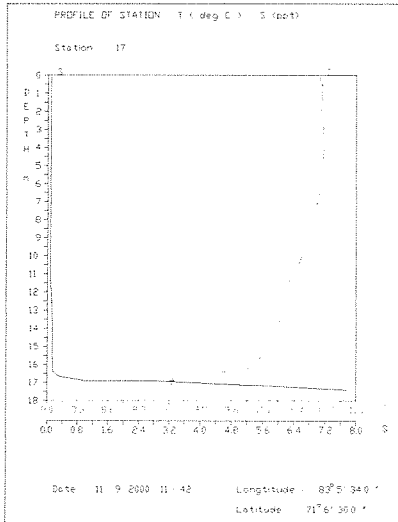
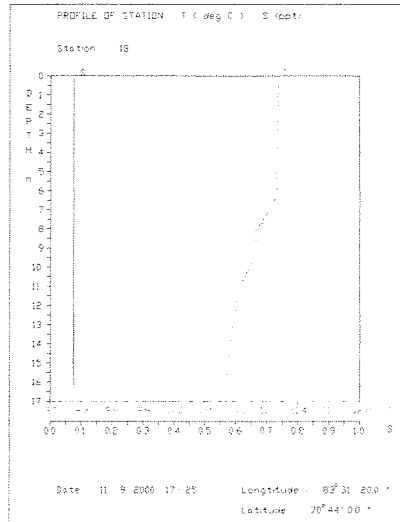


Fig.3-1 Hydrophysical stations on the 35nd cruise of RV "Akademik Boris Petrov".

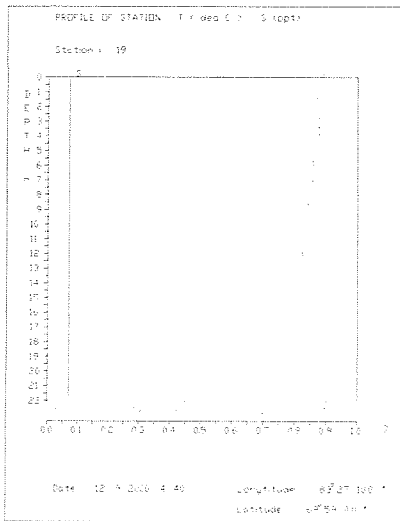
Sea water
wedge



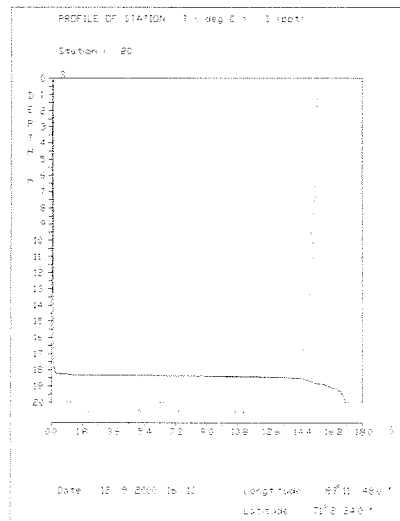
a)



b)

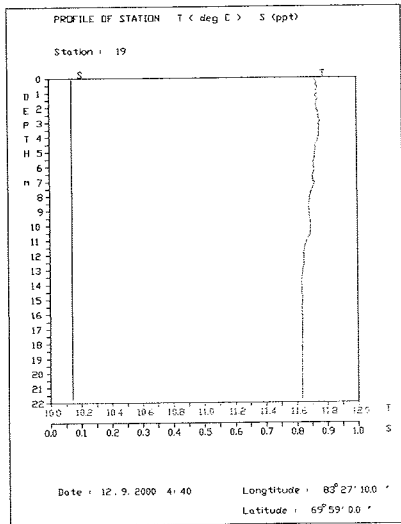


c)

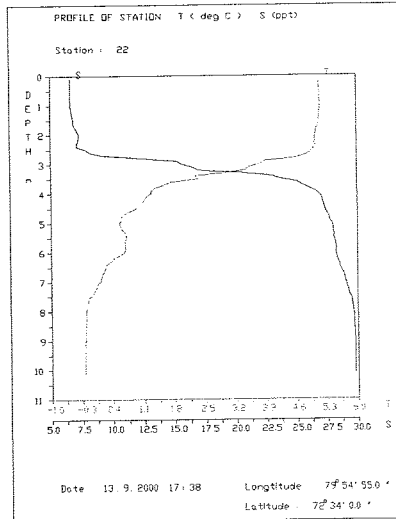


d)

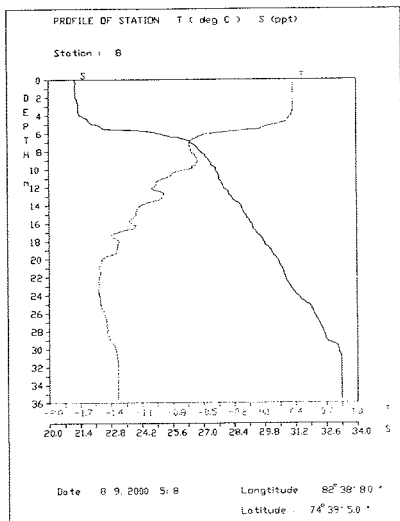
Fig.3-2. CTD profiles on stations 17 (a), 18 (b), 19 (c) and 20 (d).



a)

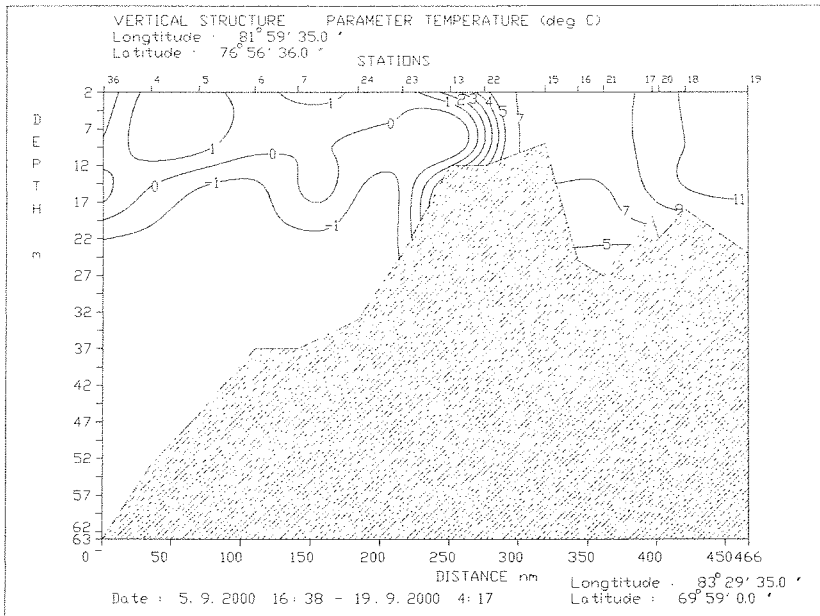


b)

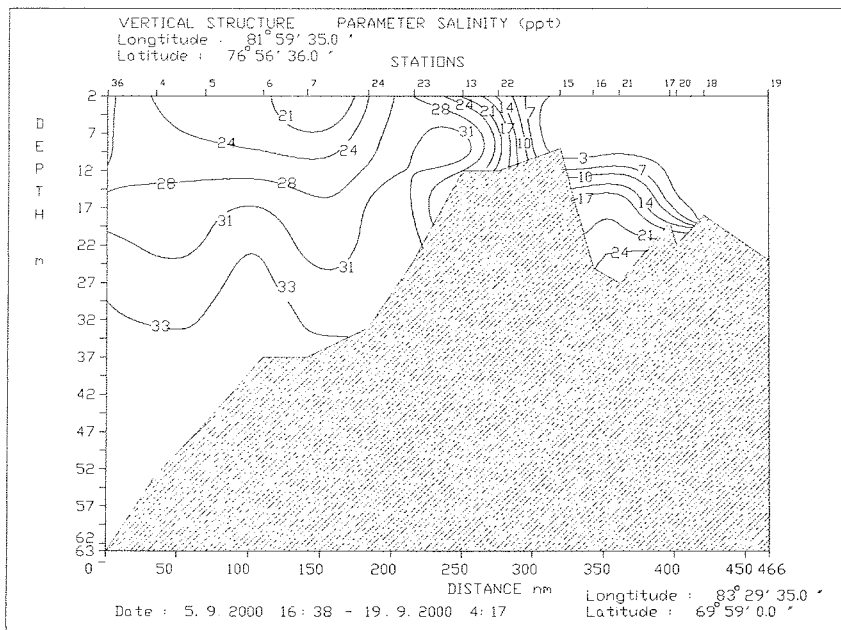


c)

Fig.3-3 Characteristic CTD profiles : river, on station 19 (a); estuary, on station 22 (b) and marine, on station 8 (c).

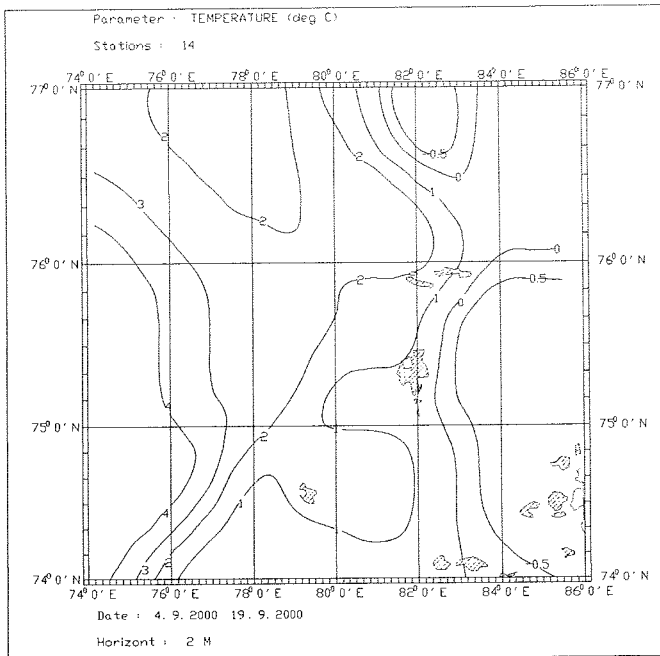


a)

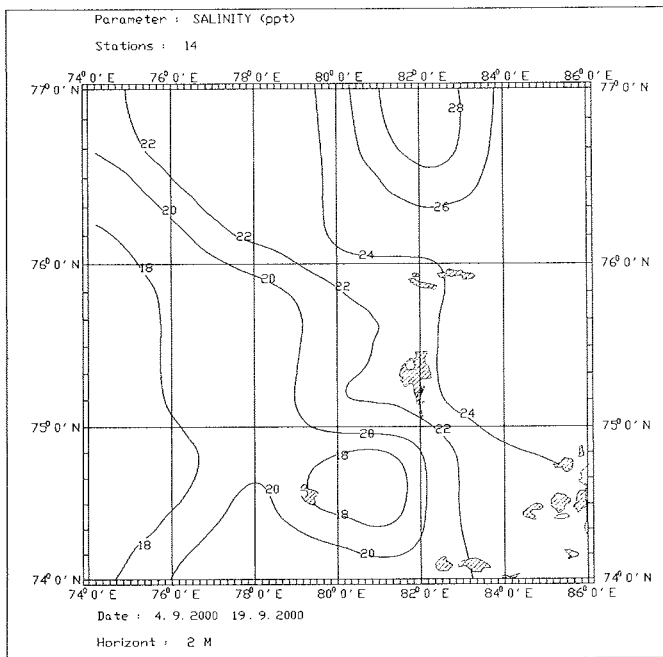


b)

Fig.3-4. Vertical distribution of temperature (a) and salinity (b) on a quazimeridional section.

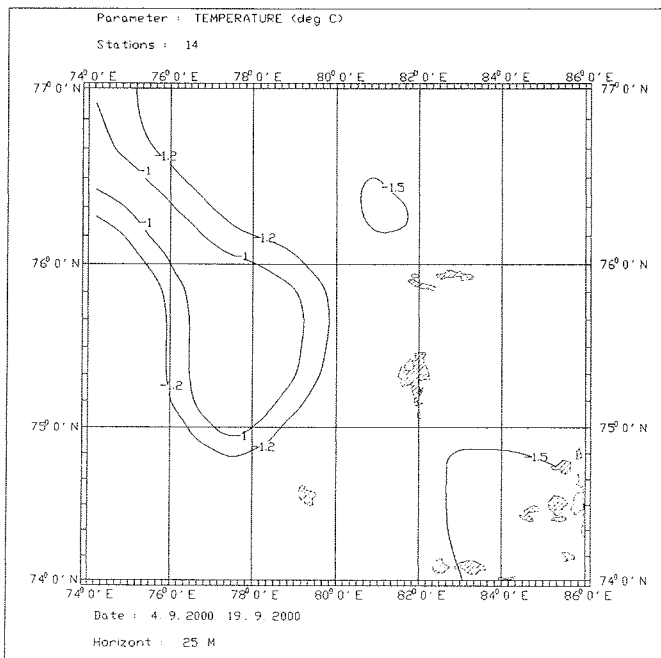


a)

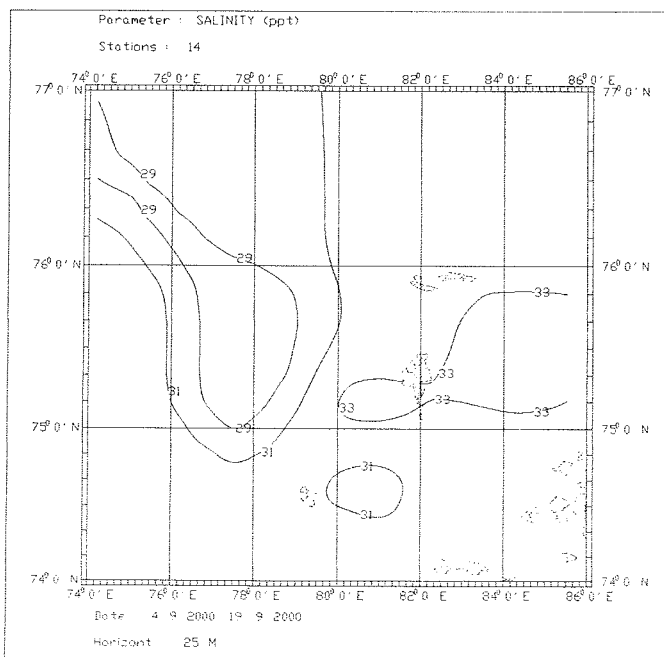


b)

Fig.3-5 Temperature (a) and salinity (b) in 2 m water depth, measured on the 35nd cruise of RV “Akademik Boris Petrov”.



a)



b)

Fig.3-6 Temperature (a) and salinity (b) in 25 m water depth, measured on the 35nd cruise of RV “Akademik Boris Petrov”.

3.2 Distribution of surface-water salinity

H. Köhler¹ and J. Simstich²

¹ Institute of Biogeochemistry and Marine Chemistry, Hamburg

² Geomar Research Center for Marine Geosciences, Kiel

Introduction

Ob and Yenisei release immense amounts (about $1600 \text{ km}^3 \text{ a}^{-1}$; cf. Fig. 6-1) of freshwater into the Kara Sea. Thus surface salinity in the Kara Sea is strongly affected by river discharge. Due to the density difference, the river water mixes poorly in the vertical and spreads far north as a thin layer above the saltier marine water. Compared to the river runoff, other aspects influencing the surface salinity like ice melt and wind conditions play only a secondary role. Considering the high annual discharge fluctuations, it is obvious that the surface salinity is subject to a strong temporal variation. Salinity values from this years expedition illuminate the short-scale variability at the surface of the Kara Sea.

Methods

Water samples were taken at all 40 CTD stations. To improve spatial resolution 82 additional samples were taken by scooping water in a bucket during our cruise. Salinity was determined by using a handheld conductivity meter of type LF 320/330 from WTW, Weilheim, Germany, with a measurement error of $\pm 0.1\%$. Our observations were carried out between September 2 and 22 and covered a range from pure freshwater in the Yenisei river up to almost pure marine water of 31‰ in the Kara Strait area.

The salinity data is mapped in Figures 3-7 and 3-8. To show the temporal variations during the investigation period, values taken before reaching the southernmost Yenisei station on September 12 are presented as circles whereas samples taken afterwards are shown as crosses.

Results and discussion

As expected the general pattern showed the typical estuarine situation: Salinity increased with the distance from the freshwater sources. Highest surface salinities above 31‰ occurred in the southwestern Kara Sea. Apparently, advecting saline surface water of the Barents Sea dominated over the freshwater input from Ob or Pechora. In the northeastern Kara Sea we observed also high salinities of more than 27‰, showing the relatively small freshwater influence in this area during sampling in late September.

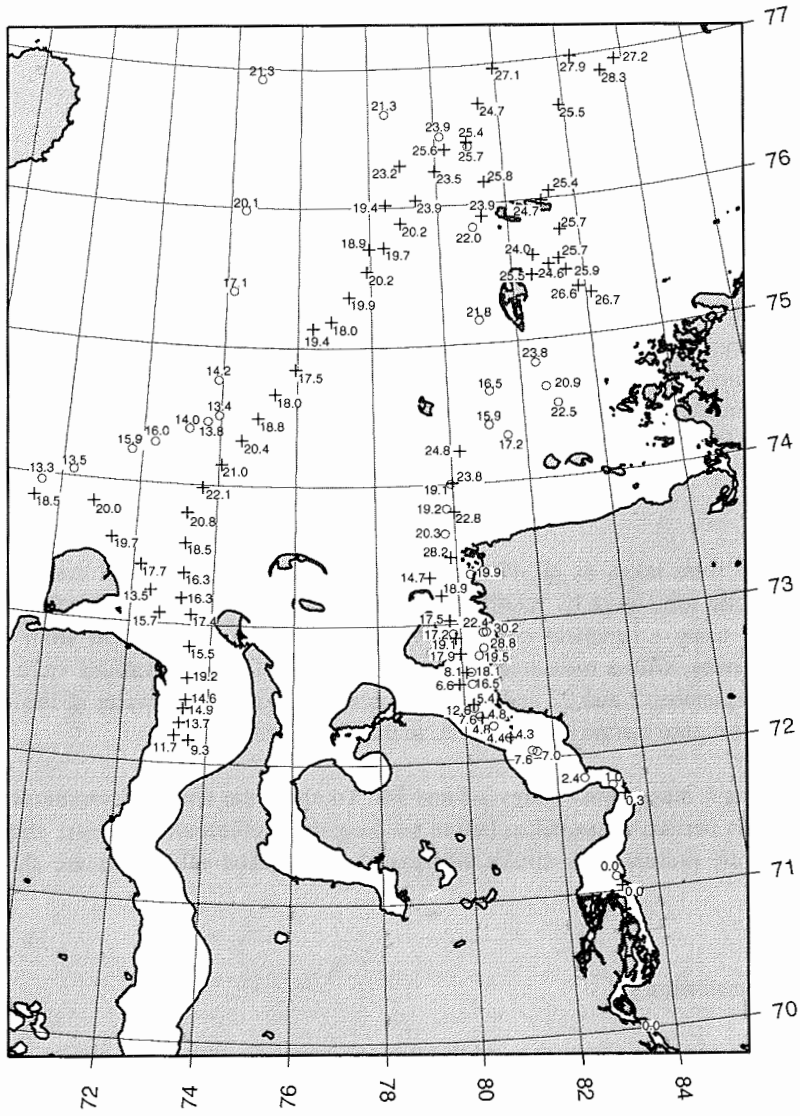


Fig.3-7: Surface-water salinity distribution (further expansions see text).

3.3 Is water from the rosette sampler a suitable approximation for bottom water? — Comparison of salinity in rosette and multicorer.

J. Simstich

GEOMAR Research Center for Marine Geosciences, Kiel, Germany

Introduction

Studies on sediment surface processes need proper bottom water samples for comparison. Apart from some sophisticated devices for bottom water sampling, it is a reasonable alternative to take the water from multicorer tubes instead. This water is true bottom water with only a very small fraction of pore water released from the sediment during handling on board (Mackensen et al. 2000). However, for some reasons it is not possible to employ the multicorer device on every station. In these cases one might feel tempted to use the water from the deepest reached level of CTD/Rosette as a substitute for bottom water. Is this an advisable procedure? For safety reasons the CTD/Rosette sampler has to stop 2-3 m above sea bottom - is the deep water there the same as the bottom water? As salinity is a conservative tracer for water masses, an answer to the former question could come from the comparison of salinity values of multicorer and CTD/Rosette samples.

Method

As "bottom water" the water above the sediment column in multicorer tubes was sampled and as "deep water" the water from the deepest depth reached in the CTD/Rosette casts, respectively. Sampling devices on board of RV "Akademik Boris Petrov" were a standard 12-tubes version multicorer, manufactured by Wuttke, Henstedt-Ulzburg, Germany and a rosette sampler with 24 bathometer bottles from Niskin. Salinity was measured with a LF320/SET conductivity meter from WTW, Weilheim, Germany, with an accuracy of 0.1 salinity units.

Results

In Figure 3-9 deep water salinity from the deepest rosette samples is plotted on the y-Axis against bottom water salinity from the multicorer samples of the same station on the x-Axis. It is obvious that at stations where deep water salinity exceeds 20 the salinity values of deep and bottom waters are very similar. The bottom water is a little bit more salty than the deep water. The salinity differences range from -0.9 to 2.1 with a mean of 0.4, i.e. there is only a small salinity increase in the water column between the deepest rosette samples and the bottom. In contrary Figure 3-9 shows a poor correlation on stations, where the deep rosette water is below 20. There, salinity of deep water is significantly lower than at the bottom, pointing to a strong salinity increase below the deepest reached rosette level towards the bottom.

Discussion

The outlier data point to the right in Figure 1 leads to a reasonable interpretation of the results: This sample (BP99-08) incidentally was not taken from the deepest reached CTD/Rosette level at 18 m but at 14 m, which is within the halocline. The summer halocline is very sharp in the Kara Sea; a big salinity increase up to 20 occurs within a 2-4 m thick interval. Below this level the salinity values generally change only moderately, and the water mass which is present in the deepest CTD generally touches the bottom. In these cases rosette water could substitute bottom water if the difference of approx. 0.4 is acceptable for the subject of study.

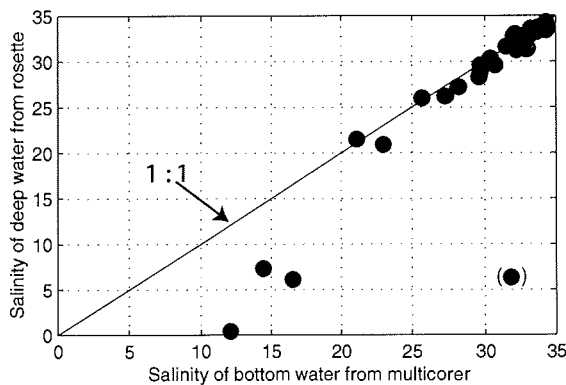


Fig. 3-9: Salinity values of bottom water from multicorer plotted against salinity values of deep water from deepest reached CTD/Rosette sampler level at the same station.

Hence, in shallow areas, where the halocline touches the bottom, the CTD/Rosette sampler stops within or above the halocline. The salinity is still increasing below the sampler and reaches highest values directly on the bottom. An extreme situation was recovered at station BP00-17 in the Yenisei, where the salinity increased within the multicorer tubes from 8.6 to 12.2 within 40 cm (L.Kodina, pers. comm.). Therefore, in shallow areas the deep rosette water is not at all suitable as substitute for bottom water.

The map in Figure 3-10 shows that the bottom salinity in the Kara Sea is strongly influenced by bottom topography. The saltiest water can be found in the deep areas to the north, whereas the freshest water is to be found in the river estuaries itself. Salty marine water intrudes tongue-like in the deep river troughs far to the south. As CTD-casts generally stop some meters above the bottom, existing maps and hydrological profiles based on such data might underestimate the true bottom water salinity in the shallow southern part of the Kara Sea. Marine water probably intrudes much deeper into the estuaries than previously known.

Conclusion

In those areas where the halocline doesn't touch the bottom and where the water salinity in the deepest rosette bottle exceeds 20, this water might be used as a reference for bottom water. Conservative tracers like salinity and oxygen isotope ratios might be unchanged or show only small changes between deepest CTD/Rosette level and ocean bottom. Presumably this is not the case for any water property which is affected by ocean bottom processes like remineralisation, resuspension etc.

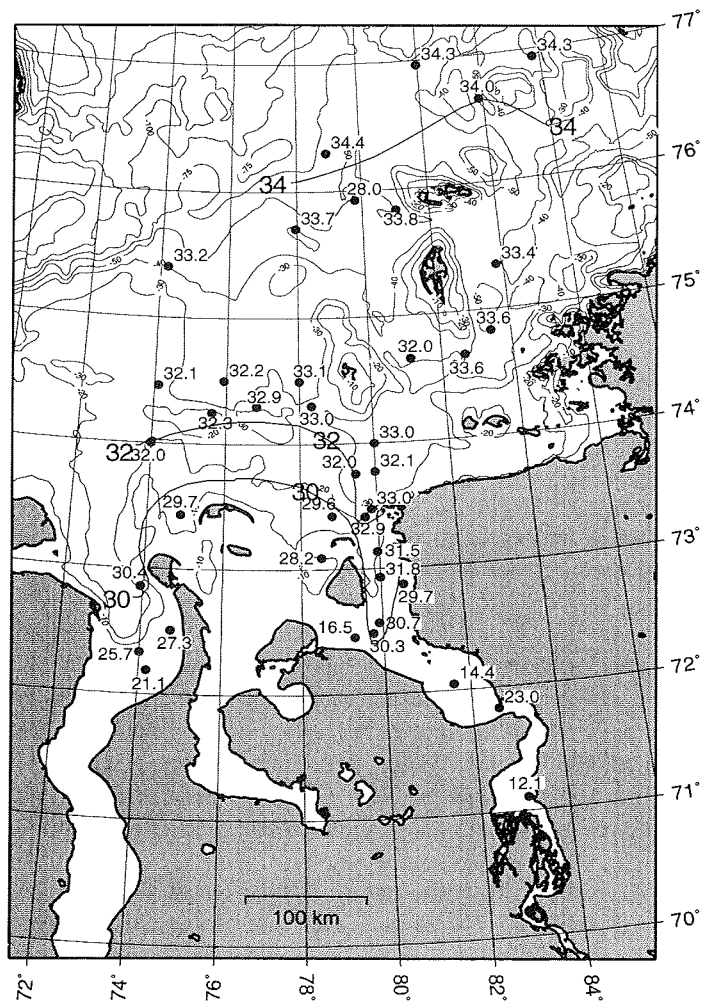


Fig. 3-10: Salinity values and isohalines of bottom water from multicorer samples.

3.4 Nutrient distribution along the Yenisei-Kara Sea transect in September 2000

Sukhoruk V.I.¹, Tokarev V.G.², Vlasova L.N.², Shmel'kov B.S.² and Kodina L.A.²

¹P.P. Shirshov Institute of Oceanology RAS, Atlantic Branch

²Vernadsky Institute of Geochemistry and Analytical Chemistry RAS, Moscow, Russia

During the 35-th cruise of the R/V "Akademik Boris Petrov" hydrochemical investigations of the water column were carried out along a longitudinal transect from the river Yenisei to the Kara Sea. The objectives were to study the sedimentation processes related to the run-off of the Yenisei, the spatial distribution pattern of hydrochemical parameters of Kara Sea waters and their impact on primary bioproductivity and environmental conditions for pelagic and benthic organisms.

According to the distribution of surface water salinity along the transect, the river water ($S < 0,1$) propagated from the Yenisei northwards and reached $71^{\circ}00' N$ (St. 17, 20). Further northwards the salinity increased slowly due to external forcing (winds, tides) and mixing/stirring with sea water. A quasi-vertical boundary between the relatively fresh transformed river ($S < 8$) and saline marine water ($S \approx 24-28$) was revealed at the sea surface between stations 13 and 22 ($72^{\circ}30'-73^{\circ}00' N$) as a narrow frontal zone with sharp horizontal gradients of salinity. Northward from the frontal zone the vertical distribution of salinity can be schematically described by a two-layer structure with a defined halocline between subsurface transformed ($S \approx 24-28$) and deep saline ($S > 32$) sea waters. For a more detailed hydrology description see Stephantsev and Shmel'kov (this vol.).

The following hydrochemical parameters were determined in the water samples taken at 3 horizons in a vertical section: total alkalinity (T_{Alk}), dissolved silica ($Si - SiO_3^-$), inorganic phosphate ($P - PO_4^{3-}$), total phosphorus (P_{total}), organic phosphorus (P_{org}), nitrites ($N - NO_2^-$) and nitrate ($N - NO_3^-$). Water samples have been analyzed without prefiltration, immediately after the Rosette sampler returned to the ship's deck. Standard hydrochemical methods were used for nutrient analysis in the shipboard laboratory [Methods, 1978].

Results

The results obtained are presented in the Table 3-1 and in the Figures 3-11 to 3-14. The distribution pattern of nutrient concentrations is in agreement with the observed hydrological regularities. Based on the vertical distribution pattern of the hydrochemical parameters the longitudinal Yenisei transect has been subdivided into three zones:

1. The zone of predominant influence of fresh riverine waters (Sts.19-22) is characterized by maximum concentrations of silicium ranging from $59,2 \mu M/L$ to $128 \mu M/L$ (Fig.3-11a), by inorganic phosphate concentrations higher than $0,55 \mu M/L$ (Fig.3-11b), total phosphorus concentrations higher than $0,65 \mu M/L$ (Fig.3-12a) and nitrite concentrations of about $0,3 \mu M/L$ (Fig.3-12b) (Stunzhas, 1995).

2. The mixing zone of sea and brackish waters (St. 22-24) is characterized by intermediate values of T_{Alk}/S - ratio (alkalinity coefficient) (Fig.3-13a,b) and other nutrients. All hydrochemical parameters indicate a frontal zone (St. 22,13,23) through distinct concentration gradients.

3. The zone of marine transformed waters in the northern part of the transect (Sts. 27-29) is characterized by a decline in concentrations of silicium, phosphates, total phosphorus and nitrites. The influence of river waters extended to the northernmost station of the transect in the surface water layer (Figs.3-11 to 3-14).

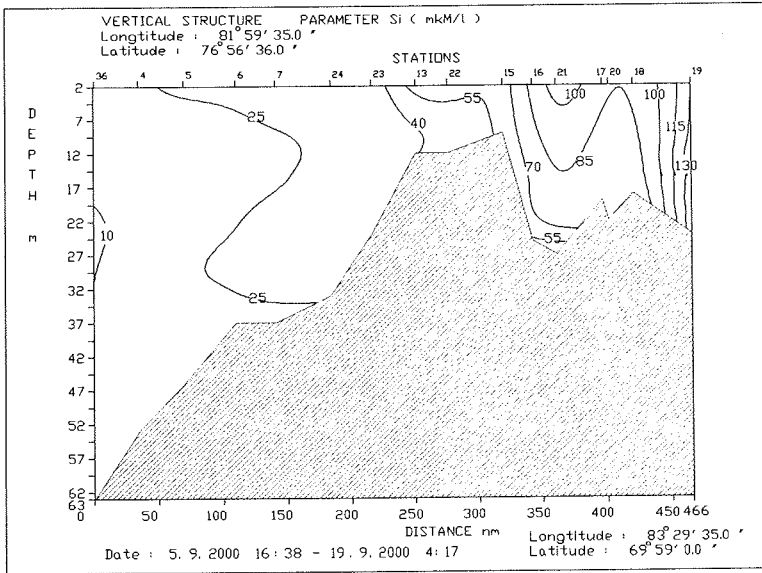
Comparison of the data from the three zones give evidence of substantially higher nutrient concentrations in the Yenisei fresh water and of lower concentrations and a weak organic matter mineralization in the colder and more saline waters of the northernmost marine part of the transect.

The distribution of alkalinity coefficient and silicium in vertical profiles indicate that river run-off [Rusanov and Vasil'ev, 1976] influence both intermediate and near-bottom waters. This indicates that the different water masses of the shallow Kara Sea are mixed thoroughly.

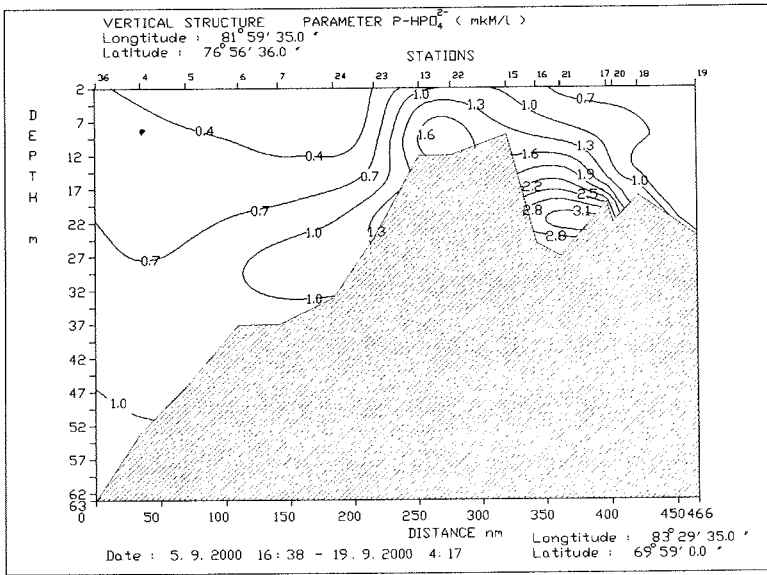
The distribution pattern of nutrients set by the composition of the river discharge and the basin hydrodynamics, as deduced from the distribution pattern of the T-S parameters along the longitudinal transect (Stephantsev and Shmelkov, this vol.), may sometimes be disturbed by biogeochemical mineralization of labile organic compounds, as well as by active nutrient uptake by phytoplankton during photosynthesis and therefore is controlled by the bioproductivity and phytoplankton biomass (Makarevich and Larionov, this vol.).

Nutrient concentrations in near-bottom water points to a low rate of organic matter degradation and remineralization near the bottom causing a high preservation in the low temperature (as low as $-1,8^{\circ}\text{C}$) environment. High benthos abundances observed at some stations (Lubin and Eckert, this vol.) may be considered as a consequence of this situation.

Comparison of the data from the expeditions in 1999 and 2000 (Sukhoruk and Tokarev, 2000) demonstrate some variations in nutrient concentrations and distribution patterns due to the seasonal differences and weather conditions. Temperature and strength of winds, ice conditions and Yenisei water level are the most effective factors (Burenkov and Vasil'kov, 1994; Makkaveev and Stunzhas, 1994).

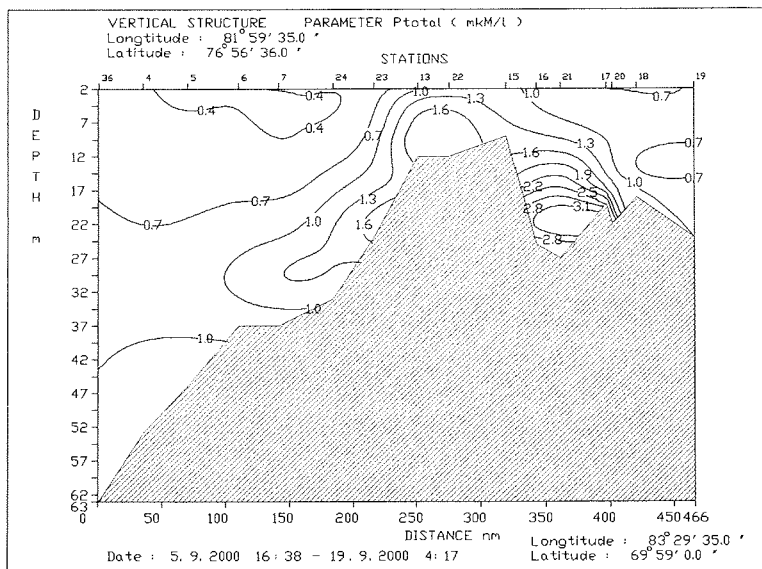


(a)

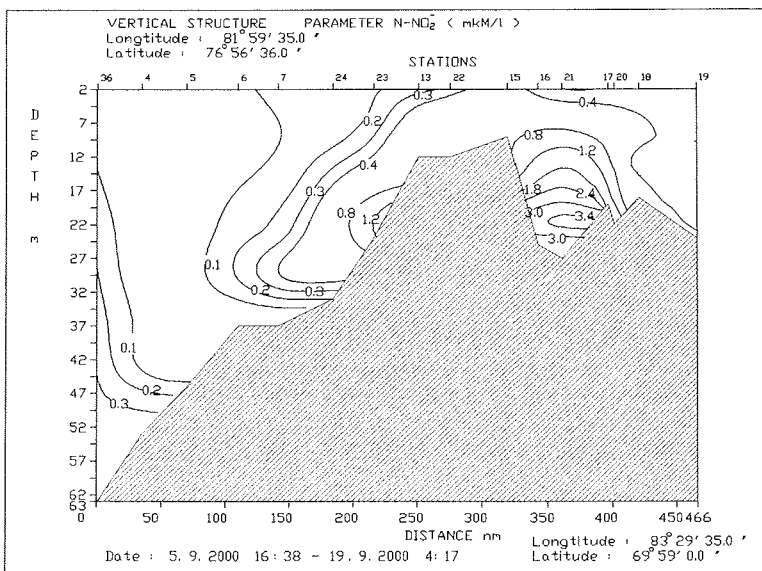


(b)

Fig.3-11: Vertical distribution of S_i (a) and $P-HPO_4^{2-}$ (b) on a quazimeridional section.

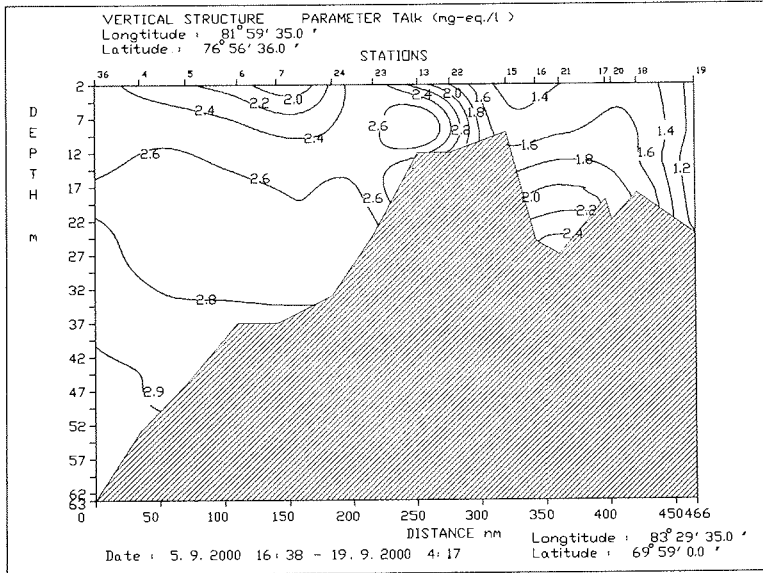


(a)

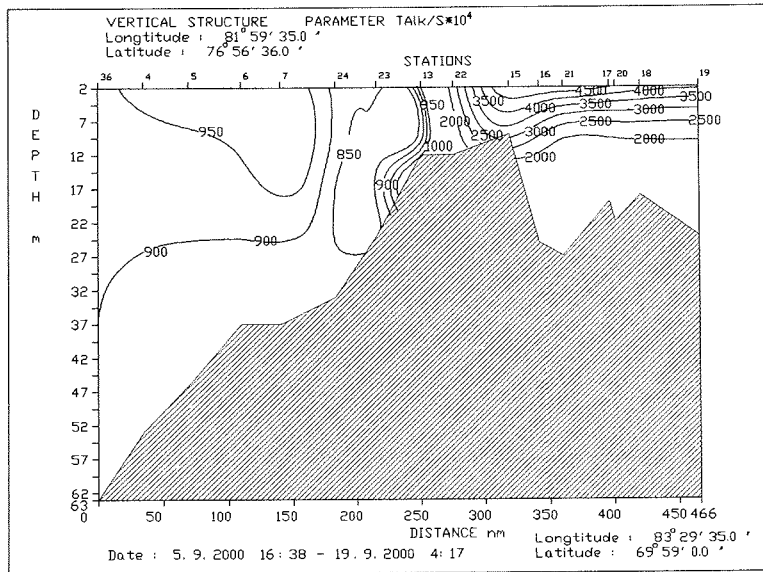


(b)

Fig.3-12: Vertical distribution of P_{total} (a) and $N-NO_2^-$ (b) on a quazimeridional section.

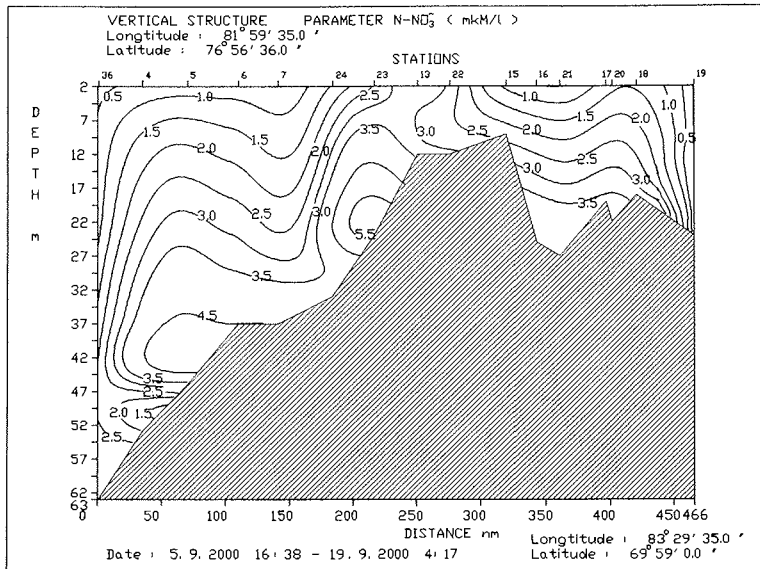


(a)

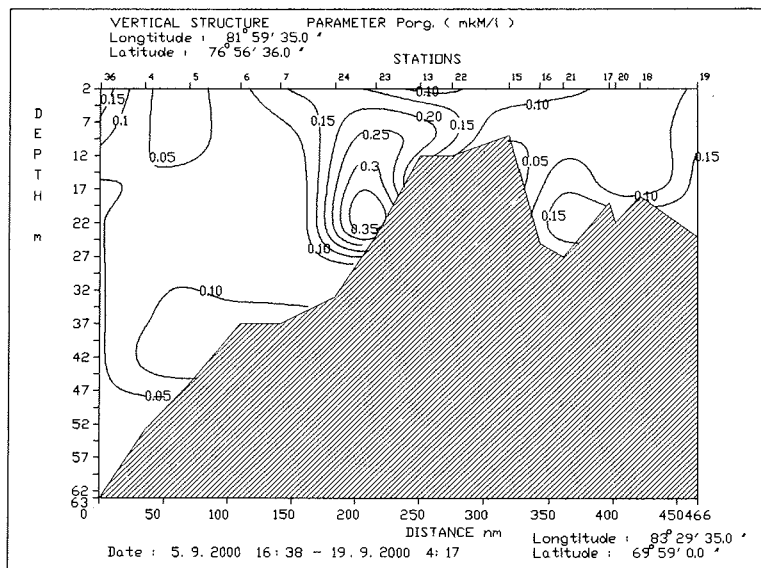


(b)

Fig 3-13: Vertical distribution of TALK (a) and TALK / S (b) on a quazimeridional section.



(a)



(b)

Fig.3-14: Vertical distribution of N-NO₃⁻ (a) and P_{org} (b) on quazimeridional section.

Table 3-1: Nutrients in the Kara sea.

Station, -	Water depth, -	S, ‰	Talk, mg-eq/L	CONCENTRATION, $\mu\text{M/L}$						TAIK/S, $\times 10^4$
				P, total	PO ₄ ³⁻ -P	P org.	NO ₂ - N	NO ₃ - N	SiO ₄ ³⁻ - Si	
2	0	17,6	1,8	0,38	0,30	0,08	0,10	0,09	42,1	1022
	12	20,0	2,2	0,30	0,30	0,00	0,02	0,40	30,1	1100
	45	33,6	2,6	0,89	0,85	0,04	0,38	0,58	20,2	774
4	0	25,7	2,4	0,45	0,30	0,15	0,07	0,80	21,7	934
	13	29,1	2,7	0,55	0,40	0,15	0,14	0,53	12,6	928
	50	34,1	2,8	0,93	0,90	0,03	0,24	0,34	25,5	821
5	0	22,0	2,2	0,35	0,32	0,03	0	0,46	26,4	1000
	10	27,9	2,6	0,49	0,45	0,04	0,010	1,92	20,3	932
	50	33,7	2,9	1,08	0,95	0,13	0,023	5,08	23,8	860
7	0	16,5	1,6	0,42	0,28	0,14	0,19	0,76	36,9	970
	11	25,3	2,5	0,40	0,35	0,05	0,10	1,49	24,6	989
	37	32,8	2,7	1,80	1,73	0,07	0,56	2,89	37,4	824
8	0	20,9	2,2	0,22	0,10	0,12	0,07	0,57	29,2	1052
	23	26,4	2,8	0,40	0,10	0,30	0,13	2,23	20,0	1060
	39	33,3	2,9	1,20	0,10	1,10	0,33	4,55	33,2	871
13	0	22,8	1,7	0,90	0,90	0	0,22	4,50	59,2	745
	4	25,5	2,7	1,20	1,05	0,15	0,24	4,64	44,4	1059
	13	29,6	2,9	2,90	2,65	0,25	1,13	1,69	41,4	980
15	0	6,8	1,5	1,00	0,83	0,17	0,09	1,15	57,0	2205
	16	7,3	1,8	0,85	0,81	0,04	0,06	1,07	67,6	2465
16	0	2,3	1,3	1,05	0,90	0,15	0,47	0,80	59,2	5652
	15,5	13,5	1,8	1,80	1,80	0	0,87	3,55	50,8	1333
	25	20,1	2,2	2,75	2,70	0,05	3,24	4,60	52,4	1094
17	0	0	1,5	0,65	0,60	0,05	0,27	3,12	57,0	40000
	16	0,4	1,6	0,65	0,65	0	0,46	3,51	67,6	
19	0	0	1,1	0,7	0,6	0,1	0,33	0,06	128	-
	21,7	0	1,1	0,8	0,6	0,2	0,33	0,15	140	
20	0	0	1,5	0,65	0,55	0,10	0,27	0,25	104,3	3333
	19	5,7	1,9	1,30	1,22	0,08	0,90	3,41	71,4	
21	0	0	1,4	0,8	0,65	0,15	0,30	0,06	107,8	2414
	5,6	5,8	1,4	0,7	0,65	0,05	0,30	1,29	98,7	
	24,5	22,9	2,4	3,7	3,5	0,2	3,82	4,25	70,0	
22	0	6,6	1,4	0,95	0,85	0,10	0,33	1,15	98,0	2121
	3	11,7	1,9	1,03	0,95	0,08	0,39	1,64	800	
	10	29,4	2,7	0,95	0,75	0,20	0,10	4,09	30,9	

Table 3-1: cont.

23	0	28,4	2,5	0,42	0,30	0,12	0,16	1,92	25,6	880
	11,7	30,5	2,5	0,75	0,45	0,30	0,27	4,21	27,8	819
	25,0	33,0	2,7	1,82	1,42	0,40	1,18	6,37	32	818
24	0	23,9	2,2	0,40	0,10	0,30	0,10	0,49	24,6	920
	11	26,1	2,6	0,40	0,20	0,20	0,13	1,45	17,4	996
	31	32,3	2,8	0,95	0,88	0,07	0,52	5,84	25,6	867
26	0	19,2	1,9	0,2	0,10	0,10	0,16	0,59	30,8	989
	17	26,7	2,5	0,3	0,10,	0,20	0,07	0,63	9,0	936
	61	33,7	2,8	1,0	0,75	0,25	0,72	6,26	19,4	830
27	0	23,2	2,2	0,45	0,10	0,35	0,13	0,81	17,4	942
	12	25,7	2,4	0,44	0,25	0,15	0,10	0,63	22,4	934
	74	34,2	2,8	0,92	0,90	0,02	0,38	3,09	15,4	818
28	0	25,6	2,5	0,50	0,45	0,05	0,13	0,49	16,5	978
	16	29,2	2,6	0,65	0,50	0,15	0,16	1,03	12,8	890
	47	34,1	2,9	0,90	0,80	0,10	0,38	4,83	10,5	850
29	0	-	-	0,60	0,45	0,15	0,13	1,75	12,1	-
	17	-	-	0,73	0,50	0,23	0,13	0,60	4,2	-
	49	-	-	1,10	0,90	0,20	4,38	4,85	18,1	-
30	0	24,9	2,4	0,50	0,45	0,05	0,12	0,56	26,8	964
	27	25,1	2,4	0,55	0,45	0,10	0,10	0,73	22,6	956
	29	29,6	2,7	0,85	0,55	0,30	0,18	1,19	15,2	912
	52	33,9	2,8	1,10	0,95	0,15	0,13	3,41	40,4	826
35	0	26,6	2,5	0,60	0,45	0,15	0,07	0,36	21,2	940
	14	30,4	2,8	0,70	0,55	0,15	0,12	2,12	21,2	921
	46	33,2	2,8	2,00	1,78	0,22	0,07	2,75	33,2	843
36	0	27,1	2,5	0,62	0,40	0,22	0,04	0,31	14,7	922
	14,0*	31,1	-	0,70	0,65	0,05	0,13	0,56	4,50	900
	14,5	27,4	2,5	0,65	0,60	0,05	0,10	0,79	21,5	912
	63,0	33,9	3,0	1,23	1,20	0,03	0,42	3,18	23,3	885

4. Sediment trap investigations in the Kara Sea

D. Unger, S. Schayen, and B. Gaye

Institute for Biogeochemistry and Marine Chemistry, University of Hamburg, Germany

Introduction

The transfer of particulate material from the surface layer to the deeper water column and sediment plays a major role in the global biogeochemical cycles of elements such as carbon, nitrogen and silica. The measurement of flux rates and the sampling of the sinking material from the water column can be conducted by means of sediment traps. Sediment trap studies being carried out in numerous regions of the world ocean have considerably improved our knowledge of the factors controlling the formation, amount and quality of sinking particles (see Ittekkot, 1996; Honjo, 1996 for an overview). This information contributes significantly to the interpretation of the sedimentary record. Flux measurements from the Arctic ocean especially over longer periods are scarce due to logistical problems arising from the ice coverage. The observed range of flux rates varies from only a few $\text{mg m}^{-2} \text{d}^{-1}$ day in permanently ice-covered regions (Hargrave et al., 1993) up to $> 300 \text{ mg m}^{-2} \text{d}^{-1}$ under the influence of ice-rafted material near the ice edge (Hebbeln and Wefer, 1991).

Methods

Recovery of sediment traps

During the „Akademik Boris Petrov“ Cruise in 1999 into the Kara Sea two sediment trap moorings have been deployed in order to study an annual cycle of rates and seasonality of vertical particle fluxes at two stations in the Kara Sea (Unger et al., 2000). Whereas the trap moorings could be recovered after short time deployment in 1999, it was not possible to retrieve the traps after this first long-time particle flux experiment in the Kara Sea. The mooring system in the Ob estuary area was completely lost. After several attempts to retrieve the system by operating the acoustic release failed, we tried to recover the system by dredging around the exact mooring position. As this was not successful, too, we suppose that the mooring line was dislocated.

The mooring line in the estuary of Yenisei river, however, could be retrieved without problems despite heavy sea. Nevertheless, here too, the trap itself and the samples were lost. It appears that the construction of the trap used in this study (MST 6, Hydrobios) is not suitable for high energetic systems with ice and waves/currents as it is represented by the Kara Sea Shelf area. In order to enable the engineers at Hydrobios to improve the construction of the sediment traps we informed them in detail about the problems which occurred during the present study.

Deployment of sediment traps

At the Yenisei station a sediment trap type Hydrobios MST 24 was deployed (see Fig. 2-1 for location). This trap is characterized by an improved fixation system as compared to the formerly used MST 6. Additionally, in order to stabilize the funnel of the trap, the ship's mechanics furnished the trap with extra holding rods.

The trap MST 24 is equipped with a sophisticated electronical control system and 24 sampling bottles which make it possible to sample the particle flux in variable intervals according to the expected flux rates and enable us to get a highly resolved record of the annual particle flux. The chosen lengths of sampling intervals vary between 28 days during winter time and seven days during summer period (Table 4-1) when high fluvial input of solids and nutrients should lead to maximum productivity and particle fluxes.

In order to avoid degradation and diffusion processes within the cups, HgCl_2 and NaCl were added to the cupwater prior to deployment. The composition of the mooring line was comparable to that of the short time moorings in 1999 and can be depicted from Figure 4-1. A detailed description of the mooring components is given in Table 4-2. The trap is located at a water depth of approximately 20 m below the surface and thus well below the low salinity surface layer.

Table 4-1: Sampling intervals of the Yen-03 deployment.

	start	Moscow	Duration
	interval	Time	Interval (d)
Bottle 1	= 16.9.00	00:00	7
Bottle 2	= 23.9.00	00:00	7
Bottle 3	= 30.9.00	00:00	14
Bottle 4	= 14.10.00	00:00	14
Bottle 5	= 28.10.00	00:00	14
Bottle 6	= 11.11.00	00:00	28
Bottle 7	= 9.12.00	00:00	28
Bottle 8	= 6.1.01	00:00	28
Bottle 9	= 3.2.01	00:00	28
Bottle 10	= 3.3.01	00:00	28
Bottle 11	= 31.3.01	00:00	28
Bottle 12	= 28.4.01	00:00	14
Bottle 13	= 12.5.01	00:00	14
Bottle 14	= 26.5.01	00:00	14
Bottle 15	= 9.6.01	00:00	7
Bottle 16	= 16.6.01	00:00	7
Bottle 17	= 23.6.01	00:00	7
Bottle 18	= 30.6.01	00:00	7
Bottle 19	= 7.7.01	00:00	7
Bottle 20	= 14.7.01	00:00	7
Bottle 21	= 21.7.01	00:00	7
Bottle 22	= 28.7.01	00:00	7
Bottle 23	= 4.8.01	00:00	7
Bottle 24	= 11.8.01	00:00	7

Table 4-2: Mooring Information YENISEI-03

Date of Deployment 14.09.2000

Time of Deployment 17.32 –17.50 (Moscow time)

Position Anchor Drop Lat. 74° 00' 275 N
Long. 80° 00' 450 E

Water Depth 31 m

Hydro-Bios Multi Sediment Trap MST 24, IfBM HH, Ser.No. 240800
Energy Source: 3 Lithium Cells 3V, 123 A
Armed: Schayen/Neumann/Unger

Acoustic Release Benthos Model 865-A, IfBM HH, S.N. 756
Energy Source: 13V Battery Pack
Receive Frequency 10kHz = Code 1
Enable Code = C
Release Code = A
Armed: Unger/Neumann/Schayen

Cupwater Filtrated Surface Sea Water (Barents Sea)
Addition of ca. 3,3 g HgCl₂ / L
and ca. 35 g NaCl / L

Laboratory work

Total samples of the BP short time moorings have been split into 8 aliquots each at the Alfred Wegener Institut, Bremerhaven. At Hamburg, one aliquot of each sample has been filtered onto preweighted polycarbonate filters for biogenic opal analysis. The remaining aliquots were filtered onto precombusted (550°C) and preweighted GF/F filters for measurement of total carbon and nitrogen (for further analytical details see Unger et al., this vol.), stable nitrogen isotopes and amino acids.

Flux rates were determined taking into account the weight of 4/8 of the total sample, the aperture of the sediment trap funnel and the duration of sampling intervals.

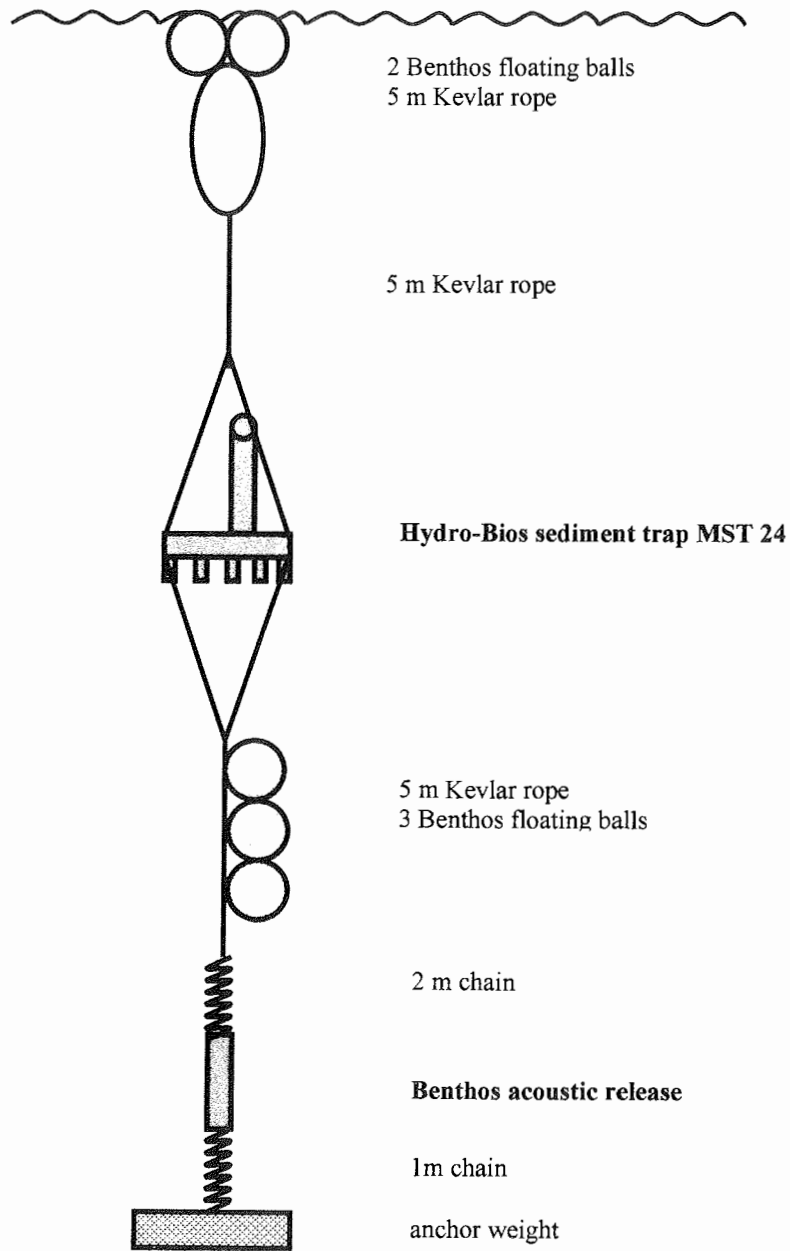


Fig. 4-1: Scheme of sediment trap mooring Yenisei-03.

First Results

First results from Kara Sea shelf area obtained during the short time deployment of sediment traps in 1999 (Unger et al., 2000) revealed very high average flux rates of $2,5 \text{ g m}^{-2} \text{ d}^{-1}$. Flux rates of this magnitude are typical for high productive and/or fluvial influenced shelf areas. Considerable differences between the settling particles from Ob and Yenisei estuaries can be noted. Average total carbon (TC) content of the Ob and Yenisei samples is 27,3 and 12,9%, respectively. Preliminary results show that the labile nitrogenous compounds represented by amino acids and amino sugars make up 13% of the total particle flux at the Ob and only 3,5% at the Yenisei station. Most probably the high TC and labile POC content in the Ob trap samples resulted from the plankton bloom in the Ob estuary and the high nutritional value of this material for zooplankton. Fecal pellets produced by zooplankton contributed significantly to the total particle flux (E.-M. Noethig, pers. comm. 2000).

However, short time measurements of particle flux represent only a snap shot of an instantaneous situation. Due to the strong seasonal variations of environmental parameters such as river runoff, ice-coverage and insolation an annual record of the particle flux and its seasonally changing composition is necessary to better understand the sedimentary record in the study area (Matthiessen and Boucsein, 1999; Boucsein et al., 1999).

Acknowledgements

We would like to express our thanks to the Captain and crew of R/V "Akademik Boris Petrov" for their excellent work during the recovery and deployment of the sediment traps and our search for the lost mooring system. We would also like to thank all colleagues on board Akademik Boris Petrov for their assistance during the cruises.

5.1 Taxonomic composition and productivity of the microalgal communities of the Ob Bay and the Yenisei Bay in the summer 1999.

Makarevich P.R. and Larionov V.V.

Murmansk Marine Biological Institute MMBI, Murmansk, Russia

In the present report, the results of a phytoplankton study carried out on the Ob-Yenisei Shallows during the 1999 cruise of RV "Akademik Boris Petrov" (August 24 – September 8, 1999). The description of the materials and methods as well as preliminary results were published earlier in the multi-disciplinary report of this expedition (Stein and Stepanets, 2000). It was also supplied with a map, and coordinates and timing of the stations.

Phytoplankton are major producers of organic matter in the Arctic seas, representing the most important link in the ecological metabolism of Arctic marine ecosystems. Our knowledge of the taxonomic composition and population parameters of the phytoplankton communities are of great importance for understanding the time-space patterns of the ecosystem processes. It is especially actual for coastal and estuarine areas which are subject to riverine runoff, a principally important factor influencing the composition and distribution of organic matter. Such a situation make it necessary to accentuate a biological component in the processes of overall transformation of organic carbon compounds.

The phytoplankton samples were conducted with a Rosette-sampler set in combination with CTD profiling. The 1 liter samples were concentrated using a reverse-flow device and preserved with 2 % buffered formaldehyde. Counting and taxonomic identification of phytoplankton were carried out in a 0.05 ml counting chamber at 300x magnification according to routine technique. The biomass was calculated using the standard mean-weight tables for Arctic pelagic algae.

Sampling layers at stations were chosen in accordance with the density structure of the water column. Three layers were usually sampled: surface layer, near-bottom layer and pycnocline. At shallower stations with the well mixed water column, only two former layers were sampled, while at deeper station an additional sample was taken immediately below the pycnocline. A total of 71 samples on 29 stations was obtained.

The taxonomic composition and biomass of pelagic algae of the Ob-Yenisei Shallows are represented in Table 5-1. Special attention has been paid to the ecological characteristics of the algal species among which three major ecological groups were present: marine species, freshwater species, and estuarine ("intermediate") species. It is necessary to note that this traditionally used classification scheme is rather conventional and characterizes pelagic organisms mainly by their origin, or, as an extreme, by their typical habitats in which a species is usually found. However, these characteristics say nothing about the physiology or salinity and temperature preferences of a given form.

The analysis of the data considered allows to outline in the study region several distinct areas that differ by both the total biomass levels and relative abundance of the ecological groups of the phytoplankton. The first area includes the mouth region of the

Ob Bay and adjacent stretch of the Kara Sea open shelf. The phytoplankton biomass here reached up to 4-9 mg liter⁻¹, exceeding 21 mg liter⁻¹ at the southernmost station (72°00' N), where salinity was as low as 0.6 ‰. More than 90 % of this biomass were formed by freshwater and, to a less extent, estuarine species: diatoms *Melosira varians* and *M. granulata*, and a chlorophycean, tentatively identified as *Rhizoclonium*. It is noteworthy that such high biomass levels were found all over the water column decreasing only slightly down to the bottom accompanied with a simultaneous decline of the taxonomic diversity. Marine forms are virtually absent at any layer, with an exception of the northern Ob Bay where rare dinophyceans were found.

The distribution boundary of the above phytoplankton community runs roughly along 73°30' N latitude. At a station located at this latitude, a unique microalgal assemblage consisting of the species of both freshwater and marine origin, was found. In the surface layer, the biomass values of both groups were approximately on parity, and down to the bottom the relative abundance of the freshwater forms increased with a maximum at the near-bottom layer in which they accounted for more than 90 % of the total biomass of the community.

The area situated north of this station was characterized by the predominance of the algae of marine origin. This community was formed by a phytoplankton assemblage typical of the Arctic seas. The dominant species here were diatoms from the genus *Thalassiosira*: *T. gravida*, *T. antarctica* (to a less extent *T. hyalina* – *T. nordenskjöldii*), together making up more than 80 % of the total phytoplankton biomass. The overall biomass level was several times lower compared to the former area, and the biomass maxima were in most cases located at the pycnocline, while there was a remarked decrease in the deeper water column. In general, this pattern corresponds with the stage of the spring bloom in the Arctic seas. Obviously, in this region of the Kara Sea, the seasonal succession pattern is the same as in other open shelf areas of the Arctic seas. However, virtually in all samples, there were rare representatives of the freshwater pelagic flora characteristic of the Ob Bay. At the near-bottom layer, their relative abundance was even higher than that of the marine species, but extremely low phytoplankton biomass values did not exclude a possibility of an error by using the relative biomass parameters.

In general, the preferentially marine character of the phytoplankton community was observed in a direction to the east. However, there was a continuous several-fold decrease of the phytoplankton biomass. In contrast, the taxonomic diversity increased. The leading role in the community played the early-spring diatoms *Nitzschia grunowii* and *Navicula vanhoeffenii*, as well as seasonally “older” species *Chaetoceros* spp. It is possible that the simultaneous presence of the early-spring and late-spring diatoms may be related to shorter duration of the phytoplankton growth season in the eastern Kara Sea.

The third area differing principally from the above ones with phytoplankton population parameters, comprised the mouth area of the Yenisei Bay and coastal waters off Taimyr Peninsula. The phytoplankton assemblages were characterized by extremely low biomass values (lower than 0.05 mg liter⁻¹). Only at a few southernmost stations, the biomass ranged from 0.1 to 0.2 mg liter⁻¹ due largely to the development of the freshwater species. On the whole, it was very difficult to establish a relative dominance of either freshwater or marine forms as on different stations the composition of the

phytoplankton was quite variable. Moreover, low biomass did not allow to qualify this area as one with active reproduction of pelagic algal populations.

Table 5-1:
The taxonomic composition and biomass (mcg/l) of the phytoplankton community in the Ob and the Enisei estuaries and the adjacent waters in August-September 1999.

Taxa	Station No.																
	Depth, m		0	7.5	24	0	7.3	12.5	0	8	27.5	0	12	18	25	0	17
BACTERIOPHYTA																	
<i>Asterionella bireakelvi</i> W.Smith																	
<i>A. formosa</i> Hassal	0.25	0.14		0.21	0.15		0.60		42.50	3.98		0.30	8.96	0.46	0.23	6.23	1.05
<i>Thalassiosira</i> sp.	1396.90	128.05		2444.57	101.27	188.58	1024.39	279.38	10.48	6.42							
<i>T. gravida</i> Cleve	39.66	6.54		5.62													
<i>T. nordenskiöldii</i> Cleve	1887.48	176.55	22.47	2097.20	67.41	112.99	171.20	68.48									
<i>T. antarctica</i> Comber				272.60	7.70	14.11	74.40										
<i>T. inyalina</i> (Grunow) Gran							9.14										
<i>T. bioquata</i> (Grunow) Osterfeld	4.57																
<i>T. fallax</i> Meunier	8.45																
<i>Thalassiosira</i> sp.				0.74	1.77		0.88		34.00	0.39		23.40	4.20	3.00	1.20	0.18	9.00
<i>Thalassionema nitzschioides</i> Grunow																	
<i>Fractilaria capucina</i> Desm.																	
<i>F. crotonensis</i> Kitton																0.25	
<i>F. cylindrus</i> Grunow																	
<i>Fractilaria</i> sp.																	
<i>Navicula vanthoeffenii</i> Gran	9.28	0.40		1.81	2.77	0.58	3.40	0.33				7.21	2.04				2.93
<i>Navicula</i> sp.			0.03														
<i>Nitzschia grunowii</i> Hasle	88.51	3.65	0.50	66.38	11.62	4.43	44.26	6.71	1.24								
<i>N. ionissima</i> (Breb.) Ralfs	0.04	0.06	0.01	0.10	0.02	0.05	0.18	0.07	0.01								
<i>N. closterium</i> W.Smith				0.01			0.08										
<i>N. seriata</i> Cleve				0.70	0.20	0.17	4.05	0.10									
<i>N. arctica</i> Cleve	0.56	0.12	0.08														
<i>N. radiolatus</i> W.Smith																	
<i>Pennatophyceae</i> spp. (unidentified)			0.03				0.32					0.14	0.33	0.10		1.50	4.95
<i>Gyrodinium</i> sp.												6.14	5.46	1.14	3.34	90.96	
<i>Melosira diaphana</i> (Ehr.) Ralfs	1.82	0.83	0.91														
<i>M. moniliformis</i> (O.E. Muellet) A.																	
<i>M. humboldtiana</i> (Bilim.) A.	3.30	3.60	3.60	21.00	14.40	14.40	9.60	7.20	3.60								
<i>M. varians</i> A.	13.03			165.64	47.84	13.48	6.29	6.29									
<i>M. urpersi</i> A.																	
<i>M. dipha</i> Kütz																	
<i>Porosira glacialis</i> (Grunow) Joerg.					2.98		24.82	1.49	1.49								
<i>Cyclotella</i> sp.																	
<i>Coscinodiscus</i> sp.																	
<i>Chaetoceros fragilis</i> Meunier	1.27			0.89			7.93	0.32				0.60	0.40				8.27
<i>C. teres</i> Cleve							0.58	5.18									0.33
<i>C. diadema</i> (Ehr.) Gran	5.83	4.54	0.46				3.67	0.92									
<i>C. socialis</i> Leuder																	
<i>C. debilis</i> Cleve																	
<i>C. septentrionalis</i> Oestrup																	

Table 5-1: (continued).

Taxa	Station No.														
	0	7.5	24	0	7.3	12.5	0	8	27.5	0	12	18	25	St. 6	St. 7
Depth, m															
BACILLARIOPHYTA															
<i>Chaetoceros wighamii</i> <i>Brigitte</i>															
<i>C. curvisetus</i> <i>Cleve</i>															
<i>C. mitra</i> (<i>Bailey</i>) <i>Cleve</i>															
<i>C. similis</i> <i>Cleve</i>															
<i>Chaetoceros</i> sp.	3.60			13.50	3.60	2.00	1.86	8.40		2.70				0.05	
<i>Synedra</i> sp.															
<i>Tabellaria fenestrata</i> (<i>Lubbock</i>) <i>Kütz.</i>															
CHLOROPHYTA															
<i>Ankistrodesmus convolutus</i> <i>Corda</i>														0.01	
<i>Rhizoclonium</i> sp.														24.83	
<i>Chlorophyta</i> spp. (unidentified)															
<i>Scenedesmus quadricauda</i> <i>Breb.</i>															
CYANOPHYTA															
<i>Anabaena</i> sp.															
<i>Merismopedia glauca</i> <i>Chod.</i>															
ELLENOPHYTA															
<i>Eutreptia lanowii</i> <i>Steur.</i>						0.18	0.36	0.18							
<i>Eutreptia</i> sp.															
DINOPHYTA															
<i>Amylax catenata</i> (<i>Levander</i>) <i>Meunier</i>	158.68	27.27	11.90	24.79	65.45	56.86	79.34	4.63	2.98				0.66		1.49
<i>Amphidinium</i> sp.															
<i>Glenodinium</i> sp.					0.60										
<i>Goniaulax triacantha</i> <i>Joerg.</i>															
<i>Gyrodinium pelliculidum</i> (<i>Wulff</i>) <i>Schiller</i>				0.10			0.76	0.08							
<i>G. pingue</i> (<i>Schuetz</i>) <i>Kofoid et Swezy</i>							0.72	0.22							0.16
<i>Gymnodinium</i> sp.															
<i>Prorocentrum micans</i> <i>Ehr.</i>															
<i>Prorocentrum granii</i> (<i>Osterfeld</i>) <i>Balech</i>	2.82			47.73	66.66	3.76	5.01	3.13	0.94	1.41					1.41
<i>P. breve</i> (<i>Paulsen</i>) <i>Balech</i>						9.20	4.60			10.35					18.90
<i>P. pyriforme</i> (<i>Paulsen</i>) <i>Balech</i>															
<i>P. pallidum</i> (<i>Osterfeld</i>) <i>Balech</i>							6.52								
<i>P. pelliculidum</i> <i>Bergb.</i>											1.25	1.04			
<i>P. brevipes</i> (<i>Paulsen</i>) <i>Balech</i>					1.25								0.39		0.87
<i>P. curvipes</i> (<i>Osterfeld</i>) <i>Balech</i>															
<i>P. thorianum</i> (<i>Paulsen</i>) <i>Balech</i>							9.22								
CHRYSOPHYTA															
<i>Chrysohyta</i> spp. (unidentified)															
<i>Ebria tripartita</i> (<i>Schumann</i>) <i>Lemm.</i>	1.34	0.62	0.34	0.56	1.01	0.90	1.79			0.50					0.50
<i>Dinobryon baillatum</i> (<i>Schuetz</i>) <i>Lemm.</i>															
Total biomass (mca/l)	3611.061	365.10	40.33	5164.15	396.70	421.69	1536.80	435.69	27.55	117.94	29.62	5.74	16.69	144.78	43.06

Table 5-1: (continued).

Taxa	Station No.										St. 13					
	Depth, m															
	0	12	15	0	10	25	0	6.5	12	35	0	8	15	24	0	
BACILLARIOPHYTA																
<i>Asterionella bleekeri</i> W. Smith																
<i>A. lornosa</i> Hassel	0.52	0.66	1.45	0.10	0.25	0.15	0.55	1.59		0.23	2.18	11.62	0.33	0.60	1.69	
<i>A. lornosa</i> Grunow			11.64	9.12	43.64		244.46	314.30	13.99		87.31	94.58	2.91		419.07	
<i>T. gravida</i> Cleve					97.78										179.76	
<i>T. nordenskiöldii</i> Cleve															67.35	
<i>T. antarctica</i> Comber																
<i>T. nyalina</i> (Grunow) Gran							16.00									
<i>T. biculata</i> (Grunow) Oosterfeld																
<i>T. fallax</i> Meunier																
<i>Thalassiosira</i> sp.																
<i>Thalassionema nitidocloides</i> Grunow	15.70	4.00	5.00				60.00	26.40	2.40	0.80	5.30			2.40		
<i>Fragilaria capucina</i> Desm.																
<i>F. cyclonensis</i> Kitton																
<i>F. cylindrus</i> Grunow																
<i>Fragilaria</i> sp.	12.63	0.63		19.24	7.21				1.38	0.50				0.15		
<i>Navicula vanthoffenii</i> Gran							0.43	0.71							0.87	
<i>Navicula</i> sp.															0.06	
<i>Nitzschia grunowii</i> Hasle			6.68				11.06	41.49			2.21	24.20	0.23		1.80	
<i>N. longissima</i> (Breb.) Halls			0.02				0.02	0.01	0.02			0.05			0.20	
<i>N. closterium</i> W. Smith							0.03	0.04							0.04	
<i>N. seriata</i> Cleve			0.11				0.55	0.35	0.30					0.08	8.36	
<i>N. arctica</i> Cleve			0.80								0.83	1.05				
<i>N. acicularis</i> W. Smith		0.01					0.05					0.01				
Pennatophyceae spp. (unidentified)	0.07	0.08	0.15		0.09	0.03		0.18	0.12	0.06	1.20	0.53	0.10	0.18		
<i>Gyrodinium</i> sp.																
<i>Meiopsis</i> sp.	1.74			1.82	8.19	5.00					4.55	4.17	1.14	2.27		
<i>M. granulata</i> (Ehr.) Halls																
<i>M. moniformis</i> (O.F. Mueller) Aa.																
<i>M. muricoides</i> (Dillw.) Aa.																
<i>M. varians</i> Aa.					5.39	3.60		10.80	18.00	1.35				6.74		
<i>M. lundensis</i> Aa.																
<i>M. gibber</i> Krieger												3.56				
<i>Porosira glacialis</i> (Grunow) Joerg.	1.74	0.62					4.47	15.63	1.49	0.13		1.86			29.78	
<i>Cyclotella</i> sp.	1.02			1.19	0.99	0.79										
<i>Coscinodiscus</i> sp.	0.46		0.33													
<i>Chaetoceros fragilis</i> Meunier							3.01	1.11				1.26			0.71	
<i>C. teres</i> Cleve																
<i>C. diadema</i> (Ehr.) Gran								2.52	0.52						0.82	
<i>C. socialis</i> Lauder															0.81	
<i>C. debilis</i> Cleve															0.11	
<i>C. septentrionalis</i> Oestrup																

Table 5-1: (continued).

Taxa	Station No.												St. 13	
	Depth, m													
	0	12	15	0	10	25	0	6.5	11	12	15	24	0	
BACILLARIOPHYTA														
<i>Chaetoceros wighamii</i> Brightw.														
<i>C. curvisetus</i> Cleve														
<i>C. mitra</i> (Bailey) Cleve														
<i>C. similis</i> Cleve							3.79							
<i>Chaetoceros</i> sp.	1.35			1.80			9.30	15.60	1.80		1.50	1.75		7.50
<i>Synedra</i> sp.														
<i>Tabellaria fenestrata</i> (Lunbysen) Kuetz.														
CHLOROPHYTA														
<i>Arthrodesmus convolutus</i> Coe		0.35			0.71	0.54							0.53	
<i>Rhizoclonium</i> sp.														
<i>Chlorophyta</i> spp. (unidentified)														
<i>Scenedesmus quadricauda</i> Grab.														
CYANOPHYTA														
<i>Anabaena</i> sp.														
<i>Metschnikowia glauca</i> Grub.													0.32	
EUGLENOPHYTA														
<i>Eutreptia lanowii</i> Steyr.	0.60				0.13									
<i>Eutreptia</i> sp.							0.13							
DINOPHYTA														
<i>Amvixax catenata</i> (Levander) Meunier	4.46			4.96	1.98		3.97	0.99			2.48			137.85
<i>Amphidinium</i> sp.				0.12										
<i>Gonaulax triacantha</i> Joerg.				0.31										
<i>Gyrodinium pelliculidum</i> (Wulff) Schiller														
<i>G. pingue</i> (Schuett) Kofoid et Swezy	0.51			0.11			0.23	0.43			0.42	0.36		0.97
<i>Gymnodinium</i> sp.							0.22	1.01			0.10			
<i>Prorocentrum micans</i> Ehr.					0.11									
<i>Protoperidinium grani</i> (Ostenfeld) Balech	1.41			0.94			1.88	9.39			1.10	2.35		17.84
<i>P. breve</i> (Paulsen) Balech				6.90							8.05			
<i>P. pyriforme</i> (Paulsen) Balech														
<i>P. pallidum</i> (Ostenfeld) Balech							6.30							
<i>P. pelliculidum</i> Bergh														
<i>P. brevipes</i> (Paulsen) Balech		2.08	1.04		1.25									2.49
<i>P. curvipes</i> (Ostenfeld) Balech														0.58
<i>P. thorianum</i> (Paulsen) Balech														
CHRYSOPHYTA														
<i>Chrysophyta</i> spp. (unidentified)														
<i>Ebria tripartita</i> (Schumann) Lemm.	2.02	0.56		1.01		0.34	0.67	9.74			1.68	0.56		0.82
<i>Dinobryon balticum</i> (Schuett) Lemm.														1.68
Total biomass (mca/l)	44.23	8.99	27.22	46.66	188.68	10.45	521.20	594.13	40.02	3.07	299.74	565.89	6.54	12.34
														861.16

Table 5-1: (continued).

Taxa	Station No.	St. 13	7	St. 17	16	0	St. 18	12	0	St. 19	11,5	0	St. 20	6	11,5	0	St. 23	0	St. 24	
Depth, m	7	32	7	16	16	0	8,7	12	0	10,5	11,5	0	6	6	11,5	0	0	0	0	
BACILLARIOPHYTA																				
<i>Asterionella bleakevi</i> W. Smith							86,32	8,90	276,89	56,68	68,27	361,88	185,92	24,07	176,96	9,50				
<i>A. formosa</i> Hassel	1,25		143,18	17,43	209,16	77,76			39,67		2,31	363,66	119,02		13,75					
<i>A. lundii</i> (Grunow) Grunow	1152,4		3,72																	2281,6
<i>I. gravida</i> Cleve																				9,25
<i>I. nordenskiöldii</i> Cleve																				564,96
<i>I. antarctica</i> Comber	231,12	5,78																		230,90
<i>I. hyalina</i> (Grunow) Gran	42,33																			
<i>I. bioculata</i> (Grunow) Ostensfeld																				
<i>I. fallax</i> Meunier										5,00		300,00	80,00	6,00						11,20
<i>Thalassiosira</i> sp.													0,92							0,52
<i>Thalassionema nitzschoides</i> Grunow																				
<i>Fragilaria capucina</i> Desm.					1,69				0,91	0,81		0,38		0,70	0,91					
<i>F. crotonensis</i> Kirtsov																				
<i>F. cylindrus</i> Grunow																				
<i>Fragilaria</i> sp.		0,69	0,60																	
<i>Navicula vanhoefenii</i> Gran	3,09																			
<i>Navicula</i> sp.	0,06	0,09						0,40												
<i>Nitzschia grunowii</i> Hasle	2,16																			0,30
<i>N. longissima</i> (Grab.) Ralls	0,57		0,35		0,20							0,04			0,02					0,03
<i>N. closterium</i> W. Smith			0,17					0,07												0,14
<i>N. seriata</i> Cleve	9,12																			3,51
<i>N. arctica</i> Cleve	1,20																			0,32
<i>Neocleptis W. Smith</i>																				
<i>Pennatophyceae</i> sp. (unidentified)	0,09		0,26	1,86	1,80				0,13	0,07		0,13		0,40						0,03
<i>Gyrodroma</i> sp.									0,60	0,25		0,35		0,15						0,78
<i>Melosira granulata</i> (Gr.) Ralls			261,51	709,49	291,07		545,76	4851,20	472,99	61,40	74,28	1303,8	145,54	49,27	354,74	12,73				
<i>M. ruficornis</i> (O. F. Muell.) Ag.																				
<i>M. ruficornis</i> (O. F. Muell.) Ag.			4767,14	5417,35	3988,90		3413,92	404,28	5390,40	621,58	2594,1	5794,7	988,24	370,59	3211,8	1976,5				
<i>M. varans</i> Ag.																				
<i>M. lutea</i> Ag.																				
<i>M. dubia</i> Kuetz																				
<i>Porosira glacialis</i> (Grunow) Jørg.	20,10																			1,99
<i>Cyclotella</i> sp.	0,40	0,40	0,99		9,92		7,93													10,74
<i>Coscinodiscus</i> sp.	0,40		0,23																	0,53
<i>Chaetoceros fragilis</i> Meunier																				0,58
<i>C. teres</i> Cleve																				
<i>C. diadema</i> (Ehr.) Gran																				
<i>C. socialis</i> Lauder																				
<i>C. debilis</i> Cleve																				
<i>C. septentrionalis</i> Oestrup																				

Table 5-1: (continued).

Tava	Station No.											
	11	18	0	8	15.5	23	0	26	0	28	31	
BACILLARIOPHYTA												
<i>Asterionella bleakevii</i> W.Smith			0.41			0.51					0.17	
<i>A. formosa</i> Hassel	1.20	3.69	3.66							0.10	0.31	0.21
<i>Thalassiosira</i> sp.											1.22	
<i>T. gravida</i> Cleve	82.65	6.98	2139.00	680.99	26.77	3.20		796.23	768.29	541.30		
<i>T. nordenskioeldii</i> Cleve			101.79	12.36								
<i>T. antarctica</i> Conner	43.87		1063.58	500.76	7.70	1.82		161.78	134.82	77.04		
<i>T. ryalina</i> (Grunow) Gran	26.30			101.02				150.09	76.97			
<i>T. bioculata</i> (Grunow) Osterfield			13.34									
<i>T. fallax</i> Meunier												
<i>Thalassiosira</i> sp.	9.50		142.31				14.50			38.40		1.20
<i>Thalassiosira</i> sp.			0.84									
<i>Fragilaria capucina</i> Desm.												
<i>F. crotoneusis</i> Kitton												
<i>F. cylindrus</i> Grunow		4.02	2.47		0.25	0.14			0.65	1.14	0.54	0.31
<i>Fragilaria</i> sp.												
<i>Navicula vanthoefenii</i> Gran												
<i>Navicula</i> sp.												
<i>Nitzschia grunowii</i> Hasle	1.57		25.82	2.47	1.33			45.80	20.75	8.30		
<i>N. longissima</i> (Breb.) Ralfs			0.65	0.11	0.02					0.15		
<i>N. closterium</i> W.Smith	0.01		0.13	0.05				0.06	0.05	0.41		
<i>N. seriata</i> Cleve			20.09	1.22				0.58				
<i>N. arctica</i> Cleve	0.54											
<i>N. aciculata</i> W.Smith												
<i>Pennatophyceae</i> spp. (unidentified)		0.05	0.11				0.04			0.05		0.06
<i>Gyrodinium</i> sp.												
<i>Metosira</i> sp.	35.32	145.54	3.18		2.43	8.34				9.10	6.14	7.58
<i>M. moniliformis</i> (O.F.Mueller) Ac.												2.65
<i>M. turmidoides</i> (Dillw.) Ac.	242.01	795.08	8.40		8.98		61.09	5.40	12.60			
<i>M. varians</i> Ac.								2.02				
<i>M. lurgersi</i> Ac.												
<i>M. dubia</i> Kuetz.	0.74		3.47	17.87				2.73	3.72	19.36		
<i>Porosira diacelis</i> (Grunow) Joerg.										0.20		
<i>Cyclotella</i> sp.	0.20	0.33		0.76	0.26		0.56	7.37	6.73	1.32	7.14	0.83
<i>Coscinodiscus</i> sp.										0.20		
<i>Chaetoceros fragilis</i> Meunier												
<i>C. teres</i> Cleve												
<i>C. diadema</i> (Ehr.) Gran												
<i>C. socialis</i> Lauder												
<i>C. debilis</i> Cleve								6.96				
<i>C. septentrionalis</i> Oestrup												

Table 5-1: (continued).

Taxa	Station No.		St. 24		St. 25		St. 26		St. 28		St. 29		St. 30		St. 31	
	11	18	0	8	15.5	23	0	0	8.5	21	0	0	10.5	0	11.5	
BACILLARIOPHYTA																
<i>Chaetoceros wighamii</i> Brightw.																
<i>C. curvisetus</i> Cleve																
<i>C. mitra</i> (Bailey) Cleve																
<i>C. similis</i> Cleve																
<i>Chaetoceros</i> sp.				4.28	0.56							1.88				
<i>Synechia</i> sp.			11.90	4.05					59.40	90.00		3.16				
<i>Tabellaria fenestrata</i> (Lyngbyae) Kuetz.												19.20				
CHLOROPHYTA																0.42
<i>Ankistrodesmus convolutus</i> Corda																
<i>Rhizobolium</i> sp. (unidentified)																
<i>Chlorophyta</i> sp. (unidentified)	0.94	6.55	0.14	1.32	0.04											0.62
<i>Scenedesmus quadricauda</i> Grub.																
CYANOPHYTA																
<i>Anabaena</i> sp.																
<i>Menistropedia glacata</i> Grub.																
EUGLENOPHYTA																
<i>Eutreptia lanowii</i> Steur.							0.09									
<i>Eutreptia</i> sp.																
DINOPHYTA																
<i>Amplex catenata</i> (Levander) Meunier			109.92	2.98	0.66	0.99	1.32		0.99			4.96		13.39		
<i>Amphidinium</i> sp.																
<i>Glenodinium</i> sp.																
<i>Gomaulax triacantha</i> Joerg.								4.79								
<i>Gyrodinium pelliculidum</i> (Wulff) Schiller								0.13				1.25				
<i>G. pingue</i> (Schuett) Koloid et. Swezy				0.10				0.20				0.11				
<i>Gymnodinium</i> sp.			0.38												0.22	
<i>Prorocentrum micans</i> Ehr.																
<i>P. brevis</i> (Paulsen) Balech	6.89		3.29	14.08				3.44	2.82			1.88			1.88	
<i>P. pyriforme</i> (Paulsen) Balech	6.90															
<i>P. pallidum</i> (Ostenfeld) Balech																
<i>P. pelliculidum</i> Bergh.																
<i>P. brevipes</i> (Paulsen) Balech			1.45	2.91	0.83			1.66	1.45	2.49						
<i>P. curvipes</i> (Ostenfeld) Balech								0.58								
<i>P. thorianum</i> (Paulsen) Balech																
CHRYSOPHYTA																
<i>Chrysothrix</i> spp. (unidentified)																
<i>Ebria tripartita</i> (Schumann) Lemm.	0.34		1.57	0.28	0.22				1.01	1.34		0.67			0.67	
<i>Dinobryon balticum</i> (Schuett) Lemm.																
Total biomass (mca/l)	460.23	962.24	3657.90	1347.61	50.01	15.75	79.17	1249.53	1122.72	0.63	719.41	10.64	27.21	16.12	12.68	

Table 5-1: (continued).

Taxa	Station No.		Station No.		Station No.		Station No.		Taxa	Station No.		Station No.	
	Depth, m	15	0	16	0	16	0	16		Depth, m	15	0	16
		St. 31	St. 32	St. 35	St. 31	St. 32	St. 35	St. 31	St. 32	St. 35	St. 31	St. 32	St. 35
BACILLARIOPHYTA													
<i>Asterionella bleakaleyi</i> W.Smith													
<i>A. formosa</i> Hassa			0,25										
<i>Thalassiosira baltica</i> Grunow + (Loban.) Gran				146,67	680,99								
<i>T. gravida</i> Cleve				34,92									
<i>T. nordenskoeldii</i> Cleve					83,46								2,10
<i>T. antarctica</i> Comber													
<i>T. hyalina</i> (Grunow) Gran													
<i>T. bicucullata</i> (Grunow) Ostenfeld													
<i>T. fallax</i> Meunier													
<i>Thalassiosira</i> sp.													
<i>Thalassionema nitroschoides</i> Grunow			5,00	12,00	0,44								
<i>Fractilia capucina</i> Desm.													
<i>F. irrotentensis</i> Kitan		1,47											
<i>F. cylindrus</i> Grunow			1,60	2,30									
<i>Fragilaria</i> sp.													
<i>Navicula vanhoeffenii</i> Gran			0,05		3,53	1,36							
<i>Navicula</i> sp.													
<i>Nitzschia grunowii</i> Hasle				23,51	2,19								
<i>N. longissima</i> (Breb.) Ralls			0,02	2,24	0,52								
<i>N. closterium</i> W.Smith				0,32	0,07								
<i>N. seriata</i> Cleve			0,21	5,47	22,28								
<i>N. arctica</i> Cleve				7,21	0,48								
<i>N. sticticaris</i> W.Smith													
<i>Pennatophyceae</i> spp. (unidentified)		2,00											
<i>Gyrodinium</i> sp.													
<i>Melosira granulata</i> (Ehr.) Ralls		39,80											
<i>M. moniliformis</i> (O.F.Mueller) Ab.		30,00											
<i>M. nummuloides</i> (Dillw.) Ag.		123,53											
<i>M. varians</i> Ag.													
<i>M. lurgensis</i> Ag.													
<i>M. dubia</i> Kuetz													
<i>Porosira glacialis</i> (Grunow) Joerg.													
<i>Cyclotella</i> sp.													
<i>Coscinodiscus</i> sp.													
<i>Chaetoceros fragilis</i> Meunier		4,96											
<i>C. teres</i> Cleve													
<i>C. diadema</i> (Ehr.) Gran													
<i>C. socialis</i> Lauder													
<i>C. debilis</i> Cleve													
<i>C. septentrionalis</i> Oestrup													
BACILLARIOPHYTA													
<i>Chaetoceros wickhamii</i> Brightw.													
<i>C. curvisetus</i> Cleve													
<i>C. mitra</i> (Bailey) Cleve													
<i>C. similis</i> Cleve													
<i>Chaetoceros</i> sp.													
<i>Synedra</i> sp.													
<i>Tabellaria tenuistria</i> (Lobanov) Kuetz.													
CHLOROPHYTA													
<i>Ankistrodesmus convolutus</i> Corda													
<i>Phaeocystis</i> sp. (unidentified)													
<i>Chlorophyta</i> spp. (unidentified)													
<i>Scenedesmus quadricauda</i> Bab.													
CYANOPHYTA													
<i>Anabaena</i> sp.													
<i>Merismopedia diluata</i> Chod.													
EUGLENOPHYTA													
<i>Eutreptia lanowii</i> Steur.													
<i>Eutreptia</i> sp.													
DINOPHYTA													
<i>Amplex catenata</i> (Levander) Meunier													
<i>Amphidinium</i> sp.													
<i>Glenodinium</i> sp.													
<i>Goniolax inaeantha</i> Joerg.													
<i>Gyrodinium pelliculatum</i> (Wulff) Schiller													
<i>G. sinoue</i> (Schuett) Kofoid et Swezy								0,19					
<i>Gymnodinium</i> sp.													
<i>Prorocentrum micans</i> Ehr.													
<i>Prorocentrum granii</i> (Ostenfeld) Balech													
<i>P. breve</i> (Paulsen) Balech													
<i>P. pyriforme</i> (Paulsen) Balech													
<i>P. pallidum</i> (Ostenfeld) Balech													
<i>P. pelliculatum</i> Bergh													
<i>P. brevipes</i> (Paulsen) Balech													
<i>P. curvipes</i> (Ostenfeld) Balech													
<i>P. thorianum</i> (Paulsen) Balech													
CHRYSOPHYTA													
<i>Chrysophyta</i> spp. (unidentified)													
<i>Ehria imparita</i> (Schumann) Lemm.													
<i>Dinobryon balticum</i> (Schuett) Lemm.													
Total biomass (mca/l)		201,76	14,06	74,07	338,77	842,23							

Table 5-1: (continued).

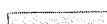



Taxa	Station No. Depth, m	St. 35 32	St. 37 0	St. 38 0	St. 39 0	Taxa	Station No. Depth, m	St. 35 32	St. 37 0	St. 38 0	St. 39 0
<i>Asterionella bleackleyi</i> (W. Smith)						<i>Chaetoceros wighamii</i> Grunow					
<i>A. gracilis</i> (Zsolt)						<i>C. curvisetus</i> Cleve		4.82		3.62	
<i>Thalassiosira baltica</i> (Grunow) (Z. Utermöhl) Gran						<i>C. mitra</i> (Bailey) Cleve					
<i>T. gravida</i> Cleve			0.10	0.15		<i>C. similis</i> Cleve					
<i>T. nordenskiöldii</i> Cleve			593.68	1711.20	2304.9	<i>Chaetoceros</i> sp.		7.20	10.80	2.40	3.60
<i>T. antarctica</i> Comber			3.57			<i>Synechococcus</i> sp.					
<i>T. hyalina</i> (Grunow) Gran		4.28	937.32	1322.52	796.08	<i>Taxodiella transsibirica</i> (Yurkavich) Kuehltz					
<i>T. bioculata</i> (Grunow) Oesterfeld			22.13	115.45		CHLOROPHYTA					
<i>T. fallax</i> Meunier						<i>Ankistrodesmus convolutus</i> Coroa					
<i>Thalassiosira nitidissima</i> Grunow						<i>Rhizoclonium</i> sp.					
<i>Fragilaria capucina</i> Desm.			0.72	0.17	0.88	<i>Chlorophyta</i> spp. (unidentified)		0.53			
<i>F. globularis</i> Krifton						<i>Scenedesmus quadricauda</i> Ereb.					
<i>F. cylindrus</i> Grunow						CYANOPHYTA					
<i>Fragilaria</i> sp.						<i>Anabaena</i> sp.					
<i>Navicula vanthoeffemii</i> Gran			5.21	1.79	1.95	<i>Merismopedia alauca</i> Chod.					
<i>Navicula</i> sp.					1.30	EUGLENOPHYTA					
<i>Nitzschia grunowii</i> Hasle			7.30	9.96	9.40	<i>Eutreptia lanowii</i> Steur					
<i>N. longissima</i> (Ereb.) Ralfs			0.18	0.65	0.12	<i>Eutreptia</i> sp.					
<i>N. closterium</i> W. Smith			0.06	0.07	0.16	DINOPHYTA					
<i>N. serjata</i> Cleve			33.93	43.55	18.23	<i>Amilax catenata</i> (Lewander) Meunier		19.83	71.41	34.38	
<i>N. arctica</i> Cleve					1.28	<i>Amphidinium</i> sp.					
<i>N. acicularis</i> W. Smith						<i>Goniolax triacantha</i> Joerg.		0.60		1.20	
Pennatophyceae spp. (unidentified)						<i>G. pinque</i> (Schuett) Kotabid et Swezy		0.44	0.11	0.65	
<i>Gyrodinium</i> sp.						<i>Gyrodinium pellucidum</i> (Wulff) Schiller					
<i>Melosira granulata</i> (Ehr.) Ralfs						<i>Gymnodinium</i> sp.					
<i>M. moultonensis</i> (O. F. Mellen) Ag.						<i>Prorocentrum micans</i> Ehr.					
<i>M. mundulocis</i> (Dillix) Ag.						<i>Prorocentrum granii</i> (Osterfeld) Balech		3.76	23.47	16.90	7.51
<i>M. varians</i> Ag.			9.00			<i>P. breve</i> (Pausen) Balech					
<i>M. turpensis</i> Ag.			103.77	127.35		<i>P. pyriforme</i> (Pausen) Balech					
<i>M. dubia</i> Kuehltz						<i>P. pallidum</i> (Osterfeld) Balech					
<i>Porosira glacialis</i> (Grunow) Joerg.			12.66	11.91	14.89	<i>P. pellucidum</i> Balech		1.25	8.72	2.49	3.32
<i>Cyclotella</i> sp.			2.48			<i>P. brevipes</i> (Pausen) Balech					
<i>Coscinodiscus</i> sp.			0.99			<i>P. curvipes</i> (Pausen) Balech					
<i>Chaetoceros fragilis</i> Meunier			0.66	0.99	1.19	<i>P. thotianum</i> (Pausen) Balech					
<i>C. teres</i> Cleve						CHRYSOPHYTA					
<i>C. diadema</i> (Ehr.) Gran					3.67	<i>Chrysophyta</i> spp. (unidentified)				1.81	
<i>C. socialis</i> Laufer					5.71	<i>Ebria tripartita</i> (Schumann) Lemm.		0.34	0.11	1.34	1.79
<i>C. debilis</i> Cleve						<i>Dinobryon balticum</i> (Schuett) Lemm.		0.10	0.11	0.45	
<i>C. septentrionalis</i> Oestrup			0.25	0.41		Total biomass (mca/l)	8.41	1743.00	3300.00	3366.84	1529.50

Table 5-1: (continued).

Taxa	Station No.	St. 19 - bis*	Taxa	Station No.	St. 19 - bis*	Taxa	Station No.	St. 19 - bis*
	Depth, m	0		Depth, m	0		Depth, m	0
BACILLARIOPHYTA			BACILLARIOPHYTA			CYANOPHYTA		
<i>Asterionella bleakeyi</i> <i>W. Smith</i>						<i>Merismopedia clauca</i> <i>Chod.</i>		
<i>A. formosa</i> <i>Hassal</i>		1002,64	<i>M. varians</i> <i>Ag.</i>		2785,04	EUGLENOPHYTA		
<i>Thalassiosira baltica</i> <i>Grunow f. Joerg.</i> <i>Gran</i>		43,64	<i>M. rubra</i> <i>Ag.</i>			<i>Eutreptia lanowii</i> <i>Steur</i>		
<i>T. gravida</i> <i>Cleve</i>			<i>M. dubia</i> <i>Kütz.</i>			<i>Eutreptia</i> sp.		
<i>T. nordenskiöldii</i> <i>Cleve</i>			<i>Porosira glacialis</i> <i>(Grunow) Joerg.</i>		4,63	DINOPHYTA		
<i>T. antarctica</i> <i>Comber</i>			<i>Cyclotella</i> sp.			<i>Amylax catenata</i> <i>(Levander) Meunier</i>		
<i>T. hyalina</i> <i>(Grunow) Gran</i>			<i>Coscinodiscus</i> sp.			<i>Amphidinium</i> sp.		
<i>T. bioculata</i> <i>(Grunow) Ostenfeld</i>			<i>Chaetoceros fragilis</i> <i>Meunier</i>			<i>Glenodinium</i> sp.		
<i>T. fallax</i> <i>Meunier</i>			<i>C. teres</i> <i>Cleve</i>			<i>Goniaulax triacantha</i> <i>Joerg.</i>		
<i>Thalassiosira</i> sp.			<i>C. diadema</i> <i>(Ehr.) Gran</i>			<i>Gyrodinium pellucidum</i> <i>(Wulff) Schiller</i>		
<i>Thalassionema nitzschioides</i> <i>Grunow</i>			<i>C. socialis</i> <i>Lauder</i>			<i>G. pingue</i> <i>(Schuett) Kofoid et Swezy</i>		
<i>Fragilaria capucina</i> <i>Desm.</i>			<i>C. debilis</i> <i>Cleve</i>			<i>Gymnodinium</i> sp.		
<i>F. crotonensis</i> <i>Kitton</i>			<i>C. septentrionalis</i> <i>Oestrup</i>			<i>Prorocentrum micans</i> <i>Ehr.</i>		
<i>F. cylindrus</i> <i>Grunow</i>			<i>Chaetoceros wighamii</i> <i>Brightw.</i>			<i>Protoperidinium granii</i> <i>(Ostenfeld) Balech</i>		
<i>Fragilaria</i> sp.		0,70	<i>C. curvisetus</i> <i>Cleve</i>			<i>P. breve</i> <i>(Paulsen) Balech</i>		
<i>Navicula vanhoefenii</i> <i>Gran</i>			<i>C. mitra</i> <i>(Bailey) Cleve</i>			<i>P. pyriforme</i> <i>(Paulsen) Balech</i>		
<i>Navicula</i> sp.			<i>C. similis</i> <i>Cleve</i>			<i>P. pallidum</i> <i>(Ostenfeld) Balech</i>		
<i>Nitzschia grunowii</i> <i>Hasle</i>			<i>Chaetoceros</i> sp.			<i>P. pellucidum</i> <i>Borgh</i>		
<i>N. longissima</i> <i>(Breb.) Ralfs</i>			<i>Synechra</i> sp.		0,13	<i>P. brevipes</i> <i>(Paulsen) Balech</i>		
<i>N. closterium</i> <i>W. Smith</i>		0,01	<i>Tabellaria tenostata</i> <i>(Lanbyae) Kütz.</i>			<i>P. curvipes</i> <i>(Ostenfeld) Balech</i>		
<i>N. seriata</i> <i>Cleve</i>			CHLOROPHYTA			<i>P. thorianum</i> <i>(Paulsen) Balech</i>		
<i>N. arctica</i> <i>Cleve</i>			<i>Ankistrodesmus convolutus</i> <i>Corda</i>			CHRYSOPHYTA		
<i>N. acicularis</i> <i>W. Smith</i>		0,16	<i>Rhizoclonium</i> sp.		826,18	Chrysophyta spp. (unidentified)		
<i>Pennatophyceae</i> spp. (unidentified)			<i>Chlorophyta</i> spp. (unidentified)			<i>Ebria tripartita</i> <i>(Schumann) Lemm.</i>		
<i>Gvrosioma</i> sp.			<i>Scenedesmus quadricauda</i> <i>Breb.</i>			<i>Dinobryon balticum</i> <i>(Schuett) Lemm.</i>		
<i>Melosira granulata</i> <i>(Ehr.) Ralfs</i>		16372,80	CYANOPHYTA			Total biomass (mca/l)		
<i>M. moniliformis</i> <i>(O.F. Müller) Ag.</i>		677,57	<i>Anabaena</i> sp.					21713,50

* St. 19 - bis - station with a salinity minimum, taken from the vessel under way .

Shaded are:

-  marine forms
-  estuarine forms
-  freshwater forms
-  forms with unclear origin

5.2 The taxonomic and ecological descriptions of the phytoplankton assemblages from the Yenisei Bay and adjacent waters of the Kara Sea in September 2000

Larionov V.V. and Makarevich P.R.

Murmanask Marine Biological Institute MMBI, Murmansk, Russia

The phytoplankton study carried out in 2000, compared to 1999, surveyed a much wider area of the Kara Sea, including the mouth region of the Yenisei River in the south, and the marginal ice-edge zone in the north. However, in the Ob Bay only one station was sampled at which sampling was conducted under the conditions of intense storm-driven mixing from the surface to bottom. Therefore, this station has been omitted from further consideration.

The methods of sampling and sample treatment were described in Chapter 5.1. A total of 62 samples from 27 stations were collected. The taxonomic composition and biomass of the phytoplankton are presented in Table 5-2.

Our results have shown that the distributional patterns of the qualitative and quantitative parameters of the phytoplankton in the study area in 2000 differed drastically from those observed in 1999. This is true first of all for the taxonomic composition of the microalgal assemblages both in the whole study area and separately at different stations. The species number recorded in 2000 was 1.5 times higher than that in 1999 largely because of richer assortments of two algal groups. One of them was Dinophyceae, and their more richer diversity was apparently due to seasonally later sampling. This group consisting of a number of mixotrophic and heterotrophic forms, is a major component of the summer phytoplankton assemblages in the Arctic seas. In 2000, the sampling program was carried out two months later which allowed to study a summer stage of the phytoplankton seasonal succession in the area of interest. There are numerous diatoms from the genus *Chaetoceros*, most of which belonging to the late-spring and early-summer forms.

The second assemblage consisted of the representatives of two classes which were of freshwater origin, namely chlorophyceans and cyanophyceans. At the mouth of the Yenisei River, in the Yenisei Bay and in some adjacent coastal areas there was an assemblage represented almost exclusively by freshwater species, and the main contribution to the total phytoplankton biomass was due to the diatoms *Melosira granulata* (similarly to the Ob Bay in 1999), and, to a lesser extent, *M. varians*, *Asterionella formosa* and *Fragilaria crotonensis*. However, a co-dominance of a number of the species belonging to the above two algal groups was observed. Some of them, such as, i.g., *Rhizoclonium* sp. (Chlorophyceae) and *Aphanizomenon flos-aquae* (Cyanophyceae), sometimes accounted for a great percentage of the total biomass.

In this area, this diversity, however, did not influence the integral quantitative parameters of the phytoplankton. The recorded biomass values only rarely reached 1 to 2 mg liter⁻¹, and only at one station (st. 17) values higher than 4.5 mg liter⁻¹ (at 17 m) and higher than 9.5 mg liter⁻¹ (at 18 m) were recorded.

The distributional boundary of this freshwater assemblage during the study period is at about 73°00' N latitude. Station 23, located 30' to the north, was characterized by a typical marine phytoplankton assemblage populating the surface layer, and only in deeper water there were freshwater species. At station 24, another half of a degree to the north, exclusively populations of marine forms were found all over the water column, and only at the near-bottom layer *Melosira granulata* was encountered. It is interesting that the further a given station was off the mouth region of the Yenisei Bay, the deeper became the localization of the freshwater species. Obviously, some kind of "expansion" of marine pelagic algae took place in the surface layer in the study area.

The open shelf water area situated to the north and north-east from the above region is dominated by the above-mentioned summer assemblage. Here, the composition of the phytoplankton was predominated by numerous dinoflagellates and diatoms *Chaetoceros* spp. The algal populations were distributed rather uniformly in either horizontal or vertical directions.

Stations 7, 8, 9, and 35, located at the marginal ice-edge zone, differed drastically from the rest of the study area. The bulk of the biomass was formed by two diatom species, early-spring *Nitzschia grunowii* and late-spring *Chaetoceros socialis*; the population maxima were recorded at the pycnocline. Their presence evidenced the formation of a typical spring bloom, which in this region, ice-free for a very short season, is more "compressed" in time and is characterized by lower cell numbers and biomass and by a tendency for a "migration" to the south, in the direction of the estuarine zone.

Simultaneously, the intense development of freshwater microalgae took place in the Yenisei Bay and adjacent coastal waters, with a time lag of about two weeks compared to the Ob Bay near-mouth region. The assemblage was characterized by the high taxonomic diversity and consisted largely of *Melosira* spp., with the chlorophytes and cyanophytes as co-dominant components. However, the overall phytoplankton biomass was more than an order of magnitude lower than that in the Ob Bay and adjacent coastal areas of the Kara Sea.

Table 5-2:
The taxonomic composition and biomass (mcg/l) of the phytoplankton community in the Ob and the Enisei estuaries and the adjacent waters in September 2000.

Taxa	St.1	St.2	St.3	St.4	St.5	St.7	St.8	St.9
Station No.	0	12	44	0	0	0	0	0
Depth, m								
BACILLARIOPHYTA								
<i>Asterionella bisatolevi</i> W.Smith								
<i>Asterionella Hassali</i>								
<i>Tetulia Menziesii</i>								
<i>T. gravida</i> Cleve	15.72							
<i>T. nordenskioldii</i> Cleve	2.38					3.20	4.66	6.98
<i>T. antarctica</i> Comber						1.29	1.82	2.21
<i>T. hvalina</i> (Grunow) Gran								
<i>T. anguste-lineata</i> (A.Schmidt) Fryxell et Grunow	7.51					2.29	4.59	
<i>Thalassiosira</i> sp.								
<i>Thalassionema nitzschioides</i> Grunow				0.28	0.22	0.11		
<i>Thalassiothrix longissima</i> Cleve et Grunow						2.01	2.76	1.76
Fragilariaceae Kirton								
<i>Fragilaria</i> sp.						0.54		
<i>Navicula vanhoefenii</i> Gran								
<i>N. granii</i> (Joerg.) Gran	6.30					0.28	0.59	0.22
<i>Navicula</i> sp.		0.03						
<i>Nitzschia grunowii</i> Hasle								
<i>N. longissima</i> (Grab.) Falis			0.11					
<i>N. serrata</i> Cleve	0.05	0.03	0.01	0.04	0.02	0.01	16.08	27.62
<i>N. aciculata</i> W.Smith							0.36	0.06
<i>N. closterium</i> W.Smith							1.11	0.21
<i>Eukampia groenlandica</i> Cleve							0.02	
<i>E. zodiakus</i> Ehr.				0.58	2.31	0.87		0.01
Pennatophyceae spp. (unidentified)								
<i>Pleurosigma elongatum</i> W.Smith		0.07	0.19				0.25	0.07
<i>Pleurosigma</i> sp.								
<i>Melosira granulata</i> (Ehr.) Falis	2.27		2.27				2.50	2.27
<i>M. arctica</i> (Ehr.) Dieke								
Chaetocerales AP								
<i>Cyclotella</i> sp.		0.33						0.40
<i>Coccinodiscus oculus-iridis</i> Ehr.								
<i>Chaetoceros fragilis</i> Meunier								2.05
<i>C. diadema</i> (Ehr.) Gran								
<i>C. socialis</i> Lauder								
<i>C. radians</i> Schuett								
<i>C. brevis</i> Schuett				0.59				
<i>C. turcellatus</i> Bailey								
<i>C. debilis</i> Cleve							0.79	38.48
<i>C. subtilis</i> Cleve	0.16			0.11			0.38	1.00
<i>C. gracilis</i> Schuett								0.16

Station No.	Taxa								
	St.1	St.2	St.3	St.4	St.5	St.7	St.8		
Depth, m	0	12	44	0	12	11	0	0	9
<i>Chaetoceros decipiens</i> Clave	4.52	6.28	3.77	8.29	9.04	3.52	3.52	1.38	4.40
<i>C. concavicornis</i> Mangin				3.62	1.81				4.40
<i>C. lachniscus</i> Schuett				0.49	0.40	1.05			1.05
<i>C. compressus</i> Laufer									
<i>C. mitra</i> (Bailey) Clave									
<i>C. similis</i> Clave									
<i>Chaetoceros</i> sp.									
<i>Synedra</i> sp.									
<i>Tabellaria tenastrata</i> (Lyngbøe) Kuetz									
<i>Tabellaria hockjocosa</i> (Roth) Kuetz									
<i>Diatoma elongatum</i> (Lyngbøe) Ag.									
CHLOROPHYTA									
<i>Ankistrodesmus convolutus</i> Gorda									
<i>A. falcatus</i> Rafn									
<i>Achnanthes rapidioides</i> Brunth.									
<i>A. hantzschii</i> Lagern.									
<i>Rhizoclonium</i> sp.									
<i>Chlorophyta</i> spp. (unidentified)									
<i>Golenkina radiata</i> Naeg.									
<i>Spaenodesmus quadricauda</i> Breb.									
<i>S. acuminatus</i> (Lagerh.) Chod.									
<i>Pediastrum duplex</i> Meyen									
<i>P. clathratum</i> Lemm.									
<i>Pediastrum</i> sp.									
<i>Diclitrix</i> sp.									
CYNOPHYTA									
<i>Aphanizomenon flos-aquae</i> (L.) Ralfs									
<i>Anabaena</i> sp.									
<i>Mentzopedia glauca</i> Chod.									
<i>Mentzopedia</i> sp.									
<i>Microcystis aeruginosa</i> Kuetz.									
<i>Nostoc</i> sp.									
<i>Oscillatoria</i> sp.									
EUGLENOPHYTA									
<i>Eutreptia lanowii</i> Steur.									
<i>Euglenophyta</i> spp. (unidentified)									
DINOPHYTA									
<i>Dinophyta</i> spp. (unidentified)	1.80								
<i>Amylax catenata</i> (Levander) Meunier	9.92	3.97	1.98	0.99		3.35	5.00	1.98	0.60
<i>Gonaulax tricaantha</i> Joera	0.40					0.60			

Table 5-2: (continued)

Table 5-2: (continued).

Taxa	Station No.										St. 1 Depth, m		
	St. 1	St. 2	St. 2	St. 3	St. 4	St. 5	St. 7	St. 7	St. 8	St. 8			
	0	0	44	0	0	12	44	0	0	37	0	6	9
DINOPHYTA													
<i>Amphidinium crassum</i> Lohmann	0.11	0.08		0.23	0.23			0.13			0.15		0.11
<i>A. sphenoides</i> Wulff													
<i>Amphidinium</i> sp.													
<i>Dinophysis acuminata</i> Claparède et Lachman				3.05	1.02								
<i>D. arctica</i> Mereschkowsky				0.29	0.29								
<i>D. norvegica</i> Claparède et Lachman				1.27									
<i>Gyrodinium lachnyna</i> (Meunier) Koloid et Swezy	7.78	6.48		3.89	3.89	7.78	7.13	5.18			4.54	7.78	
<i>G. fusiforme</i> Koloid et Swezy		1.91		1.64	3.28	1.64	1.84						
<i>G. nasutum</i> (Wulff) Schiller		0.90		0.77								1.35	
<i>G. prunus</i> (Wulff) Lebour				0.11						0.10			
<i>G. prius</i> (Schuett) Koloid et Swezy					0.53								
<i>G. wulffii</i> Schiller													
<i>Gyrodinium</i> sp.													
<i>Gymnodinium veneticum</i> Ballantine		0.14		0.34	0.24	0.15		0.31			1.35		0.11
<i>Gymnodinium</i> sp.				0.65	0.32	0.54	0.20	1.72			0.50	0.32	
<i>Protoperidinium granii</i> (Ostenfeld) Balech					0.94						1.10	1.88	
<i>P. breve</i> (Paulsen) Balech													
<i>P. pyiforme</i> (Paulsen) Balech		4.20			6.30								
<i>P. mita</i> (Pavillard) Balech		0.63											
<i>P. pellucidum</i> Berg	21.18	16.61		1.25	8.72	4.98	12.46				10.38	1.25	
<i>P. brevipes</i> (Paulsen) Balech	3.47	5.79		0.58	8.68	1.74	1.16	0.58			1.35	0.58	0.68
<i>P. conicoideus</i> (Paulsen) Balech	3.75												
<i>P. curvipes</i> (Ostenfeld) Balech					0.93						0.93		
<i>P. cerasus</i> (Paulsen) Balech													
<i>P. bipes</i> (Paulsen) Balech					0.15					0.27	0.17	0.15	
<i>P. globulum</i> (Stein) Balech													
<i>P. monacanthus</i> (Broch) Balech													
<i>Protoperidinium</i> sp.							1.80			6.00			
<i>Protoperidinium</i> sp.	1.17	0.78											
<i>Scirpsioella trochoidea</i> (Stein) Leeblich III				1.20	0.47								
CRYPTOPHYTA													
<i>Cryptophyta</i> spp. (unidentified)	5.44												0.39
CHRYSOPHYTA													
<i>Chrysochyta</i> spp. (unidentified)													
<i>Ebria tripartita</i> (Schumann) Lemm.	0.34	0.22				0.34					0.62		
<i>Dicyochoa speculum</i> Ehr.	0.04			0.37	0.75								
<i>Dinobryon balticum</i> (Schuett) Lemm.	84.10	55.15	0.43	4.77	48.30	34.81	50.99	27.81	17.72	50.81	84.52	101.42	11.60
Total biomass (mcg/l)													

Table 5-2: (continued).

Taxa	Station No.	St. 8	St. 9	St. 9	St. 9	St. 13	St. 14	St. 15	St. 16	St. 17	
	Depth, m	37	14	44	0	3.5	10	0	15.4	0	
BACILLARIOPHYTA											
<i>Asterionella bleekerei</i> W. Smith											
<i>A. formosa</i> Hassall											
<i>A. rotula</i> Weidner											
<i>T. gravida</i> Cleve	3.20										
<i>T. nordenskiöldii</i> Cleve	3.34		4.43								
<i>T. antarctica</i> Comber			4.60								
<i>T. hyalina</i> (Grunow) Gran			5.00		2.73	0.08	0.14	0.12	0.17	1.73	0.69
<i>T. angustilineata</i> (A. Schmidt) Fryxell et Hasle					2.29	2.73	3.54				0.27
<i>Thalassiosira</i> sp.					0.73						28.15
<i>Thalassionema nitzschoides</i> Grunow											
<i>Thalassiothrix longissima</i> Cleve et Grunow			25.85				1.51			0.23	0.55
<i>Thalassiothrix longissima</i> Cleve et Grunow										0.44	8.78
<i>Thalassiothrix longissima</i> Cleve et Grunow										0.70	28.62
<i>Thalassiothrix longissima</i> Cleve et Grunow										0.70	
<i>Fragilaria</i> sp.			0.66				0.31				
<i>Navicula vanhoefenii</i> Gran											1.63
<i>N. granii</i> (Joerg.) Gran											
<i>Navicula</i> sp.											
<i>Nitzschia grunowii</i> Hasle	0.48	30.90	163.07	5.16	0.47	0.85	0.24	0.19			
<i>N. ionnissima</i> (Breb.) Fells		0.05	0.05	0.01	0.07	0.05	0.09	0.02			
<i>N. seriata</i> Cleve		0.12	0.79	0.21		0.07					
<i>Nitzschia</i> sp.											
<i>N. aculeata</i> W. Smith					0.01	0.01					0.13
<i>N. closterium</i> W. Smith											
<i>Eukampia groenlandica</i> Cleve											
<i>E. zodiakus</i> Ehr.		1.06									
<i>Pennatophyceae</i> spp. (unidentified)	0.12	0.45	0.18	0.07	0.35	0.11	1.33	1.43	29.45	198.59	2.30
<i>Pennatophyceae</i> spp. (unidentified)			1.95						0.45	0.87	6.02
<i>Pleurosigma</i> sp.											17.28
<i>Pleurosigma</i> sp.											
<i>Melosira granulata</i> (Ehr.) Fells				1.06	16.15	16.15	111.73	31.53	77.32	167.06	687.28
<i>M. arctica</i> (Ehr.) Dickie											1018.8
<i>M. varians</i> A. B.											237.71
<i>Cyclotella</i> sp.											270
<i>Coscinodiscus oculus-iridis</i> Ehr.											270
<i>Chaetoceros fragilis</i> Meunier											2280.1
<i>C. diadema</i> (Ehr.) Gran											2.92
<i>C. socialis</i> Lauder					1.29	0.36	1.68	0.63		1.35	1.80
<i>C. radians</i> Schuett	11.92		1.87							0.56	5.69
<i>C. brevis</i> Schuett			119.13								
<i>C. furcillatus</i> Bailey		1.05									
<i>C. debilis</i> Cleve											
<i>C. subtilis</i> Cleve		0.33			0.38	0.05	0.32				
<i>C. cracilis</i> Schuett											

Table 5-2: (continued).

Taxa	St. 8	St. 9	St. 13	St. 14	St. 15	St. 16	St. 17
Station No. Depth, m	37	14 1.51	0 3.5	0 10	0 6.5	0 15.4	0 23
BACILLARIOPHYTA							
<i>Chaetoceros decipiens</i> Cleve							
<i>C. concavicornis</i> Marain							
<i>C. lachniosis</i> Schuett.							
<i>C. compressus</i> Lauder							
<i>C. mitra</i> (Bailey) Cleve							
<i>C. similis</i> Cleve							
<i>Chaetoceros</i> sp.			0.85		0.75 0.10	3.50	0.10 0.46
<i>Synedra</i> sp.							
<i>Tabellaria fenestrata</i> (Lubbock) Kuetz.							
<i>Tabellaria loxalea</i> (Roth) Kuetz.							
<i>Diatoma elonatum</i> (Lubbock) Aq.							7.22
CHLOROPHYTA							
<i>Ankistrodesmus convolutus</i> Corda							0.03
<i>A. taicatus</i> Ralls				0.02	1.79	0.31	0.11
<i>Acinastrum rhabdoides</i> Brunnth.							0.30
<i>A. hantzschii</i> Lagerh.					2.08	3.30	22.24
<i>Rhizoclonium</i> sp.						1.80	7.17
<i>Chlorophyta</i> spp. (unidentified)							1.20
<i>Golenkinia radiata</i> Naeg.							0.03
<i>Scenedesmus quadricauda</i> Breb.				0.07	0.30	0.77	0.16
<i>S. acuminatus</i> (Lagerh.) Chod.							0.46
<i>Pediastrum duplex</i> Meyer							0.02
<i>Pediastrum</i> sp.						0.07	0.05
<i>Ulothrix</i> sp.							0.01
CYANOPHYTA							
<i>Aphanizomenon flos-aquae</i> (L.) Ralls				0.96	1.81	6.25	13.53
<i>Anabaena</i> sp.						1.24	0.22
<i>Merismopedia lauca</i> Chod.					0.43	0.32	1.25
<i>Merismopedia</i> sp.							0.17
<i>Microcystis aeruginosa</i> Kuetz.							0.18
<i>Nostoc</i> sp.							2.11
<i>Oscillatoria</i> sp.							0.16
EUGLENOPHYTA							
<i>Eutreptia lanowii</i> Steur		0.24	0.27			2.00	
<i>Euglenophyta</i> spp. (unidentified)							
DINOPHYTA							
<i>Dinophyta</i> spp. (unidentified)		2.25					
<i>Amplex catenata</i> (Levander) Meunier		3.64					
<i>Goniaulax inaequalis</i> Jørgen.		1.10					

Table 5-2: (continued).

Taxa	Station No.		St. 8		St. 9		St. 13		St. 14		St. 15		St. 16		St. 17		
	Depth, m		37	0	14	44	0	3,5	10	0	0	6,5	0	15,4	23	0	17
DINOPHYTA																	
<i>Amphidinium crassum</i> Lehmann				0.11													
<i>A. longum</i> Lehmann				0.13													
<i>A. sphenoides</i> Wulff																	
<i>Amphidinium</i> sp.											0.12						
<i>Dinophysis acuminata</i> Claparede et Lachman																	
<i>D. arctica</i> Mieraschikowsky																	
<i>D. norvegica</i> Claparede et Lachman																	
<i>Gyrodinium lachryma</i> (Meunier) Koloid et Swezy				3.89													
<i>G. fusiforme</i> Koloid et Swezy				1.64													
<i>G. nasutum</i> (Wulff) Schiller																	
<i>G. minus</i> (Wulff) Lebour																	
<i>G. pinque</i> (Schuett) Koloid et Swezy																	
<i>G. wulffii</i> Schiller																	
<i>Gyrodinium</i> sp.																	
<i>Gymnodinium veneticum</i> Ballentine				0.09	2.70												
<i>Gymnodinium</i> sp.				0.40	0.10												
<i>Gyrodinium</i> sp.			0.14	0.94			0.11		0.94		0.94						
<i>Proroperidium granii</i> (Ostenfeld) Balech																	
<i>P. breve</i> (Paulsen) Balech																	
<i>P. pyiforme</i> (Paulsen) Balech				2.66													
<i>P. nitida</i> (Pavliard) Balech				8.09													
<i>P. pellucidum</i> Bergt				0.58													
<i>P. brevipes</i> (Paulsen) Balech				0.58													
<i>P. conicoides</i> (Paulsen) Balech																	
<i>P. curvipes</i> (Ostenfeld) Balech																	
<i>P. carasus</i> (Paulsen) Balech				0.96													
<i>P. bipes</i> (Paulsen) Balech				0.27													
<i>P. globulatum</i> (Stein) Balech				15.18													
<i>P. monacanthus</i> (Broch) Balech																	
<i>Proroperidium</i> sp.					4.50												
<i>Scrippsiella trochoidea</i> (Stein) Loeblich III																	
CRYPTOPHYTA																	
<i>Cryptophyta</i> spp. (unidentified)											0.21	0.56					
CHRYSOPHYTA																	
<i>Chrysophyta</i> spp. (unidentified)																	
<i>Ebria tripartita</i> (Schumann) Lemm.				1.23							0.34		0.34				
<i>Ditychia speculum</i> Ehr.																	
<i>Dinobryon balticum</i> (Schuett) Lemm.			0.74	95.19	342.79	6.51	26.65	23.26	115.70	77.61	114.24	392.82	698.19	238.64	1023.3	2383.7	4531.6
Total biomass (mgd/l)																	

Table 5-2: (continued).

Taxa	Station No. 17		Station No. 19		Station No. 22		Station No. 23		Station No. 24		Station No. 26				
	Depth, m	18	0	21.5	4	10	0	11.5	31	0	11.5	32	0	17.6	62
BACILLARIOPHYTA															
<i>Asterionella bleakelevi</i> W. Smith		122.18	48.21	39.84	1.10	0.36	0.24		0.11					0.21	
<i>A. borealis</i> Hassall															
<i>A. rotula</i> Meunier															
<i>A. gravida</i> Cleve							12.22			13.39					
<i>A. nordenskiöldii</i> Cleve							4.16			17.83					
<i>A. antarctica</i> Comber							7.70								
<i>A. hvalina</i> (Grunow) Gran															
<i>A. anguste-lineata</i> (A. Schmidt) Frenzel et Hasle															
<i>Thalassiosira</i> sp.		14.84													
<i>Thalassiosira nitzschoides</i> Grunow															
<i>Thalassiosira longissima</i> Cleve et Grunow															
<i>Fragilaria crotonensis</i> Kitton		47.67	26.84	4.83	0.48					10.29					0.29
<i>Fragilaria</i> sp.															
<i>Navicula vanhoefenii</i> Gran															
<i>Navicula</i> sp.															
<i>Nitzschia grunowii</i> Hasle															
<i>N. longissima</i> (Breb.) Ralls							6.40			0.30					
<i>N. serjata</i> Cleve							0.03			0.06					
<i>N. acicularis</i> W. Smith		0.29					0.12			0.22				0.01	0.02
<i>N. closterium</i> W. Smith				0.16											
<i>Eukampia groenlandica</i> Cleve															
<i>E. zodiakus</i> Ehr.							0.01								
<i>E. zodiakus</i> Ehr.							1.15							0.67	
<i>Pennatophyceae</i> spp. (unidentified)		24.58	9.50	16.80	1.12	8.02	0.78	0.67	0.32	1.44	0.37	0.56	0.78	0.16	0.51
<i>Pleurosigma elongatum</i> W. Smith														1.95	
<i>Pleurosigma</i> sp.															
<i>Melosira granulata</i> (Ehr.) Ralls		9314.3	950.5	1940.5	57.15	352.02	96.72		2.73	14.10			2.65		1.97
<i>M. arctica</i> (Ehr.) Dickie		27.29	23.70	23.02											
<i>M. arctica</i> sp.		17.55	3.50	24.13	0.40										
<i>Cyclotella</i> sp.							0.33			0.43					1.06
<i>Coscinodiscus oculus-iridis</i> Ehr.															
<i>Chaetoceros fragilis</i> Meunier															
<i>C. diadema</i> (Ehr.) Gran								49.63		2.93				1.30	
<i>C. socialis</i> Lauder										36.38					
<i>C. radialis</i> Schuett								0.65							
<i>C. brevis</i> Schuett					0.21										
<i>C. furcellatus</i> Bailey															
<i>C. debilis</i> Cleve								9.86		3.83					
<i>C. subtilis</i> Cleve								0.22		0.16				0.07	0.06
<i>C. gracilis</i> Schuett															

Table 5-2: (continued).

Taxa	Station No.	St. 17	St. 19	St. 22	St. 23	St. 24	St. 26
Depth, m	1.8	0	4	10	11.5	11.5	17.6
BACILLARIOPHYTA							
<i>Chaetoceros decipiens</i> Cleve							6.03
<i>C. concavicornis</i> Mannin							3.01
<i>C. lachnoides</i> Schuett				0.73		1.63	
<i>C. compressus</i> Lauder							
<i>C. mitra</i> (Bailey) Cleve					0.70		
<i>C. similis</i> Cleve			1.00	3.24			0.67
<i>Chaetoceros</i> sp.						1.05	
<i>Synedra</i> sp.							
<i>Tabellaria fenestrata</i> (Lindb.) Grun.	1.38	1.85					
<i>Tabellaria loeblichii</i> (Grun.) Kuetz.	0.83	10.37	1.16				
<i>Diatoma elongatum</i> (Lindb.) Grun.							
CHLOROPHYTA							
<i>Ankistrodesmus convolutus</i> Cora		0.04					
<i>A. falcatus</i> Ralfs	0.03	0.02	0.06	0.03			
<i>Acinastum rachioides</i> Brunnth.		0.19	0.04				
<i>A. hantzschii</i> Lagerh.	0.24	0.20					
<i>Rhizosolium</i> sp.	6.10	3.15	2.13				
<i>Chlorophyta</i> spp. (unidentified)		0.92	0.81	0.14			
<i>Golenkinia raclata</i> Neeg.		0.24	0.12	0.14	0.08		
<i>Scenedesmus quadricauda</i> Brab.	0.07	0.55	0.12				
<i>S. acuminatus</i> (Lagerh.) Chod.		0.02	0.01	0.02			
<i>Pediastrum duplex</i> Meyen							
<i>P. clathratum</i> Lemm.							
<i>Pediastrum</i> sp.	0.02	0.37					
<i>Ulminik</i> sp.							
CYANOPHYTA							
<i>Aphanizomenon flos-aquae</i> (L.) Ralfs	4.59	2.00	32.17				
<i>Anabaena</i> sp.	2.01	0.17	0.97				
<i>Merismopedia clauca</i> Chod.		0.13	0.14				
<i>Merismopedia</i> sp.							
<i>Microcystis aeruginosa</i> Kuetz.							
<i>Nostoc</i> sp.		0.43					
<i>Oscillatoria</i> sp.	0.93						
EUGLENOPHYTA							
<i>Eutreptia lanowii</i> Steur.						0.09	
<i>Euglenophyta</i> spp. (unidentified)							
DINOPHYTA							
<i>Dinophyta</i> spp. (unidentified)							
<i>Amplex catenata</i> (Levander) Meunier							
<i>Goniaulax triacantha</i> Jørg.							

Table 5-2: (continued).

Taxa	Station No.		St. 17		St. 19		St. 22		St. 23		St. 24		St. 26			
	Depth, m		18	0	21.5	0	4	10	11.5	31	0	11.5	32	0	17.6	62
DINOPHYTA																
<i>Amphidinium crassum</i> Lohmann																
<i>A. longum</i> Lohmann																
<i>A. sphaeroides</i> Wulff																
<i>Amphidinium</i> sp.																
<i>Dinophysis acuminata</i> Claparede et Lachman																
<i>D. arctica</i> Mereschkowsky																
<i>D. norvegica</i> Claparede et Lachman																
<i>Gyrodinium lachryma</i> (Meunier) Kofoid et Swezy										3.89				4.54	6.48	
<i>G. tusiforme</i> Kofoid et Swezy															1.37	
<i>G. nasutum</i> (Wulff) Schiller																
<i>G. prunus</i> (Wulff) Lebour																
<i>G. pinque</i> (Schuett) Kofoid et Swezy																
<i>G. wulffii</i> Schiller																
<i>Gyrodinium</i> sp.																
<i>Gymnodinium veneticum</i> Ballantine																
<i>Gymnodinium</i> sp.										0.10						
<i>Protoperdinium granii</i> (Ostenfeld) Balech										0.31						
<i>P. breve</i> (Paulsen) Balech										0.94						
<i>P. pyriforme</i> (Paulsen) Balech										6.90						
<i>P. mite</i> (Paulsen) Balech																
<i>P. pelliculum</i> Berg										0.94						
<i>P. brevipes</i> (Paulsen) Balech										1.25						
<i>P. concolor</i> (Paulsen) Balech										0.58						
<i>P. curvipes</i> (Ostenfeld) Balech																
<i>P. oerbasus</i> (Paulsen) Balech										4.77						
<i>P. bipes</i> (Paulsen) Balech										1.64						
<i>P. globulum</i> (Stein) Balech																
<i>P. monacanthus</i> (Brach) Balech																
<i>Protoperdinium</i> sp.																
<i>Scoppsiella trochiloides</i> (Stein) Loeblich III														0.55	0.20	
CRYPTOPHYTA																
<i>Cryptophyta</i> spp. (unidentified)																
CHRYSOHYTA																
<i>Chrysohyta</i> spp. (unidentified)																
<i>Ebria tripartita</i> (Schumann) Lemm.											0.81					0.28
<i>Dictyocha speculum</i> Ehr.																
<i>Dinobryon balticum</i> (Schuett) Lemm.																
Total biomass (mca/l)	9584.9	1080.9	2088.2	61.01	361.13	105.82	162.95	57.08	16.94	106.90	53.67	11.00	34.12	15.16	9.77	

Table 5-2: (continued).

Taxa	St. 27	St. 28	St. 29	St. 30	St. 31	St. 35	St. 36
Depth, m	0	16	0	26	51	14,5	17,5
BACILLARIOPHYTA							
<i>Asterionella bleakeyi</i> W.Smith							
<i>A. formosa</i> Hassall					6.41		
<i>A. formosa</i> (Hassall) Grunow						5.62	
<i>I. gravida</i> Cleve	0.59			2.45	3.47	13.10	4.66
<i>I. nordenskioeldii</i> Cleve					5.56	3.75	
<i>I. antarctica</i> Comber							
<i>I. hvalina</i> (Grunow) Gran							
<i>T. anguste-lineata</i> (A. Schmidt) Fuxell et Hasle		1.46					
<i>Thalassiosira</i> sp.							
<i>Thalassionema nitzschoides</i> Grunow	0.11	0.06	0.17	0.11			
<i>Thalassiothrix longissima</i> Cleve et Grunow		0.22				3.77	2.26
Fragilaria crotonensis Kirtlan							
<i>Fragilaria</i> sp.							
<i>Navicula vanhoefenii</i> Gran				0.23		0.63	2.57
<i>N. granii</i> (Loefer) Gran							
<i>Navicula</i> sp.		0.06					
<i>Nitzschia grunowii</i> Hasle	0.14	0.30	0.26	13.43	2.88	14.06	56.80
<i>N. longissima</i> (Gréb.) Falis		0.30	0.02	0.03	0.03	0.04	0.01
<i>N. senata</i> Cleve		0.01	0.02	0.10	0.11	0.11	0.05
<i>N. aciculata</i> W.Smith							
<i>N. closterium</i> W.Smith						0.01	
<i>Eukampia groenlandica</i> Cleve	1.15			0.58	0.48		
<i>E. zodiakus</i> Ehr.						0.38	
Pennatulaceae spp. (unidentified)						0.48	
<i>Pleurosigma elongatum</i> W.Smith		0.06	0.30	0.45	1.12	1.44	0.29
<i>Pleurosigma</i> sp.					3.15	0.16	0.32
<i>Melosira grandis</i> (Ehr.) Falis					4.17		
<i>M. arctica</i> (Ehr.) Dickie	3.64				1.74		
<i>M. varians</i> Ag.					0.17		
<i>Cyclotella</i> sp.							
<i>Coscinodiscus oculus-iridis</i> Ehr.							
<i>Chaetoceros fragilis</i> Meunier							
<i>C. diadema</i> (Ehr.) Gran	1.60		1.64		2.75	72.13	9.21
<i>C. socialis</i> Laufer		0.75		13.61	1.57	15.96	3.10
<i>C. radians</i> Schuett				0.35			
<i>C. brevis</i> Schuett							
<i>C. furcellatus</i> Bailey							
<i>C. debilis</i> Cleve							
<i>C. subtilis</i> Cleve		0.13	0.05		0.07		
<i>C. gracilis</i> Schuett		0.03	0.03				

Table 5-2: (continued).

Taxa	Station No.	St. 27		St. 28		St. 29		St. 30		St. 31		St. 35		St. 36		
	Depth, m	0	0	1.6	0	1.7	0	2.6	5.1	0	0	14.5	4.6	0	17.5	6.3
BACILLARIOPHYTA																
<i>Chaetoceros decipiens</i> Cleve		4.52	12.06	21.48	13.19	41.57	7.03	8.16	2.89					7.28	3.52	2.51
<i>C. concavicornis</i> Mangin		1.81	6.33	6.03	9.34	13.11	3.77	2.26		3.62	3.77			5.73	0.60	
<i>C. lacinosus</i> Schuett						0.72										
<i>C. compressus</i> Lauder											1.21					
<i>C. mitra</i> (Bailey) Cleve																
<i>C. similis</i> Cleve																
<i>Chaetoceros</i> sp.			3.60			0.90	2.60	2.00					1.10			
<i>Synedra</i> sp.																
<i>Tabellaria fenestrata</i> (Lynbyae) Kuetz																
<i>Tabellaria flocculosa</i> (Roth) Kuetz																
<i>Diatoma elongatum</i> (Lynbyae) Ag																
CHLOROPHYTA																
<i>Ankistrodesmus convolutus</i> Corda																
<i>A. falcatus</i> Ralfs																
<i>Aotinastrum raphidoides</i> Brunnh.																
<i>A. hantzschii</i> Lagerh.																
<i>Rhizoclonium</i> sp.																
<i>Chlorophyta</i> spp. (unidentified)																
<i>Golenkinia radiata</i> Naeq.																
<i>Scenedesmus quadricauda</i> Breb.																
<i>S. acuminatus</i> (Lagerh.) Chod.																
<i>Pediastrum duplex</i> Meyen																
<i>P. clathratum</i> Lemm.																
<i>Pediastrum</i> sp.																
<i>Ulothrix</i> sp.																
CYANOPHYTA																
<i>Aphanizomenon flos-aquae</i> (L.) Ralfs																
<i>Anabaena</i> sp.																
<i>Merismopedia laevis</i> Chod.																
<i>Merismopedia</i> sp.																
<i>Microcystis aeruginosa</i> Kuetz.																
<i>Nostoc</i> sp.																
<i>Oscillatoria</i> sp.																
EUGLENOPHYTA																
<i>Eutreptia janowii</i> Steur.																
<i>Euglenophyta</i> spp. (unidentified)																
DINOPHYTA																
<i>Dinophyta</i> spp. (unidentified)																
<i>Amylax catenata</i> (Levander) Meunier																
<i>Goniaulax triacantha</i> Joera.																

60

Table 5-2: (continued).

Taxa	Station No. Depth, m	St. 38 0	St. 40 0	Taxa	Station No. Depth, m	St. 38 0	St. 40 0	Taxa	Station No. Depth, m	St. 38 0	St. 40 0
BACILLARIOPHYTA				BACILLARIOPHYTA				DINOPHYTA			
<i>Asterionella bleakeri</i> W. Smith				<i>Chaetoceros desibians</i> Cleve				<i>Amplex catenata</i> (Levander) Meunier			
<i>A. funicosa</i> Hassall				<i>C. subtilis</i> Cleve				<i>Goniolax trifacantha</i> Joerg.			
<i>T. rotula</i> Meunier				<i>C. concavicornis</i> Martin				<i>Amphidinium crassum</i> Lohmann			
<i>T. gravida</i> Cleve				<i>C. laciniosus</i> Schuetz				<i>A. longum</i> Lohmann			
<i>T. nordenskioldii</i> Cleve				<i>C. compressus</i> Lauder				<i>A. sphenoides</i> Wulff			
<i>T. antarctica</i> Comber				<i>C. mitra</i> (Bailey) Cleve				<i>Amphidinium</i> sp.			
<i>T. inyalina</i> (Grunow) Gran				<i>C. similis</i> Cleve				<i>Dinophysis acuminata</i> Claparede et Lachman			
<i>T. anguste-lineata</i> (A. Schmidt) Fryxell et Hasle				<i>Chaetoceros</i> sp.				<i>D. arctica</i> Mereschkowsky			
<i>Thalassiosira</i> sp.				<i>Synedra</i> sp.				<i>D. novaejica</i> Claparede et Lachman			
<i>Thalassiosira nitzschoides</i> Grunow				<i>Tabellaria lanceolata</i> (Lubbock) Kuetz				<i>Gyrodinium lechma</i> (Meunier) Kobid et Swezy			
<i>Thalassiosira longissima</i> Cleve et Grunow				<i>Tabellaria loricata</i> (Lubbock) Kuetz				<i>G. lusitane</i> Kobid et Swezy			
<i>Thalassiosira etionensis</i> Kifer				<i>Diadema elongatum</i> (Lubbock) Ag.				<i>G. nasutum</i> (Wulff) Schiller			
<i>Fraxillaria</i> sp.				CHLOROPHYTA				<i>G. pinque</i> (Schuetz) Kobid et Swezy			
<i>Navicula vanhoefeni</i> Gran				<i>Ankistrodesmus convolvulus</i> Corda				<i>G. wulffii</i> Schiller			
<i>N. granii</i> (Joerg.) Gran			0.21	<i>A. falcatus</i> Ralls				<i>Gyrodinium</i> sp.			
<i>Navicula</i> sp.				<i>Actinastrum radioloides</i> Burmth.				<i>Gymnodinium</i> sp.			
<i>Nitzschia grunowii</i> Hasle				<i>A. hantzschii</i> Lagerh.				<i>Gymnodinium veneticum</i> Ballantine			
<i>N. longissima</i> (Breb.) Ralls			0.02	<i>Rhizosolenium</i> sp.				<i>Protoperidinium granii</i> (Ostenfeld) Balech			
<i>N. seriata</i> Cleve				<i>Chlorophyta</i> spp. (unidentified)				<i>P. breve</i> (Paulsen) Balech			
NAUCLEIUS				<i>Colerkinia radata</i> Nasc.				<i>P. pyriforme</i> (Paulsen) Balech			
<i>N. aciculatus</i> W. Smith				<i>Solenodesmus quadricauda</i> Breb.				<i>P. mita</i> (Pavillard) Balech			
<i>N. closterum</i> W. Smith				<i>S. acuminatus</i> (Lagerh.) Chod.				<i>P. pelliculatum</i> Bergh			
<i>Eukampia groenlandica</i> Cleve				<i>Pediastrum duplex</i> Meyen				<i>P. brevipes</i> (Paulsen) Balech			
<i>E. zodiacus</i> Ehr.			0.16	<i>P. clathratum</i> Lemm.			0.11	<i>P. contoides</i> (Paulsen) Balech			
<i>Pennatophyceae</i> spp. (unidentified)			0.03	<i>Pediastrum</i> sp.				<i>P. curvipes</i> (Ostenfeld) Balech			
<i>Pleurosigma elongatum</i> W. Smith				<i>Ulothrix</i> sp.				<i>P. carasus</i> (Paulsen) Balech			
<i>Pleurosigma</i> sp.				CYANOPHYTA				<i>P. bipes</i> (Paulsen) Balech			
<i>Melosira granulata</i> (Ehr.) Ralls			29.79	<i>Alphanomenon flos-aquae</i> (L.) Ralls			515.44	<i>P. globulum</i> (Stein) Balech			
<i>M. arctica</i> (Ehr.) Dickie				<i>Alabaena</i> sp.				<i>P. moracanthus</i> (Brecht) Balech			
<i>M. setiensis</i> Ag.				<i>Mensoplecta diauca</i> Chod.				<i>Protoperidinium</i> sp.			
<i>Cyclotella</i> sp.				<i>Mensoplecta</i> sp.				<i>Scrippsiella trochoidea</i> (Stein) Loeblich III			
<i>Coscinodiscus oculus-iridis</i> Ehr.			0.17	<i>Microcystis aeruginosa</i> Kuetz.				<i>Dinophyta</i> spp. (unidentified)			
<i>Chaetoceros fragilis</i> Meunier			0.43	<i>Nastoe</i> sp.				CHRYSOPHYTA			
<i>C. diadema</i> (Ehr.) Gran				<i>Oscillatoria</i> sp.				<i>Chrysophyta</i> spp. (unidentified)			
<i>C. socialis</i> Lauder				EUGLENOPHYTA				<i>Ebria tripartita</i> (Schumann) Lemm.			
<i>C. radians</i> Schuetz				<i>Eutreptia lanowii</i> Steur.				<i>Dictyocha speculum</i> Ehr.			
<i>C. brevis</i> Schuetz				<i>Euglenophyta</i> spp. (unidentified)				<i>Dinobryon balticum</i> (Schuetz) Lemm.			
<i>C. furcellatus</i> Bailey				CRYPTOPHYTA				Total biomass (mca/l)	30.14	516.22	
<i>C. debilis</i> Cleve				<i>Cryptophyta</i> spp. (unidentified)							
<i>C. gracilis</i> Schuetz											

Destinations as in Table 5-1

5.3 The role of zooplankton for the turn-over of organic matter in the Kara Sea - First results and basic facts

I. Suck

Alfred Wegener Institute for Polar and Marine Research, Bremerhaven, Germany

Introduction

The Kara Sea is strongly influenced by the freshwater input of the two large Siberian rivers Yenisei and Ob (Gordeev et al 1996). On one hand this leads to a stratification of the water column, and on the other hand it results in a high input of riverborn organic matter, mainly detritus and particulate carbon (Lisitzin 1995). Until now, little is known on how zooplankton, especially copepods, may function as "pelagic pumps" enhancing the sedimentation rate of the imported carbon. During the Arctic winter copepods as well as other organisms are faced with an extreme situation concerning light and thus food regime. Some species normally feeding on algae, may overcome these problems by producing resting eggs which may sink to the bottom and overwinter close to or even in the sediment.

Objectives

The knowledge of the distribution of the zooplankton communities, i. e. abundances and biomass, is essential for further evaluation of carbon utilization and the estimation of the transport of the organic matter from surface waters to the benthos (benthic-pelagic coupling). Therefore, one of the emphases of this cruise was put on quantitative sampling to get a *status quo* of the distribution pattern of the zooplankton in the Kara Sea with special regard to the hydrography which is strongly influenced by the freshwater input.

Further samples were taken in order to select single animals for dry weight and C/N analyses necessary for biomass estimations. Samples for stable isotope analyses incl. faecal pellet examination were taken as zooplankton feeds selectively on certain sources. Such analyses may help to estimate the significance of biological processes for the turn-over of organic and inorganic matter. Experiments on egg-production and faecal-pellet-production were conducted to investigate the possible energy exploitation with regard to reproduction and food, as well as the maturity stage of the females. In order to find out whether resting eggs of certain species exist, sediment and near bottom water samples were taken.

Material and Methods

Zooplankton

During the "Akademik Boris Petrov" Cruise 2000 plankton samples were taken at 20 stations (Table 5-3) using a Nansen closing net (mesh size 150µm). The nets were towed vertically with a velocity of about 0.5 ms⁻².

In order to get a detailed picture of the distribution of the species composition with respect to the stratification of the water column, sample depths were chosen according to the a priori gathered CTD data for mainly salinity and also temperature. The first net was taken from the bottom to the lower border of the pycnocline (if present) or the lower border of the mixed water body between the low-saline surface waters and the higher-saline bottom waters, respectively. The second sampling depth was chosen in that way that only the low-saline surface water mass was sampled, excluding the pycnocline. In order to get a full picture of the species composition a complete haul from bottom to surface was performed. The obtained quantitative samples were fixated in 4% buffered formalin solution and will be identified to species and stage level at the Shirshov Institute (Moscow) and at the AWI (Bremerhaven)

Additional nets for zooplankton were taken, mainly below the pycnocline, in order to get living animals for further investigation (genetic analysis, dry weight, C/N analyses) at the home institute. and experiments (egg- and faecal pellet production) onboard. Until the start of the investigation or experiments, these animals were kept in large beakers in the in-situ water and were incubated in a 4°C refrigerator.

Multiple Corers

In order to test whether resting eggs are produced by copepods in the investigated area - these eggs are either found in surface sediments or in the water layer near the bottom - Multiple Corer (MUC) surface samples (approx. 0-5 cm) were taken at 14 stations. Depending on the number of the MUCs employed at each station 2*3 or 1*3 cores were sampled. In addition the bottom water was sieved through a 50 µm net, and the thus acquired material was fixated, as the sediment samples, in 4% buffered formalin solution. At two stations where no MUC samples were taken, sediment surface and water samples were taken from the Giant Box Corer. All of these samples will also be used for meroplankton studies, and will be examined in the home laboratory.

Egg-/faecal pellet production

This standard experiment in copepod research to gather information about the animals food exploitation and energy utilisation, was performed with animals from 5 stations (Table 5-3). Animals of sts 05 and 07 were placed individually in Cell Wells® using in-situ water, and checked every six hours for 24 hours for eggs (and faecal pellets). Whereas for sts 05 and 07 in-situ water was used females of station 28 were kept in filtered seawater (32.3 psu) (individually kept in Cell Wells®). Females of sts 30 and 36 were kept in filtrated sea-water (32.3 psu) in a small beaker containing a net insertion (300 µm mesh size) and checked for eggs and faecal pellets after 26 (sta.30) and 24 hours (sta.36), respectively.

Dry weight, C/N and stable isotope analyses

To obtain dry weight values of certain species with special emphasis on female *Calanus glacialis*, individual adult animals were selected, put into pre-weighted Aluminium Caps and deep frozen immediately. The stations were selected in order to obtain dry weight values along a transect from the river estuary to the open southern Kara Sea. In addition to the *Calanus glacialis* females, adult specimens of several other species were frozen as well. Animals selected for later C/N and stable isotope analyses were placed into silvercaps and deep frozen afterwards. In this case several specimens of the dominant species were chosen regardless of station. The different analyses will be carried out in the home laboratory.

Preliminary Results

In comparison to last years' data the freshwater influence seems to have been much lower. One hint is that the salinity which is, apart from the river stations, high at the bottom and in general high at the surface as well with around 20 psu. This situation may be due to more frequent storms during the summer resulting in an extensive mixing of the water column and thus in a lack of a sharp halocline. Instead, at most stations a large salinity transition zone could be detected. Two of the zooplankton stations (sts 17 and 19) were true river stations whereas at sta. 15 the salinity was a little higher (6.7-7.3 psu). At sta. 16 the bottom salinity was even higher (20.1 psu) although this station was situated further south than sta. 15. It will be interesting to see whether brackish or even marine species are able to live in this high-saline residue water lens.

Distribution

In general, Copepoda clearly dominated the planctonic community as expected. The northern part of the sampling area was characterised by a high abundance of truly marine species such as *Calanus glacialis*, *Pseudocalanus* spp. and *Microcalanus* spp. whereas the southern area was dominated by brackish species such as *Drepanopus bungei* (Brodskii 1967; Dussard and Defay 1995), *Jaschnovia tolli* (Markhaseva 1996) and *Limnocalanus macrurus* (Sars 1903; Brodskii 1967), even though compared with last year's results the abundance of *L. macrurus* was much lower (Fetzer and Arndt 2000). The area in between the two mentioned ones may be divided into an eastern part which is characterised by a more brackish water community, and a western part which is dominated by marine species. In general, the abundance of adults of any species was rather low, with slightly higher portion of adults (e.g. of *Calanus glacialis*) in the north, mainly females. In addition numerous Chaetognatha were found at all stations along with some Hydromedusae. Meroplankton, especially ophioplutei, other Echinodermata and Mollusca, showed high abundances at the northernmost stations (e.g. sta.28) which corresponds with the high abundance of adult Ophiuroidea found at this station.

Calanus glacialis females were mainly found at stations in the northern Kara Sea, namely sts 02, 05, 08, 28 and 35, suggesting that adults of this species are to be found in higher latitudes of the Kara Sea at this time of the year or in general, whereas all other catches from stations close to the Yenisei estuary were dominated by copepodite stages. *C. glacialis* males were very rarely found.

During the five combined egg-production and faecal-pellet-production experiments none of the females produced any eggs nor faecal pellets. This corresponds in part with the results of the former Kara Sea Cruises in 1997, when no eggs but some faecal pellets were produced (Halsband 1997; Halsband and Hirche 1999), and in 1999 when no eggs nor faecal pellets were produced by *Calanus glacialis* females either (Fetzer and Arndt 2000). The reasons for the lack of egg-production are unclear, but further investigation of the gonads may show that females used for the experiments were not fecund yet. Furthermore the food supply might have been unfavourable at the time of sampling, at least in the lower layers of the water column the animals originated from. Dredging them through the desalinated surface layer may have resulted in irritation of the animals and thus in an "untypical" behaviour.

Table 5-3: Stationlist Plankton

Date	Stat.	Lat (N)	Long (E)	Depth [m]	Pycnokline/ mixed water [m]	Zooplankton nets taken	experiments	Meroplankton	MUC	EBS [t] V= 1 kn	Comments
4.9.00	02	75°24.114'	74° 11.82'	50	12-22	5 nets: 44-25 (2); 8-0 (2); 44-0	DW; CN	2 nets: 45-22; 22-0	2 * 3		
5.9.00	04	76°24.989'	81°0.486'	54	9-20	2 nets: 45-0; 8-0	--	3 nets: 45-20; 20-0; 45-0	GKG		
6.9.00	05	75°50.22'	81°0.32'	50	8-30	3 nets: 44-30 (2); 44-0	EP; DW, CN	2 nets: 45-30; 30-0;	2 * 2	3 min	Net torn due to strong winds and waveaction
7.9.00	07	74°39.456'	81°08.75'	37	7-30	5 nets: 32-25 (2); 7-0 (2); 32-0	EP; DW	3 nets: 32-25; 25-0; 32-0	2 * 3	3 min	
8.9.00	08	74°39.554'	82°38.553'	41	6-23	4 nets: 35-25 (2); 5-0; 35-0	DW	3 nets: 35-25; 25-06-0	1 * 3	5 min	
8.9.00	09	74°50.006'	83°25.898'	44,5	15-25	3 nets: 39-25; 13-0; 39-0	--	3 nets: 39-15; 15-0; 25-0	1 * 3	--	
9.9.00	13	72°56.018'	80°33.232'	13	2-6	4 nets: 10-4 (2); 2-0; 10-0	DW; CN	3 nets: 10-6, 4-0; 6-0	2 * 3	3 min	
10.9.00	15	72°2.992'	81°36.157'	6,5	--	2 nets: 5-0 (2)	--	no nets	2 * 3		Short net used
10.9.00	16	71°49.903'	82°36.991'	26	13-17	4 nets: 22-17 (2); 13-0; 22-0	DW; CN	3 nets: 24-17; 17-0; 13-0	2 * 3	5 min	
11.9.00	17	71°6.506'	83°5.533'	18	17	1 net:: 15-0					
12.9.00	19	69°58.856'	83°27.192'	22	--	1 net: 19-0					no pycnokline
13.9.00	21	71°41.489'	83°29.291'	24	--	--			--	5 min	
13.9.00	22	72°33.990'	79°54.927'	11	--	--			--	5 min	

Table 5-3: cont.

Date	Stat.	Lat (N)	Long (E)	Depth [m]	Pycnocline/ mixed water [m]	Zooplankton nets taken	experiments	Meroplankton	MUC	EBS [1] V= 1 kn	Comments
14.9.00	23	73°28.542'	79°51.348'	33	6-17	4 nets: 30-17; 4-0; 30-0 (2)	DW; CN	3 nets: 30-17; 17-0; 6-0	2 * 3	5 min	
14.9.00	24	74°0.505'	79°59.945'	31	10-24	4 nets: 28-24; 10-0; 28-0; 28-10	DW; CN	3 nets: 28-24, 24-10; 24-0	--	--	
15.9.00	26	75°42.512'	77°57.589'	68	14-36	5 nets: 60-40 (2); 15-0; 60-0; 40-0	DW; CN	3 nets: 60-40; 40-0; 17-0	1 * 3	5 min	
15.9.00	27	76°18.045'	78°55.977'	78	5-45	3 nets: 75-45; 5-0; 75-0		3 nets: 75-45; 45-0; 6-0	2 * 3	--	
16.9.00	28	76°39.33	83°52.61'	50	14-35	4 nets: 47-35; 13-0; 47-0; 47-15?	EP; DW; CN	3 nets: 47-35; 35-0; 14-0	1 * 3	5 min	Last net's depth not clear (used for exp.)
16.9.00	29	76°56.172'	85°45.793'	68	13-20	4 nets: 62-22; 10-0; 62-0; ??	DW	3 nets: 62-22; 22-0; 13-0	--	--	Last net closed uncontrolled (exp.)
17.9.00	30	75°59.188'	83°2.174'	51	25-40	3 nets: 25-0; 48-0 (2)	EP; DW; CN	3 nets: 63-22; 22-0; 16-0	GKG; 2 * 3		Net not closed (3 trials): no bottom sample
18.9.00	35	75°20.827'	83°48.086'	46	12-25	5 nets: 43-25; 11-0 (2); 43-0; 43-15	DW	3 nets: 43-25; 25-0; 14-0	2 * 3	5 min	
19.9.00	36	76°57.707'	81°57.79'	66	15-20	4 nets: 63-22 (2); 15-0; 63-0	EP; DW; CN	3 nets: 63-20; 20-0; 15-0	2 * 3	5 min	

5.4 Distribution of meroplankton and juveniles along a transect in the eastern Kara Sea

I. Fetzer

Alfred Wegener Institute for Polar and Marine Research, Bremerhaven, Germany

Introduction

Indirect development with a pelagic larval stage represents the most widely spread developmental mode of benthic marine invertebrates in the temperate latitude. This guarantees a wide distribution of the species and a good ability for quick exploitation of new territories. Many of those planktonic forms look somehow like tiny copies of the adults but have special mainly ciliated swimming organs, which reduce after settling. Other types of larvae, e.g. the plutei larvae of echinoderms, have to undergo major morphological changes before settling.

The lack of larvae in samples from polar waters inspired hypotheses that many polar species reproduce directly without a planktonic stage. Thorson (1936, 1946, 1950) postulated that the number of species with a planktonic larval stage decrease with increasing geographical latitude and increasing water depth due to the shortening of time for development and food accessibility. This as 'Thorson's rule' (Mileikovsky 1971) known paradigm, is widely accepted although new discoveries of more and more pelagic larvae, especially in the Antarctic waters and the deep sea, arose doubts on the validity of such generalisations.

Except the studies of Thorson and Mileikovsky, very little is known on the ecology of meroplankton in the Arctic. The structure of a community is determined by the supply of larvae, their transport mechanism and settlement success (Butman 1987). Also how far environmental factors may influence the distribution and the mortality of the pelagic stages and their later juvenile stages and how far postlarval processes are actually responsible for creating the observed distribution of adult infauna, is unknown. Benthic investigations usually do not ask whether distinct assemblages may result from different postlarval processes, but only care about the adult stages (Butman 1987, Olafson et al. 1994). Burkovsky et al. (1997) stated the importance of juveniles structuring a littoral macrobenthic community and their relationship to environmental factors. They showed that the correlation factor for the juvenile abundance to the measured environmental factors were usually higher than for the adult abundance. Nevertheless it is commonly accepted that an understanding of benthic communities without the knowledge of larval and juvenile ecology is almost impossible (Sheltema 1986).

The aim of this study is to investigate the presence and distribution of the larvae and juveniles of benthic invertebrates in the Kara Sea in relation to their adults with respect to the structuring effects of the freshwater influence of the rivers and their imported materials.

Material and Methods

The meroplankton was collected with a Nansen closing net (NCN; 55 μ m mesh size; 0.5m/sec hauling speed) at 20 stations (Table 5-4). According to the structure of the water column (archived by instant CTD data) three net samples were taken by vertical hauls: One from the bottom to the lower part of the pycnocline, one through the pycnocline to the surface, and one through the upper water layer from the upper part of the pycnocline to the surface. To gather information about the occurrence of larvae close to the sea floor, since they cannot be reached by the plankton net an Epibenthic Sledge (EBS) equipped with a Supra-benthic net of 80 μ m mesh size, was used.

The Sledge was dredged between 3-5 minutes, at 1knot speed, according to bottom sediment structure. In order to assess the number and distribution of already settled postlarvae and juveniles, the upper 5cm of undisturbed surface samples archived by a Multicorer (MUC; 28cm² surface cover), were taken. At every station 3-6 tubes were sampled. Before removing the sediment, the supernatant water above each core was sieved through a 50 μ m mesh and stored separately. All samples were preserved in 4% buffered formaline until further identification.

Table 5-4: Meroplankton station list with overview of sampling devices used. Numbers referred to samples achieved per device and time of towing, respectively. MUC = Multicorer; NCN = Nansen closing net; EBS = Epibenthic Sledge

No.	Station			Depth (m)	Device			
	Date	Time (GMT)	Lat ° N		Lon ° E	MUC [N]	NCN [N]	EBS [min]
2	4.9	5:53	75°24'	74° 11'	50	6	2	
3	5.9	4:38	76°55'	74°46'	193	4		
5	6.9	4:20	75°50'	81°00'	50	4	3	3
7	7.9	6:22	74°39'	81°08'	38	6	3	3
8	8.9	4:58	74°39'	82°38'	41	3	3	5
9	8.9	10:55	74°50'	83°25'	45	3		3
13	9.9	12:38	72°56'	80°33'	13	6	3	3
15	10.9	8:05	72°02'	81°36'	6	6		
16	10.9	13:36	71°49'	82°36'	26	6	3	5
17	11.9	11:27	71°06'	83°05'	18	2		
22	13.9	17:36	72°33'	79°54'	11			5
23	14.9	4:36	73°28'	79°51'	33	6	3	5
24	14.9	14:01	74°00'	79°59'	31		3	
26	15.9	7:20	75°42'	77°57'	68	3	3	5
27	15.9	15:28	76°18'	78°55'	78	6	3	
28	16.9	3:40	76°39'	83°52'	50	3	3	5
29	16.9	11:14	76°56'	85°45'	68	6	3	
30	17.9	8:45	75°59'	83°02'	52	6	3	
35	18.9	9:43	75°20'	83°48'	46	6	3	5
36	19.9	3:35	76°57'	81°57'	66	6	3	
$\Sigma=20$						$\Sigma=88$	$\Sigma=44$	$\Sigma=11$

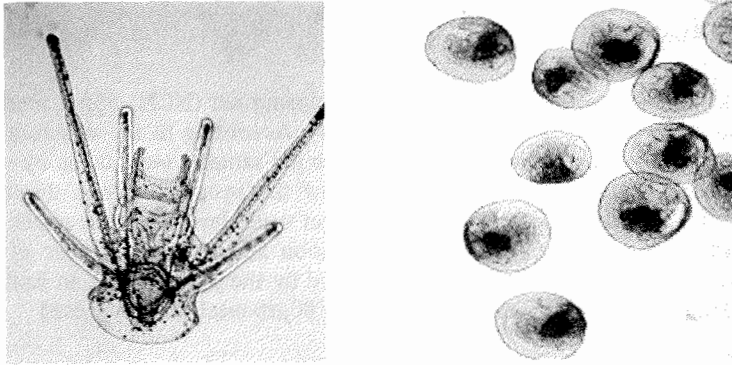


Fig 5-1: Samples of meroplanktic stages of marine Invertebrates:
a) Pluteus larvae (Echinodermata: Ophiurida); b) Veliger (Bivalvia: Lamellibranchia);

Results and Discussion

The northern and eastern parts of the investigation area were mainly dominated by pluteus larvae of the at some stations very abundant brittle star *Ophiura* sp. (Fig. 5-1), as well as larvae of the common starfish *Asterias* sp. while in the middle part many spionid larvae (Spionida: *Marenzelleria* sp., *Prionospio* sp.) were found in the net samples. Already former investigations reported the occurrence of spionid and ophiurid larvae as typical in this region of the Kara Sea throughout the year (Formin 1989). The distribution of the pelagic stages corresponds well with the main occurrence of their adults, since adult ophiurids were found mainly in northern parts, while spionids distributed more close to the estuaries. For echinoderms, usually the dominant taxon in high latitudes (Piepenburg et al. 1986, Piepenburg 1988, Piepenburg and Juterzenka 1994), the low water salinity is the most probable limiting factor induced by the freshwater input of the rivers (Schmidt-Nielsen 1994). However, their larvae seem more tolerable to low salinities since they were found in all samples even at the more southern stations (see also Halsband and Hirche 1999). Spionid polychaetes, on the other hand, seem to be more tolerable to lower salinities and therefore thrive well in the carbon enriched bottoms of the middle parts (Cochrane et al. 1997). Since the larvae were found so close to their adults it seems that they were released into the water column recently and have not been strongly dispersed yet. Additionally, mortality pressure must have been low on them yet because of their high abundances.

Also trochophoral stages and postlarvae of polychaetes of the orders Cirratulida (*Chaetozone* cf. *setosa*, *Tharix* cf. *marioni*), Cossurida (*Cossura longacirrata*), Flabelligerida (*Brada* sp.) Capitellida (*Capitella* sp.) and Phyllodocida (Phyllodocidae; *Aeglophamus malmgreni*, *Nephtys ciliata*, *Micronephtys minuta*; Spaeodoridae) could be identified. Most pelagic stages were evenly distributed within the observed area but almost no larvae were present in the estuary of the Yenisei River. Also hardly any juvenile stages were found here. In this area the current regime and rapid changes in temperature and salinity may limit the dispersal and survival of the meroplankters.

In general, very few bivalve and gastropod larvae were present in the net samples. In boreal regions they occur very early in spring in the water column. In addition, many already settled specimen of rather big size (250-500µm) were found in the sediment samples. This confirms that most of the larvae have already settled some time ago. Here, juveniles of *Portlandia* cf. *arctica/aestuariorum*, *Thyasira* sp., *Serripes* cf. *groenlandica* and *Nuculana* sp. were found in the samples.

The above mentioned results only refer to those species that have been so far identified yet. But still many juveniles and pelagic stages could not be recognised until now. Of the bigger animals the decision, whether they are already adult or still juvenile, has to be done for many samples. Further interpretation of the distribution pattern of both juveniles and larvae in relation to hydrographic factor, food conditions in the sediment and water column and other abiotic factor that may have an influence on the distribution, still have to be done in order to estimate their importance on the structuring of the adult macrofauna within the Kara Sea ecosystem.

5.5 Macrobenthos of the Yenisei River and inner Kara Sea.

Lubin P. A.¹ and Eckert, C.²

¹Murmansk Marine Biological Institute, Murmansk, Russia,

²Alfred Wegener Institute for Polar and Marine Research, Potsdam, Germany

The aim of the present study was to analyse the structure, species composition, abundance and biomass of benthic macrofauna in the Yenisei Bay and adjacent waters of the Kara Sea. As one of the main objectives within the framework of the Russian-German project "Siberian River Run Off" (SIRRO) is to investigate the fate of fluvial material along transects from the river estuaries of Ob and Yenisei up to the central Arctic Ocean. The extension of the study area as compared to our former cruises to a northern position at 76 ° 30' N was important.

Research methods

Quantitative macrozoobenthic samples were collected either by using a van-Veen grab covering an area of 0.1 m² or by a Large Box Corer (LBC) sampling 0.25 m². For statistical reasons the van-Veen grab was used 3 or 5 times at each station. Qualitative samples were collected using a Sigsby trawl with a mouth opening of 1 m and 10 mm mesh size of the net. Additionally, an Epibenthic sled (EBS) was used with an epibenthic (500 µm mesh size) and a suprabenthic net (80 µm mesh size). Usually, trawling time was about 10-15 minutes. Grab samples were sieved over 0.5 mm screen. The quantitative material was preserved with 4% buffered formaldehyde. The qualitative samples were pre-sorted at high taxonomic level and some of them became preserved with 75% ethanol, others with 4% formaldehyde. Selected individuals of dominant species obtained by trawl catches were deep-frozen for future radioactivity analysis. Other individuals such as asteroids and holothurians were deep-frozen at - 80 °C for biochemical analyses.

Collected materials

During the cruise 105 quantitative samples were taken with the van-Veen grab at 24 stations (see Table 5-5). Additionally, 16 samples with the LBC were obtained most of them at the same location as the van-Veen grabs. Qualitative samples were taken using the Sigsby trawl at 8 stations. Of more quantitative nature 13 EBS samples supplement the total collection of benthos material.

Preliminary results

Similar to the results of our former cruises, crustaceans, polychaetes, molluscs, echinoderms, and sipunculids were representatives of the dominant taxonomic groups in the study area. Polychaetes were abundant at all stations, except the stations in the Yenisei Estuary. The crustaceans were dominated by amphipods and isopods while bivalves were the most abundant molluscs. In the north-eastern part of the study area gastropods, often together with symbiotic sea anemones, occurred in the dredge samples.

A preliminary distribution analysis of the most abundant macrozoobenthic organisms seems to allow a subdivision of the study area into different zones starting from the Yenisei River to the adjacent shallow Kara Sea. The zones are composed by characteristic benthos assemblages and dominant species are most likely distributed along the major hydrographic pattern in salinity distribution.

Species typical for brackish and even freshwater were collected for example at station 019 belonging to Oligochaeta, Amphipoda, Bivalvia, Gastropoda and Chironomidae.

In the estuarine zone (stations 15-17, 21), characterized by salinity values ranging from 0.6 to 25 ‰, dominant species in our samples were euryhaline forms such as *Pontoporeia affinis*, *Gammaracanthus loricatus*, *Mesidotea (Saduria) entomon* (see also Fig. 5-2d) and *Portlandia aestivalis*. At locations with salinity values at the lower end of the above mentioned range mainly *G. loricatus* and *M. entomon* were sampled (stations 16, 21). As the salinity increases to 28 ‰ (stations 14, 22) *Macoma calcarea* appears in the composition of this estuarine community.

With an increase in salinity to 33 ‰ (stations in the northern part of the study area), a more marine character of the benthos assemblages was observed characterized by Echinoderms, Nemertini, Spongia and Alcionaria.

At station 09 (74° 50'100''N, 83° 25'900''E) the richest, in terms of species number, sample was taken. The dredge sample contained numerous echinoderms, crustaceans, polychaetes, molluscs, echinoderms, sipunculids, cnidaria, and sponges (Fig. 5-2a). We assume that Fe-Mn-hydroxid concretions found in the samples are responsible for this exceptional diversity allowing hard bottom fauna to settle there. In the area around station BP00-09 the sea floor was found to be covered with flat round and mainly kidney-shaped Fe-Mn-hydroxid nodules. The concretions reach various diameters between 5 and 20 cm. They are the basis of a hard bottom fauna with High Arctic components. Other notable, but smaller, concentrations of Fe-Mn-nodules with influence of the benthos fauna were detected at station BP-00-04 and BP-00-30.

At station BP00-28 (76° 39' 330''N, 83° 52'610''E) benthic fishes (Fig. 5-2c) and asteroids, at station BP 29 (76° 56' 170''N, 85° 45'790''E) a large individual of *Gorgonocephalus arcticus* (Fig. 5-2b) were collected, indicating fully marine and high Arctic conditions at the seafloor.

Table 5.-5: List of benthological stations during SIRRO 2000

Station	Date	Depth(m)	LBC	vVeen	Dredge	Sigsbi trawl	EBS
BP-00-02	04.09.2000	50	0	3	1	1	0
BP-00-04	05.09.2000	54	1	3	0	0	0
BP-00-05	06.09.2000	50	1	3	0	0	1
BP-00-07	07.09.2000	38	1	3	1	1	1
BP-00-08	08.09.2000	41	1	3	0	1	1
BP-00-09	08.09.2000	45	1	3	1	1	0
BP-00-13	09.09.2000	13	1	3	0	0	1
BP-00-14	09.09.2000	19	0	3	0	0	0
BP-00-15	10.09.2000	6	1	5	0	0	0
BP-00-16	10.09.2000	26	1	5	0	0	2
BP-00-17	11.09.2000	18	1	5	1	1	0
BP-00-19	12.09.2000	22	0	3	0	0	1
BP-00-21	13.09.2000	24	0	5	0	1	0
BP-00-22	13.09.2000	11	1	5	0	0	1
BP-00-23	14.09.2000	33	1	5	1	0	1
BP-00-24	14.09.2000	31	0	5	0	0	0
BP-00-25	14.09.2000	59	0	5	0	0	0
BP-00-26	15.09.2000	68	0	5	1	0	1
BP-00-27	15.09.2000	78	0	5	0	0	0
BP-00-28	16.09.2000	50	1	5	0	0	1
BP-00-29	16.09.2000	68	0	5	1	0	1
BP-00-30	17.09.2000	30	1	3	1	0	0
BP-00-31	17.09.2000	43	1	0	0	0	0
BP-00-35	18.09.2000	46	1	5	0	0	1
BP-00-36	19.09.2000	66	1	5	0	1	1
BP-00-38	20.09.2000	20	0	5	0	0	0
Σ			16	105	8	7	14

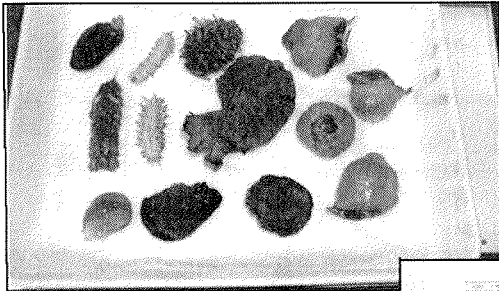


Fig. 5-2a: Polychaetes, sponges, and symbiotic sea anemons with gastropods

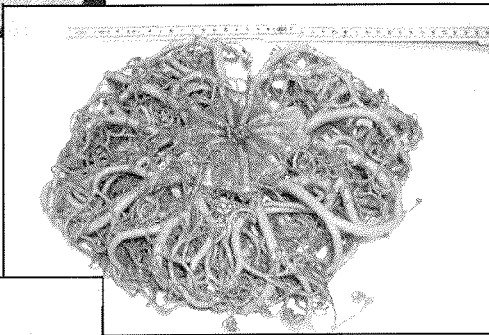


Fig. 5-2b: *Gorgonocephalus arcticus*

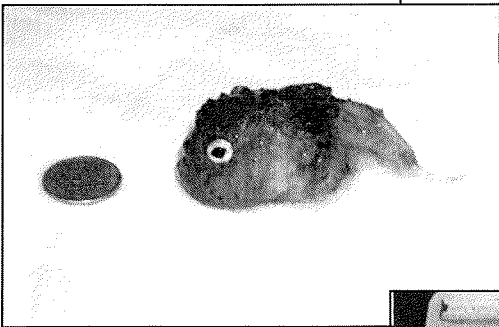


Fig. 5-2c: Arctic benthic fish

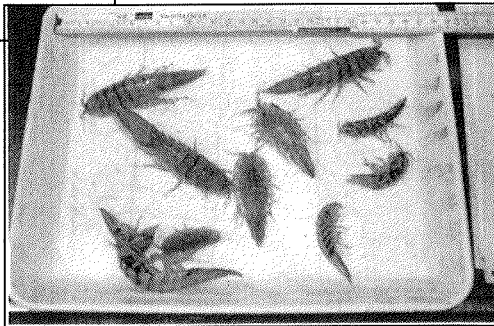


Fig. 5-2d: *Mesidotea entomon*

6. Marine Geology

R. Stein¹, K. Dittmers¹, E. Ivanova², M. Kraus¹, S. Krivanek³, M. Levitan^{2,4}, J. Matthiessen¹, F. Schoster¹, J. Simstich³, and T. Steinke¹

¹Alfred Wegener Institute for Polar and Marine Research, Bremerhaven

²Shirshov Institute of Oceanology RAS, Moscow

³GEOMAR Research Center for Marine Geosciences, Kiel, Germany

⁴Vernadsky Institute of Geochemistry and Analytical Chemistry RAS, Moscow

The Arctic Ocean and its marginal seas are key areas for understanding the global climate system and its change through time (for overviews see ARCSS Workshop Steering Committee, 1990; NAD Science Committee, 1992; and further references therein). The present state of the Arctic Ocean itself and its influence on the global climate system strongly depend on the large river discharge which is equivalent to 10 % of the global runoff. Today, the freshwater inflow by the major rivers reaches a total of 3300 km³/yr.

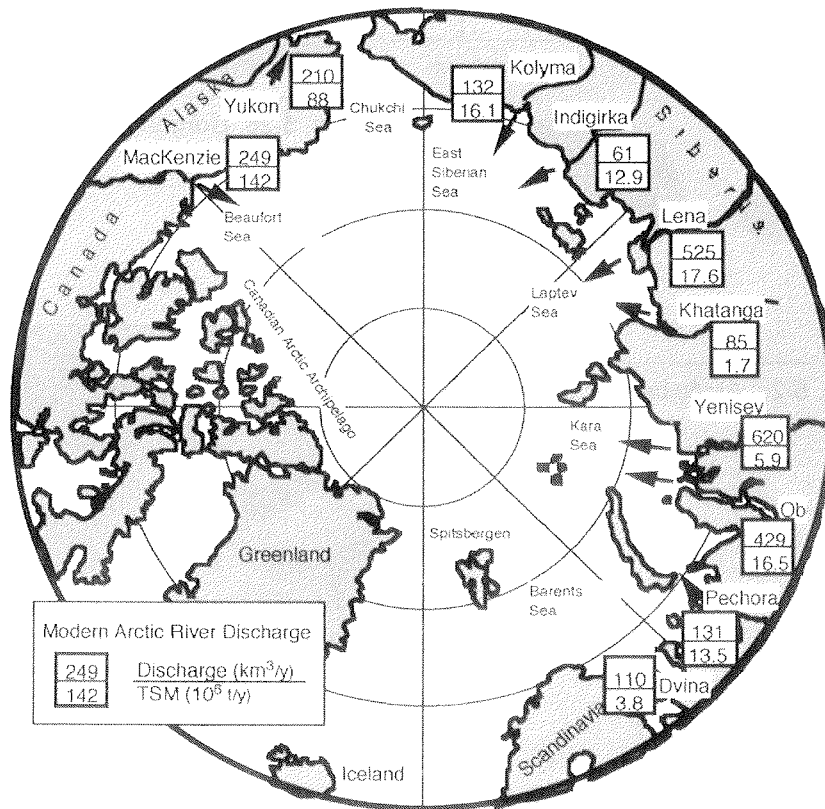


Fig. 6-1: Modern annual circum-Arctic river discharge, according to Aagaard and Carmack (1989) and Gordeev et al. (1996). TSM = total suspended matter.

Of particular importance are the Kara and Laptev seas receiving almost 2,000 km³/yr. of river discharge (Aagaard and Carmack, 1989; Gordeev et al., 1996), which constitutes more than 50% of the total Arctic continental run-off. The major part of this volume is provided by the Siberian rivers Ob, Yenisei, and Lena (Fig. 6-1).

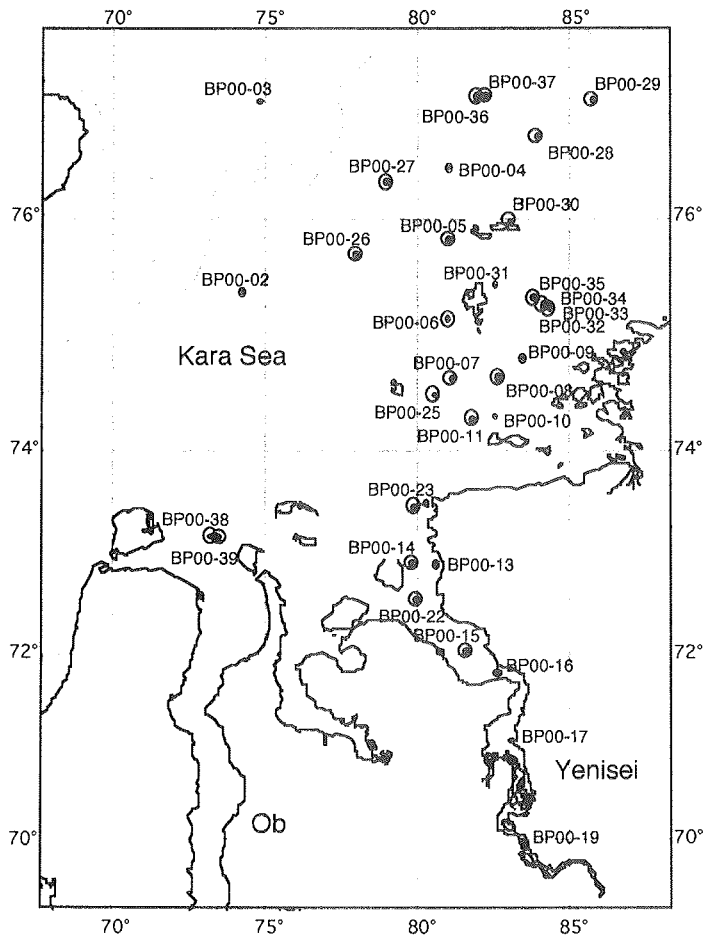


Fig. 6-2: Geological sampling stations of the "Akademik Boris Petrov" Expedition 2000. Stations where gravity cores were obtained are circled.

Furthermore, large amounts of dissolved and particulate (organic and inorganic) material are transported by the major Arctic rivers (Fig. 6-1). The annual discharge of total suspended sediments by the Ob River, for example, is $16.5 * 10^6$ tons. Dissolved and particulate organic carbon supply by the Ob River is estimated to reach about $2.8 * 10^6$ and $0.3 * 10^6$ tons per year, respectively (Gordeev et al., 1996). Although most of this material is deposited in the estuary and inner Kara Sea close to the river mouth (Lisitzin, 1995), significant amounts are further transported by currents and sea ice onto the outer continental margin and the open ocean, which may contribute significantly to the entire Arctic Ocean sedimentary and chemical budgets.

The overall goal of the RV "Akademic Boris Petrov" Expedition 2000 is to study these processes in the Ob and Yenisei estuaries and the adjacent inner Kara Sea in detail. Within this concept, a major interest of the marine geological investigations of the material obtained during this expedition (Fig. 6-2) is the quantification and characterization of the supply of siliciclastic and organic material by the rivers Ob and Yenisei, its accumulation in the estuaries, its transfer onto the open Kara Sea shelf, and its changes in time and space.

The methods to be used are summarized in Annex Table 9-3. The investigations will be performed on suspended matter, sediment-trap material, surface sediments and sediment cores.

6.1 Sediment sampling program

F. Schoster¹, K. Dittmers¹, E. Ivanova², S. Kriwanek³, M. Levitan^{2,4}, J. Simstich³, R. Stein¹, and T. Steinke¹

¹ Alfred Wegener Institute for Polar and Marine Research, Bremerhaven

² Shirshov Institute of Oceanology RAS, Moscow

³ GEOMAR Research Center for Marine Geosciences, Kiel, Germany

⁴ Vernadsky Institute of Geochemistry and Analytical Chemistry RAS, Moscow

In comparison to the expeditions of the "Akademik Boris Petrov" in the years 1997 and 1999 the working area was larger reaching up to almost 77° in the north and 70° in the south (Matthiessen and Stepanets 1998, Stein and Stepanets 2000). It was of major interest to take samples along the salinity gradient from the southern Kara Sea, the outer Yenisei Estuary into the Yenisei River to get the pure fresh water endmember (Fig. 6-2). The water column and the sediments were generally sampled at the same stations in order to study the relationship between modern processes in the surface waters and their reflection in the surface sediments.

Based on the sediment echograph profiling the geological stations were selected. After arriving and anchoring at the station the water sampling started. When this was finished the geological sampling started usually with the Giant Box Corer and the Multicorer in order to take samples from the surface and near-surface sediments. For long sediment cores the Gravity Corer was used in lengths of 3, 5 and 8 m.

Giant Box Corer

The Giant Box Corer (weight of ca. 500 kg, volume of sample 50*50*60 cm; manufactured by Fa. Wuttke, Henstedt-Ulzburg, Germany) was successfully used 42 times on 22 stations. Three times the box corer was empty due to technical problems, only two box corers were disturbed, and only one box corer was overfilled due to overpenetration. The recovery generally varied between 25 and 50 cm. The box cores were sampled for the following investigations:

a. surface sediments

- stable isotope analysis of benthic calcareous organisms (Geomar)
 - 10*10 from the upper 1 cm (100 cm³) fixed with bengal-rose-methanol-solution
 - 10*10 from the upper 5 mm (50 cm³)
- benthic foraminifera and stable isotopes (Shirshov-Institute)
 - 1-3 times 10*10 from the upper 1 cm (100 cm³) fixed with bengal-rose-methanol-solution
- studies on benthic macrofauna (AWI-Biology)
- organic geochemistry (Vernadsky-Institute)

b. profiles (tubes 120 mm in diameter)

- sedimentology, grain-size and clay mineralogy (AWI-Geology)
- organic geochemical bulk parameters (TOC, CaCO₃, C/N-ratio, Rock Eval pyrolysis) and biomarkers as well as $\delta^{13}\text{C}$ of specific biomarkers (AWI-Geology)
- organic geochemistry, radio-nuclides (Vernadsky-Institute)
- benthic foraminifera (Shirshov-Institute)

In addition, at 4 stations Mn-nodules were sampled (Tab. 6-1). Mn-oxides are precipitated onto stones, molluscs and polychaete tubes.

Table 6-1: Occurrences of Mn-nodules in the working area of the cruise of "Akademik Boris Petrov" Expedition 2000.

Station	Mn-Crusts precipitated mainly on
BP00-04	molluscs
BP00-06	polychaete tubes
BP00-09	polychaete tubes and portlandia
BP00-30	pebbels and gravel

Multicorer

The standard 12-tubes-version multicorer (weight of 495 kg; manufactured by Fa. Wuttke, Henstedt-Ulzburg, Germany) with an inner tube diameter of 6 cm was used. The penetration weight was always 250 kg. The multicorer was successfully used 30 times on 18 stations, and usually recovered undisturbed surface sediments and overlying bottom water. Only one multicorer was empty due to technical problems.

surface sediments

- Copepodes (Juveniles) (AWI-Biology)
3-4 tubes, 30 – 80 cm³
- Phyto-zoo-plankton (AWI-Biology)
2-3 tubes, 20 – 60 cm³
- stable isotope analysis of benthic calcareous organisms (Geomar)
1-3 tubes, 10 – 60 cm³, from the upper 1 cm fixed with bengal-rose-methanol-solution to stain living organisms
- inorganic geochemistry (AWI-Geology)
2 tubes, ca. 20 cm³
- clay minerals (AWI-Geology)
1 tube, 10 – 20 cm³
- palynology (AWI-Geology)
1 tube, 10 – 20 cm³
- biomarkers and $\delta^{13}\text{C}$ of specific biomarkers (AWI-Geology)
1 tube, 10 – 20 cm³, stayed frozen at -20°C
- organic geochemical bulk parameter (TOC, C/N, Rock Eval pyrolysis, CaCO₃) (AWI-Geology); 1 tube, 10 – 20 cm³

profiles

- organic geochemical analysis (C_{org}/N , carbonate, biogenic silica (Opal), carbohydrates, amino acids) (IfBM)

1 tube, samples (20 cm^3) from the upper 3 cm, stored frozen at -20°C , tube sampled at 5 cm intervals and additionally at lithological changes, stored at -20°C

- organic geochemistry (Vernadsky-Institute)

In addition, bottom water (100 ml), was sampled from the multicorer tubes for stable isotope measurements (Geomar).

Gravity Corer

The Gravity Corer has a penetration weight of 1.5 t and is used in 3, 5 and 8 m long core barrels. The diameter is 12 cm. The gravity corer was used on 26 stations for 37 times. Only two cores were empty due to stiff or hard sediment layers near to the surface. The other cores vary in the recovery of sediments from 0.34 up to 7.32 m (Fig. 6-3, Table 6-2). Most of the cores showed a brownish colored sediment at the top indicating that the near-surface sediments have been recovered. After recovery the cores were cut in segments of 100 cm length and stored in the cold. Also the core catcher was sampled. Double cores were taken at 5 stations and four times at another 2 stations (Table 6-2). One to two from these cores was opened, described and sampled for methane/pore water and/or heavy mineral investigations. Core descriptions are presented in the annex.

Table 6-2: Penetration and recovery of gravity corer. (SL-3 (5 or 8): 3 (5 or 8) m core barrel (m/pw: methane and pore water sampling, hm/bf: sampling for heavy minerals and benthic foraminifera, CC: core catcher).

Core	Gear	Water depth (m)	Penetration (m)	Recovery (m)	Remarks
BP00-02/4	SL-5	49.6	2.6	0.68	H ₂ S smell
BP00-04/3	SL-5	54	0	0	
BP00-05/5	SL-5	50		0.34	
BP00-06/1	SL-5	38	3	2.88	
BP00-07/4	SL-5	38	7	5.03	about upper 1m lost
BP00-07/5	SL-8	38	8.5	6.32	hm/bf
BP00-07/6	SL-8	38	8.5	6.65	m/pw
BP00-07/7	SL-8	38	8.5	7.32	
BP00-08/4	SL-5	41	2.5	1.9	stiff black sediment in CC
BP00-10/1	SL-5	29	0	0	
BP00-11/1	SL-8	42	3.5	3.22	
BP00-14/3	SL-5	19.2	3	2.43	CC: sandy
BP00-14/4	SL-5	19.2	4	2.56	CC: sandy, m/pw
BP00-15/5	SL-5	5.8	4.5	3.69	
BP00-15/6	SL-5	5.8	4.8	4.38	m/pw
BP00-22/4	SL-5	11	5	4.38	m/pw
BP00-22/5	SL-5	11	5	4.36	
BP00-23/6	SL-5	33	4.5	4.17	
BP00-23/7	SL-5	33	4.5	4.27	m/pw
BP00-25/1	SL-8	59	5.5	3.32	
BP00-26/4	SL-5	65	4.5	3.96	
BP00-27/3	SL-8	78	8.5	6.7	
BP00-28/5	SL-5	50	4.2	1.21	
BP00-29/4	SL-5	68	4	3.29	
BP00-30/3	SL-8	52	8.5	7.32	
BP00-32/1	SL-8	32	8	5.74	
BP00-33/1	SL-3	22	1	0.53	very stiff clay
BP00-34/1	SL-5	39	5	4.52	CC: sandy
BP00-35/5	SL-5	46	4	2.61	
BP00-35/6	SL-5	46	4	2.58	
BP00-36/1	SL-8	66	8	5.74	m/pw
BP99-36/2	SL-8	66	8	5.73	hm/bf
BP00-36/3	SL-8	66	8	5.87	
BP00-36/4	SL-8	66	8	5.63	
BP00-37/1	SL-8	63	6.5	4.33	
BP00-38/2	SL-8	20	7.8	6.52	
BP00-39/1	SL-8	14	3.2	1.28	hm

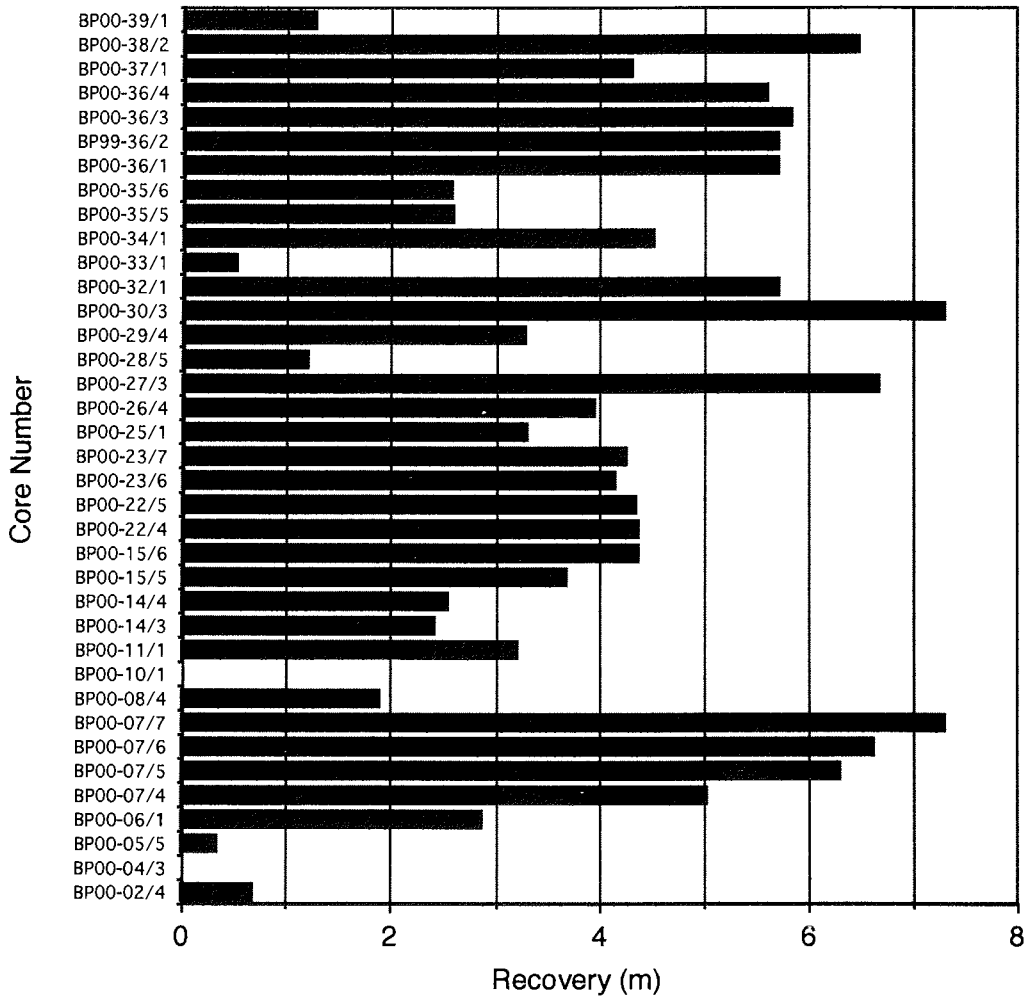


Fig. 6-3: Recovery of gravity cores during “Akademik Boris Petrov” Expedition 2000.

6.2. 3.5 kHz and ELAC sediment echograph profiling

K. Dittmers and R. Stein

Alfred Wegener Institute for Polar and Marine Research, Bremerhaven

RV "Akademik Boris Petrov" is equipped with an ELAC echograph LAZ 72 constructed by Honeywell-Nautik, Kiel, Germany. The system can be used for either fishfinding, surveying, navigation or oceanography and thus offers different operating modes. For sediment profiling the echosounder had to be set to an operating frequency of 12 kHz, an impulse length of 1 ms and 200 W transmitting power to show best possible results. Analogical recording was carried out by plotting the received signal directly on Spark recording paper. Limiting profiling factors were the relatively high frequency which did not provide higher resolution of layered sediments and the small water depth causing a very strong backscatter signal from the seafloor and high amplitude multiple echos especially when increasing the transmitting power. Despite these limiting factors the ELAC echograph was a very successful tool to distinguish between soft clayey sediments which show higher penetration, and single seismic reflectors and sandy sediments of higher density characterized by a hard reflector and no deeper penetration.

In addition to the ship's ELAC profiler, a 3.5 kHz profiling survey was carried out. For this, a „Geochirp“ towfish, mounted with four Massa 137 Transducers connected parallel, was used overboard as acoustic source and receiving unit (Fig. 6-4). It was lowered by a gasoline-powered winch manufactured by Swissrope (Switzerland). Depending on water depth and speed it was submerged 6-12 meters. Onboard a ORE 140 Transceiver for receiving and transmitting and a Geoacoustics SES („Sonar Enhancement System" model Se 8815) for enhancement, triggering and digital recording (Exabytetape with Seg-Y data format) were used (Fig. 6-4). A custom-made Sony DAT recorder was employed for recording the source trigger signal and the received signal in order to get blind copies. The „normal“ analogous signal was plotted by a Ultra Electronics 120 Series Linescan recorder at a paper speed of 1000-1500 mm/s.

In open seas and under heavy weather conditions a TSS model 305 Swell filter was switched between the signal and the SES. The trigger time of the SES was adjusted consequently with a sample period of 25 and a repeat period of 250 ms. The same rate (25ms) is the digitising frequency of the tape recorder.

The ORE Transceiver was run with a pulse length of 0.2 to 0.5 ms depending on the desired depth of penetration. The higher pulse length resulted in a deeper penetration but decreased the resolution. The transmitting power was between 2.5 and 5 kW, and a gain of factor 20 was applied.

Limiting profiler resolution factors were:

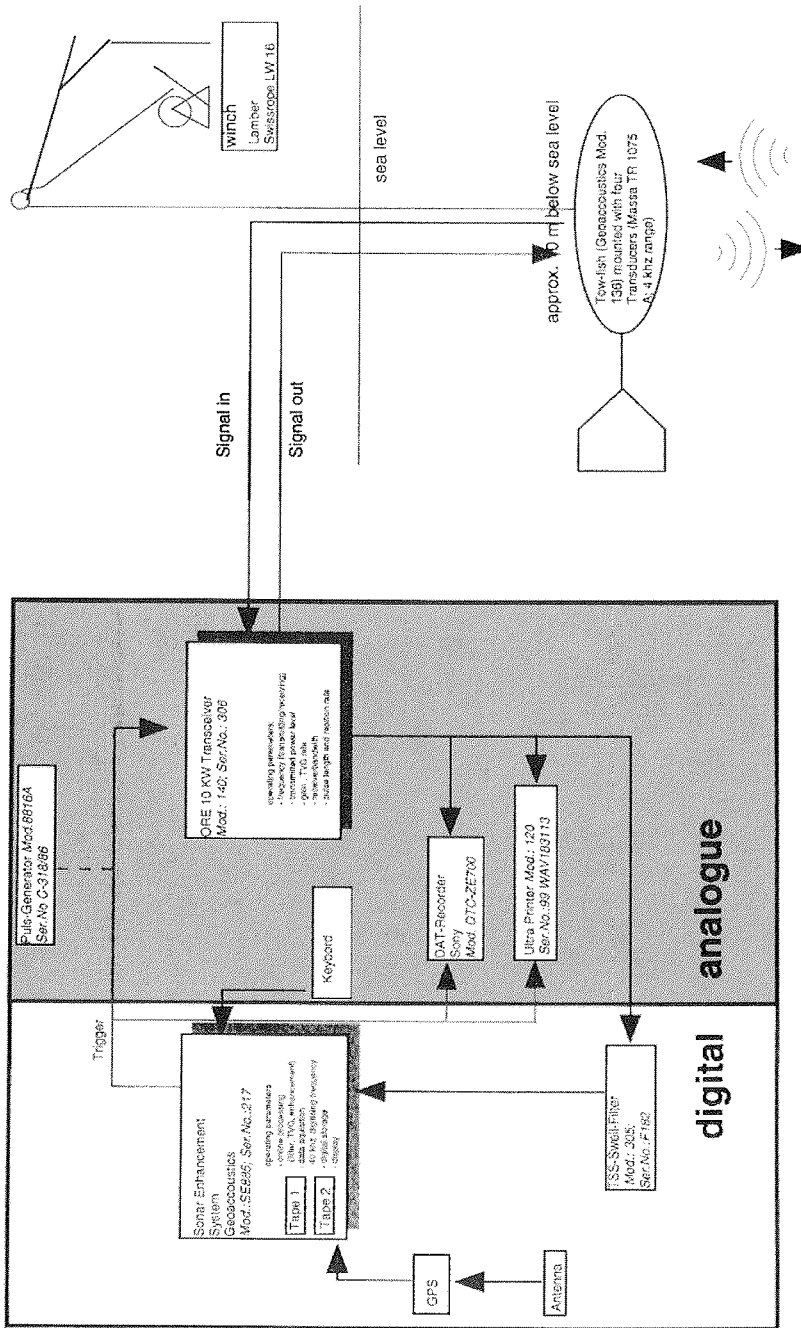
- wave noise (including roll and heave of the vessel). This was emphasized, because the fish was used in the bow part of the ship to avoid noise from the engines;

- noise in the fish. Especially at higher speed the cables started to „work“; this was intensified because a separate deck cable was used for signal transmission to/from the transducers in the fish beneath the cable that supported the fish .

The ELAC echograph was in continuous operation along all cruise tracks between arrival and departure at the working area in the Kara Sea. The 3.5 kHz sediment profiling system was used on selected profiles to get more detailed information about the structures of the near-surface sediments. In general, the aims of the sediment profiling were:

- * to select coring stations for gravity coring;
- * to get a detailed picture of the modern bottom topography; and
- * to get information about the thickness and structure of the youngest (Holocene?) sedimentary cover and the pre-Holocene bottom topography

In the following, three selected examples of the profiling results are presented.



Data aquisition - enhancement - signal generation - receiving

Fig. 6-4: Scheme showing the functioning of the 3.5 kHz system

Channel systems in the southern Kara Sea

Two profiles obtained by the 3.5 kHz system are shown in Figures 6-5 and 6-6. Figure 6-5 displays a narrow about 25 m deep v-shaped channel filled with young (Holocene?) sediments. Core BP00-07 (for location see Fig. 6-2) was recovered just from the central part of the channel. Outside the channel, the thickness of young sediments decreases sharply to less than 3 m.

The profile presented in Figure 6-6, is from a channel-like structure extending for some 5 km to the SE. Note the swell superimposed on the reflectors which is due to wave movement of the vessel. This profile can be divided into two parts. In the NW corner of the profile, thin young (Holocene?) sediments ("Unit I"; cf. Chapter 6.7) are overlying the hard acoustic "basement". No structures are recorded below the "basement" reflector. Furthermore, indication of possible ice gouging is obvious. Towards the SE, well-stratified sediments with higher penetration up to 10 m and several sharp continuous reflectors, are overlying the acoustic "basement". These sediments are truncated by young (Holocene?, "Unit I") sediments on top (discordance). The thickness of the sediments of Unit I is decreasing to zero in the middle part of the profile. This is corroborated by the lithostratigraphy of Core BP00-11/1 where the thickness of lithological Unit I is < 10 cm (cf., Chapter 6.7, Fig. 6-27). Unfortunately, the gravity corer at position BP00-11 was only able to penetrate the upper about 3 m of sediment and got stuck in the first reflector.

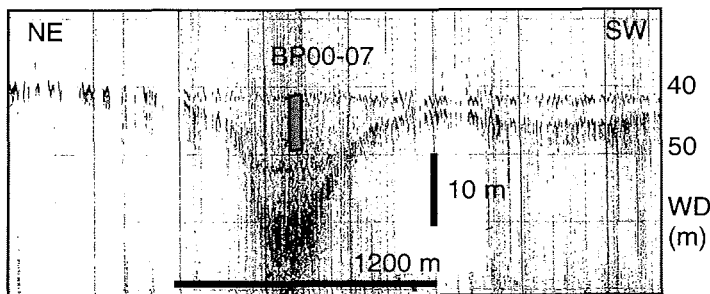


Fig. 6-5: 3.5 kHz profile across the position of Core BP00-07 (for location see Fig. 6-2).

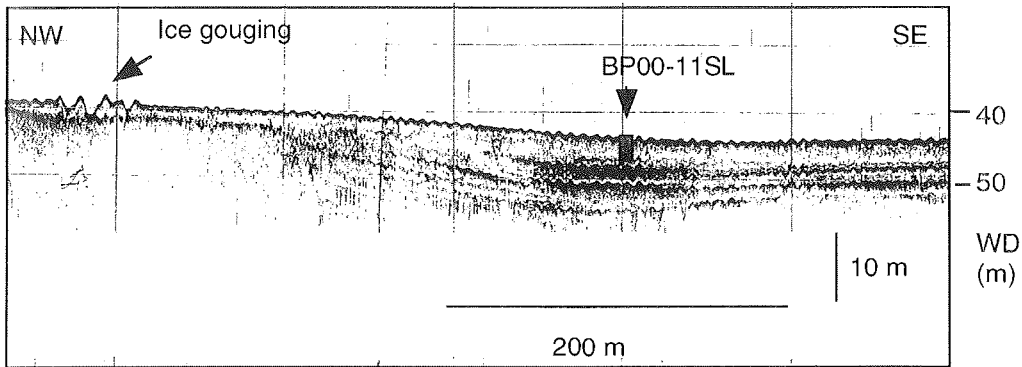


Fig. 6-6: 3.5 kHz profile across the position of Core BP00-11 (for location see Fig. 6-2).

End morain (?) east of the "Islands of Arctic Institute"

Based on an ELAC sediment echograph survey, an end-morain-like structure was recovered in the eastern part of our study area (Fig. 6-7; for location of ELAC profile (5) see Fig. 6-24). Young (Holocene?) sediments are overlying a strong reflector which is cropping out at the top of the structure (for further details see Chapter 6.7).

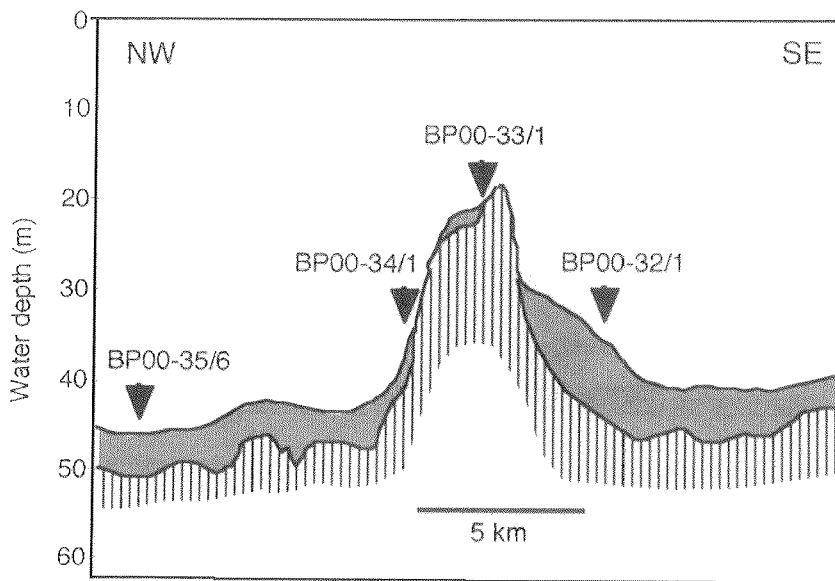


Fig. 6-7: Scheme of ELAC sediment echograph profile across end-morain-like structure with locations of sediment cores (cf. Chapter 6.7)

6.3 Core Logging: Magnetic Susceptibility

K. Dittmers, R. Stein, and T. Steinke

Alfred Wegener Institute for Polar and Marine Research, Bremerhaven

Magnetic susceptibility is commonly used as an indicator for the mineralogical composition of the sediments and for lateral core correlation (e.g., Kleiber and Niessen, 2000). It is defined as the dimension-less proportional factor of an applied magnetic field in relation to the magnetization in the sample (here expressed in SI units).

In order to determine magnetic susceptibility of gravity cores and box cores directly onboard "Akademik Boris Petrov", a simple core logging device was built. A Bartington MS2C-2 magnetic loop sensor was mounted in the middle of an about 250 cm long bench. The sensor was connected with a Bartington measuring unit MS2. A single sealed sediment core was taken and driven along the bench at increments of 2 cm. To avoid bordering effects at the end of the cores the bench was designed to hold two cores. 10 cm before the end of a core reached the loop, the new core was added. Before starting the measurements, all core segments were stored at least for 36 hours in the laboratory to become adapted to room temperature (18-20°C).

At the location of Station BP00-07 (Fig. 6-2), four sediment cores (BP00-07/04 to BP00-07/07) were obtained. Two of them (BP00-07/04 and BP00-07/06) were logged (Fig. 6-8). Based on the magnetic susceptibility records, both cores can be clearly correlated. Furthermore, in Core BP00-07/04 the upper about 2m were lost due to high overpenetration of the gravity corer, which is also obvious from the logging results.

All sediment cores obtained during the "Akademik Boris Petrov" Expedition 2000 and described at AWI (cf. Chapter 6.7), were logged before opening the cores using the "Multi Sensor Core Logger (MSCL-14)". A detailed description of the MSCL system is given by Kuhn (1995), its calibration is described by Weber et al. (1997). By means of the MSCL system, records of magnetic susceptibility, wet bulk density, and p-wave velocity can be obtained.

As an example, magnetic susceptibility and wet bulk density records are shown for Core BP00-26/4 in Figure 6-9. The upper silty clayey, bioturbated Unit I is characterized by low susceptibility and density values whereas high susceptibility and density values were recorded in the coarse-grained lithological Unit II. Similar records were determined in numerous cores from the Kara and Laptev seas (e.g., Kleiber and Niessen, 2000; Stein and Fahl, 2000; Stein et al., 2001). In these cores, this change in susceptibility is AMS¹⁴C-dated to about 10 ka, i.e., the base of the Holocene, and can be used as stratigraphic marker.

Further detailed evaluation and interpretation of all logging records as well as the correlation with the lithostratigraphy and other sedimentological and mineralogical data sets (e.g., grain size, clay minerals etc.) will be performed by K. Dittmers (AWI).

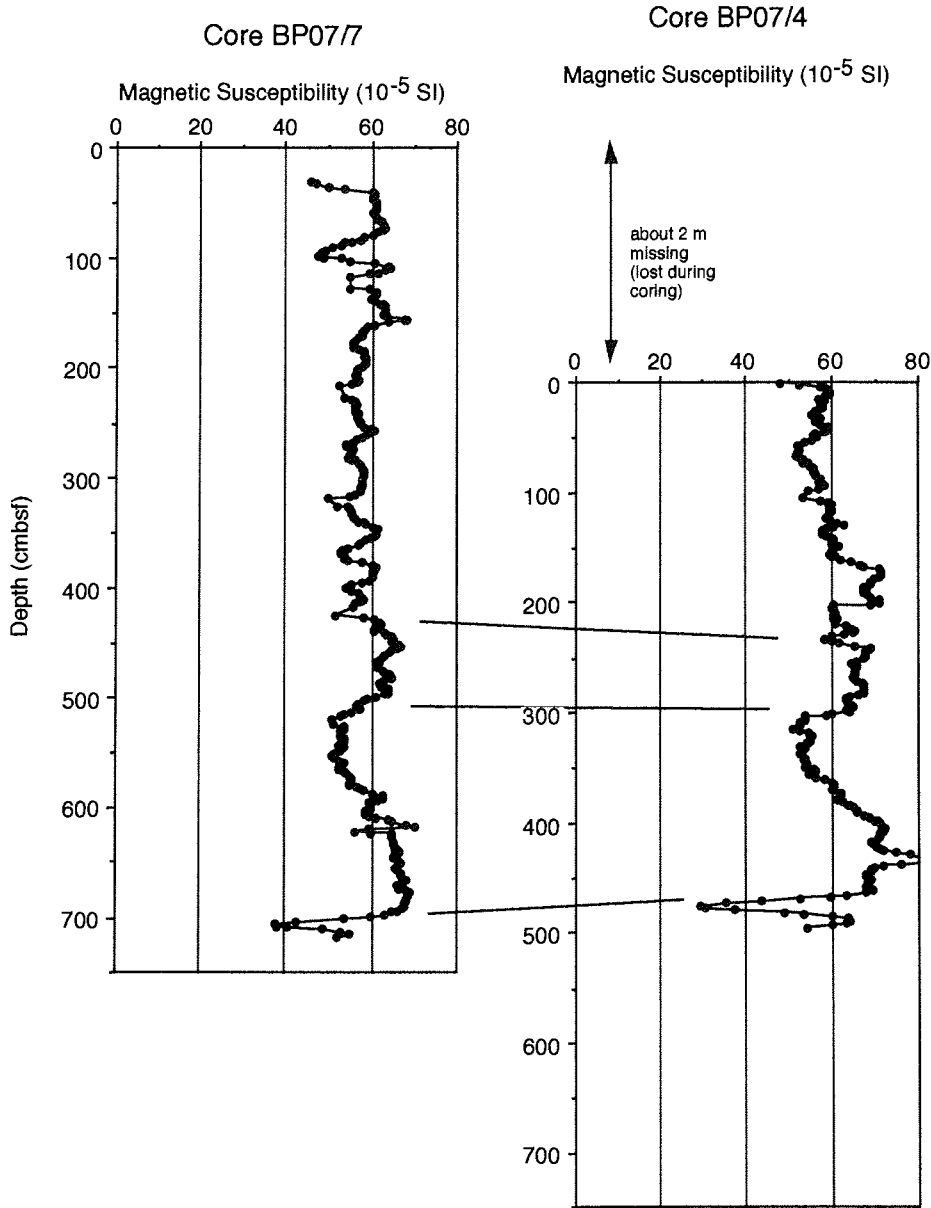


Fig. 6-8: Magnetic susceptibility records of cores BP00-07/04 and BP00-07/06.

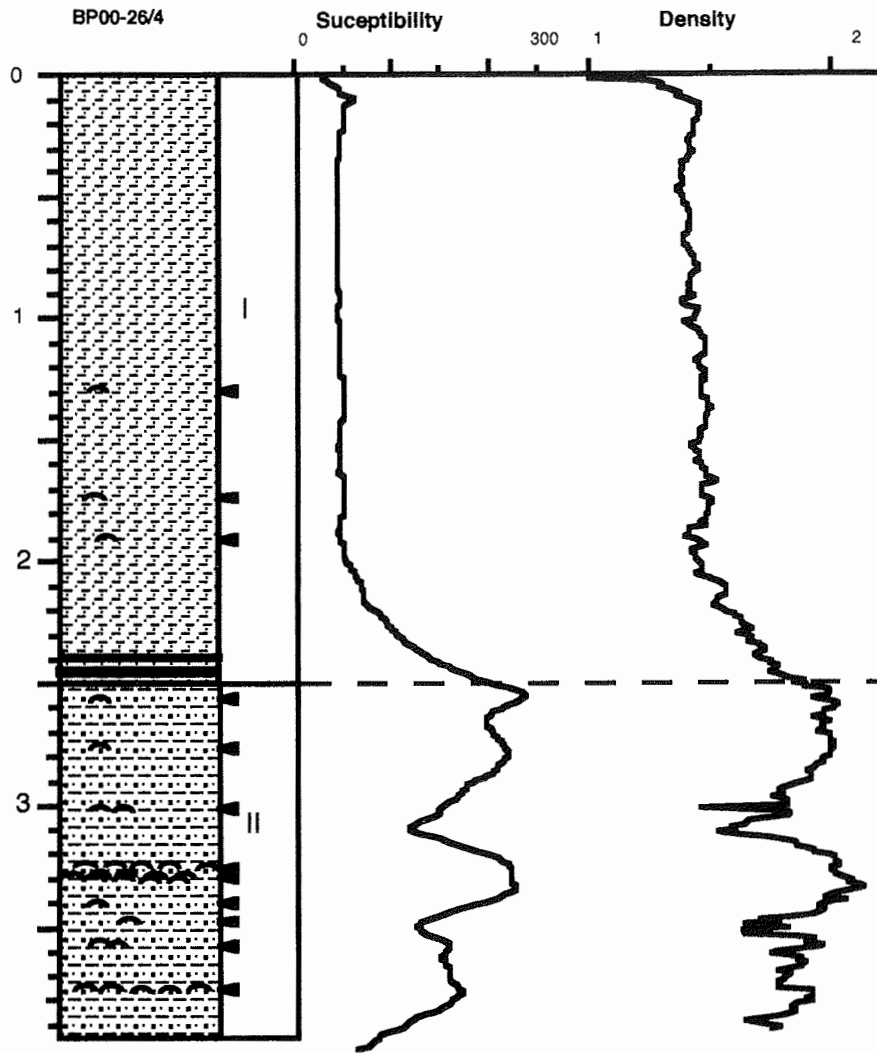


Fig. 6-9: Lithostratigraphy and magnetic susceptibility and wet bulk density records of Core BP00-26/4.

6.4 Facies variability of surface sediments along the Yenisei transect based on grain-size composition, heavy and light mineral data

M. Levitan^{1,2}

¹ Shirshov Institute of Oceanology RAS, Moscow

² Vernadsky Institute of Geochemistry and Analytical Chemistry RAS, Moscow

Introduction

In the middle of 90-s years of the last century we proposed a general scheme of facies zonation for the Kara Sea recent sediments (Levitan et al., 1996). According to the scheme, there are two main facies zones: Western Kara (FI) and Ob-Yenisei (FII). Recently this division was supported by data on IRD composition (Lisitsin et al., 2000).

Mineralogical (Levitan et al., 1998, 1999; Müller and Stein, 1999), geochemical (Nürnberg, 1996; Boucsein et al., 1999; Krasnyuk and Vansteyn, 1999; Schoster and Stein, 1999) and micropaleontological (Khusid and Korsun, 1996; Polyakova, 1999; Mukhina and Yushina, 1999; Matthiessen, 1999) data revealed a clear facies difference between western (Ob) and eastern (Yenisei) parts of FII zone.

It takes sense to remind that northward FII zone consists of FIIA, FIIB, FIIC and FIID subzones, where FIIA means river sediments, FIIB – sediments of a mixing zone of fresh and sea water, FIIC – sediments of negative, zero or low sedimentation environments, and FIID – sediments of accumulation areas in the northern troughs.

In 35-th cruise of R/V “Akademik Boris Petrov” (2000) our main efforts were concentrated in the eastern part of FII zone. Just now, based on available materials and – first of all – on data of V.I. Gurevich (1995) and above listed references, it is possible to give more detailed facies zonation for the eastern FII zone.

FIIA subzone consists of FIIA/1 and FIIA/2 areas, where FIIA/1 – areas of zero or negative sedimentation (bottom erosion) with bedrock outcrops within Yenisei River valley; FIIA/2 – areas of active winnowing of fine fractions and passive concentration of pebble, gravel (mainly) and sand fractions due to strong currents. During 49-th cruise of R/V “Dmitry Mendeleev” (1993) and 35-th cruise of R/V “Akademik Boris Petrov” we failed to find any areas of significant sediments’ accumulation in the lowest part of Yenisei River valley.

FIIB subzone includes areas FIIB/1 and FIIB/2, where FIIB/1 – areas of relatively coarse (sandy and silty) sediments in the southernmost part of FIIB subzone. The genesis of these sediments is related to hydrodynamical barrier existing due to the meeting of strong current of Yenisei with the “wall” of sea water. FIIB/2 sediments are located northward from the barrier and have more clayey composition. Here pure marine components play more important role.

It is well known that FIIC subzone is characterized for the vast area of neotectonic emergence with significant role of bottom currents eroding and winnowing fine grain-size fractions from bottom sediments. One can divide FIIC subzone for three areal regions (FIIC/1, FIIC/2, FIIC/3) and two linear areas (FIIC/4 and FIIC/5), where FIIC/1

means areas with bedrock outcrops (Cretaceous and Cenozoic rocks), FIIC/2 – outcrops of Quaternary (mainly Upper Pleistocene) relict (residual and/or palimpsest) sediments, FIIC/3 – areas of recent sandy winnowed, reworked and – sometimes – redeposited sediments. To make difference between FIIC/2 and FIIC/3 sediments we have to use radiochemical (^{210}Pb , ^{137}Cs etc.) and geochronological (^{14}C and others) indicators.

At least since the 70-s years of the last century it is known about flooded hydrographic network of the Pleistocene age in the FIIC subzone (Lastochkin, 1977). The network consists of paleo-Yenisei (for the eastern part of FIIC) River valley and its tributaries of different orders. Later this hydrographic pattern became expressed more complicatively on maps according to Musatov (1989). Based on echosound and seismoacoustic data it is possible to reveal FIIC/4 – paleo-valleys filled by sediments, and FIIC/5 – empty paleo-valleys with bedrock outcrops due to strong bottom currents channelized by valleys. In sum areas of FIIC/1-3 facies distribution occupy up to 80-90% of FIIC area. Boundaries of these areas with FIIC/4-5 are very sharp, and just on these boundaries we observe very large gradients of different facies indicator concentrations.

As FIIC subzone was not investigated during the 35-th cruise of R/V “Akademik Boris Petrov” this paper will not consider its inner structure in this paper.

Facts and methods

In this paper, I will describe grain-size composition, heavy and light minerals in the surface-layer (0-1 cm) sediments obtained by means of box-corers during the 35-th cruise of R/V “Akademik Boris Petrov”. Location of studied stations is shown on Figure 6-10. Analyses of grain-size composition (by Petelin method), heavy and light minerals were performed in analytical laboratory of Shirshov Institute by V.P.Kazakova and A.N.Rudakova. Analytical methods were described earlier (e.g. Levitan et al., 1996). Recently it was shown that results of Atterberg and Petelin analyses for siliciclastic sediments are very similar (Alekseeva and Svalnov, 1999). Earlier the author used a grain-size classification by Bezrukov and Lisitsin (1960) where gravel/sand, sand/silt and silt/clay boundaries were 1 mm, 0.1 mm, and 0.01 mm, respectively. Since this paper I will use the classification by Frolov (1995) in which these boundaries are 2 mm, 0.05 mm, and 0.001 mm, respectively. From the one hand, this classification is closer to the nature of sedimentation processes (for example, to the behavior of different grain-size fractions during transportation by currents). From the other hand, the classification is not so far from traditional western classifications with boundaries 2 mm, 0.63 mm, 0.002 mm, respectively. It allows to make a better comparison of Russian and western results of grain-size analysis.

Results

Grain-size composition

Results of grain-size analyses are shown in Table 6-3 and Figure 6-11. I should note that areas of ancient bedrock outcrops (FIIC/1 and FIIC/1) are not reflected in the data. There is also no full characteristics of FIIC/2-3 sediments because in many places they contain Mn nodules of pebble size (see areas of Mn nodule distributions in the atlas of

Gurevich, 1995). Furthermore, water depth of the Yenisei profile does not exceed 70 meters (6 m at St. 15 to 66 m at St. 36).

Nevertheless, facies variability along the Yenisei profile is quite obvious. Pure river sediments (FIIA/2) are strongly enriched by pebble, gravel and sand (in sum ca. 90%). Among FIIB facies, southernmost facies of mixing zone (FIIB/1) has the smallest content of clay fraction and the highest one of sand and silt fractions. It seems that we can reveal proximal facies (more coarse) located near Yenisei River delta, and distal facies (more fine) located northward. At Stations 22 and 23 light enrichment of sand can be attributed to their small distance from the Taymyr Peninsula coast. Products of coastal abrasion could accumulate by means of different sedimentation processes including, for example, the melting of fast ice. Clayey silts dominate among FIIB/2 facies.

Totally different grain-size composition of FIIC/2-3 and FIIC/4 facies is excellently expressed in Figure 6-11. Sometimes different sedimentation processes can result in similar grain-size composition. From one hand, some FIIC/2-3 sediments are similar to FIIB/1 sediments (compare data for stations 17 and 7). This may suggest that sediments of Station 7 belong to FIIC/2 facies. Earlier I mentioned that there were very large gradients of grain-size composition along boundaries between areal and linear facies in FIIC subzone. The difference between relatively coarse surface sediments from box-corer (Station 7) and more or less fine sediments from Site 7 coretop (see Stein and Levitan, this vol.) may reflect this gradient. On the other hand, some FIIB/2 sediments are similar to FIIC/4 sediments (compare Stations 13 and 5). If sediments of Station 13 have been accumulated as result of fresh and sea water mixing, the origin of Station 5 sediments is due to accumulation of fine (clay and silt) fractions winnowed from sediments of surrounding areas, and riverine matter plays not so important role. One can suggest that in such case differences in mineral or chemical composition should be more obvious than grain-size composition.

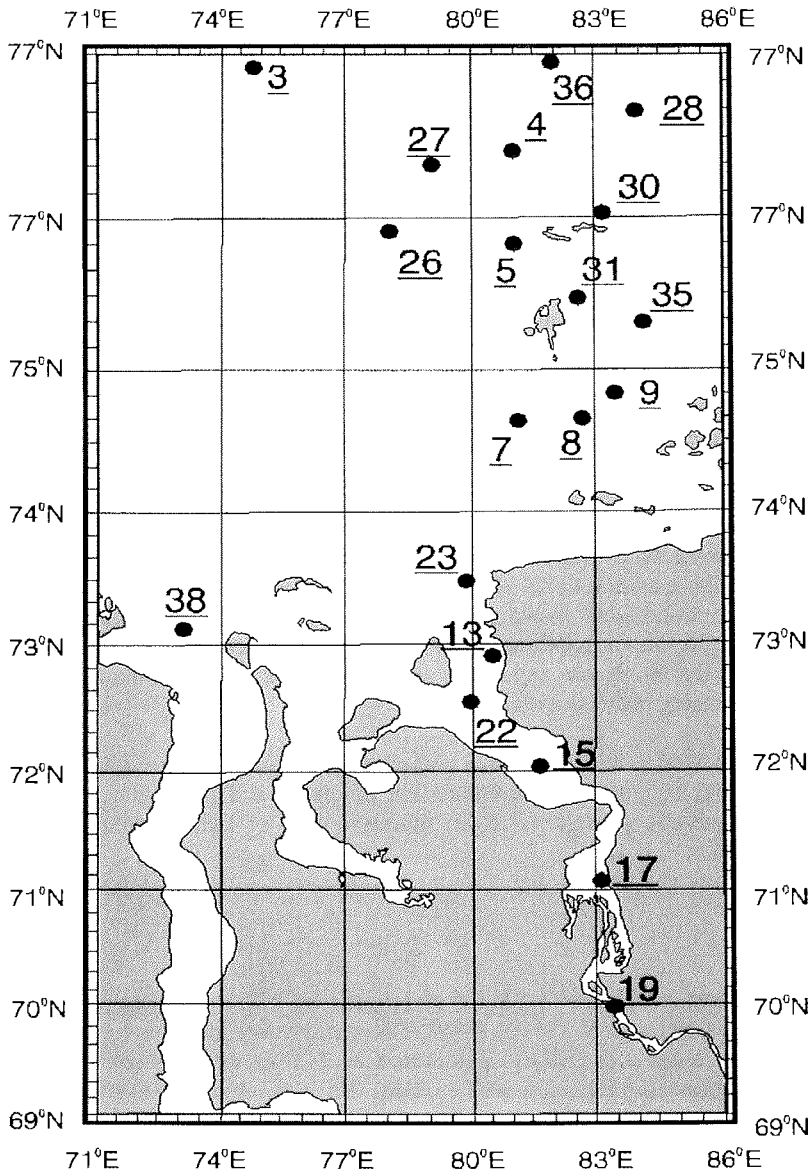


Fig. 6-10: Location map for studied surface sediment samples. Numbers – 35 cruise of R/V “Akademik Sergey Vavilov” stations

Light minerals

Results of light mineral analysis are shown in Table 6-4 and Figure 6-12. Light minerals dominate in fraction 0.1-0.05 mm: their content varies from 81.13% in river sediments (St. 19) to 99.47% in sediments of St. 31. Main minerals of light subfraction are as follows: quartz, potassium feldspars (with $n < 1.54$), lithoclasts. Plagioclases have a much smaller content (less than a few percent). The term "lithoclasts" in this paper means a large group of rock grains (mainly), undetermined light minerals (for example, peliticized feldspars), grains with Fe oxide coatings, etc. In FIIA and FIIB subzones content of lithoclasts has a positive correlation with sand+silt concentration but FIIC sediments have another characteristics. Content of lithoclasts exceeds an amount of quartz in the most of FIIA and FIIB sediments (with exception of St. 13) (Fig. 6-12).

In all sediments quartz content is more than the amount of feldspars, and the Q/FSp ratio exceeds 1.0: more than 2.0 at St. 19, 23, 7, 5, 4 and between 1.0 and 2.0 at St. 17, 15, 22, 13 and 36 (Fig. 6-12). Levitan et al. (1998) have mentioned that there are at least two varieties of quartz in the surface Kara Sea sediments: supplied by Siberian rivers and produced by bottom erosion from old sediments. Thus, it is proposed that quartz in FIIA/2 and FIIB sediments is mainly derived from Yenisei River discharge (with the exception of St.23 where an additional sediment matter supply from Yamal Peninsula). The assemblage of light minerals in sediments of FIIC subfacies has a different origin. Interestingly that St. 36 has an individual assemblage which differs from St. 7, 5 and 4 (Fig. 6-12). It seems that St. 36 has an another source province for light minerals. Later we'll check this idea using heavy mineral data.

The amount of lithoclasts is too high for a correct determination of the light mineral assemblage origin but in general the combination of quartz and potassium feldspars allows to propose granitic complexes as an initial sources of light minerals in the fraction 0.1-0.05 mm.

Heavy minerals

Heavy minerals content is shown in Table 6-5 and Figure 6-13. The new data confirmed the former results of Levitan et al. (1996, 1999). That main heavy minerals for this part of the Kara Sea are: black ores (BIO_r), clinopyroxenes (ClPx), epidotes (Ep), normal hornblendes (HBl), garnet (Gr). Sometimes Fe oxides (Fe) play an important role.

It is well known that enhanced amounts of BIO_r (magnetite, titanomagnetite, ilmenite) are located just close to their sources. This trend is obvious for St. 19 (FIIA/2 sediments), St. 22 and 23 (additional supply from Yamal Peninsula), and St. 36 (Fig. 6-13). Sediments of St. 36, as mentioned earlier, differ from the more southern stations: besides of enhanced amount of BIO_r they are enriched by olivine, apatite, and rutile, and have too low concentration of garnet. The same is obvious for St. 35.

Fe oxides have highest amounts (up to 29.2%) in sediments of FIIB/1 subfacies. Such way a hydrodynamical barrier plays the most important role in their sedimentation. This proxy might be used in paleoceanographic studies of the Yenisei region.

CIPx can be considered as the main indicator for Yenisei riverine input. It's well known that their origin is related mainly to erosion of P-T trapps in Tungusian syncline of East Siberia. But these rocks also are cropping-out in Taymyr mountains and are recorded in sediment sequences of West Siberia as sills and sheets. Earlier (Levitan et al., 1996) it was shown that one of the best proxies of riverine input in the studied region is the CIPx/Ep ratio. In general this ratio is diminished northward (Fig. 6-13). Enhanced values of CIPx/Ep ratio (more than 11.0) in sediments of Stations 22 and 23 confirm the idea of additional input of sediment matter from Taymyr Peninsula. Again, sediments of St. 35 and 36 have a higher CIPx/Ep ratio than sediments of southern FIIC stations.

Normal hornblendes are enriched in FIIB/2 sediments (St. 13) but – on the other hand – in sediments of FIIC/2-3 subfacies (St. 7 and 4) as well (Fig. 6-13). The last event is typical for vast areas of the Kara Sea where old sediments were undergone to bottom erosion (Levitan et al., 1996, 1999). The enrichment of St. 13 sediments by HBI is probably due to its high buoyancy. The same behavior is observed for Ep: this mineral also has higher concentrations in St. 13 and FIIC sediments where dilution by CIPx is relatively low. Garnet demonstrates only local enrichment in Stations 29 and 31 sediments. It can be explained by local sources of the mineral.

Yenisei Profile

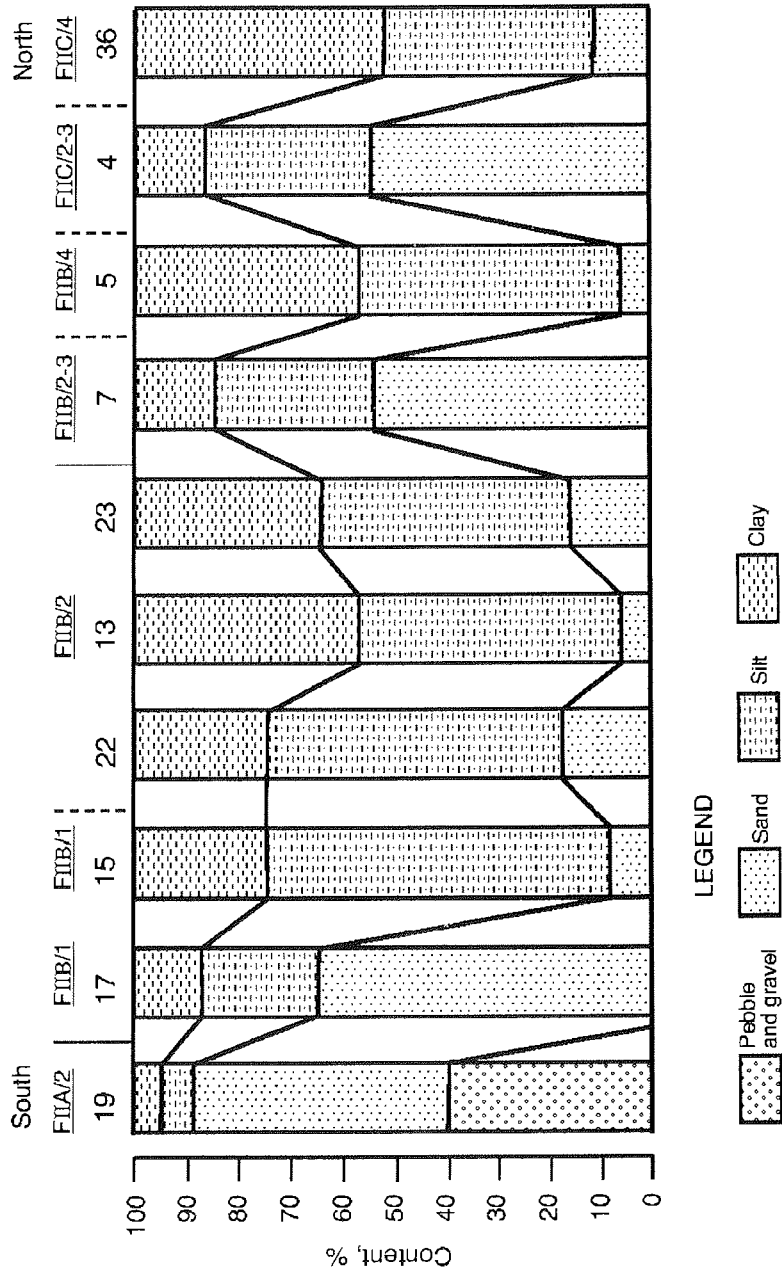


Fig. 6-11: Grain-size composition of the Yenisei profile surface sediments.

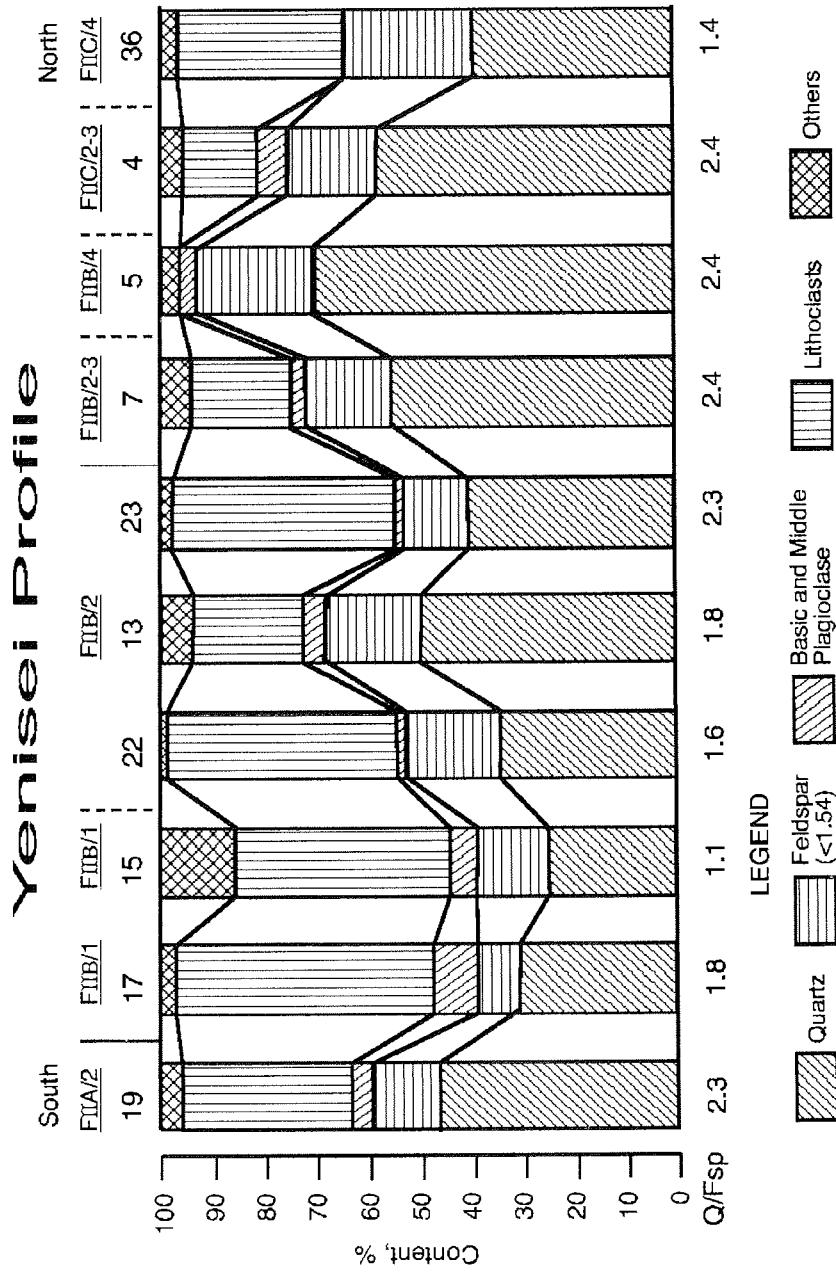


Fig. 6-12: Light minerals of the Yenisei profile surface sediments.

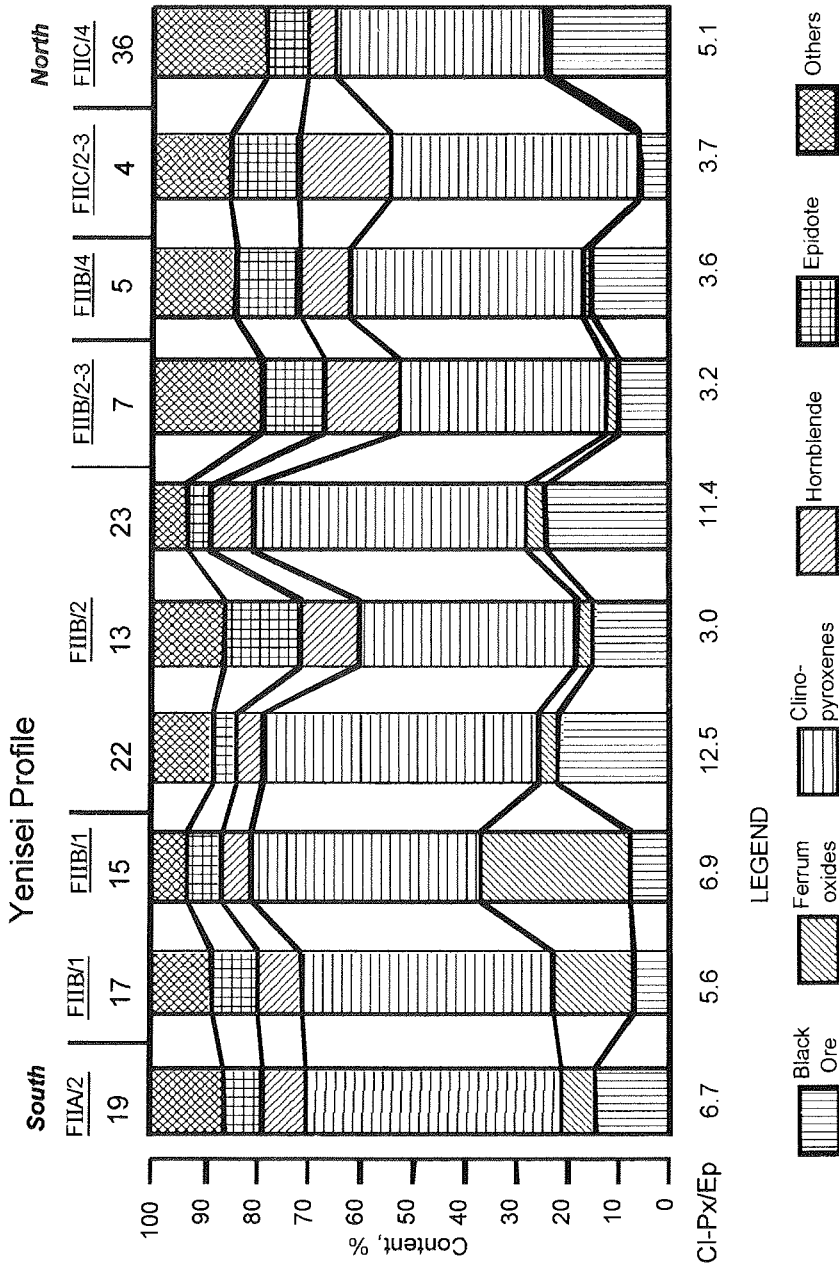


Fig. 6-13: Heavy minerals of the Yenisei profile surface sediments.

For the Yenisei profile (Fig. 6-13) three main assemblages of heavy minerals occur: BIOR-CIPx (for St. 19, 22, 23, 36), Fe-CIPx (for St. 15 and 17), and Ep-HBI-CIPx (sometimes with BIOR) for the other stations. Local sources (islands of Yenisei shoal; outcrops of old bedrocks at the sea floor, on Taymyr Peninsula, and, perhaps on Severnaya Zemlya Archipelago) also give their input in formation of composition of heavy mineral assemblages.

Conclusions

The facies zonality along the Yenisei profile has been studied using grain-size composition, light and heavy minerals in the fine sand fraction (fr. 0.1-0.05 mm). Facies pattern is due to many factors such as environment, neotectonic regime, topography, different source provinces, transportation processes, etc. From our point of view, the relative importance of used parameters as facies indicators is diminishing in the row: grain-size composition – heavy minerals – light minerals.

River sediments (FIIA/2) have the coarsest composition. The fraction 0.1-0.05 mm is strongly enriched by BIOR and CIPx. Proximal sediments of the mixing zone (FIIB/1) have a rather coarse composition and high content of Fe oxide and CIPx. In general, distal sediments of this zone have a finer composition and demonstrate the strong influence from local sediment matter sources. We have revealed a sharp differences between more coarse FIIC/2-3 and more fine FIIC/4 sediments but the composition of the fine sand fraction is more or less similar (relatively low CIPx/Ep ratio, enhanced role of HBI, etc.). According to all mineralogical data, sediments of the northernmost profile area (for example, St. 36) have their individual source province which is different from more southern areas of FIIC subzone.

One of the most reliable mineral indicators to trace Yenisei River influence is the CIPx/Ep ratio. The influence is the strongest for FIIA/2 and FIIB/1 sediments. We have to underline the great importance of sediment matter local sources related to bedrock outcrops at the sea floor, islands and adjacent land masses. The general similarity of fine sands mineral composition of St. 13, from the one hand, and St. 7, 5, 4, from the other hand, forces us to join them into one terrigenous-mineralogical province which is different from the northern province (St. 35, 36). Facies zonality and provenance have their own structure regularities.

Acknowledgements

I am grateful to the crew of R/V "Academic Boris Petrov" and my colleagues from sedimentological team for fruitful cooperation during the cruise. My special thanks to co-chief scientists O.V. Stepanets and R. Stein.

Table 6-3: Grain-size composition of the Eastern Kara Sea surface sediments (wt.%)

Site	Grain-size fractions (mm)										
	>10	10-7.	7.-5.	5.-3.	3.-2.	2.-1.	1-0.5	0.5-0.25	0.25-0.1	0.1-0.05	
BP00/03						1,91	0,24	0,61	3,27	4,2	
BP00/04						0,68	0	0,8	28,23	26,57	
BP00/05								0,05	0,68	2,64	
BP00/07						0,27	0,13	0,23	29,83	25,86	
BP00/08						0,48	0,21	0,26	3,21	5,79	
BP00/09						0,28	0	1,9	13,53	3,62	
BP00/13						1,33	0,14	0,21	1,19	1,33	
BP00/15						0,16	0,05	0,16	0,93	5,58	
BP00/17						1,47	8,04	34,32	20,48	2,7	
BP00/19	29,26	4,86	4,6	0,87	0,53	0,95	6,27	1,77	37,35	1,4	
BP00/22						2,39	0,32	1,68	7,75	4,52	
BP00/23							0,27	0	10,19	5,45	
BP00/26							0,32	0,32	1,24	1,51	
BP00/27							0,37	0,23	0,37	0,52	
BP00/28						0,47	0,24	0,77	19,3	27,44	
BP00/29						0,9	0,17	0,69	43,94	11,65	
BP00/30						1,11	0,17	0,33	3,39	10,08	
BP00/31						0,71	0,37	0,92	4,85	11,53	
BP00/35						0,2	0,27	0,27	0,62	1,52	
BP00/36						0,2	0,2	0,4	3,63	8,78	
BP00/38						0,5	0,12	0,19	1,55	2,67	

Table 6-3: cont.

Site	Grain-size fractions (mm)								
	0.05-0.01	0.01 - 0.005	0.005-0.001	<0.001	gravel and pebble	sand	silt	clay	sediment
BP00/03	3,65	24,75	30,38	30,99	0	10,23	58,78	30,99	clayey silt
BP00/04	9,5	9,26	10,88	14,08	0	56,28	29,64	14,08	silty sand
BP00/05	5,29	19,59	30,4	41,35	0	3,37	55,28	41,35	clayey silt
BP00/07	2,99	5,48	18,87	16,34	0	56,32	27,34	16,34	silty sand
BP00/08	2,46	23,8	28,73	35,06	0	9,95	54,99	35,06	clayey silt
BP00/09	1,03	18,83	23,32	37,49	0	19,33	43,18	37,49	sandy clayey silt
BP00/13	2,8	19,69	31,57	41,74	0	4,2	54,06	41,74	clayey silt
BP00/15	29,93	13,9	21,33	27,96	0	6,88	65,16	27,96	clayey silt
BP00/17	2,99	6,13	9,62	14,25	0	67,01	18,74	14,25	silty sand
BP00/19	0,13	3,27	3,92	4,88	40,06	47,74	7,32	4,88	pebble sand
BP00/22	2,65	14,09	39,43	27,17	0	16,66	56,17	27,17	clayey silt
BP00/23	5,17	21,39	21,18	36,35	0	15,91	47,74	36,35	clayey silt
BP00/26	1,44	15,65	38,17	41,35	0	3,39	55,26	41,35	clayey silt
BP00/27	0,91	19,61	35,98	42,01	0	1,49	56,5	42,01	clayey silt
BP00/28	5,79	13,36	15,77	16,86	0	48,22	34,92	16,86	silty sand
BP00/29	0,9	10,66	11,65	19,44	0	57,35	23,21	19,44	silty sand
BP00/30	4,07	9,38	29,58	41,89	0	15,08	43,03	41,89	clayey silt
BP00/31	4,85	14,29	20,12	42,36	0	18,38	39,26	42,36	silty clay
BP00/35	0,48	15,71	27,98	52,95	0	2,88	44,17	52,95	silty clay
BP00/36	8,37	7,23	24,31	46,88	0	13,21	39,91	46,88	silty clay
BP00/38	2,48	13,06	33,33	47	0	5,03	48,87	47	clayey silt

Table 6-4: Concentration of light minerals in fraction 1-0.05 mm (%).

Site	Quartz	Chaiced.	FSp<1.54	Microcline	Basic and middle Pl	Acid Pl	Biotite	Muscovite	Chlorite	Glaukonite	Serpentine	CaCO3	Undeterm. rocks and minerals	Plant rem.
BP00/03	19,4	0	3,0	0,3	1	0,3	0,3	0,3	0	0	0	0	75,4	0
BP00/04	58,6	0,6	17,7	0	5,5	1,6	0,3	0,3	0,3	0	0	0,3	14,8	0
BP00/05	54,9	0	18,3	1,1	2,2	1,1	0	0	0,5	0	0	0,5	21,4	0
BP00/07	54,9	1,1	16,6	0,6	3,2	2,9	0,6	0	0,3	0,3	0	0,6	18,9	0
BP00/08	50,4	0,8	16,5	2	6,7	1,6	0	0,8	0	0	0	0,4	20,8	0
BP00/09	50,3	0,8	17,4	0,8	6,5	2,4	0	0,4	0,4	0,4	0,4	0	20,2	0
BP00/13	49,5	0	18,9	0,9	4,3	4	0,3	0,6	0,3	0,3	0	0	20,9	0
BP00/15	24,2	0	13,7	1,6	5,3	2,1	2,1	2,6	5,3	0	0	1,1	42	0
BP00/17	29,9	1,6	8,2	0	8,6	0	0	0	0,8	0,8	0	0	50	0
BP00/19	45,7	1,5	13,5	1	4	1	0,5	0	0	0	0	0	32,8	0
BP00/22	33,5	0	19	0,3	1,3	0,3	0,3	0,3	0,3	0	0	0	44,7	0
BP00/23	39,5	0	13	0	1,5	2,5	0	0	0	0	0	0	43,5	0
BP00/26	38	0	21,7	0	0,4	1,2	0	0	0	0	0	0	38,7	0
BP00/27	31,3	0	23,7	0	3,6	0,6	0	0	1,2	0	0	0	39,6	0
BP00/28	34,3	0	25,7	0,3	0,6	0,6	0,3	0	0,6	0	0	0	37,6	0
BP00/29	48,6	0	19,2	0	1	0,3	0	0	0,3	0	0	0	30,6	0
BP00/30	26,9	0	9	0,3	0,3	0,6	0	0	0,3	0	0	0	62,6	0
BP00/31	45,7	0	13,5	0,4	0	0,4	0	0	0,4	0	0	0	39,6	0
BP00/35	46,3	0	16,5	0,3	0,3	0,6	0	0	0,3	0	0	0	35,7	0
BP00/36	39,1	0	25,4	1,5	0,6	1,2	0	0,3	0,3	0	0	0	31,6	0
BP00/38	30,1	0	13,1	0	1,4	0,3	0	0,3	0,3	0	0	0	50,1	4,9

Table 6-5: Content of heavy minerals (%) (Fr.0.1-0.05 mm).

Site	BiO	Fe oxide	Oi	CIPX	Eg	Romb Px	Norm HBI	Bas. HBI	Trem-act.	Ep	Garnet	Zr	Tormal.
BP00703	6.8	14.7	0.2	44.6	0	0.5	10	0	0.7	8.9	2.8	3	0.2
BP00704	6	0.3	0.5	48.1	0.2	1	17.4	0	1.2	13.1	3.4	2.2	0
BP00705	14.9	1.3	0.5	45.4	0	0.7	10.2	0	1.8	12.7	2.1	2	0.5
BP00707	9.3	2.8	0.6	40.1	0	0.6	14.4	0.3	1.9	12.4	2.5	0.6	0.3
BP00708	10.7	2.2	0.7	47.9	0	0.4	11.2	0.2	0.4	14.1	1.8	1.5	0.2
BP00709	10.1	1.3	1.3	48.6	0	0.6	12	0	0.3	11.4	3.6	1.4	0.6
BP00713	14.6	2.9	0.7	42.2	0	0.7	11.3	0	0.7	14.2	2.1	1.1	0.7
BP00715	7.2	29.2	1	44.4	0	0	5.8	0	0	6.4	1.8	1.4	0.2
BP00717	6.8	15.6	2.2	48.3	0	0	8.7	0	1.1	8.7	1.9	0.5	0.3
BP00719	14.5	6.3	2	48.9	0.4	0.8	9	0	0	7.3	3.2	3.2	0
BP00722	21.4	3.6	0	53.6	0	0.3	5.3	0	0	4.3	4.8	2.3	0.3
BP00723	23.5	3.5	0	51.1	0	0	8.1	0	0	4.5	1.7	2	0.5
BP00726	18.8	0.3	0	61.3	0	0.3	5.6	0	0	1.7	3.3	2.7	0.3
BP00727	35.6	3.2	0	44.4	0	0	3.2	0	0	2.7	2.7	2.1	0
BP00728	33.8	2.1	1.5	29.7	0	0.3	5.3	0	0	6.1	7.9	2.8	0.5
BP00729	36.4	2.1	0.4	22.6	0	0.2	4.2	0	0	4.8	11.6	3.8	0
BP00730	40.5	2	0	29.7	0	0.3	1.3	0	0	3.9	8.8	6.1	0
BP00731	35.4	0.7	1.6	28.9	0	0.2	1.9	0	0	8.3	12.4	5.9	0.4
BP00735	30.3	0.5	1	39.2	0	0.5	6.9	0	0	5.7	7.4	3.5	0
BP00736	22.9	1.1	4.4	40.6	0	0.5	5.2	0	0	8	0.5	3.8	0.5
BP00738	25.7	1	0	35.9	0	0.8	6.5	0	0	1.6	6.5	10.5	0

Table 6-5: cont.

Site	Ap	Sphen	Ru	Distene	Stav	Sill	Andal	Leikox	CaCO3	Chl	undeterm
BP00/03	1.6	1.6	0	0.2	0.2	0	0	0.3	0	0	3.7
BP00/04	0.8	1.4	0.4	0.2	0	0	0.2	0	0	0	3.6
BP00/05	0.8	0.8	0.3	0.3	0.3	0.3	0	0	0	0	5
BP00/07	0.6	2.5	0.3	0.3	0.3	0.3	0	0.6	0.6	0.3	8.4
BP00/08	0.7	1	0.4	0.7	0.4	0	0.2	0.2	0.4	0	4.6
BP00/09	0.6	1.7	0.3	0.3	0.3	0	0	0.3	0	0	5.3
BP00/13	1.1	1.1	0.4	0.1	0	0	0	0	0	0	5.8
BP00/15	0.6	0.6	0.2	0.2	0.2	0	0	0	0.2	0	0.6
BP00/17	0.8	0.5	0.5	0	0	0	0	0	0	0	4.1
BP00/19	0.4	2	0	0.4	0	0	0	0	0	0	1.6
BP00/22	0.6	0.3	0.3	0.6	0	0	0	0	0	0	2.3
BP00/23	0.3	0.5	0	0	0	0	0	0	0	0	1.7
BP00/26	1.3	1	0	0.7	0	0	0	0	0	0	2.7
BP00/27	1	1	0	0	0	0	0	0	0	0	3.9
BP00/28	1.3	0	0.5	0	0	0.3	0	0	0	0	7.9
BP00/29	1.4	0.7	0.7	0.2	0.2	0.7	0	2.7	0	0	7.7
BP00/30	1.3	1	0.8	0.8	0	0	0	0	0	0	3.4
BP00/31	0.7	0.5	0.5	0.5	0	0	0	0.7	0	0	1.5
BP00/35	2	0.5	0	0	0	0	0	0	0	0	2.5
BP00/36	2.4	0.8	1.1	0.3	0	0.5	0	0.5	0	0	6.9
BP00/38	1.4	1	0.2	0	0	0	0	0.8	0	0	8.1

6.5 Distribution of aquatic palynomorphs along the salinity gradient in the Kara Sea

J. Matthiessen and M. Kraus

Alfred Wegener Institute for Polar and Marine Research, Bremerhaven

In the frame of the joint Russian-German project SIRRO palynological investigations are conducted on surface sediments and sediment cores from the southern Kara Sea. Both terrestrial and aquatic palynomorphs are studied to address paleoenvironmental change in the Kara Sea during the Holocene and to establish links between the marine and terrestrial paleoclimate evolution. In order to achieve these goals the relationship between distribution pattern of pollen in modern terrestrial and marine sediments, and the ecological preferences of aquatic palynomorphs must be known. Therefore, surface sediments that were collected during expeditions of RV "Dmitriy Mendeleev" in 1993 (Lisitsyn and Vinogradov, 1995), and RV "Akademik Boris Petrov" in 1997, 1999 and 2000 (Matthiessen and Stepanets, 1998; Stein und Stepanets, 2000, this vol.) are studied for their palynomorph content to describe the distribution of palynomorphs in the estuaries of Ob and Yenisei and in the Kara Sea. Here we report on results of our ongoing studies considering only the distribution of marine dinoflagellate cysts and selected freshwater algae along the salinity gradient.

Results and Discussion

The basic methodology and initial results of the studies on the sample set from the expedition of "Akademik Boris Petrov" in 1997 are described by Matthiessen (1999) and Matthiessen et al. (2000). We supplemented this data set by further analysis of samples from the expedition of RV "Dmitriy Mendeleev" in 1993 which extends the geographical coverage from the Kara Sea southward into the inner estuaries of the rivers Ob and Yenisei and northward towards the Arctic Ocean (Fig. 6-14).

In Figure 6-15 we show the distribution of dinoflagellate cysts and of the selected chlorococcalean algae genus *Pediastrum* spp. along the Ob and Yenisei transects. Abundances of palynomorphs are expressed as concentrations per gram dry sediment. Both transects display a comparable distribution of palynomorphs. *Pediastrum* spp. is abundant in the inner estuaries and show a pronounced decline in the outer estuaries probably corresponding to the seaward boundary of the "marginal filter" (Lisitzin, 1995). Dinoflagellate cysts are inversely correlated to *Pediastrum* spp. The estuaries are marked by low concentrations increasing offshore north of 73°N.

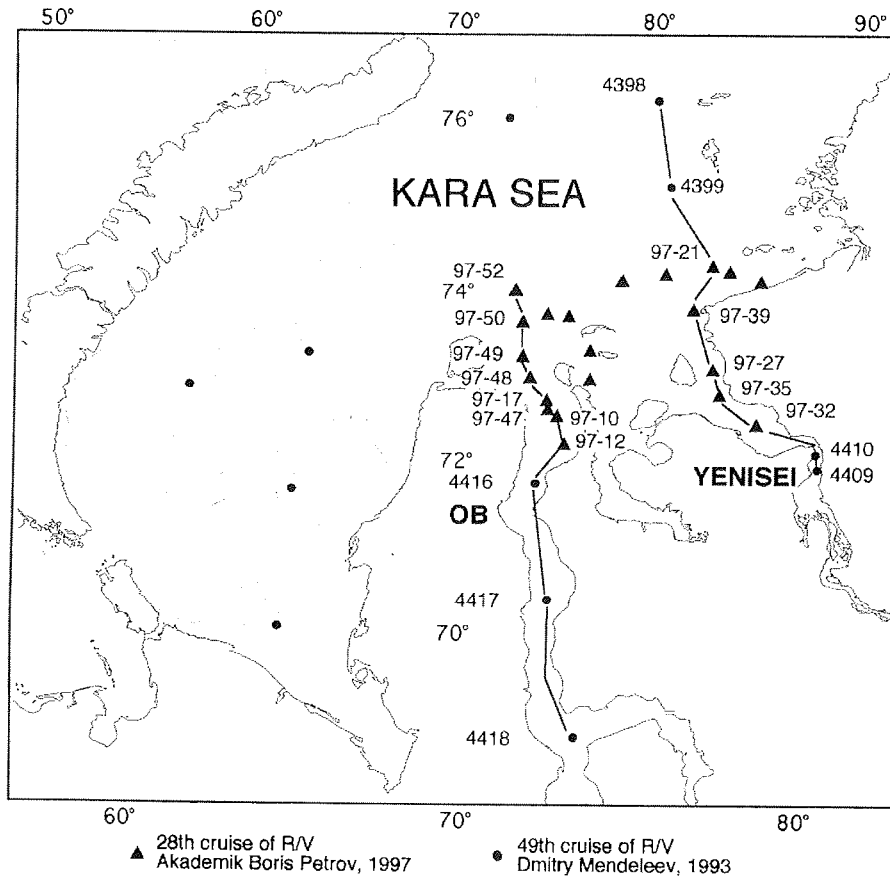


Fig. 6-14: Sample coverage in the Kara Sea. The station numbers of the selected samples along the two transects are shown. Isohalines of the surface layer are from Burenkov and Vasilkov. (1995).

These distribution patterns suggest that *Pediastrum* spp. may be a good micropaleontological marker of input of fine-grained suspension into the southern Kara Sea from the rivers Ob and Yenisei (cf. also Matthiessen et al., 2000). However, the database must be extended in order to test this assumed relationship. It could also be of some interest to analyse a seasonal cycle of input of riverine sediments and associated freshwater palynomorphs by means of sediment traps.

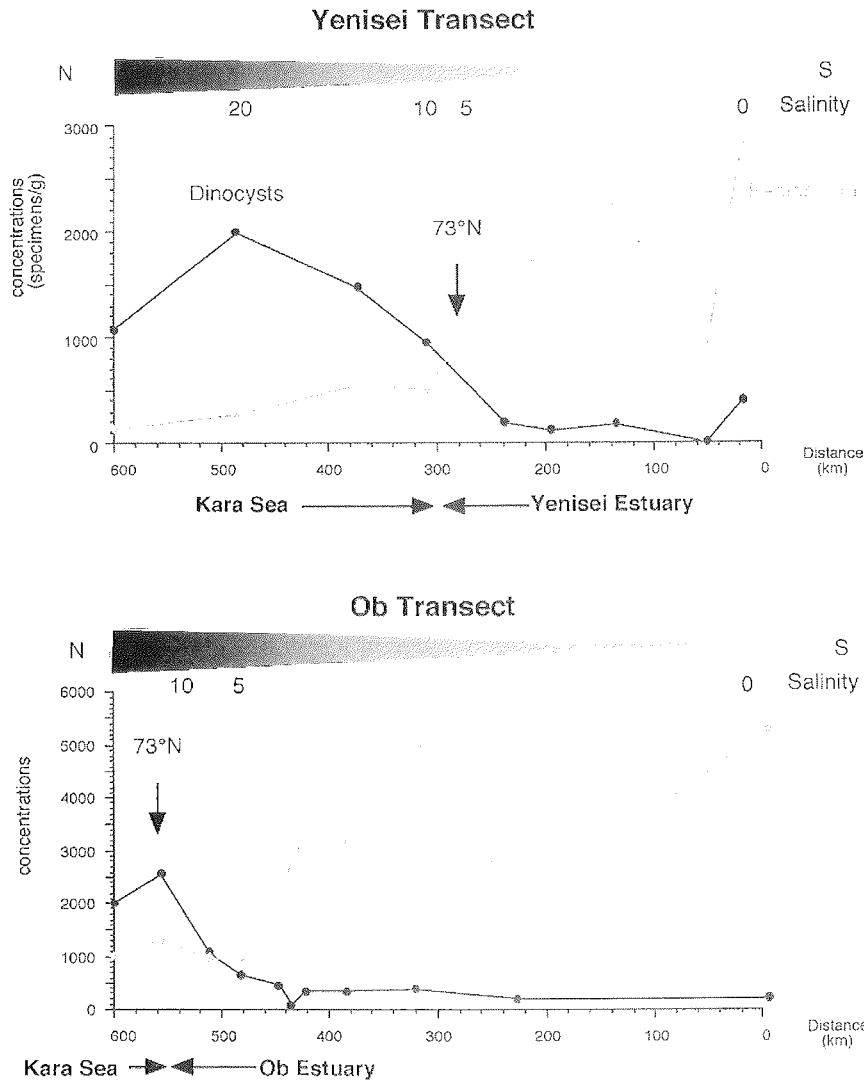


Fig. 6-15: Distribution of dinoflagellate cysts and *Pediastrum* spp. along the Ob and Yenisei transects. Salinity data are from Burenkov and Vasilkov (1995).

On the other hand, the common occurrence of dinoflagellate cysts in the inner Kara Sea show that they may be useful for paleoenvironmental reconstructions at salinities higher than 10. The occurrence in the inner estuaries, although with extremely low concentrations, suggests that marine waters may intrude occasionally from the Kara Sea into these freshwater environments.

6.6 Grain-size and sediment composition of sediment cores based on lithological core description and smear-slide estimates

R. Stein¹ and M.A. Levitan^{2,3}

¹Alfred Wegener Institute, Columbusstraße, Bremerhaven, Germany

²Shirshov Institute of Oceanology RAS, Moscow

³Vernadsky Institute of Geochemistry and Analytical Chemistry RAS, Moscow

Onboard "Akademik Boris Petrov", a selected set of sediment cores were already opened, described and sampled for smear-slide analyses. These sediment cores are situated on a S-N profile from the Yenisei Estuary towards the inner Kara Sea between 72°N and 77°N (see Fig. 6-2 for core locations). Except for the southernmost Core BP00-15/4, all other cores contain an upper clayey silt to silty clay unit (Unit I), underlain by a more coarse-grained unit (Unit II) (Fig. 6-16). Unit I is probably of Holocene age, resulting in sedimentation rates between 23 and > 66 cm/ky (for further details see Chapter 6.7).

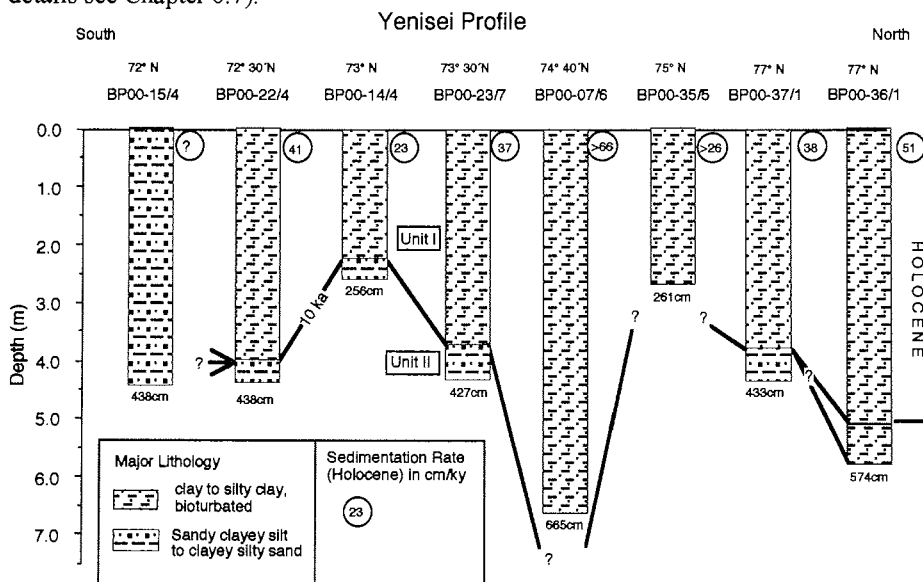


Fig. 6-16: Lithologies of sediment cores opened onboard "Akademik Boris Petrov" during the expedition. Estimates of Holocene sedimentation rates based on the assumption that Unit I represents the Holocene (i.e., the last 10000 years BP).

Based on smear slide analyses and lithological core description (cf., Annex 9.2), a first rough information about grain-size distribution and sediment composition could be obtained.

Core BP00-15/4

The southernmost Core BP00-15/4 consists of very dark grayish brown, olive gray, and very dark gray clayey sandy silt to clayey silty sand (Fig. 6-17). Maximum silt content was determined in the lower part of the core. Quartz is the dominant mineral throughout

the core (up to about 50%). The next important compounds are feldspars and rock fragments (10-20%). Heavy minerals reach values between 1 and <10%. The content of clay minerals seems to be decreased in the lower part of the sequence. Significant amounts of diatoms and plant debris occur throughout the core.

Core BP00-22/4

The sediments of Core BP00-22/4 are mainly olive gray, very dark gray and black bioturbated silty clays (Unit I; Fig. 6-16); the sand content is mainly < 5% (Fig. 6-18). In the lowermost part (> 400cm; Unit II), the sand content increases ("clayey silty sand"). Clay minerals are the dominant fraction in Unit I (40-60%), followed by the mineral quartz (20-25%). Quartz always occur in higher amounts than feldspars. Heavy minerals and rock fragments reach values of 1-5%. The content of diatoms is very variable (1-10%). In Unit II, the content of quartz, feldspars, and rock fragments are similar; each component occurs in percentages of about 20%. Clay minerals decreases to about 15%. In comparison to Unit I, the amount of plant debris is significantly higher (10%).

Core BP00-14/4

Core BP14/4 consists of an upper Unit I dominated by olive gray to dark olive gray bioturbated silty clay, and a lower Unit II composed of clayey silty sand (Figs. 6-16 and 6-19). Silty laminae occur between 25 and 65 cm. Clay minerals (45-60%) and quartz (20-30%) are the most important compounds of Unit I (Fig. 6-19). Feldspars, rock fragments, and heavy minerals occur in amounts of about 3-10% each. Diatoms and plants debris are less important (< 2%). In the more sandy Unit II, quartz increases to values of 40-50% whereas clay minerals decrease to < 30%.

Core BP00-23/7

Core BP00-23/7 is composed of dark olive gray, very dark gray, and black bioturbated silty clay (Unit I, 0-374 cm), and clayey silty sand (Unit II; below 374cm) (Figs. 6-16 and 6-20). Unit I mainly consists of clay minerals (30-60%) and quartz (20-35%). Feldspars reach values of 10-15%. Rock fragments and heavy minerals only occur in percentages of <10%. In Unit II, quartz and rock fragments become the dominant compounds. Plant debris increases towards the lower part of the core.

Core BP00-07/6

Core BP00-07/6 only consists of dark olive gray, very dark gray, and black bioturbated silty clay (Unit I; Fig. 6-16). Clay minerals (about 35-60%) and quartz (30-40%) are the most important components (Fig. 6-21). All other minerals only occur in amounts of <10%.

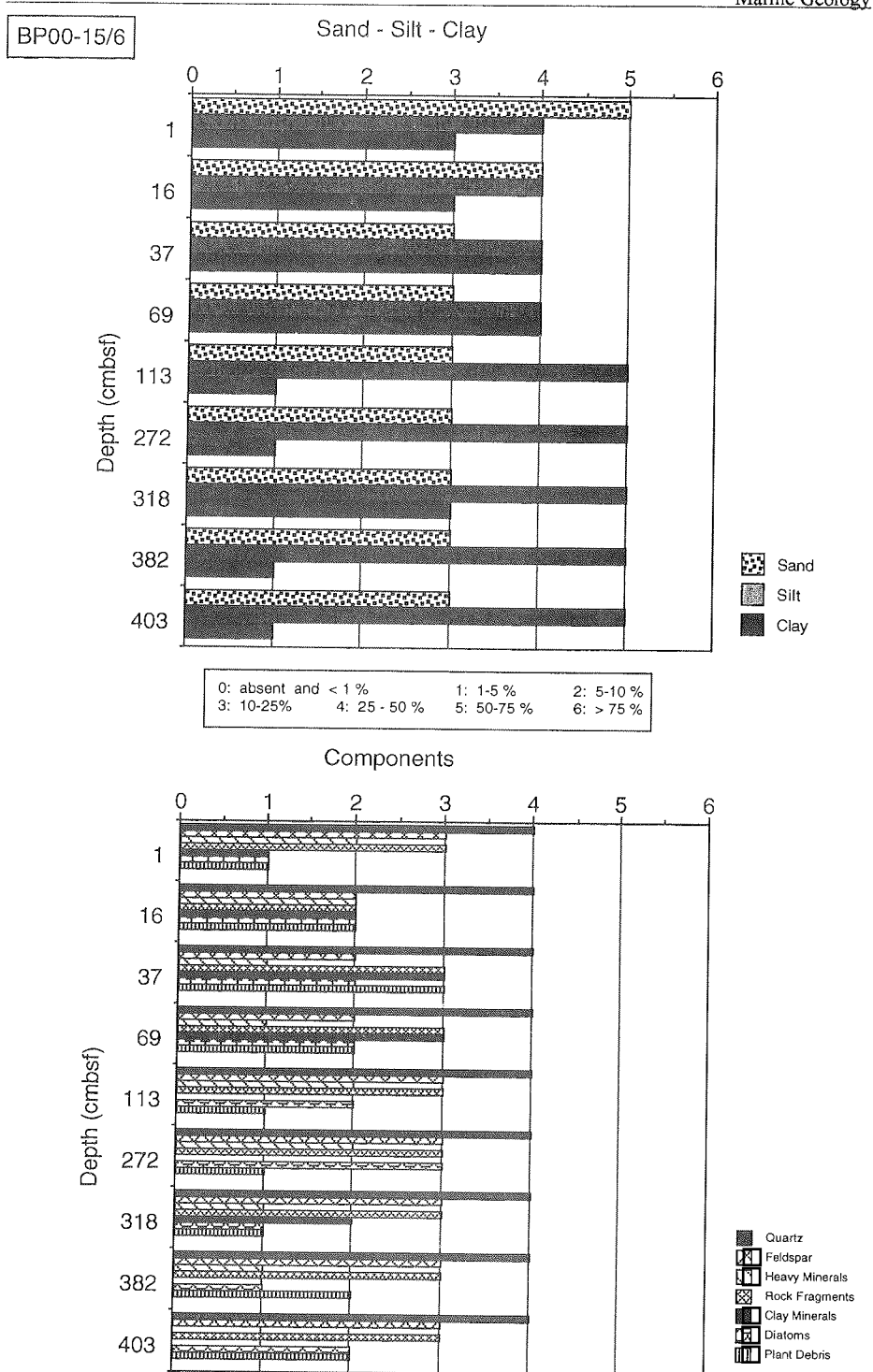


Fig. 6-17: Grain size and composition of selected samples from Core BP00-15/6, based on smear-slide estimates.

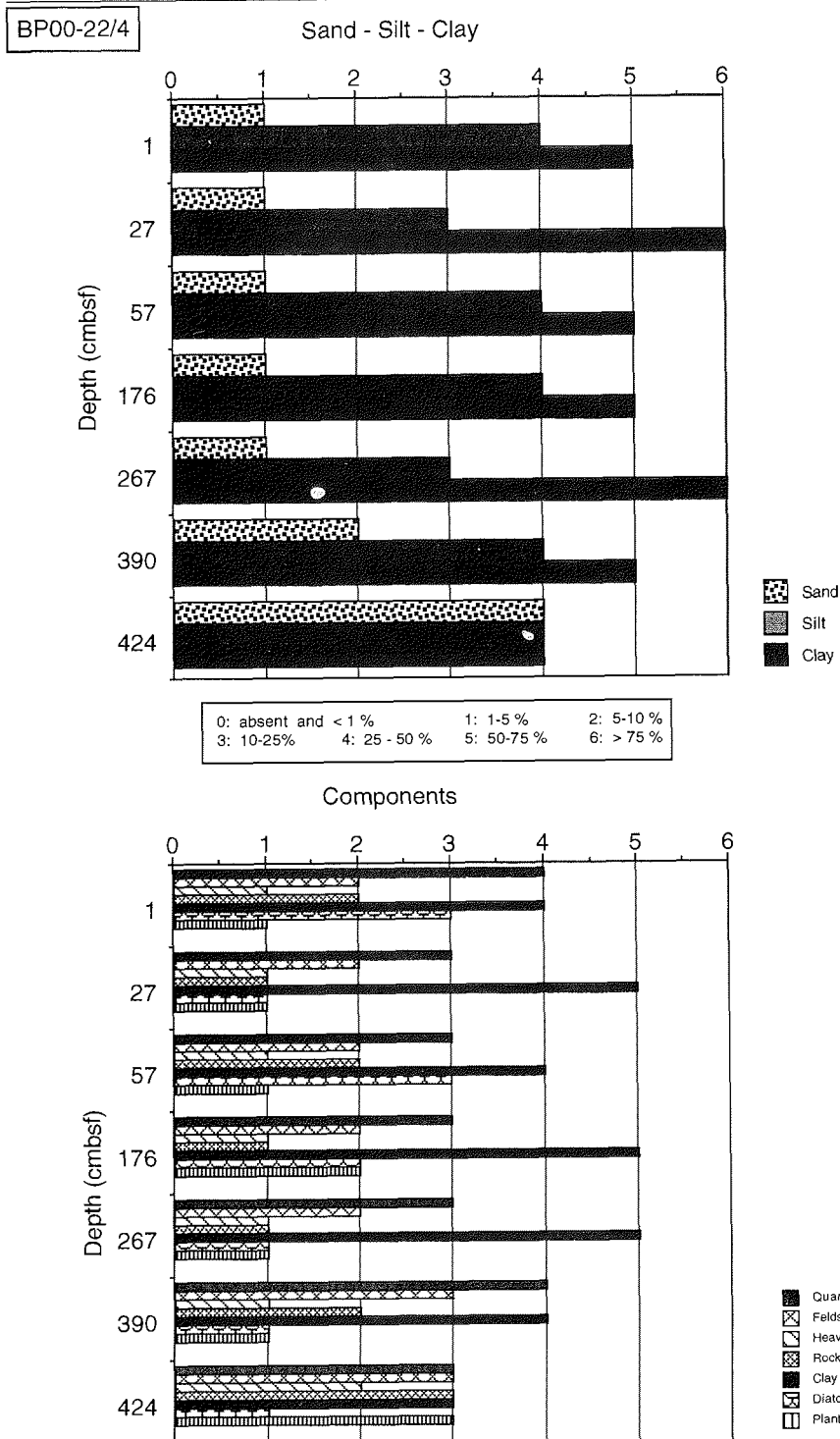


Fig. 6-18: Grain size and composition of selected samples from Core BP00-22/4, based on smear-slide estimates.

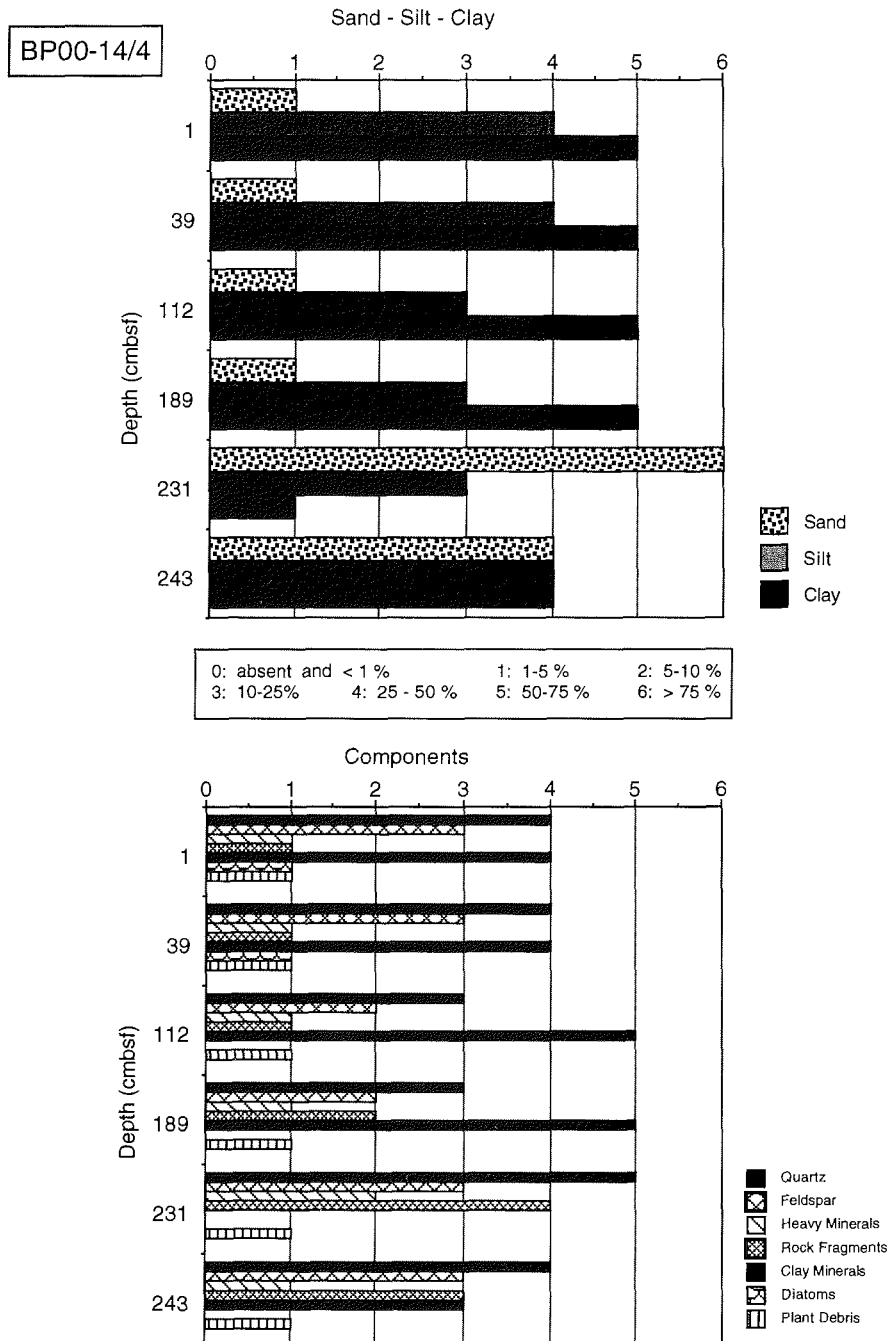


Fig. 6-19: Grain size and composition of selected samples from Core BP00-14/4, based on smear-slide estimates.

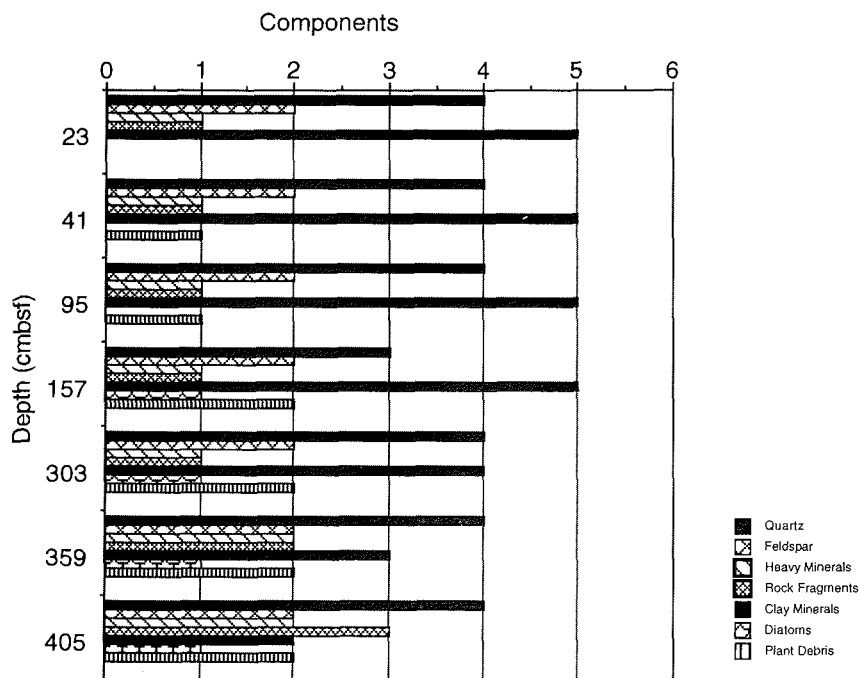
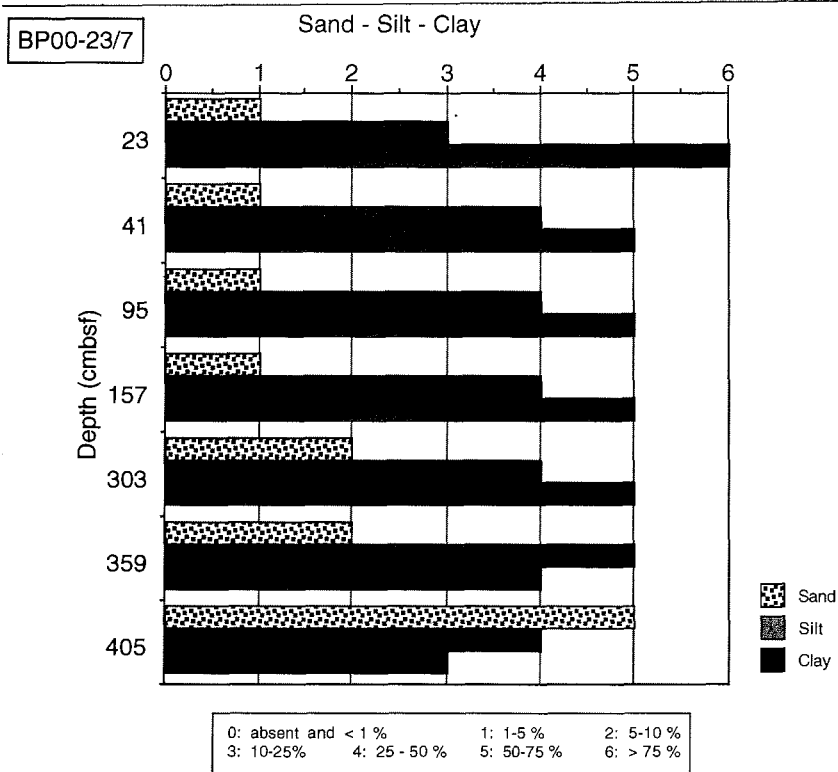


Fig. 6-20: Grain size and composition of selected samples from Core BP00-23/7, based on smear-slide estimates.

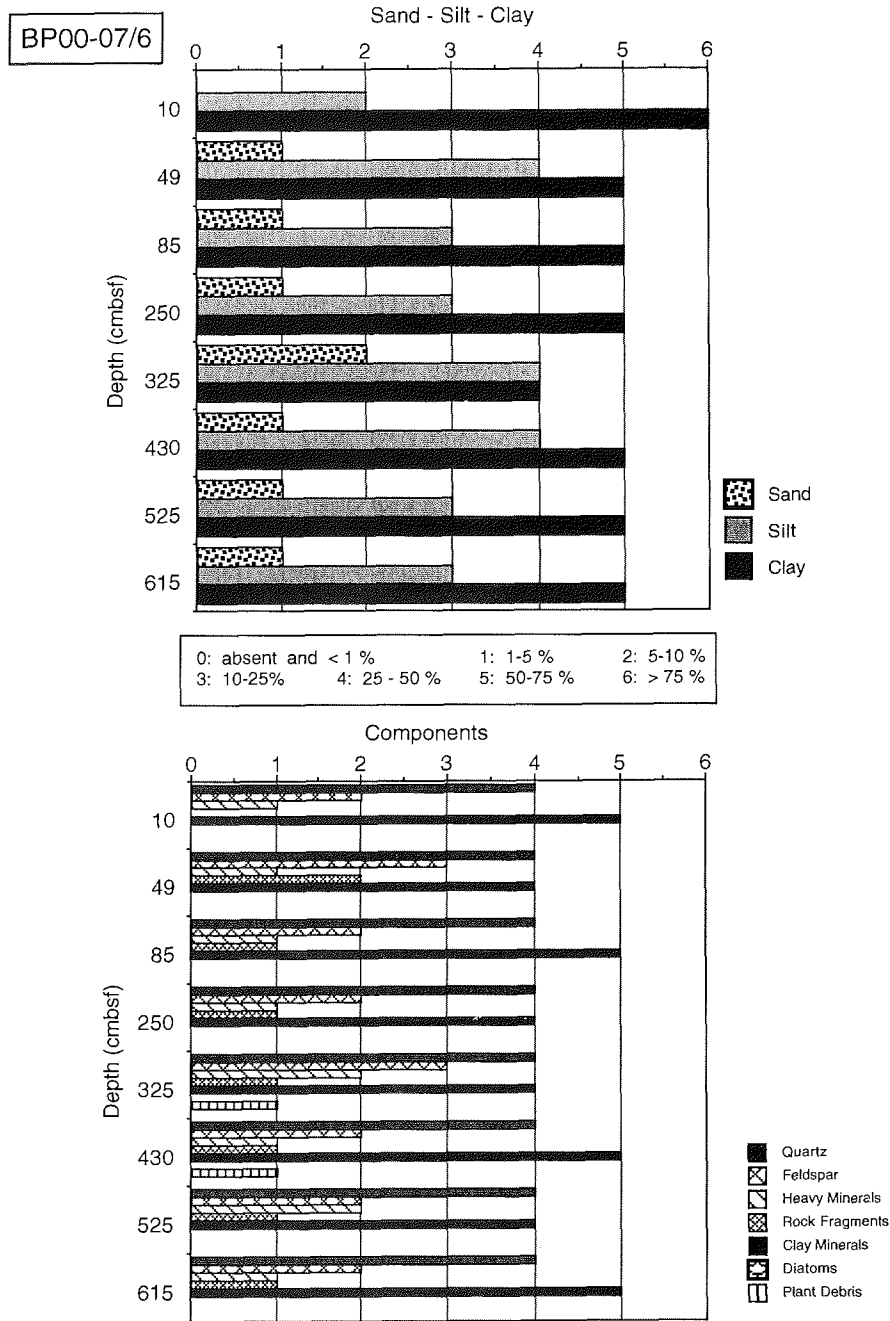


Fig. 6-21: Grain size and composition of selected samples from Core BP00-07/6, based on smear-slide estimates.

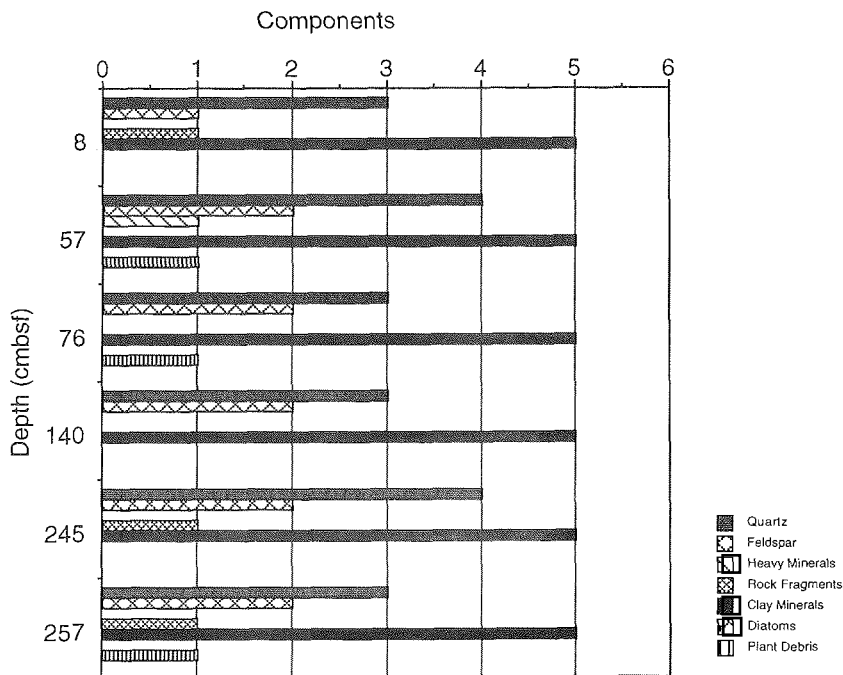
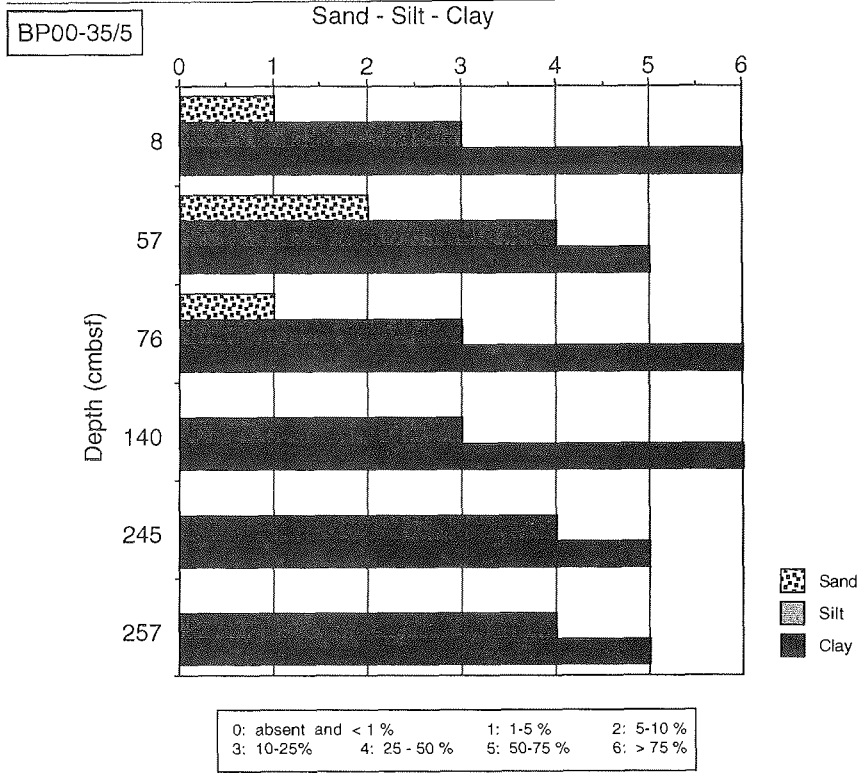


Fig. 6-22: Grain size and composition of selected samples from Core BP00-35/5, based on smear-slide estimates.

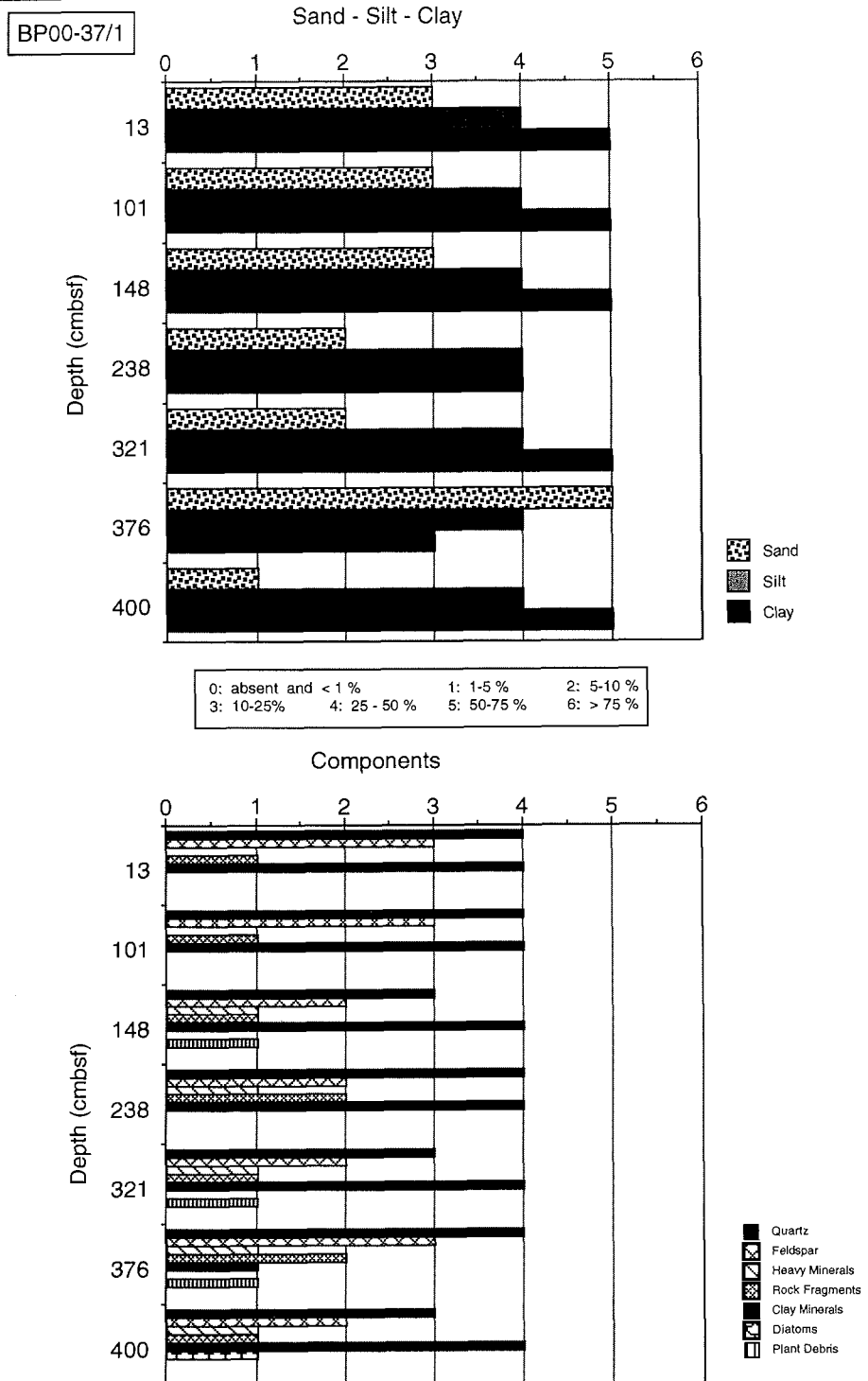


Fig. 6-23: Grain size and composition of selected samples from Core BP00-37/1, based on smear-slide estimates.

Core BP00-35/5

As Core BP00-07/6, Core BP00-35/5 only consists of dark olive gray, very dark gray, and black bioturbated silty clay; sand is mostly absent (Fig. 6-22). Clay minerals (60-70%) are predominant. Quartz and feldspars reach values of 20-25% and 5-10%, respectively. All other compounds are insignificant (<2%).

Core BP00-37/1

The sediments of Core BP00-37/1 are composed of dark gray to black silty clay (Unit I), underlain by sandy silty clay with frequent sandy layers (Unit II) (Fig. 6-23). The silty clay and sandy silty clay sediments consist of clay minerals (35-50%), quartz (15-30%), and feldspars (5-15%), respectively (Fig. 6-23). All other compounds only occur in values <5%. The sandy layers have a different composition. Quartz (45%), feldspars (25%), and rock fragments (15%) are the three most important components whereas clay minerals decrease to about 5%.

Before an interpretation of the sediment composition in terms of sedimentary facies variability (cf., Chapter 6.4) and depositional environment is possible, more precise data on grain size and mineralogical composition using more sophisticated techniques (e.g., microscopy of heavy minerals, X-Ray diffraction, etc.) as well as a stratigraphic framework have to be produced.

6.7 Lithostratigraphy of gravity cores and correlation with sediment echograph profiles ("Akademik Boris Petrov" Kara Sea expeditions 1999 and 2000)

R. Stein

Alfred Wegener Institute, Columbusstraße, Bremerhaven, Germany

Introduction

During the "Akademik Boris Petrov" Kara Sea Expedition a total of 35 gravity cores with lengths between 0.5 and 7.3 meters were obtained (Fig. 6-24; cf. Fig. 6-3). Onboard "Akademik Boris Petrov", a selected set of eight sediment cores were already opened, described and sampled for smear-slide analyses (see Chapter 6.6). All other cores were opened, photographed, and described at AWI. Color slides from the core sections are available at AWI (request to R. Stein, AWI). Furthermore, from all these cores sediment slabs were taken for X-Ray photographs. In most of the cores, abundant bivalves were found which were sampled for future AMS¹⁴C dating (Table 6-6; cf. Figs. 6-25 to 6-30).

The main purpose of this chapter is (1) to summarize the major lithologies of the sedimentary sequences based on lithological core descriptions, (2) to obtain a lithostratigraphic framework, (3) to correlate selected sediment cores with ELAC sediment echograph profiles obtained during the "Akademik Boris Petrov" 1999 Expedition (cf., Stein and Stepanets, 2000), and (4) to give a first rough estimate of Holocene sedimentation rates. These data should be the basis for future sampling and more detailed sedimentological, micropaleontological, and geochemical studies of the BP2000 sediment cores. The complete core descriptions are presented in the appendix 9.2.

Lithostratigraphy

For presentation and description of the major lithologies, the sediment cores are grouped into six transects (Transects A to F; Fig. 6-24).

In the northern Ob Estuary, a 6.5 m long sediment core was obtained (Transect A, Core BP00-38/2; Fig. 6-25). The sedimentary sequence can be divided into two lithological units. The upper about 6.3 meters consist of bioturbated silty clay to clayey silt with bivalves occurring almost throughout the unit. Thin silty-sandy layers are obvious at 132 cm and 352 cm core depth. The lowermost 22 cm are more sandy sediments (Unit II). In Core BP00-02/4 situated in the southern Kara Sea north of the Ob Estuary, the thickness of the upper silty-clayey unit is much more reduced (about 30 cm; Fig. 6-25). In the lower part of the only 70 cm long core, abundant sandy intervals occur (Unit II).

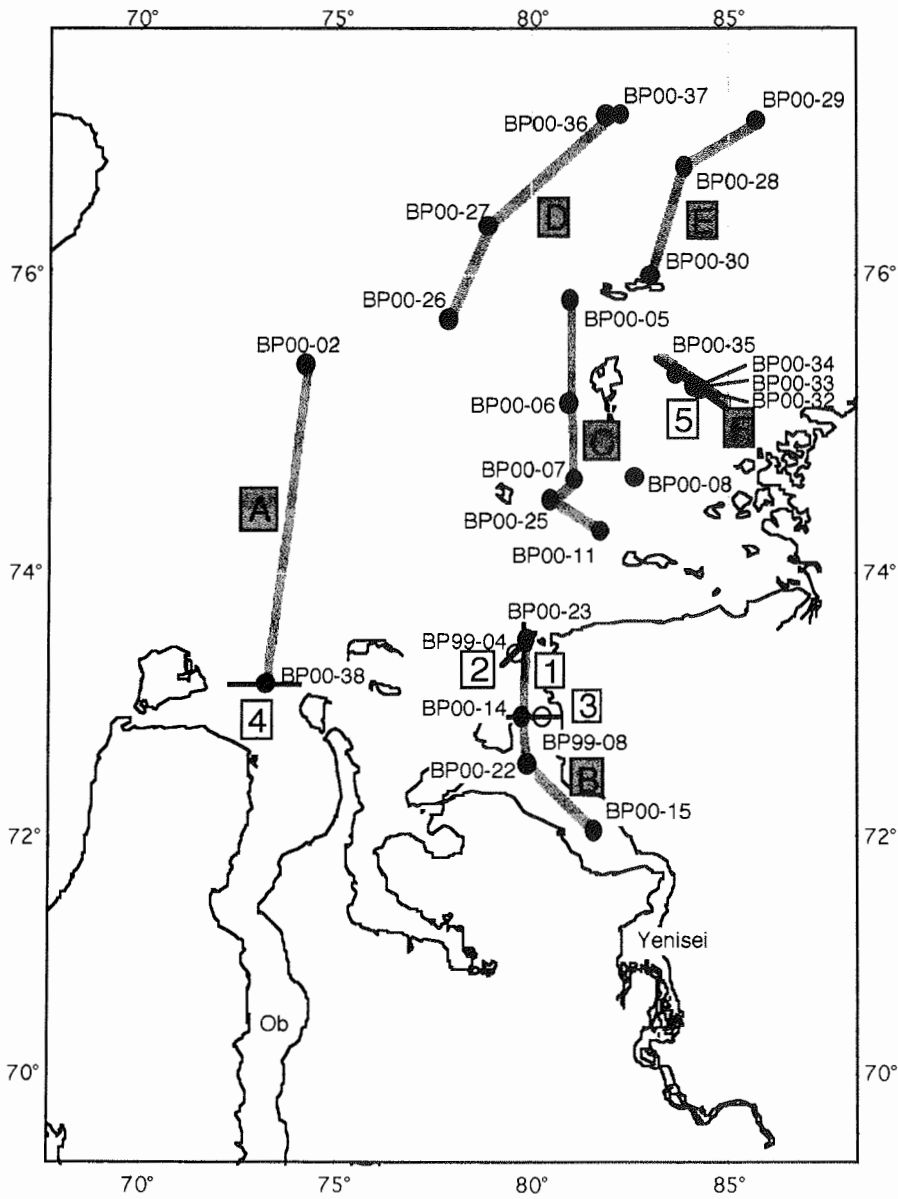


Fig. 6-24: Location of gravity cores obtained during "Akademik Boris Petrov" Expedition 2000. In addition also the position of cores BP99-04 and BP99-08 are shown. A to F indicate transects for which the lithologies are shown in Figures 6-25 to 6-30. Numbers 1 to 5 indicate ELAC sediment echograph profiles presented in Figures 6-30 to 6-34.

Table 6-6: Compilation of all bivalve samples taken from the sediment cores (available for AMS¹⁴C datings and studies of bivalves).

BP'00-06/1 SL		BP'00-14/3 SL		BP'00-27/3 SL		BP'00-32/1 SL	
no	depth (cm)	no	depth (cm)	no	depth (cm)	No	depth (cm)
1	7	1	56	1	66	1	114
2	23	2	68	2	81	2	118
3	35	3	182,5	3	84	3	226
BP'00-07/7 SL		4	183	4	91	4	231
no	depth (cm)	5	223	5	95	5	238
1	01. Mrz	BP'00-15/5 SL		6	98	6	261
2	31	no	depth (cm)	7	101	7	276
3	120	1	247.5*	8	229	8	277
4	125	BP'00-22/5 SL		9	293	9	298,5
5	131-133	no	depth (cm)	10	322	10	312
6	135	1	5	11	375	11	317
7	201	2	10,5	12	507	12	326
8	220	3	139	13	632	13	327
9	239	4	195,5	14	637	14	331
10	254	5	256	BP'00-28/4 SL		15	337
11	280	6	376	no	depth (cm)	16	338
12	325	BP'00-23/6 SL		1	15	17	346
13	326	no	depth (cm)	2	44	18	348
14	330	1	37	3	55	19	350
15	335	2	44	4	107	20	359
16	406,5	3	73	5	118	21	361
17	461	4	88	BP'00-29/4 SL		22	362
18	488	5	102	no	depth (cm)	23	367
19	559	6	107	1	65	24	377
20	580	7	113,5	2	69,5	25	388,5
21	581	8	133	3	71	26	407,5
22	586	9	137	4	80-85	27	412
23	625	10	143	5	88	28	432
24	628	11	181	6	104	29	506
25	650	12	263	7	121	30	533
26	652	13	369*	8	124	31	547
27	661	14	397*	9	138	BP'00-32/1 SL	
28	663	BP'00-25/1 SL		10	145,5	No	depth (cm)
29	671	no	depth (cm)	11	150	1	114
30	690	1	70	12	161,5	2	118
31	690	2	73	13	162	3	226
32	700	3	77	14	166	4	231
BP'00-08/4 SL		4	88	15	306-307	5	238
no	depth (cm)	5	114	16	313,5	6	261
1	12	6	116	BP'00-30/3 SL		7	276
2	80	7	122	no	depth (cm)	8	277
BP'00-11/1 SL		BP'00-26/4 SL		2	94	9	298,5
no	depth (cm)	No	depth (cm)	3	104	10	312
1	18	1	87	4	118,5	11	317
2	81	2	128	5	125	12	326
3	104	3	173,5	6	136	13	327
4	151	4	257	7	140,5	14	331
5	151	5	276	8	145	15	337
6	163	6	301	9	153	16	338
7	184	7	300-302	10	221	17	346
8	192	8	324-329	11	536	18	348
9	206	9	341	12	595	19	350
10	206	10	349	13	627,5	20	359
11	226	11	356-358	14	651	21	361
12	227	12	357	BP'00-32/1 SL		22	362
13	238,5	13	375,5	No	depth (cm)	23	367
14	240	BP'00-26/4 SL		1	114	24	377
15	258	1	87	2	118	25	388,5
16	258,5	2	128	3	226	26	407,5
17	259	3	173,5	4	231	27	412
18	289	4	257	5	238	28	432
19	306,5	5	276	6	261	29	506
20	317	6	301	7	276	30	533
		7	300-302	8	277	31	547
		8	324-329	9	298,5		
		9	341	10	312		
		10	349	11	317		
		11	356-358	12	326		
		12	357	13	327		
		13	375,5	14	331		
				15	337		
				16	338		
				17	346		
				18	348		
				19	350		
				20	359		
				21	361		
				22	362		
				23	367		
				24	377		
				25	388,5		
				26	407,5		
				27	412		
				28	432		
				29	506		
				30	533		
				31	547		

Table 6-6: cont.

BP'00-34/1 SL		BP'00-36/4 SL		BP'00-38/2 SL	
No	depth (cm)	No	depth (cm)	No	depth (cm)
1	44,5	1	12,5	1	7
2	46,5	2	23	2	10
3	61	3	24,5	3	43,5
4	68,5	4	27	4	45
5	81	5	33	5	114
6	98	6	42	6	160
7	103	7	44	7	166,5
8	105	8	59	8	179,5
9	107	9	70	9	190
10	112	10	73	10	213
11	115	11	77	11	213,5
12	116,5	12	82	12	228
13	123,5	13	99,5	13	249,5
14	127,5	14	100	14	250
15	131	15	115	15	250-251
16	135	16	120,5	16	265
17	136	17	130	17	287,5
18	141	18	131,5	18	290
19	155,5	19	136	19	296,5
20	168	20	139,5	20	300
21	198	21	142,5	21	309,5
22	207	22	144	22	310
23	215	23	150	23	321
24	222	24	150,5	24	331
25	231	25	156,5	25	341
26	243	39	297	26	349
27	254	26	159	27	351
28	258	27	161	28	355
29	268	38	278,5	29	372
30	270	28	180	30	381
31	271,5	29	187	31	408,5
32	275	40	330	32	457
33	284,5	30	190	33	462
34	292	31	197	34	481
35	300	32	199	35	483
36	301,5	33	212,5	36	495
37	306	34	222	37	505
38	310	35	240	38	507
39	323	36	251	39	510
40	332	37	261	40	520
41	342	41	365	41	533
42	399	42	395,5		
		43	397		
		44	402		
		45	408,5		
		46	483*		
		47	509		
BP'00-35/6 SL					
No	depth (cm)				
1	15				
2	20				
3	63				
5	125				
6	127,5				
7	129,5				
8	130-131				
9	130-133				
10	145				
11	146				
12	171				
13	187				
14	203				
15	203				
16	205,5				
17	218				
18	236				
19	237				
20	243				
21	248				

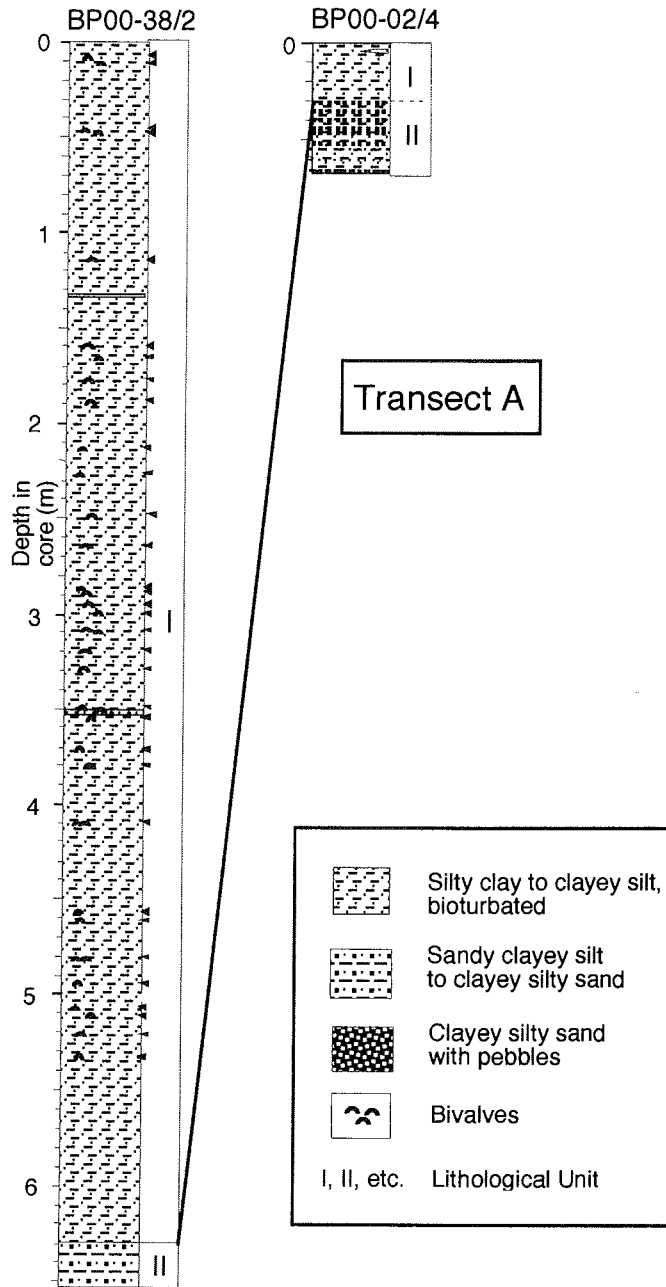


Fig. 6-25: Lithologies of sediment cores from Transect A. For location of transect see Fig. 6-24.

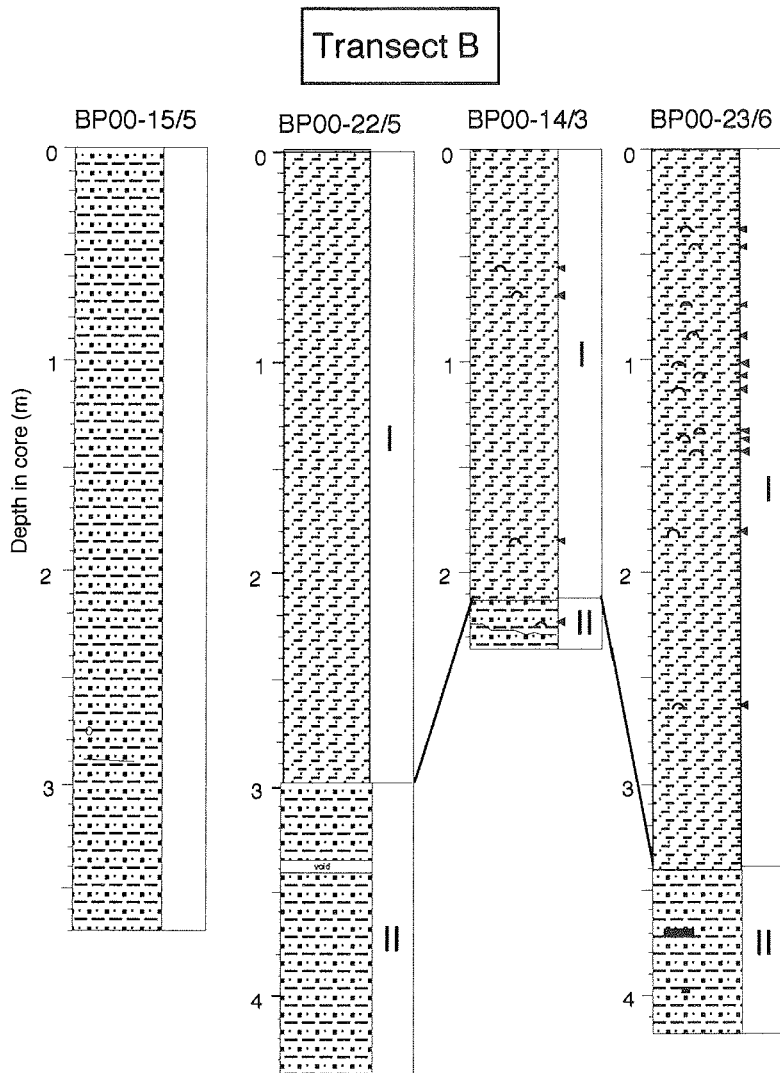


Fig. 6-26: Lithologies of sediment cores from Transect B. For location of transect see Fig. 6-24, for legend see Fig. 6-25.

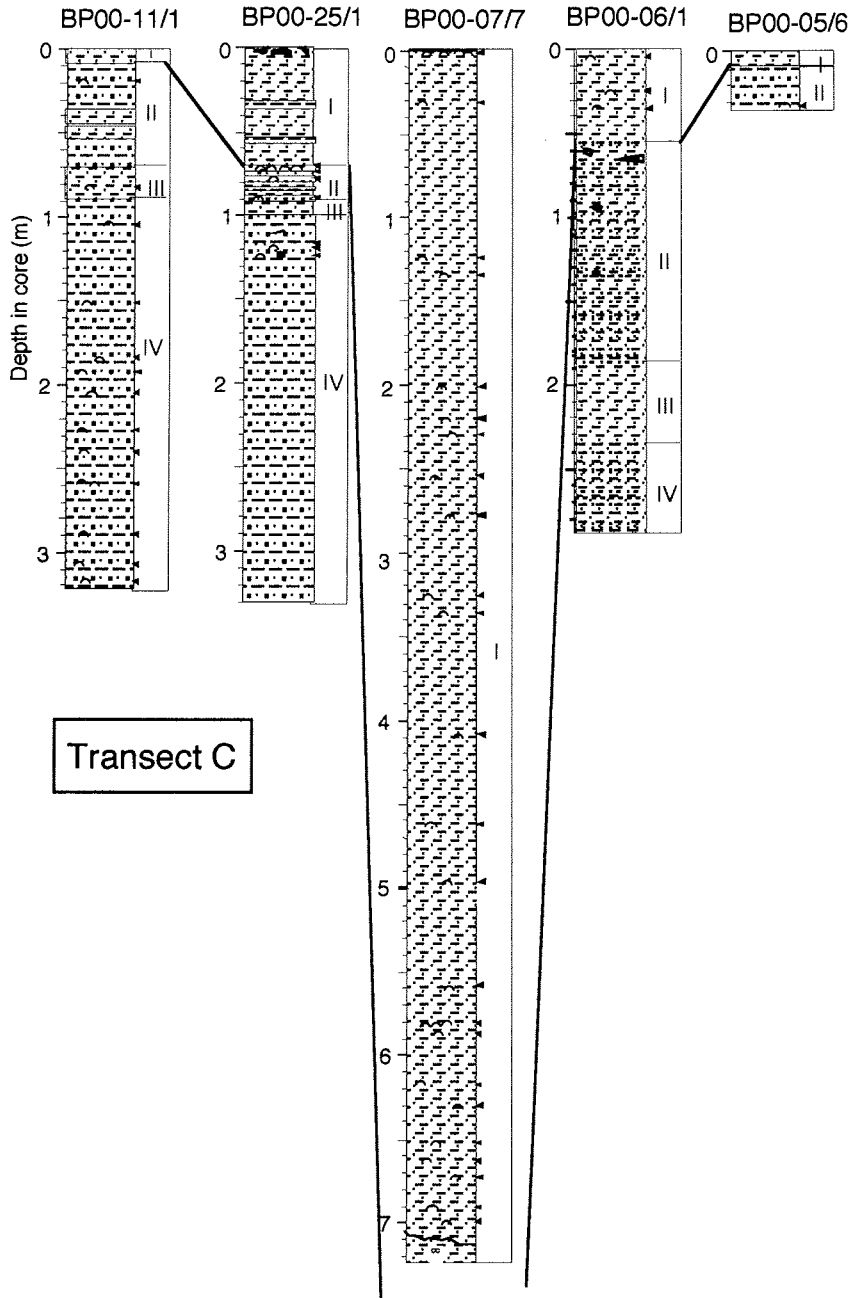


Fig. 6-27: Lithologies of sediment cores from Transect C. For location of transect see Fig. 6-24, for legend see Fig. 6-25.

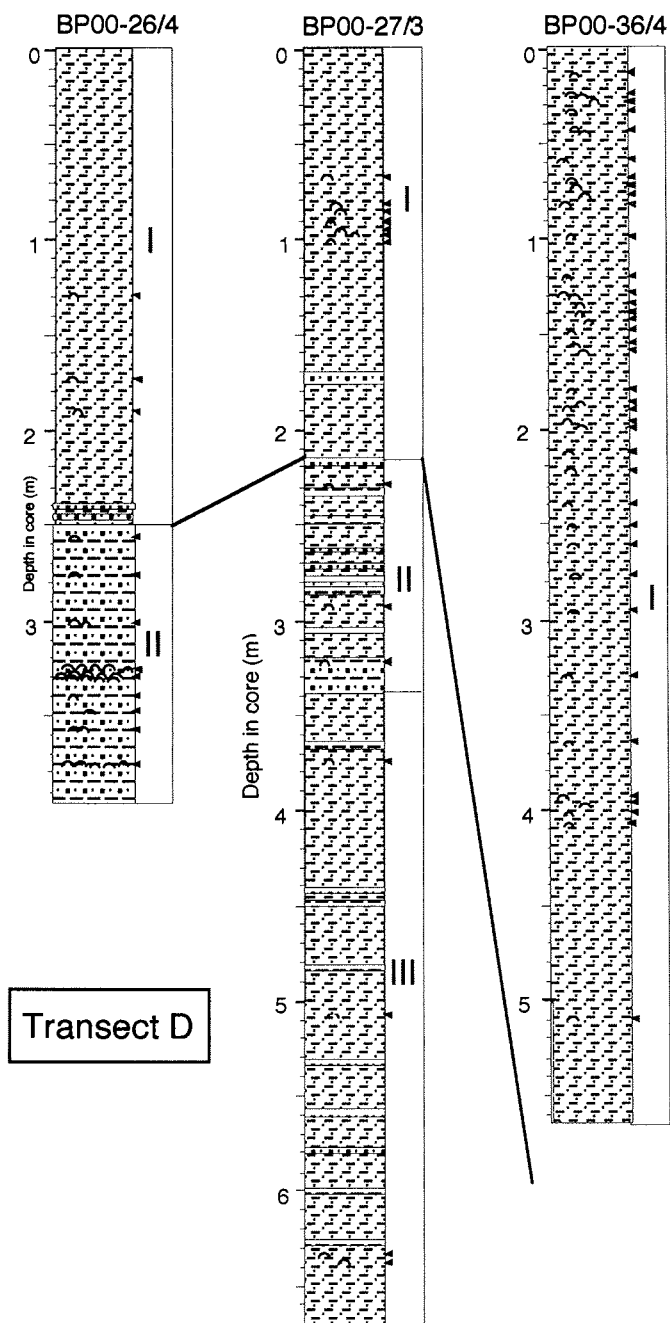


Fig. 6-28: Lithologies of sediment cores from Transect D. For location of transect see Fig. 6/-24, for legend see Fig. 6-25.

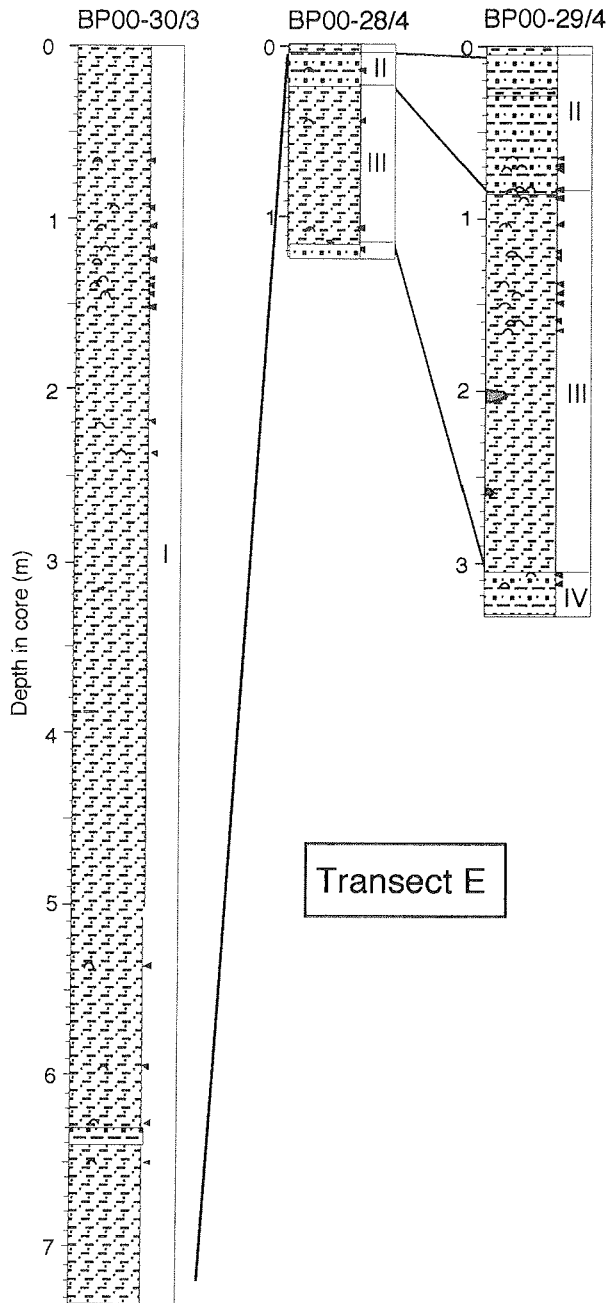


Fig. 6-29: Lithologies of sediment cores from Transect E. For location of transect see Fig. 6-24, for legend see Fig. 6-25.

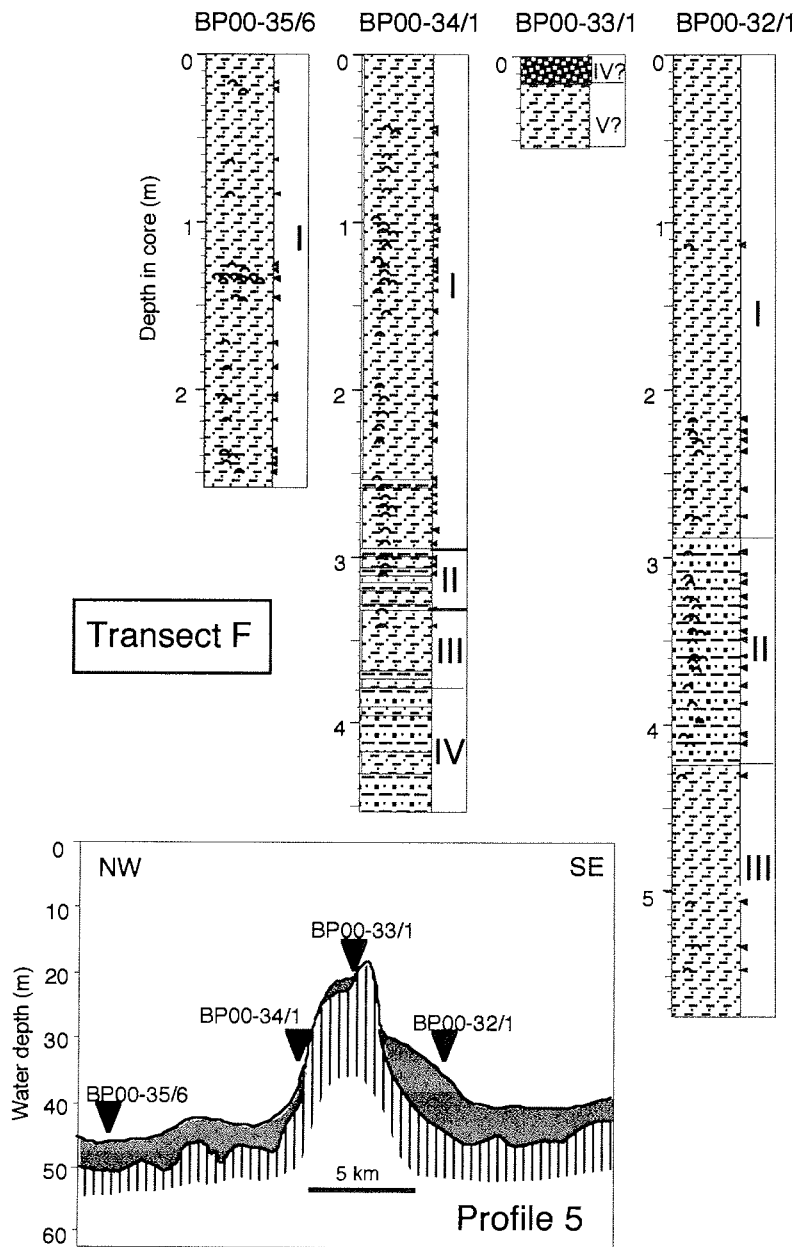


Fig. 6-30: Lithologies of sediment cores from Transect F. For location of transect see Fig. 6-24, for legend see Fig.6-25. In addition, a scheme of the ELAC sediment echograph profile is shown (profile 5 in Fig. 6-24).

The four Yenisei cores BP00-14/3, BP00-15/5, BP00-22/5, and BP00-23/6 (Transect B, Fig. 6-26) are additional cores taken at the same position than those described in Chapter 6.6. With the exception of the southernmost Core BP00-15/5 characterized by one unit of clay silty sand to clayey sandy silt, these cores consist of an upper bioturbated clayey silt to silty clay Unit I and a lower more sandy Unit II (for more details see Chapter 6.6).

In most of the cores obtained from the southern Kara Sea north and northeast of the Yenisei, the lithology is more variable than described for the Yenisei cores (Transects C, D, E and F; Figs. 6-27 to 6-30). Silty clayey units/intervals alternate with more sandy units/intervals (Units I to IV). The thicknesses of these fine-grained and more coarse-grained units are also very variable ranging from a few centimeters to more than two meters. Thick sandy intervals of 1.3 to 2.3 m in thickness were recovered in the lower part of cores BP00-11/1, BP00-25/1, BP00-26/4, and BP00-32/1 (Figs. 6-27, 6-28, and 6-30). In Core BP00-06/1, the sandy units are characterized by abundant thin sandy layers/intervals alternating fine-grained layers. The sandy units of the different cores display very different magnetic susceptibility records (cf. Chapter 6.3). Thus, a correlation between the sediment cores only based on the lithological units should be used with caution. Additional data, especially AMS¹⁴C datings of the numerous bivalves occurring throughout most of the cores (Table 6-6), are necessary for a more precise core correlation.

The long sediment cores BP00-07/7, BP00-30/3, and BP00-36/4 (Figs. 6-27 to 6-29) consist of fine-grained silty clay to clayey silt throughout, representing Unit I. Abundant occurrences of bivalves will allow a precise AMS¹⁴C dating of the records and, thus, allow a future detailed high-resolution study of the (Holocene) paleoenvironmental history.

Exceptional lithologies were recovered in four sediment cores:

- In cores BP00-06/1 and BP00-29/4 beige-colored (carbonate?) minerals were recovered (see annex 9.2 for exact depths), possibly representing "pseudomorphs after ikaite" (glendonite?) (cf. Kodina et al., Chapter 7.9).
- At the surface of Core BP00-25/1 several large-sized (3-7 cm in diameter) manganese nodules were found.
- The upper 15 cm of Core BP00-33/1 consist of silty sand with several large-sized un-rounded pebbles. The lower 40 cm are composed of stiff (overconsolidated?) clay.

Correlation of sediment cores and ELAC sediment echograph profiles

Based on an ELAC sediment echograph survey, an end-morain-like structure was recovered in the eastern part of our study area (Fig. 6-30; for location of ELAC profile see Fig. 6-24). Young (Holocene?) sediments are overlying a strong reflector which is cropping out at the top of the structure. A transect of four cores were taken across this structure. With cores BP00-35/6 (NW of the structure) and BP00-32/1 (southeast of the structure), the young sediments overlying the basis reflector ("basement"), were recovered. Core BP00-34/1 from the NW-flank of the structure and Core BP00-33/1 taken from the top of the structure, penetrate into the "basement". The sandy sediments from the bottom of Core BP00-34/1 and, especially, the diamicton-like sediments and the underlying stiff (overconsolidated?) clay from Core BP00-33/1 may represent glaciogenic, non-marine sediments (margin of late Quaternary ice sheet?). The more

sandy sediments from the middle part of Core BP00-32/1 are probably younger and of marine origin as suggested from the abundant occurrences of bivalves. Future detailed sedimentological and mineralogical studies as well as AMS¹⁴C datings of these cores (Dittmers et al., in prep.) may give new insights into the extent and history of late Quaternary glaciation which is still under controverse discussion in the eastern part of the Kara Sea (Svendsen et al., 1999 and further references therein).

In the northern part of the Yenisei, an ELAC echography survey was carried out in 1999 (Stein and Stepanets, 2000). Three of these profiles (original profiles and the interpretation) are shown in Figure 6-31a and 6-31b (for lithologies of cores BP99-04/7, BP99-05/1, and BP00-23/6 see Fig. 6-32). In these profiles an upper acoustic Unit I can be distinguished from the underlying acoustic Unit II. Unit I which can be further divided into subunits Ia and Ib, represents the young Holocene sediments. In the N-S profile (1) the northern end of the "marginal filter" (Lisitzin, 1995) at about 73° 30'N is obvious. Within the "Marginal Filter" where freshwater and salt water mixes (salinities of about 2 to 10), rapid accumulation (precipitation) of fine-grained suspension occurs due to coagulation processes (Fig. 6-33). North of 73° 30'N, the thickness of young sediments rapidly decreases to about zero. That means, most of the riverine matter (about 90 to 95 %; Lisitzin, 1995) accumulates south of this borderline.

The three sediment cores BP99-04/7, BP99-05/1, and BP00-23/6 were obtained in the northern margin area of the marginal filter (Figs. 6-31 and 6-33). The lithological units I (Ia, Ib) and II correlate with the acoustic units I (Ia and Ib) and II. Core BP00-04/7 is composed of mainly clayey silty sediments representing Unit I (Ia and Ib) whereas the two cores BP00-23/6 and BP99-05/1 from the end of the marginal filter penetrate into the underlying Unit II. Subunit Ib seems to be absent in Core BP00-23/6 but present at Core BP99-05/1 (cf. Fig. 6-31). Based on first AMS¹⁴C datings (Stein, unpubl. data 2000), the sedimentary sequence of Core BP99-04/7 represents the last about 10000 calendar years which will allow a detailed study of the riverine sediment discharge and its variability during Holocene times (Stein et al., in prep.). First AMS¹⁴C datings of samples from Core BP99-05/1 indicate that the sandy Unit II is of pre-Holocene, post-glacial age, and that the lower part of Subunit Ia is missing due to a hiatus (Fig. 6-32 Stein, unpubl. data 2000).

The E-W ELAC Profile (3) obtained further to the south in the central part of the main depo-center of Yenisei Bay at about 73° N, indicates distinctly increased Holocene sedimentation rates (Fig. 6-34). Here, Unit I reaches a thickness of about 20 m resulting in a Holocene sedimentation rate of about 200 cm/ky. Core BP00-14/3 penetrated the entire Unit I and obtained sediments from the upper Unit II. Bivalves found in the lower part of this core, will allow a dating of the Unit I/II boundary. Core BP99-08/7 is situated in the central part of the main depo-center (Figs. 33 and 34). The recovered about 5.4 m long sedimentary sequence will probably give the possibility to perform ultra-high-resolution studies of the upper Holocene history of river discharge.

Northern Yenisei Estuary Profiles

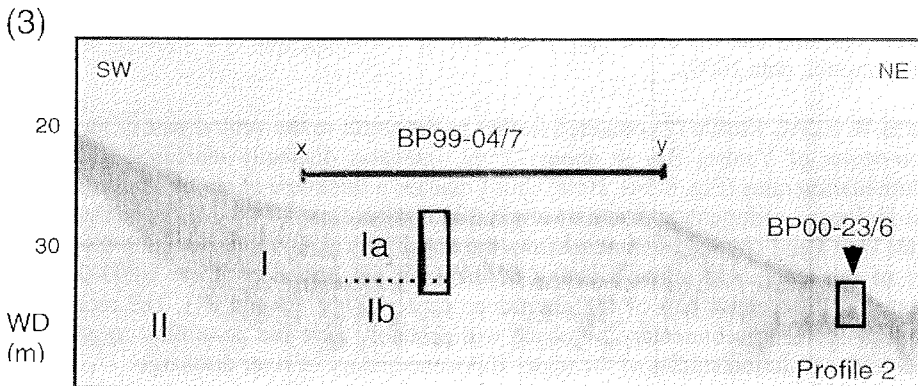
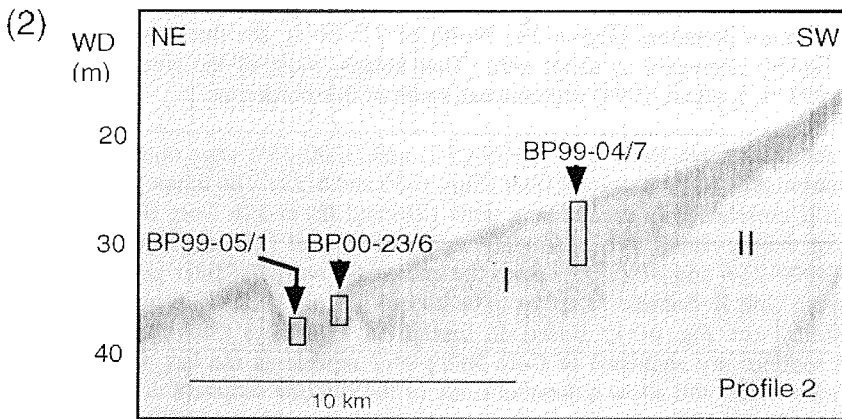
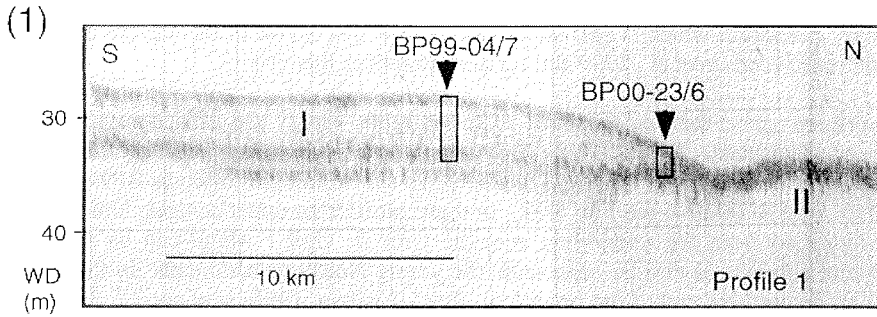


Fig. 6-31a: ELAC sediment echograph profiles obtained in the northern Yenisei Estuary. For location of profiles 1 and 2 see Figure 6-24. Acoustic units are indicated by roman numbers. In (3) profiler was running during station time at BP99-04/7 (x-y).

Northern Yenisei Estuary Profiles

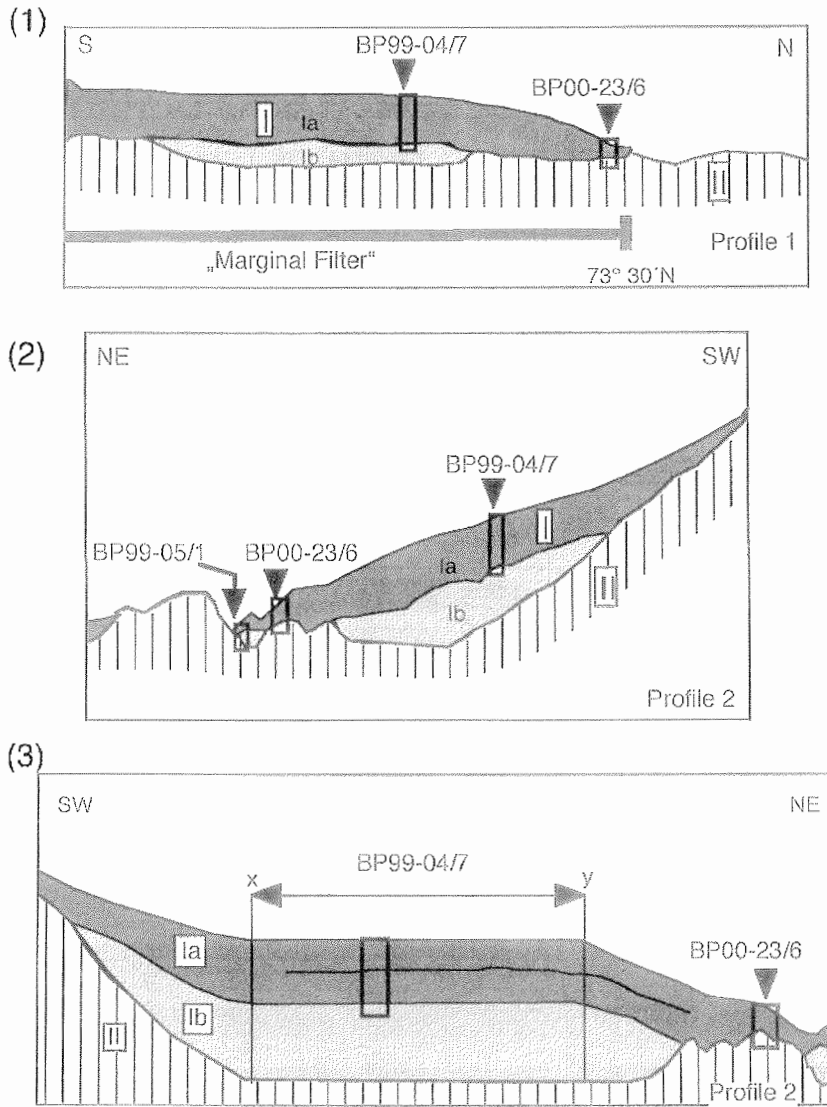


Fig. 6-31b: Interpretation of the three profiles presented in Fig. 6-31a.

Northern Yenisei Estuary Transect

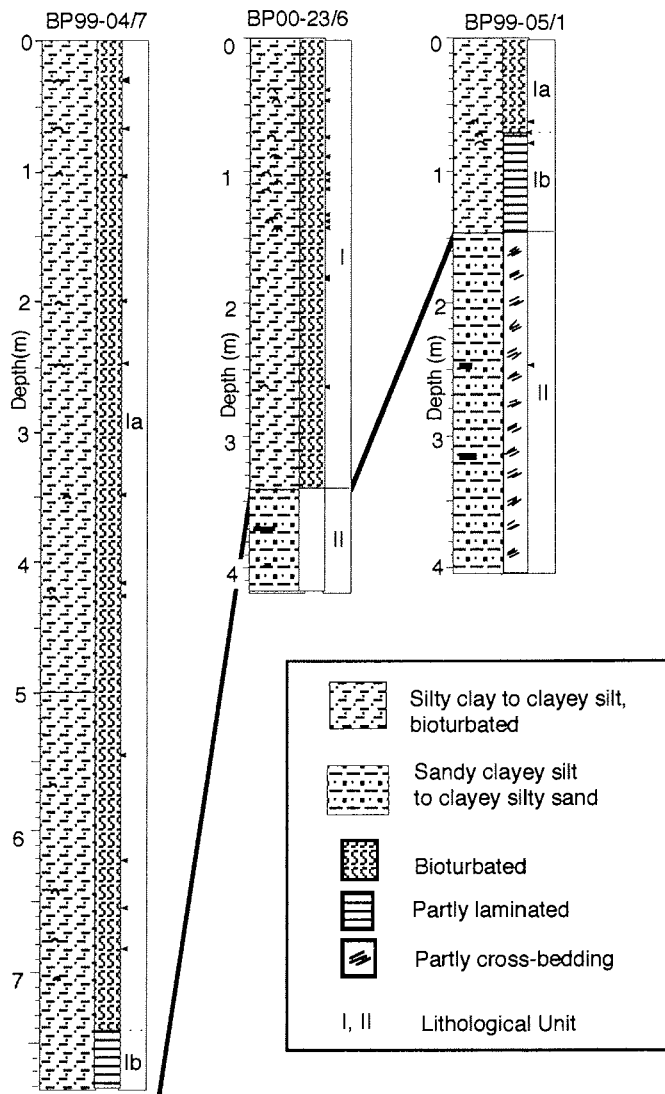


Fig. 6-32: Lithologies of the three sediment cores from the northern Yenisei Estuary. The cores are located on the ELAC profiles shown in Figure 6-31.

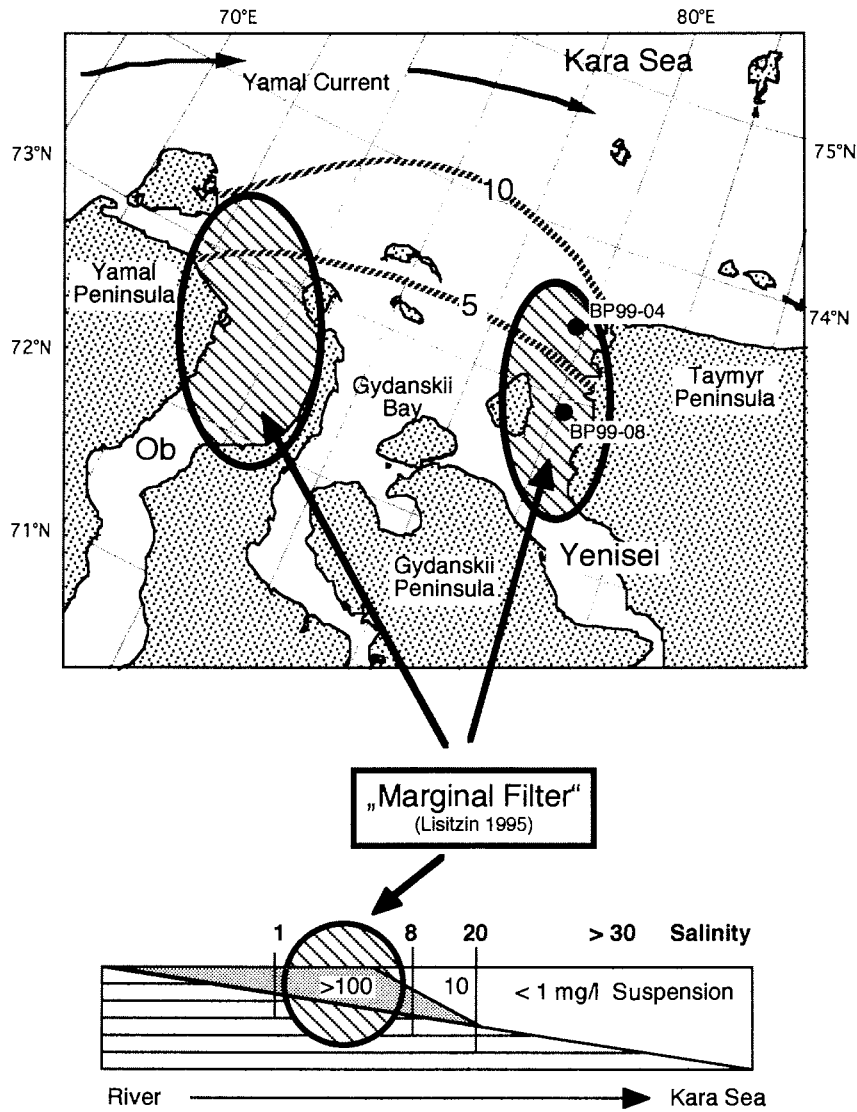


Fig. 6-33: Scheme of occurrence of "Marginal Filter" (Lisitzin, 1995) in the Ob and Yenisei estuaries. Hatched lines in the map indicate salinities (5 and 10). Within the filter, about 90 to 95% of the suspended matter is accumulating.

Yenisei Estuary Profile (73° N)

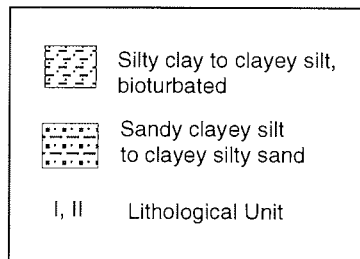
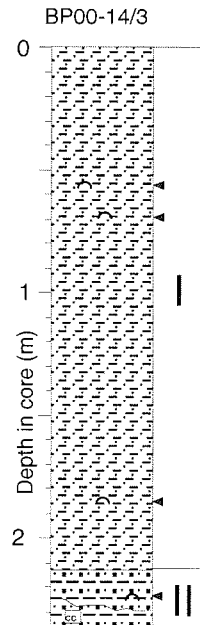
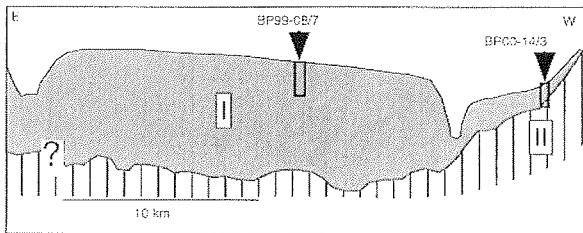
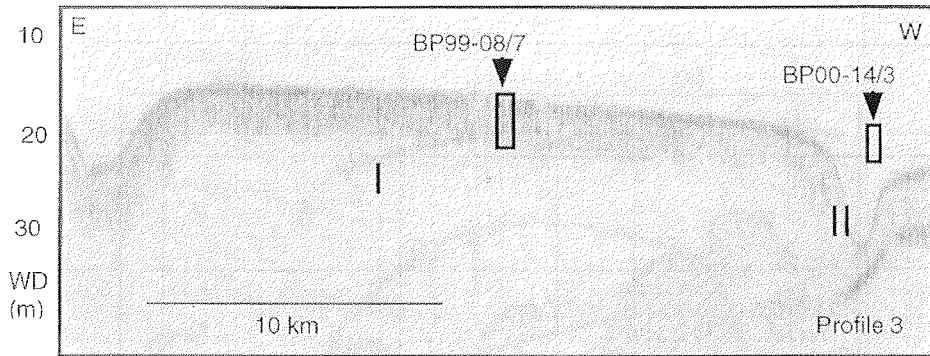


Fig 6-34: ELAC sediment echograph profile in the Yenisei at 73° N and lithology of Core BP00-14/3. For location of profile see Figure 6-24.

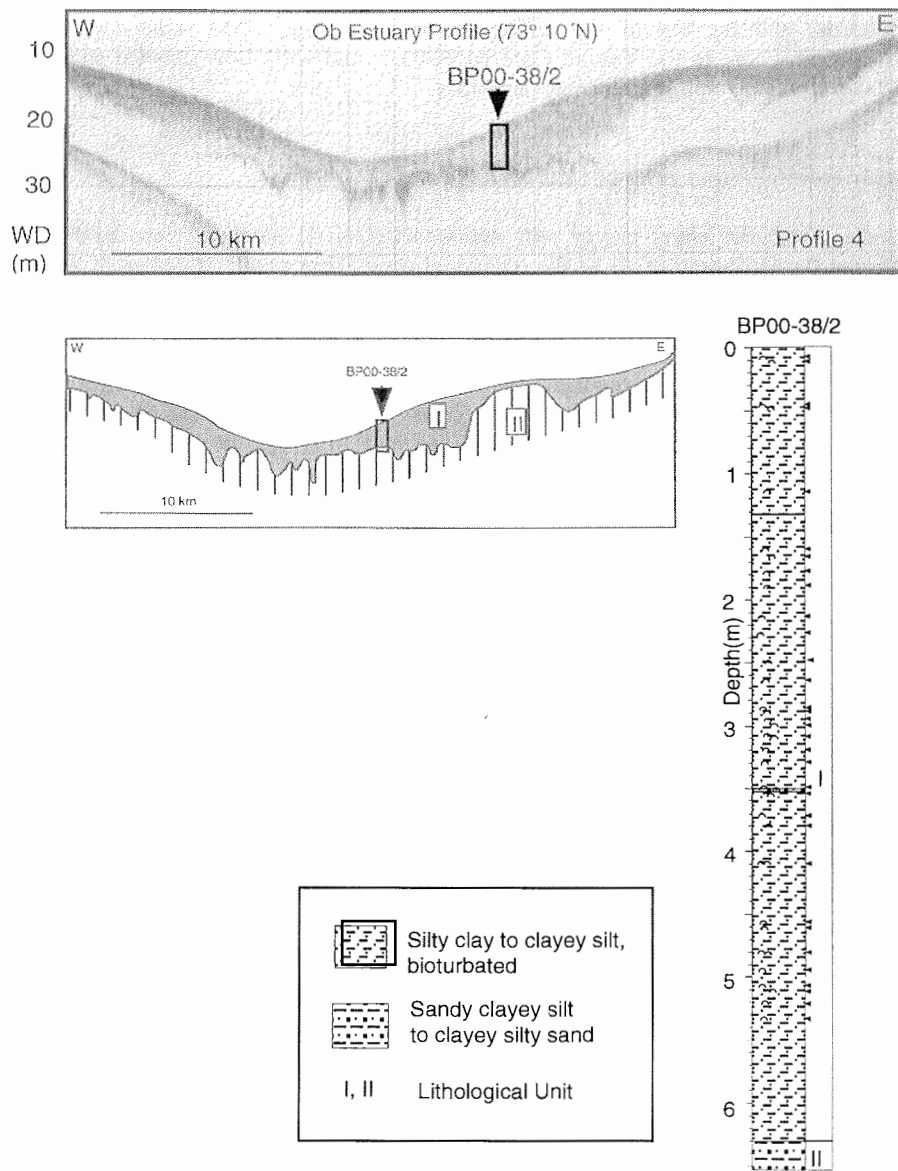


Fig. 6-35: ELAC sediment echograph profile in the northern Ob Estuary at 73° 10' N and lithology of Core BP00-38/2. For location of profile see Figure 6-24.

In the northern part of the Ob estuary, an ELAC sediment echograph survey was carried out in 1999 (Stein and Stepanets, 2000). In Profile (4) (Figs. 6-24 and 6-35), acoustic units I and II can also be distinguished. Due to a restricted permission for coring, a sampling was not possible in 1999. During the 2000 expedition, however, a long sediment core could be obtained from this area representing the lithological Unit I (Holocene) and the top of the underlying Unit II (Fig. 6-35). This core is the corresponding core to the Yenisei Core BP99-04/7, and will allow detailed studies of Ob river discharge and its Holocene variability.

Linear sedimentation rates of Unit I (Holocene)

Assuming that the upper clayey silty sediments (Unit I) dated at Core BP99-04/7, represent the Holocene in all of the recovered cores, first rough estimates of average Holocene sedimentation rates are possible (Fig. 6-36 and Table 6-7). Based on this assumption, maximum sedimentation rates $> 50\text{cm/ky}$ are reached, as suggested, in the Ob and Yenisei estuaries. Similar high sedimentation rates, however, were also recorded at some cores situated in the main channels further to the north. The silty clayey terrigenous sediments recovered at these cores suggest, that significant amounts of sediments may have passed through the marginal filter and were transported and deposited further offshore. Further detailed sedimentological and mineralogical studies, however, are necessary to determine the different sediment sources and transport processes of the sediments. Based on these data, it will be possible to quantify the amount of riverine material reaching the Kara Sea shelf.

In the inner Kara Sea outside the main channels, sedimentation rates are significantly lower ranging between 10 and less than 1cm/ky and indicating a distinctly reduced accumulation of terrigenous (riverine) material.

Outlook

Based on (a) the lithological core description, (b) future AMS¹⁴C dating of the sediment cores, (c) sedimentological, mineralogical, micropaleontological, and geochemical data sets, (d) detailed topographic maps, and (e) the evaluation of sediment echograph and 3.5 kHz profiles, a detailed reconstruction of the paleoenvironment (e.g., changes in paleo-river discharge, history of late Quaternary glaciation, etc.) and a calculation of sedimentary and organic carbon budgets will be performed (cf., Annex 9.3).

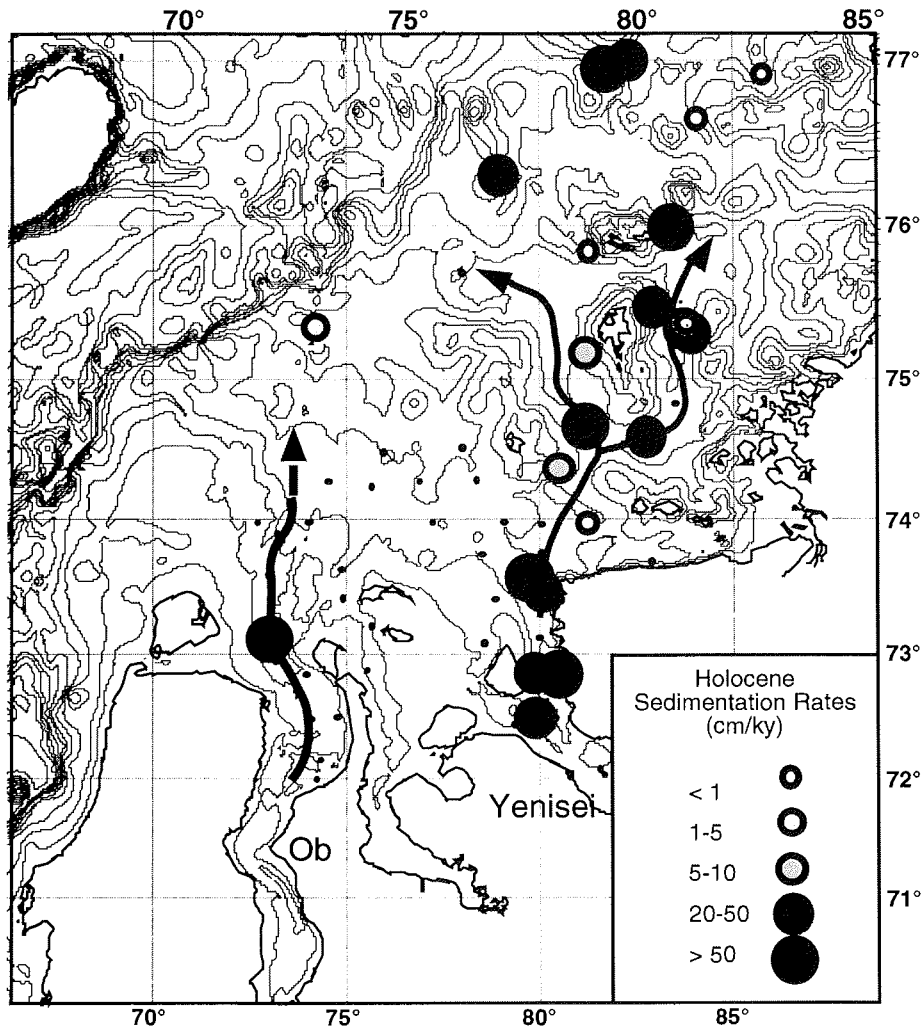


Fig. 6-36: Estimates of average Holocene sedimentation rates (cm/ky).

Table 6-7: Estimates of Holocene sedimentation rates, assuming that the upper clayey silty unit represents the Holocene, i.e., the last 10000 years BP.

Gravity Core	Latitude ° N	Longitude ° E	Depth (m)	Total Recovery (cm)	Thickness Unit I (cm)	LSR Unit I (cm/ky)
BP00-02/4	75°24.114'	74° 11.82'	49,6	68	30 (?)	3 (?)
BP00-05/6	75°50.22'	81°0.32'	50	34	8	0,8
BP00-06/1	75°10.051'	80°59.748'	38	288	88 (?)	8.8 (?)
BP00-07/6	74°39.456'	81°08.466'	38	665	> 665	> 66.5
BP00-07/7	74°39.456'	81°08.466'	38	723	> 723	> 72.3
BP00-08/4	74°39.554'	82°38.553'	41	191	>191	> 19.1
BP00-11/1	74°17.536'	81°47.141'	42	322	7	0,7
BP00-14/3	72°55.853'	79°47.381'	19.2	243	213	21,3
BP00-14/4	72°55.853'	79°47.381'	19.2	256	230	23
BP00-15/5	72°2.992'	81°36.157'	5.8	369	?	?
BP00-15/6	72°2.992'	81°36.157'	5.8	438	?	?
BP00-22/4	72°33.990'	79°54.927'	11	438	410	41
BP00-22/5	72°33.990'	79°54.927'	11	436	297	29,7
BP00-23/6	73°28.542'	79°51.348'	33	417	340	34
BP00-23/7	73°28.542'	79°51.348'	33	427	374	37,4
BP00-25/1	74°30.324'	80°31.656'	59	332	70 (100?)	7 (10?)
BP00-26/4	75°42.512'	77°57.589'	68	396	250	25
BP00-27/3	76°18.045'	78°55.977'	78	670	215 (?)	21.5 (?)
BP00-28/5	76°39.33	83°52.61'	50	121	5	0,5
BP00-29/4	76°56.172'	85°45.793'	68	329	5	0,5
BP00-30/3	75°59.188'	83°2.174'	52	732	> 732	> 73.2
BP00-32/1	75°15.392'	84°20.568'	32	574	289	28,9
BP00-33/1	75°16.760'	84°13.013	22	53	0	0
BP00-34/1	75°17.638'	84°8.728'	39	452	379 (?)	37.9 (?)
BP00-35/5	75°20.827'	83°48.086'	46	261	> 261	> 26.1
BP00-35/6	75°20.827'	83°48.086'	46	258	> 258	> 25.8
BP00-36/1	76°57.707'	81°57.79'	66	574	> 574	> 57.4
BP00-36/4	76°57.707'	81°57.79'	66	563	>563	> 56.3
BP00-37/1	76°58.007'	82°12.291'	63	433	375	37,5
BP00-38/2	73°11.807'	73°14.308'	20	652	630	63

6.8 Benthic foraminifera from the southern Kara Sea: Preliminary results

E. Ivanova

Shirshov Institute of Oceanology RAS, Moscow, Russia

Abstract

A pilot study of benthic foraminiferal assemblages was performed in 19 surface sediment samples and in 5 gravity cores to evaluate the river discharge influence on the species distribution along the Yenisei Transect up to 77°N. The most diverse Recent assemblages were recorded in the middle part of the transect, between 75°30' and 73°N. They correspond to an interval of water depth from 68 to 13 m, and to near-bottom salinity from 29 to 34‰. The diversity of species noticeably decreases inshore. At about 72°45'N, in the outer Yenisei Estuary the number of calcareous species declines whereas arenaceous taxa completely disappear. Only few likely *in situ* specimens of *Elphidium excavatum* forma *clavatum*, *E. incertum* and *E. subarcticum* are recorded in low-diverse assemblages of the inner Yenisei Estuary, at 72°N, where measured near-bottom salinity did not reach 15‰ during the sampling time. The survival of few individuals of these infaunal species at so critical salinity may be explained by deeper burrowing during short-term freshening as the environmental conditions in the estuary are very unstable. Foraminifera were not found neither in sediment samples southward nor throughout the innermost sediment core BP00-15. Rather diverse assemblages dominated by several calcareous species, such as *Elphidium* spp., *Protelphidium orbiculare*, *Cassidulina reniforme*, *Buccella* spp. characterize Holocene section in five sediment cores along the Yenisei Transect, however the abundance of foraminiferal tests is generally low. Only few specimens occur in the Pleistocene section of core BP00-14 while in other cores the Pleistocene sediments are barren or contain only reworked foraminifera. This points to a pronounced amelioration of environmental conditions in the Early Holocene compared to the Late Pleistocene.

Introduction

The vast mixing zone of fresh Ob and Yenisei waters with saline water of the adjacent Kara Sea (Burenkov and Vasilkov, 1994; Churun and Ivanov, 1998) is of a special interest for SIRRO Project. Variations in a tremendous water discharge of these Siberian rivers during the Late Quaternary should have a strong impact on the water masses transformation in the Kara Sea and to the Arctic paleoceanography. The paleoenvironments of the Kara Sea can be reconstructed by benthic foraminifera and stable isotope analyses. The study of Recent foraminiferal fauna along the transects from two estuaries to the inner Kara Sea up to 76°N was fulfilled by Khusid (1996) and that from Ob estuary up to 74°N was performed by Korsun (1998,1999), based on surface sediment samples collected during 49-th cruise of RV "Dmitry Mendeleev" and 28-th cruise of RV "Akademik Boris Petrov", respectively. Hald and Steinsund (1996) examined the effect of dissolution on foraminiferal assemblages. However, foraminiferal data for the Kara Sea remain insufficient, whereas oxygen and carbon isotope measurements in the sediment cores are practically absent.

According to SIRRO Project target the main goal of micropaleontological study onboard was to make pilot foraminiferal analyses in sampled gravity cores retrieved especially for further high resolution investigation of the inner Kara Sea paleoenvironments and their evolution during the Holocene in relation to changes in river run-off. The second task was to provide first insight into the distribution and abundance of foraminifera, mollusks and ostracods in other sediment cores opened onboard to evaluate perspectives of their dating which is necessary for geochemical and mineralogical investigations and as well of their value for paleoceanographic study. The third aim was to evaluate changes in Recent foraminiferal assemblages along the salinity gradient from Yenisei estuary to the adjacent Kara Sea up to 77°N. These new surface samples will be further used to enlarge a very limited database on foraminifera distribution in the Kara Sea (Khusid, 1996; Khusid and Korsun, 1996; Korsun, 1999).

Material and methods

The samples were obtained by box-corer and gravity corer in September 2000 during the Russian-German expedition by RV "Akademik Boris Petrov" (Table 6-8). Express study of benthic foraminifera including evaluation of relative abundance and identification of main species was made for a long gravity core BP00-7/5 with the sampling interval of 20 cm, and for cores BP00-23/7, BP00-22/4, BP00-14/4 and BP00-37/1 with the interval of 50 cm. The occurrence of mollusks, ostracods and gastropods was also noted. A preliminary investigation of benthic foraminifera assemblages was performed on 19 surface (0-2 cm) and 2 subsurface (2-4 cm) sediment samples retrieved by a box-corer at stations no. 3, 5, 7, 8, 9, 13, 15-17, 22, 23, 26, 28-31, 35, 36, 38 (Fig. 6-37). All these samples were washed through a mesh sieve 100 µm and examined under a binocular microscope. The mean weight of each sample was about 100 g.

Table 6-8: List of stations.

station	Latitude, N	Longitude, E
BP00-36	76°58'	81°58'
BP00-29	76°56'	85°46'
BP00-37	76°58'	82°12'
BP00-28	76°39'	81°53'
BP00-30	75°59'	83°02'
BP00-05	75°50'	81°00'
BP00-26	75°42'	81°58'
BO00-31	75°28'	82°33'
BP00-35	75°21'	83°49'
BO00-09	74°50'	83°26'
BP00-08	74°40'	82°39'
BP00-07	74°39'	81°08'
BP00-23	73°29'	79°51'
BP00-13	72°56'	80°33'
BP00-14	72°56'	79°47'
BP00-22	72°34'	79°55'
BP00-15	72°03'	81°36'
BP00-16	71°50'	82°37'

Study area

The surface sediment samples and gravity cores were mainly obtained along the Yenisei Transect (Fig. 6-37, Table 6-8). Water depth in the northern part of the transect reached

66-68 m, whereas in the southern part of the Yenisei Estuary, at st. 15, it was about 6 m. During the cruise, in September, near-bottom water temperature increased inshore from $-0.6\text{ }^{\circ}\text{C}$ (st. 29) to $5.5\text{ }^{\circ}\text{C}$ (st. 15) according to *in situ* multi-corer measurements (see Stepanetsev and Shmelkov, this vol.). Near-bottom salinity decreased in the same direction from 34.3‰ which is typical for the Kara Sea (Dobrovolsky and Zalogin, 1982), to 14.4‰ in Yenisei estuary (*in situ* multi-corer measurement at st.15, see Stepanetsev and Shmelkov, this vol.). In Yenisei Estuary the halocline reached the bottom during the sampling time (see Stepanetsev and Shmelkov, this vol.). Near-bottom temperature and salinity demonstrate strong seasonal and synoptical variations in the region, especially in the Yenisei estuary (Dobrovolsky, Zalygin, 1982; Churun and Ivanov, 1998). The study area is dominated by terrigenous fine-grained sediments, however, silty clayey sands were recovered at several stations (Müller and Stein, 1999; Stein and Levitan, this vol.).The TOC content in the surface sediments of the Yenisei estuary sometimes exceeds 2% and varies between 0.5 and 2 % in the adjacent Kara Sea (Romankevich et al., 1982; Boucsein et al., 1999; Fahl et al., this vol.).

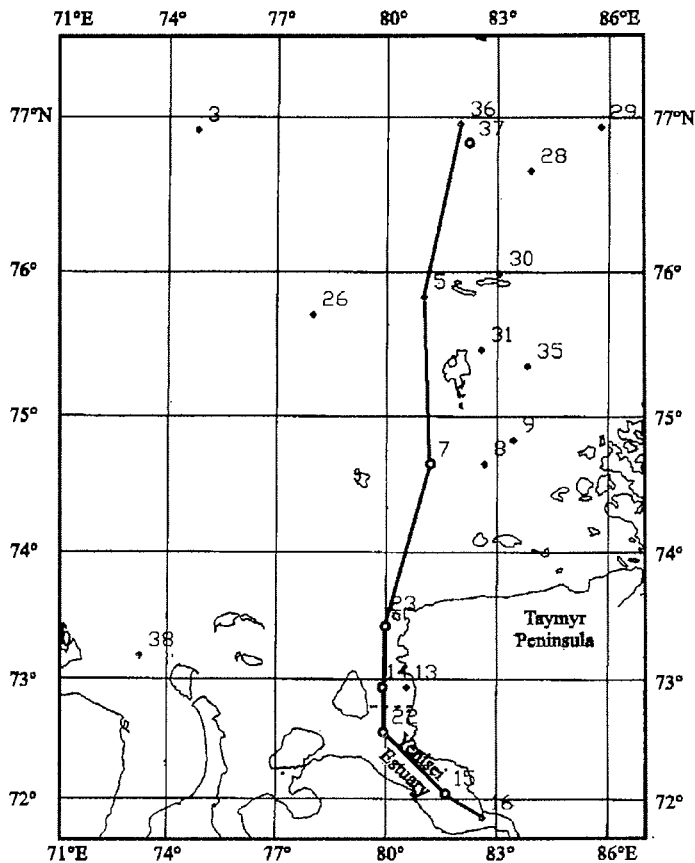


Fig. 6-37: Location of studied surface sediment samples (solid circles) and gravity cores (open circles). Yenisei Transect is shown by solid line. A drop in number of species is associated with a boundary between stations 13 and 22 shown by dashed line.

Results

As a whole, 19 well-known species of calcareous foraminifera and 4 genera of arenaceous foraminifera were identified in surface samples and sediment cores. Calcareous species generally demonstrated moderate to good state of preservation, however, the tests etched by dissolution occurred in many samples. Some mineralized, broken and/or rounded calcareous tests were noted. Arenaceous specimens were frequently broken and undistinguished to a species level, especially in sediment cores. No planktic foraminifera were found.

Recent foraminiferal assemblages

*Surface sediment samples can be subdivided into several groups depending on calcareous and arenaceous foraminifera abundance and ratio at each station:

*samples from st. 16 and 17 (Yenisei Estuary, Fig. 6-37, Table 6-9) are barren of forams, as well as that one from st. 38 located to the north of Ob Estuary, where only several tests of *E.excavatum* forma *clavatum* were found;

*arenaceous foraminifera dominate at st. 3, and demonstrate approximately the same, rather low, abundance as calcareous foraminifera at st. 35 and 36;

*calcareous foraminifera represented by 5 to 9 species dominate over arenaceous ones at st.5, 7, 9, 23, 26, 28, 30, but they are not numerous; the number of arenaceous forms decreases from surface to subsurface layer; the same tendency was noted by the author during two cruises in the Barents Sea, and by Khusid (1996) in the Kara Sea;

*foraminiferal assemblages of st. 13, 8 and 31 are the most diverse (9-12 calcareous and generally 5-8 arenaceous species), the abundance of foraminifera seems higher than at other stations.

It is interesting to note that few specimens of *Elphidium incertum*, *Elphidium subarcticum* and *E.excavatum* forma *clavatum* occurred at st.15 located in the Yenisei Estuary. The tests looked fresh and were filled with green phytoplankton (?) fragments. Therefore, I suggest that they were probably alive but not reworked from the north. As pointed out above, the near-bottom salinity at this station during sampling time was as low as 14.4‰.

A decline in species diversity (calcareous and arenaceous together) along the transect is noted near 72°45'N, between stations 13 and 22, where the number of calcareous species decreases from 9 to 3. Arenaceous foraminifera were not recorded southward of station 13. Among the common calcareous taxa, only *E.excavatum* f. *clavatum*, *E.bartletti*, *E.incertum* and *E.subarcticum* rarely occur in the Yenisei Estuary (Table 6-9, Fig.6-37), while other species, such as *Nonion labradoricum*, *Virgulina loeblichii*, *Islandiella helenae*, *Islandiella norcrossi*, *Quinqueloculina* spp. disappear along the transect, mainly between st. 7 and 23.

Table 6-9: Occurrence of main benthic foraminiferal species along the Yenisei Transect.

species/station	36	29	28	30	5	26	31	35	9	8	7	23	13	22	15	16
		**	**	**		*	**	**	**	**	**					
calcareous																
Elphidium excavatum																
f. clavatum		x		x		x		x	x	x	x	x	x	x	x	x
Elphidium incertum									x							x
Elphidium subarcticum																x
Elphidium bartletti			x	x	x	x	x			x	x	x		x		
Elphidium groenlandicum							x	x	x	x			x			
Islandiella helenae							x		x							
Islandiella norcrossi	x					x										
Cassidulina reniforme				x	x	x	x	x		x	x					
Nonion labradoricum	x			x		x	x			x						
Protelphidium orbiculare	x		x	x	x	x	x		x	x	x	x	x			
Virgulina loeblichii							x									
Buccella sp.														x		
Pyrgo williamsoni	x	x		x	x		x	x		x	x	x				
Quinqueloculina sp.	x	x	x	x		x	x	x								
arenaceous																
Trochammina sp.			x			x	x			x	x	x	x			
Reophax sp.	x		x	x	x		x		x	x		x				
Ammotium cassis	x						x		x	x		x				
Alveolophragmium crassimargo	x				x		x		x	x						

Notes: station located west of the transect is marked by asterix, stations located east of the transect are marked by two asterixes

Foraminifera distribution in the sediment cores

Foraminiferal study fulfilled onboard proved that core 7 obtained in the mixing zone of fresh Yenisei water with saline Kara Sea water can be selected for a multi-proxy high resolution study, including variations in foraminiferal assemblages, stable isotopes, ^{14}C dating (cf. Table 6-6, Stein, this vol.) etc.. 30 samples examined in this core contain more or less abundant foraminiferal tests of sufficiently good preservation generally accompanied by bivalves and ostracods (Table 6-10). Some decrease in foraminifera abundance is noted in the interval 420 to 600 cm. Variations in foraminiferal assemblages can be seen even during the express study. The northernmost core 36 seems not valid for the foraminiferal study due to a presence of dissolving gases in the sediments. Core 37 obtained about 2 miles apart from core 36 is almost barren of foraminifera. Core 39 has no value for high resolution study due to very short length (120 cm), core-catcher sample contains scarce foraminiferal tests, some of which demonstrate signs of mineralization.

Variations in foraminiferal abundance and diversity throughout the sequence were recorded in sediment cores BP00-23/7, BP00-22/4, BP00-37/1 and BP00-14/4 which reach the Pleistocene/Holocene boundary according to lithological data (Stein and Levitan, this vol.). Pleistocene sediments seem to be barren of foraminifera in three cores (Fig. 6-38), except for rare reworked dark-brown tests found at 410 cm in core

BP00-37/1, while rare but fresh and likely *in situ* specimens of four calcareous species (*Protelphidium orbiculare*, *Elphidium excavatum* f. *clavatum*, *Oolina* sp, *Polymorphina* sp.) were recorded in core 14/4, within the outer Yenisei Estuary (Table 6-10). Core BP00-23/7 demonstrates higher abundance of foraminifera in the Holocene section compared to other three cores. The Holocene sediments are generally dominated here by *Protelphidium orbiculare*, *Elphidium excavatum* forma *clavatum* and *Elphidium bartletti*; other important species include *Cassidulina reniforme*, *Pyrgo williamsoni*, *Islandiella norcrossi*, *Islandiella helenae*, *Buccella frigida*, *Elphidium groenlandicum*, *Elphidium incertum*, *Virgulina loeblichii*, *Nonion labradoricum*, *Quinqueloculina* spp., *Reophax* spp., *Trochammina* spp., *Alveolophragium crassimargo*, *Ammotium cassis*.

Three cores contain enough bivalve shells for AMS ^{14}C dating (cf. Table 6-6, Stein, this vol.), whereas in core BP00-37/1 only few ostracod shells are found in two samples (Table 6-10). Core BP00-15/4 is barren of foraminifera likely due to very low near-bottom salinity and shallow depth.

Table 6-10: Macro- and microfossils occurrence in the sediment cores along the Yenisei Transect.

core	depth, (cm)	Bivalvia	Gastropoda	Ostracoda	Benthic Foraminifera
BP00-15/4	0				
	50				
	100				
	150				
	200				
	250				
	300				
BP00-22/4	10	x			x
	60			x	x
	110				
	160	x		x	x
	215	x			
	265	x		x	
	305			x	x
	380			x	
BP00-14/4	0	x		x	x
	50	x		x	x
	110	x		x	x
	160	x		x	x
	210			x	x
	250	x		x	x
	415				
BP00-23/7	10	x	x	x	x
	60	x	x		x
	110	x	x	x	x
	160	x			x
	215			x	x
	265				x
	305	x			x
	380			x	x
415					

Table 6-10: cont.

core	depth, (cm)	Bivalvia	Gastropoda	Ostracoda	Benthic Foraminifera
BP00-07/6	0	x	x	x	x
	20	x	x		x
	40			x	x
	60	x	x	x	x
	80	x		x	x
	100	x			x
	120	x	x	x	x
	170	x	x	x	x
	200	x	x	x	x
	220	x		x	x
	240	x			x
	260	x			x
	280	x			x
	300	x			x
	320				x
	340				x
	360				x
	380	x			x
	400	x			x
	420				x
	440				x
	460				x
	480				x
	500	x			x
	520	x			x
	540				x
	560	x			x
580				x	
600	x			x	
620				x	
BP00-37/1	10			x	x
	70				x
	110			x	x
	160				x
	215				
	265				
	305				
	360				x
	410				

Discussion

The inshore trend of decline in species diversity related to decrease in salinity and shallowing of the basin was previously noted (Khusid, 1996; Korsun, 1999) for Ob and Yenisei Transects. Korsun (1999) fixed the main drop in number of species, as well as the disappearance of arenaceous taxa at about 72°30'N in the Ob Transect. Khusid (1996) found a similar change at about 73°N in the Yenisei Transect, but she had only 1 station between 72 and 74°N.

In our surface sediment samples the number of calcareous species shows maximum values, from 9 to 12, in the middle part of the transect, at stations 31, 13, 8, and at st. 26 located westward. These samples were obtained from 68 to 13 m water depths. A main drop in the number of calcareous species, as well as a disappearance of arenaceous taxa is noted between st. 13 and 22, in the outer part of the Ob Estuary, at about 72°45'N (Fig. 6-37). Korsun (1999) suggested that such a drop is related to the depth break in the Ob Estuary, but our two samples were obtained from the similar water depths of 13 and 11 m, respectively. *In situ* temperature and salinity measurements at water depth 10 m (Stephantsev and Shmelkov, this vol.) also demonstrate close values: 28.9‰ and 1.2°C at st. 13, 29.6‰ and 1.3°C at st.22. The difference in species diversity between two stations, perhaps, results from local environmental conditions. Note that site 22 is located under the main stream of fresh Yenisei water whereas near-shore site 13 may represent a refugium for foraminiferal species development due to more favorable trophic conditions. The intermediate number of species (5 calcareous and no arenaceous) at the surface sample of core BP00-14/4 obtained close to st.13 and from the same latitude (Fig. 6-37) seems to support this suggestion.

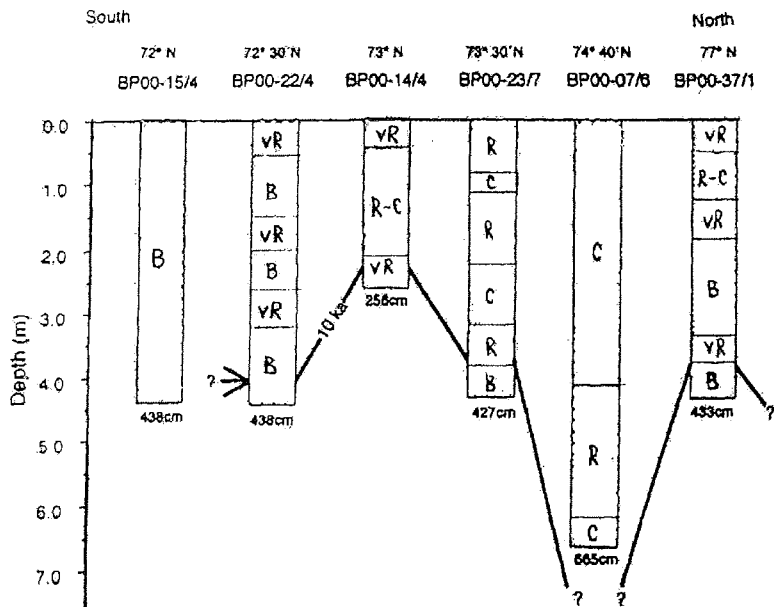


Fig. 6-38 Benthic foraminifera abundance in the sediment cores retrieved along the Yenisei Transect.

B - barren, R - rare, vR - very rare, C - common.

The Pleistocene/Holocene boundary is shown according to lithological (Stein and Levitan, this vol., Fig. 6-16)

The low-diverse assemblages of the Yenisei estuary (st.22 and 15) consist only of *Protelphidium orbiculare*, and three species of *Elphidium* genera which tolerate reduced oxygen content and low salinity, up to 20-25‰. The latter controls foraminifera distribution in the estuary (Khusid, 1996; Korsun, 1999).

The lowest salinity limit for calcareous foraminifera survival recorded by Khusid (1996) was about 27‰. However, I found probably living *in situ* specimens of *Elphidium excavatum* f. *clavatum*, *E. subarcticum* and *E. incertum* at st. 15, where near-bottom salinity during the sampling time was much lower, about 14.4‰. Only these opportunistic species can survive in harsh estuarine environments. However, it should be taken into account that strong seasonal and synoptical variations in bottom water salinity are characteristic for estuarine circulation. Korsun (1999) suggested that infaunal species can burrow deeper into the sediments with higher pore water salinity during freshening events. Corliss found living individuals of *E. excavatum* forma *clavatum* penetrated up to 10 cm into the sediment.

Variations in number and abundance of calcareous species in the outer part of the transect, between 77° and 72°45' N, should be related to local environmental changes and to preservation conditions in the surface sediments. Unlike Korsun (1999) and Khusid (1996) I did not find common specimens of *Buccella* spp. Instead, other typical arctic species, such as *N. labradoricum*, *V. loeblichii*, *E. groenlandicum* and *Pyrgo williamsoni* frequently occur in the outer part of studied area, in the bottom water salinity range from 34.3 to 28.9‰.

An occurrence of likely *in situ* specimens of four calcareous species in the alluvial Pleistocene sediments of core BP00-14/4 allow me to suggest rather high near-bottom salinity during the late deglaciation at the site actually located in outer Yenisei Estuary. On the other hand, foraminiferal tests found in Pleistocene sediments of core 37/1 located at the northern end of the transect (Fig.6-37) seem reworked by icebergs floating from Taymyr glacier or by bottom currents.

An appearance of rather diverse foraminiferal assemblages above the Pleistocene/Holocene boundary in cores BP00-22/4, BP00-23/7, BP00-14/4 and BP00-37/1 points to a pronounced change of paleoenvironment in the studied area. The most abundant foraminiferal taxa in five Holocene sequences, including core 7/6, are *Protelphidium orbiculare*, *Elphidium excavatum* f. *clavatum* and *Elphidium bartletti*, i.e. species found in the surface sediments along almost the whole Yenisei Transect, except for the innermost stations. These species survive both in saline and in brackish waters of the Arctic seas (Korsun et al., 1994; Khusid and Korsun, 1996; Korsun, 1999). Due to so high tolerance to variations in salinity they can be used for stable isotope studies in the Kara Sea as was done in the Barents and Laptev seas (Duplessy et al., in press; Bauch, unpublished data). Changes in abundance of these and of some other species common in the Arctic seas as *Cassidulina reniforme*, *Pyrgo williamsoni*, *Islandiella norcrossi*, *Islandiella helenae*, *Buccella frigida*, *Virgulina loeblichii*, *Nonion labradoricum* mainly reflect variations in surface productivity (food supply), TOC, length of ice-free season, and near-bottom salinity and temperature (Khusid, 1996; Khusid and Korsun, 1996; Korsun et al., 1994; Korsun, 1999; Polyak and Solheim, 1994) during the Holocene. These environmental variables, in turn, strongly depended on oscillations in Yenisei and Ob rivers run-off, and to a less extent on the water exchange of the Kara Sea with the Arctic Ocean and the Barents Sea.

Conclusions

The diversity of benthic foraminiferal assemblages declines at 72°45' N where the number of calcareous species strongly decreases and arenaceous taxa completely disappear.

The bottom-water salinity limit of calcareous foraminifera survival in Yenisei Estuary may be lower than previously established. Only *Elphidium excavatum* forma *clavata*, *E. incertum* and *E. subarcticum* can persist in such harsh environment.

The Holocene variations in paleoceanographic parameters of the south-eastern Kara Sea, in particular in bottom-water salinity, can be deduced from foraminiferal assemblages and stable isotope studies of sediment core BP00-07 as rather well preserved foraminiferal specimens are sufficiently abundant throughout the sequence.

An appearance of rather diverse foraminiferal assemblages at the beginning of Holocene evidences a pronounced amelioration of paleoenvironments along the Yenisei Transect between 77 and 72°30'N.

Acknowledgements

I wish to express my appreciation to the Vernadsky Institute of Geochemistry, RAS and the Alfred Wegener Institute for the opportunity to participate in the expedition. I am thankful to RV "Akademik Boris Petrov" crew and to colleagues from the geological team, who provided gravity cores and box-corer samples for the study. R.Stein and M.Levitan supplied me with the lithological data, and L.Stephantsev offered the T-S data. The crew, German colleagues from AWI and T.Pribylova helped me with the equipment. My special gratitude is to J.Simstich for a fruitful cooperation, to L.Polyak and S.Korsun for consulting on taxonomy, and to I.Sadovnikova for assistance with figure drawing. The manuscript benefited from critical reading by I.Murdmaa.

7.1 Geochemistry of Dissolved Organic Matter (DOM)

H. Köhler and K. Neumann

Institute of Biogeochemistry and Marine Chemistry, Hamburg

Introduction

Dissolved organic matter (DOM) play miscellaneous roles in aquatic ecosystems, especially in estuarine mixing zones, where the DOM originates from different sources. Some of the main features of DOM include its role as a transport agent for nutrients, radionuclids and pollutants and its influence on the submarine light conditions. Another important aspect is the function of DOM in the global carbon cycle: Oceanic DOM is one of the largest active reservoirs of organic carbon on earth. Therefore changes in the marine DOM pool are supposed to affect atmospheric carbon dioxide concentrations.

The rivers Ob and Yenisei drain immense areas ($5390 \cdot 10^3 \text{ km}^2$) of the Northern Hemisphere. About 30% of the global organic carbon soil pool are stored in their catchments, so the two rivers represent an important link between the terrestrial and marine carbon pool. Almost 40% of the total DOM ($7,3 \cdot 10^{12} \text{ gC}$) going into the Arctic Sea is contributed by the discharge of the Ob and the Yenisei (Opsahl et al. 1999). Consequently, the transformation processes occurring in the Kara Sea are of global pertinence.

Work and sampling program

Sampling was carried out between September 3 and September 22, 2000. As sampling of pure endmembers was not possible during the cruises BP 1997 and BP 1999, this time we put special emphasis on the freshwater sampling (salinity $< 1 \text{ ‰}$) in the Yenisei Estuary.

DOC Sampling

In order to improve our understanding of the riverine DOC distribution, we carried out a high-resolution sampling program for DOC: Samples (15ml) were taken at all 40 main stations at different depths by using the CTD-rosette or the large volume sampler (batomat). To improve spatial resolution we took 82 additional DOC-surface samples during the cruise of the vessel by scooping the sample water in a bucket. Samples were immediately filtered with a syringe through precombusted Whatman G/FF filters. After filtration, samples were stored in sealed glass ampoules at -20°C until analysis.

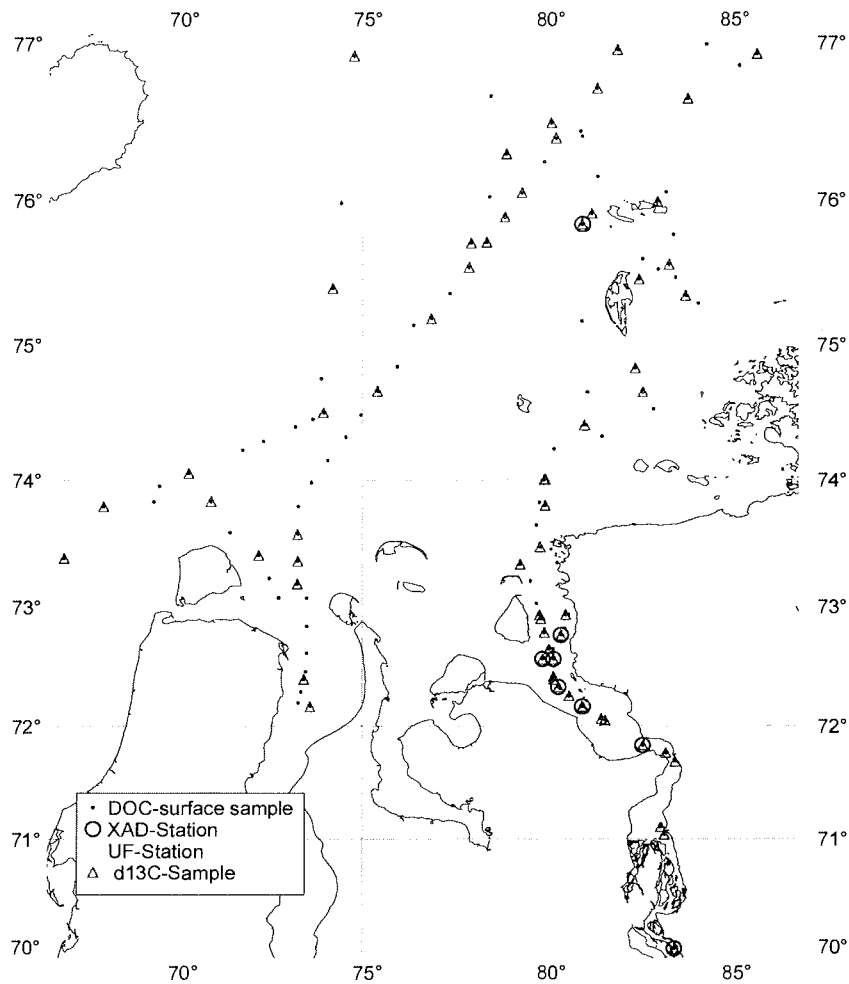


Fig.7-1: Location of sampling stations

$\delta^{13}\text{C}$ Sampling

In total 70 $\delta^{13}\text{C}$ -samples (100-250ml) were taken at 25 chosen main stations at different depths and at 45 additional spots during our cruise (Fig. 7-1). Samples were filtered (G/FF) and stored cool in acid-rinsed brown glass bottles until analysis.

A new technique, which was developed recently at our institute in Hamburg (Spitzky et al. 2001), allows us to perform $\delta^{13}\text{C}$ -analysis directly from the salt water matrix. By comparing the different $\delta^{13}\text{C}$ -values of marine and terrestrial DOM we hope to gather more information about the origin of the DOM.

Additional samples for DON-, Amino Acid- and CHO-determination were taken at all CTD- stations. These analyses will be performed at AWI.

Isolation of DOM

For detailed analyses and characterization DOM must be concentrated from the saltwater matrix. For isolation of DOM we used two different approaches: The XAD resin isolation technique concentrates components of seawater DOM that differ in chemical characteristics, such as hydrophobicity. The second approach, the tangential-flow ultrafiltration, is based primarily on physical characteristics such as molecular size and shape.

Ultrafiltration

Ultrafiltration samples were taken at 8 stations by using a large volume sampler (200l batomat). The water was pre-filtered through 3, 1 and 0,2 μm polycarbonate Nuclepore filters in a sequential manner and immediately ultrafiltered onboard the ship. Ultrafiltrations were performed by using disc-tube membrane modules (tangential-flow; Pall-Rochem), which were equipped with different membrane types (Desal, Osmonics). We mainly applied DK- and GE-membranes, which are expected to reject molecules with a molecular weight above 1000 Da and 400 Da respectively. For the freshwater samples in the estuary of the Yenisei an additional membrane (cut-off size 8 kDa) was applied. Water samples (80-300 l) were concentrated down to about 1,5L, yielding concentration factors of up to 200. DOM-concentrates were frozen until detailed analysis. DOC samples of each subfraction during the ultrafiltration process were taken.

XAD resin isolation

At two chosen stations 100 liters from the pre-filtered water (0,2 μm) were acidified to pH 2 by using hydrochlorid acid. The acidified sample was passed through a glass column filled with XAD-8 resin. Hydrophobic substances (humic and fulvic acids) are adsorbed by resin under these conditions. An alkaline solution (0,1 M NaOH) was applied to elute the hydrophobic substances. A detailed description of this method is given by Thurman and Malcolm (1981). The obtained extract of humic and fulvic acids was acidified and concentrated in a second step in a smaller column. After this procedure a concentration factor of 100 was reached. Concentrated samples were filled into brown glass bottles, reacidified to pH 2 and preserved by using HgCl_2 . To determine the hydrophobic component of total DOC we took 6 additional samples of the XAD outflow in the Yenisei Estuary.

Initial results

Concentrations of DOC ranged from 70 $\mu\text{M C l}^{-1}$ in the outer Kara Sea to 700 $\mu\text{M C L}^{-1}$ in the mouth of the Yenisei. In the Ob Estuary the maximum concentrations reached 450 $\mu\text{M C L}^{-1}$. Generally, these values agree well with the data from the cruises BP 1999 and BP 1997. However, this time we sampled the Yenisei endmember and the area north of 75° for the first time. As indicated by our salinity data (Köhler and Simstich, this vol.) the influence of both rivers in the northern part of our study area was very weak during the sampling period, so we were not surprised to find only low DOC-concentrations in the outer Kara Sea. At this stage we suppose that these lower concentrations of DOC are mainly due to mixing processes. Detailed analyses of the

fate and origin of the DOC will allow us to find out to what extent degradation processes might also play a role.

In the Yenisei Estuary we were able to isolate more than 65 % of total DOM with the XAD-resin technique. At the high-salinity endmember station (33,5 ‰) 38% of total DOM could be identified as humics. These values are clearly higher than those reported for the BP 1997 cruise (Amon and Spitzky 1999) but they agree well with the estuaries of other major world rivers (Spitzky and Leenheer, 1991).

The supplementary application of ultrafiltration and XAD-resins enabled us to isolate more than 80% of the total DOC in the Yenisei Estuary. In the open Kara Sea we separated about 60% of the bulk DOC from the salt water matrix. In general the recovery in seawater for the XAD technique is less than 30% and for ultrafiltration (1000 Da cut off) less than 40% (Benner et al., 1997; Benner 1998). It seems that the complementary usage of both techniques and the application of membranes with a cut off size of 400 Da improves the recovery quite distinctly.

More detailed information on our results will be presented elsewhere as soon as available.

7.2. The influence of dissolved organic matter on the behaviour of several radionuclides in sea and fresh water - preliminary results

O. Stepanets¹, A. Ligaev¹, A. Borisov¹, L. Kodina¹, A. Spitzky², and H. Köhler²

¹Vernadsky Institute of Geochemistry and Analytical Chemistry, RAS, Moscow, Russia

²Institute of Biogeochemistry and Marine Chemistry, University of Hamburg, Germany

The rivers Ob and Yenisei drain large areas of the Siberian Taiga. Hence the dissolved and suspended load carried by both rivers show a typical geological, geochemical and biological pattern of this unique environment. For example the high content of humic and fulvic compounds in the Ob and Yenisei can have an effect on the geochemical elements and their species in the estuaries and coastal seas.

The behaviour of radionuclides in marine environments depends on their chemical nature itself and on the physicochemical conditions in the environment. For example the alkaline element Cs and the alkaline earth element Sr are mobile in water. Plutonium radionuclides are rapidly concentrated and accumulated in the sediments, whereas usually about 90% of Cs remains dissolved in the water. Another important aspect concerning the solubility of radionuclides are the physicochemical conditions in the environment. Especially concentration and feature of the dissolved organic matter (DOM) might influence the distribution of radionuclides in natural waters. Due to the chemical structure of the DOM, some radionuclides like ⁹⁰Sr are able to build soluble complexes with organic compounds. The adsorption of ionic metal on colloids and the subsequent coagulation of colloids on large particles is the dominant removal process for metals in aquatic environments with a low concentration of suspended matter.

The main objective of our investigations is to expand our knowledge about the interactions between artificial radionuclides and dissolved organic matter. In this report we present preliminary data for the isotopes ¹³⁷Cs and ⁹⁰Sr in water samples of different salinities. All water samples were immediately filtered through 3 µm, 1 µm and 0,2 µm Nuclepore filters in a sequential manner. In a second step the prefiltered water was ultrafiltered by using a disc-tube membrane system (tangential-flow, Pall-Rochem). We applied membranes with a cut-off size of 1 kDa. Consequently, the ultrafiltered water contains only those organic molecules, which have a smaller molecular size than 1000 Da.

The counting for ¹³⁷Cs did not change significantly during the ultrafiltration process. Obviously the radionuclide ¹³⁷Cs does not interact with organic compounds. The results for Cs in near bottom water show that the suspended matter absorbs up to 1% of ¹³⁷Cs (Table 7-1). This means that the coefficient of ¹³⁷Cs concentration by suspended matter may be as high as 103-104. Apparently the suspended matter is able to transfer considerable amounts of radioactive caesium.

For the radionuclide ⁹⁰Sr from the riverine endmember sample we found clearly lower values in ultrafiltered water than in the pre-filtered water sample (Table. 7-2). We conclude that the observed difference is a result of the interaction between ⁹⁰Sr and DOM. It seems that more than 50% of ⁹⁰Sr is able to form complexes with dissolved organic matter and is retained as such in the fraction >1000 Da. In the more saline water

this effect is less clear. We suppose that the interaction between ^{90}Sr and DOM is mainly due to the concentration of humic and fulvic acids: these compounds have higher concentrations in river water than in marine waters of high salinity.

Table 7-1: Concentration of ^{137}Cs (Bq/sample) in the water and suspension.

Station	Suspension	Water
BP 95-36	0.02	3.3
BP 95-33	0.03	4.6

Table 7-2: Results of Sr-90 measurements in unfiltered water, filtered water ($1\mu\text{m}/0,2\mu\text{m}$), ultrafiltered water ($< 1000\text{Da}$) and on filter material ($>1\mu\text{m}$).

Station	Depth (m)	Salinity (psu)	Activity Sr-90, Bq/m ³			
			Not filtered water	Filter ($1\mu\text{m}$)	Filtered water ($1\mu\text{m}$)	Ultrafiltr. water
BP00-40	2	9,3		$0,5\pm 0,1$	$5,7\pm 1,1$	$2,6\pm 0,5$
BP00-19	2	$<0,1$			$4,2\pm 0,8$	$1,9\pm 0,4$
BP00-05	42	33	$1,0\pm 0,2$		$0,6\pm 0,1$	$1,0\pm 0,2^*$

*- filtered through $0,2\mu\text{m}$.

7.3 The carbon isotope composition of phytoplankton along the Ob–Kara Sea Transect in August–September 1999

Kodina L.A.

V.I.Vernadsky Institute of Geochemistry and analytical Chemistry, RAS, Moscow, Russia

Abstract

Along the Ob Transect a clear carbon isotopic variation manifested: from -25.1‰ in the sea part (salinity=11‰) to about -35‰ in the river water with salinity of 0.6‰. In opposite to Yenisei Estuary fresh-water plankton including green algae was predominant in the south Ob Bay. Sample of filamentous green algae (*Chlorophyta*, *Rhizoclonium?*) has been prepared for isotope analysis. The green algae *Rhizoclonium* was extremely depleted in ^{13}C and has an isotope composition of -37.0‰ . The diatoms from the same water have $\delta^{13}\text{C}$ -value of -27.4‰ . The difference in the $\delta^{13}\text{C}$ -values is discussed from the position of the peculiarities in biological fractionation between different algae taxa and CO_2 abundances.

Introduction

Stable carbon isotope ratio is a useful tool to study carbon cycling because it may allow to trace sources of organic matter in sediments. Carbon isotope composition of dissolved organic matter alongside with specific biomarkers has been applied in identification of water masses of different origin, in particular for detection of Arctic waters in the North Atlantic (Opsahl et al., 1999).

Distinction between two genetic types of organic matter in the Arctic Basin is complicated by the presence of sharp temperature and salinity gradients due to large input of fresh water by Ob and Yenisei rivers to the Kara Sea. The river discharge brings inorganic carbon depleted in the ^{13}C -isotope to the sea which makes a great impact to the biological carbon cycling. Evaluation of the contribution of terrigenous and plankton carbon in the organic carbon pool in the sea call for reliable data of the carbon isotope ratio for the two endmembers.

Laboratory experiments revealed the complexity of biological isotope fractionation in aquatic plants, its great variability depending on the environmental conditions and biological peculiarities of different species (Descolas-Gros. and Fontugne., 1990; Fischer, 1991; Freeman and Hayes, 1992; Goericke, Fry., 1994; Hayes, 1993; Hayes et al., 1999; Rau et al., 1982). Paucity of isotopic data on Arctic plankton invites further investigations of phytoplankton natural communities against salinity gradient in the Kara Sea.

Sampling

Sampling of phytoplankton for organic carbon isotope composition in the estuarine area of the Kara Sea has been carried out in the Joint Russian-German Cruises onboard «Akademik Boris Petrov» 1997, 1999, and 2000. Phytoplankton sampling and floristic description of the native samples were performed by Dr. V. Larionov (Makarevich and Larionov, this vol.).

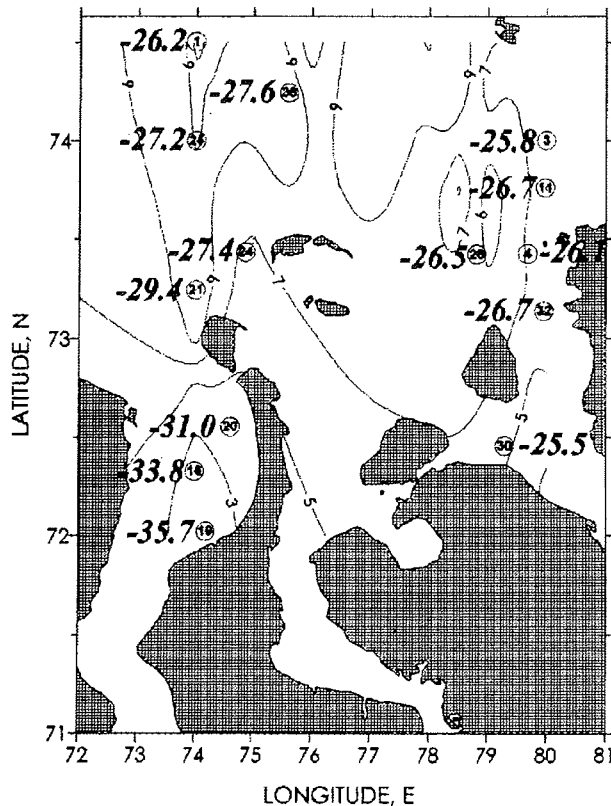


Fig.7-2: $\delta^{13}\text{C}$ - values of phytoplankton in Ob-Yenisei-Kara Sea area in Sept.1999. Station numbers are circled. Surface water salinity isolines are given.

Below we present data from the expedition August-September 1999 inside the Ob Estuary and adjacent part of the open Kara Sea.

Six stations (25,24,21,20,18,19) of the Ob- Kara-Sea Transect were sampled within 3 days (31.08 - 03.09.99) and may be considered as quasi-synoptic. Surface water salinity ranged along the transect from 0.6 to 11‰. The area map with the plankton station locations, surface water salinity and isotope composition ($\delta^{13}\text{C}$, ‰) of the plankton samples is given in Figure 7-2.

In the Yenisei Estuary 6 stations were sampled. Stations 3,4,11 were sampled at 26-28 .08.99, Sts. 28, 30, 32 - about a week later: 4-6. 09.99. Because of late ice thawing in the Yenisei mouth that year, low salinity of 5.30-8.8 ‰ was observed in the sea area and the outer Yenisei Estuary. The common feature of the Yenisei plankton stations is extremely low bioproduction with absolute prevalence of marine diatoms and marked contribution of unidentified debris at most stations. At St.32 about 50% of unidentified debris was present in the plankton sample, at St.4 about 26% (Makarevich and Larionov, this vol.). A deficiency of material did not allow to concentrate algae biomass enough for getting representative clean samples of diatomic plankton from Yenisei and native plankton samples collected without any special preparation.

For isotope analysis we intended to get phytoplankton biomass uncontaminated by some poorly characterized debris or products of consumer organisms as well as sediment particles, particularly at shallow water stations and during windy weather.

Results and discussion

There were no pronounced variations in the plankton isotope composition between the stations located in the area of low salinity in the Yenisei Estuary (Fig. 7-2). $\delta^{13}\text{C}$ -values of the bulk plankton samples were clustered between -25.5 and -26.7 ‰ without any relation to the minor variation of water salinity in the area (5.5-7.0 ‰).

A large range of isotope values for bulk phytoplankton from -26.2 ‰ to -35.7 ‰ was determined along the Ob-Kara Sea Transect. If not taken into account the two far northward stations 1 and 38, which had been sampled in a time interval of two weeks when salinity at that point changed twofold, it is evident that there exists a rather good relation between the stable carbon isotope ratio in the phytoplankton and water salinity along the longitudinal Ob Transect (Fig. 7-2). The phytoplankton carbon is getting depleted in ^{13}C -isotope southwards with decreasing salinity. Stations 25 and 24 are similar to the situation in the Yenisei Estuary in the sense that marine diatoms are far prevailing in the phytoplankton community, except that Ob plankton community is impoverished in detritus, at the St.24 fresh water diatoms are present (38% of *Melosira varians*; Makarevich and Larionov, this vol.), and fresh water green algae *Chlorophyta* appeared for the first time in the Ob Transect.

Within Ob Bay, carbon isotopes are highly ^{13}C -depleted. $\delta^{13}\text{C}$ values of algae communities range from -31.0 to -35.7 ‰. The surface water salinity (5.9 -0.6 ‰) agrees with long-term mean data from climatological database for this area (Stephantsev and Shmelkov, 2000) with strong spatial variation, resulting from changing river discharge and weather conditions (Amon, 2000).

Three stations (No 20,19,18) were studied in detail. Phytoplankton communities consisted of fresh-water algae species with subordinated brackish- water species and small percentages of marine species (at St. 20 and 18) (preliminary data from V. Larionov).

At St. 19 rather high bioproductivity was detected, and we made an effort to separate large filamentous green algae identified as *Rhizoclonium* ? (*Chlorophyta*) for isotopic analysis by screening the fresh water (S = 0.6 ‰) sample (15 l) through a hand net with

an effective pore size of 90 μm . The long green filaments were left on the screen surface, washed with distilled water and taken carefully off from the screen with needles under microscopy control. Filtrate was poisoned with HgCl_2 and left to stay under cold conditions. Precipitate was collected for isotope analysis. It was brown in colour as opposite to the bright green filaments of *Rhizoclonium*. All procedures were performed with fresh samples on board "Boris Petrov".

Carbon isotope analysis showed, that the fresh-water green algae from the Ob Bay are extremely depleted in the ^{13}C -isotope ($\delta^{13}\text{C} = -37.0\text{‰}$). Dissolved inorganic carbon at the sampling point is of -12.5‰ PDB. It means that carbon dioxide which is a photosynthesis carbon source for fresh-water green algae, is enriched in the ^{12}C -isotope by -11.3‰ at a temperature of $+4^\circ\text{C}$ relative to the dissolved bicarbonate (calculated after Mook et al., 1974) and has $\delta^{13}\text{C}$ value of -23.8‰ . Then, the photosynthetic fractionation corresponds to -13.2‰ . This is a reasonable value, if taken into account high bioproductivity of the fresh-water plankton at the sampling point. According to Hayes et al. (1999), in the modern ocean value of isotope fractionation commonly ranges between 8 and 18 ‰ in dependence on the CO_2 abundances.

In fact we distinguished isotopic heterogeneity of the microalgae community, with the green algae being the most depleted in the ^{13}C -isotope (-37‰). In the filtrate after separation of the green algae, fresh-water diatoms among which were *Melosira varians* (prevailing), *Asterionella formosa*, brackish water diatom *Melosira granulata*, were enriched in the ^{13}C to the value of -27.4‰ .

Investigations of the last decades evidence a great variability of environmental factors which influence the carbon isotope fractionation in marine photosynthesis. All variations can be explained in terms of variations in concentration of dissolved CO_2 (Freeman and Hayes, 1992; Fry and Wainright, 1991).

Diatoms are supposed to be enriched in the ^{13}C -isotope relative to other plankton because of possibility to assimilate HCO_3^- using phosphoenolpyruvate carboxylase (Descolas-Gros and Fontugne, 1990; Fontugne et al., 1991). Many diatoms and some other taxa (*Prymnesiophyceae*) possess an active transport mechanism to uptake bicarbonate and are therefore insensitive to changes in the carbon dioxide concentration in the environment (Tortel et al., 1997). The extent to which other phytoplankton groups are also enriched in ^{13}C is not yet fully known. The variability in cellular metabolism caused by changing physiological state and environmental conditions, makes any comparisons between different species difficult.

An impact of the fresh-water plankton might not be excluded as another source (in addition to the terrestrial one) of isotopically depleted carbon source in the Kara Sea. Further studies are needed to resolve its efficiency.

This paper was prepared under support of the Russian Foundation for Basic Research, Project 00-05-64575.

7.4 Particulate organic carbon in river and sea waters: Concentration and stable isotope ratio

Bogacheva M.P.¹, Kodina L.A.¹, and Ljutsarev S.V.²

¹V.I.Vernadsky Institute of Geochemistry and analytical Chemistry RAS, Moscow, Russia;

²P.P.Shirshov Institute of Oceanology RAS, Moscow, Russia)

Abstract

The present data were obtained from particulate organic matter collected during the joint Russian-German Cruise 35 of R/V "Akademik Boris Petrov" in September-October 2000 along south-north transect from the river Yenisei to the open Kara Sea area. $\delta^{13}\text{C}$ -values for river stations correspond to -30.4 and -30.5‰ PDB. POC samples are getting less depleted as the water salinity is increasing. The most enriched in ^{13}C organic carbon (-25.5‰) was observed in the sea water of high salinity (26.6 psu). POC concentrations in the river part of the transect are the highest and range between 199 and 291 $\mu\text{g/l}$. The mixing zone of the fresh river water with marine water of high salinity was marked with the sharp drop of the POC concentration and enrichment of the water suspended material in the heavy carbon isotope.

Introduction

The data were obtained from material collected during the joint Russian-German Cruise 35 on board R/V "Akademik Boris Petrov" in September-October 2000. The location of the sampling stations along the Yenisei-Kara Sea Transect extending from about 70°N to 77°N is shown in Figure 7-3. There are 17 sampling stations along the transect. Five of them (St. 19,18,17, 20,21) belong to the river part of the transect; five stations (St. 16,15,22,13, 23) are located within the Yenisei Estuary, the other stations are located in the open Kara Sea. The present study might be considered as an additional contribution to the previous investigations of particulate organic carbon isotope geochemistry in the Yenisei Estuary and adjacent Kara Sea (Kodina et al., 1999) in the sense that the present study includes some fresh water river stations (surface water $S = 0$ psu), and sea water of rather high salinity (surface water $S = 273$ psu) at the far northern station close to the ice edge.

Methods

Surface water sampling was performed with a bucket, the other samples were taken with rosette sampler or large - volume steel bathomat (200 l). Standard filtration procedure under vacuum through the fiber-glass Whatman filters GF/F was used. The filters with POM were pretreated with concentrated HCl vapour in a dessicator before organic carbon isotope analysis and determination of C_{org} concentration. Analytical methods have been described earlier (Kodina et al., 1999; Ljutsarev et al., 1994).

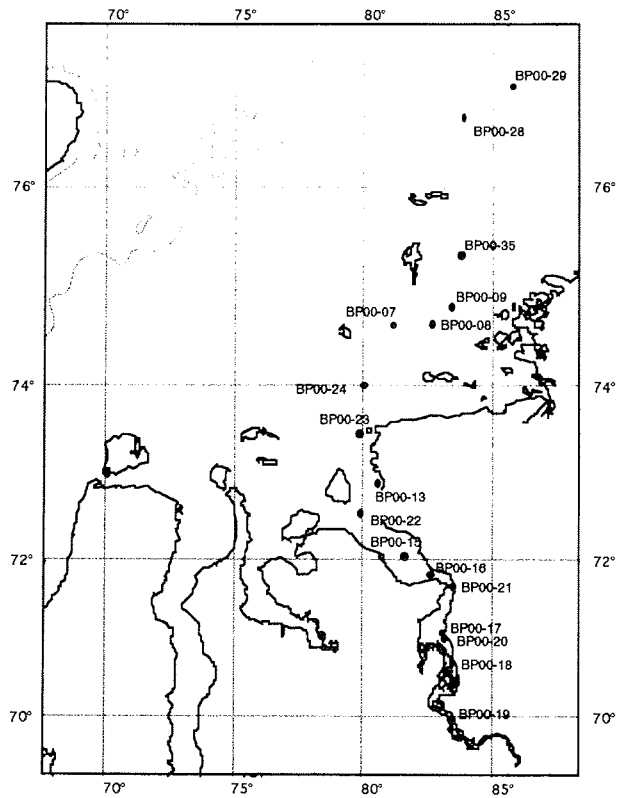


Fig.7-3: Location of POC sampling stations along the Yenisei-Kara Sea Transect.

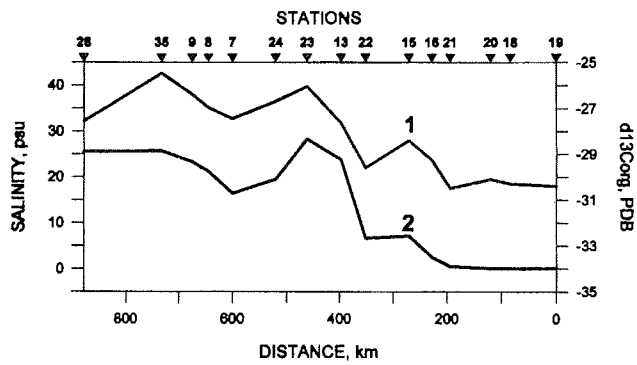


Fig.7-4: Distribution of $\delta^{13}C_{POC}$ values (% PDB) (Curve 1) and surface water salinity (Curve 2) along the transect.

Results

The results on the POC isotope composition are presented graphically in Figure 7-4 against the corresponding water salinity values. It is obvious that both curves are almost parallel. The regularity of POC isotope composition distribution pattern is governed by the water salinity: fresh-water POC samples are highly depleted in the ^{13}C isotope. $\delta^{13}\text{C}$ -values for river stations correspond to -30.4 and -30.5 ‰ PDB. POC samples are getting less depleted as the water salinity is increasing. The most enriched in ^{13}C organic carbon (-25.5 ‰) was observed in the sea water of high salinity (26.6 psu).

The fresh river water is most enriched in suspended material. POC concentrations in the river part of the transect range between values of 199 and 291 $\mu\text{g/l}$ with some fluctuations (Fig. 7-5). At St.22 ($S = 6.6$ psu) it reaches the extra value of 291 $\mu\text{g/l}$ and then drops sharply when salinity rises to 22.8 psu (St. 13) due to mixing of the high salinity marine water with fresh water (hydrological front). The mixing zone is characterized by active chemical and physical transformations resulting in precipitation of the large proportion of the dissolved and particulate material which was carried with fresh river water (Lisitsin, 1994).

As might be expected from this phenomenon, particulate material suspended in water is enriched sufficiently in the ^{13}C isotope at St.13 and northwards. This regularity of geochemical behaviour of particulate carbon and its isotopes by mixing of fresh and saline waters in the estuarine area is clearly seen in Figure 7-5. Sea water of high salinity is characterized by lowest concentrations of particulate organic carbon (as low as 20.1 $\mu\text{g/l}$).

The study has been supported by the Russian Foundation for Basic Research, Grant 00-05-64575.

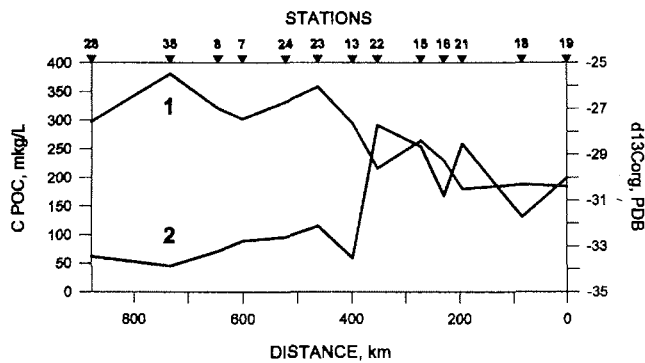


Fig.7-5: Distribution of $\delta^{13}\text{C}_{\text{POC}}$ values (‰ PDB) (Curve 1) and POC concentration ($\mu\text{g/l}$) (Curve 2) in surface water along the transect.

7.5 Geochemistry of carbon and silica: water column and sediment sampling. Material, methods and first results

D. Unger, S. Schayen, K. Neumann, and B. Gaye

Institute for Biogeochemistry and Marine Chemistry, University of Hamburg, Germany

Introduction

The Kara Sea forms part of the Eurasian continental margin and receives about one third of the freshwater and more than half of the sediments delivered to the Arctic Ocean via rivers (Pavlov and Pfirman, 1995). The freshwater supply strongly influences the hydrography in the working area leading to low salinity in surface waters and a strong stratification of the water body as observed during the "Akademik Boris Petrov" expeditions (e.g. Stephantsev and Shmelkov, 1999; Amon and Köhler, 1999). Furthermore, the riverine input has a strong impact on the distribution and quality of suspended particulates and sediments in the Ob and Yenisei estuaries and the Kara Sea (e.g. Fernandes and Sicre, 2000; Lobbes et al., 2000; Lukashin et al., 1999) which are characterized by a complex mixture of autochthonous and allochthonous sources (e.g. Kodina et al. 1999; Boucsein et al. 1999).

The investigations carried out along the salinity gradient and within the water column aim to characterize the quantity and quality of the suspended matter with special emphasis on organic and silicious material. A comparison with surface sediments and the cooperation with other SIRRO-subprojects (DOC, nutrients, biomarkers, stable Carbon isotopes) will offer a comprehensive data set which will improve our understanding of the present material transfer and transformation processes in the two estuaries. This is also a prerequisite for deciphering the sedimentary record.

Shipboard Sampling Program and Methods

During the "Akademik Boris Petrov" 2000 expedition special emphasis was put on the investigation of the eastern part of the working area between 70 and 77°N (Fig. 7-6). In course of this cruise the investigated area was substantially extended to the north and south as compared to the former cruises in 1997 and 1999, and the existing set of samples was complemented. At the southernmost part of this year's transect the water masses were of pure riverine nature (= 0‰ salinity) throughout the water column, and particulates at this station are expected to represent the material delivered to the Kara Sea by the Yenisei river at the end of the high discharge period during summer. In addition to the Yenisei riverine endmember we were provided with riverine suspended material and soil samples from the Ob river at Salekhard gained during a sampling campaign in June 2000 by H. Köhler. These samples will enable us to characterize the riverine/terrestrial material which enters the Kara Sea via the rivers Ob and Yenisei.

Water sampling for filtration of suspended matter was carried out at 28 stations (Table 7-3, Fig. 7-6). Sampling depths were chosen according to the CTD profiles. Generally, water was taken from the low salinity surface layer, from the pycnocline and the near bottom water. Surface water samples were taken by bucket, whereas water from the

intermediate and deep layers was sampled by means of a 24-bottles Niskin rosette water sampler and/or a large volume sampler (Bathomat, 200 l).

One part of the obtained water was filtered through preweighted polycarbonate membrane filters (Schleicher & Schuell) with a pore size of 0.4 μm and a diameter of 47 mm for biogenic silica (opal) analyses. The remaining water was filtered through preweighted and precombusted glass fibre filters (GF/F Whatman) with a diameter of 47 and 25 mm, respectively, for organic compound analysis and calculation of total suspended matter concentration. The filters were dried at 40°C for 24 hours.

In addition to suspended matter, surface sediment samples were collected from a multiple corer. This material was stored frozen and was freeze-dried in the home laboratory before further analysis.

Both suspension and sediment samples will be analysed for their content of organic carbon and total nitrogen, carbonate, biogenic opal (silica), lithogenic material as well as for stable nitrogen isotopes, amino acids and amino sugars.

Table 7-3: Water sampling stations, water depths, sampling depths and respective salinity, sampling device and water volume filtrated. *B=Bucket, R=Rosette Water Sampler, Ba=Bathomat (200 l).

Station BP 2000	Water Depth [m]	Sampling Depth [m]	Salinity [‰]	Sampling Device*	Water Volume [l]
02	49,6	surf	17,6	B	32,5
		11,8	20	R	13
		48	33,6	R	12,5
03	193	surf	21,3	B	47
04	54	surf	25,7	B	35,5
		12-12,8	29,1	R	2
		50	34,1	Ba	27
05	50	surf	22,0	B	50
		11-12	27,9	Ba	35,5
		44	33,7	Ba	27
06	38	surf	21,8	B	43,5
07	38	surf	16,5	B	36
		11,2-11,8	25,5	R	15
		35	32,8	Ba	19,5
08	41	surf	20,9	B	40
		5,8	23,7	R	16
		37	33,4	Ba	28
09	44	surf	23,8	B	34
		14,9	28,5	R	16
		43	33,5	Ba	30
13	13	surf	21,6	B	24
		3,5-4,1	25/25,6	R	13,5
		10,1	29,5	R	14
15	5,8	surf	6,7	B	15,5
		5,6	7,3	R	10
16	26	surf	2,3	B	17,5
		15,5	12,7	R	13
		24	20,9	Ba	9,5
17	18	surf	0	B	24,5
		~18	0,6	Ba	16

Table 7-3: cont.1

Station BP 2000	Water Depth [m]	Sampling Depth [m]	Salinity [‰]	Sampling Device*	Water Volume [l]
19	22	surf	0	B	30
20	20	surf	0	B	24
21	24	surf	0,3	B	14,5
		12	5,9	R	1
22	11	surf	6,6	B	20
		3,7	19,6	R	13,4
		4	7,8	R	
		10,7	30,4	R	15
23	33	surf	28,2	B	41
		9,2/14,2	30,3/31,7	R	10
		32	33,1	Ba	22
24	31	surf	23,8	B	37,5
		16	27,9	R	13
		32	32,3	Ba	31,5
26	68	surf	18,9	B	39,4
		17	25,6	R	16
		63	33,7	Ba	33
27	78	surf	23,2	B	45,5
		12,5	26,4	R	15
		74	34,2	Ba	34
28	50	surf	25,5	B	50,5
		16,2	29,5	R	18
		50	34,1	Ba	19
29	68	surf	27,2	B	60
		17,5	30,4	R	28
		65 ?	34,4	Ba	49
30	52	surf	24,7	B	53
		28	29,6	Ba	57
		51	33,9 ?	Ba	36
31	43	surf	25,5	B	27
35	46	surf	26,6	B	54
		13,7	30,1	R	26
		46	33,3	Ba	18
36	66	surf	27,1	B	56
		14,5 (deepML)	27,4	R	9
		17,5	29,9-30,5	R	15,5
		63	33,9	Ba	30
38	20	surf	16,3	B	17
40	9	surf	9,3	Ba	6,5

Flocculation experiment

In order to study flocculation and sorption processes occurring during the mixing of riverine and marine water masses (e.g. Hedges and Keil, 1999) we mixed water of the riverine endmember (0 ‰) with high salinity deep water of marine origin (33,7 ‰) thus obtaining 7 mixtures of different salinities (0, 3, 6, 9, 15, 25 and 33,7 ‰). Approximately 24 h after mixing the water was filtered through precombusted glass fibre filters (GF/F) for the investigation of the partitioning of carbon and nitrogen between the particulate and dissolved phases.

Laboratory Methods

At the home laboratory the amount of particulate matter on each filter was determined and the total suspended matter (TSM) concentration was calculated. The given TSM concentration at a certain station and depth is the average of several filters.

Total carbon and nitrogen were determined with a Carlo Erba Nitrogen Analyzer 1500. Average standard deviation for duplicate analysis was 0,4% for carbon and 0,06% for nitrogen. For the BP99 suspended material samples and all sediment samples the given particulate organic carbon (POC)-values are calculated by subtracting the carbonate-carbon from the total carbon (TC) content. Carbonate analysis carried out conductometrically with a Wösthoff Carmograph 6 resulted in carbonate percentages <1% (average 0,35 with 2 samples >1%) for the suspended material of BP 1999. For the suspended matter of BP 2000 only TC values are given. Due to the overall low carbonate content of the BP 1999 samples no significant differences between TC and POC are expected and a preliminary comparison of both data sets seems acceptable. We refrained from carbonate removal by acidification in order to avoid losses of nitrogenous compounds (e.g. Lohse et al., 2000).

C/N ratios were calculated from weight percentages of organic carbon (total carbon for BP2000 suspension) and total nitrogen.

First Results and Discussion

Suspended particulate matter

During the "Akademik Boris Petrov" cruise in 2000 the study area was substantially extended to the north as compared to the cruises in 1997 and 1999 (Fig.7-6). The surface waters in the northernmost part of the study area in 2000 were characterized by salinities of >25‰ whereas surface salinities at the sampling sites in 1999 did not exceed 12,7‰. The fluvial impact which is reflected in the surface salinities also influences the distribution of suspended particulate matter. Figure 7-7 shows the TSM concentration in Kara Sea surface waters as observed during the research cruises BP 1999 and BP 2000. The trend of decreasing TSM concentration in offshore direction which has been observed earlier (Shevchenko et al., 1996, Lukashin et al., 1999) could be verified in 2000 and mirrors the reduced influence of riverine particulate matter on TSM distribution in the distal part of the working area. Lowest concentrations of <0,5 mg/l were observed north of 75,5°N, highest ones were found in the estuaries. In general, our datasets of both cruises are in good agreement with each other. Some exceptional high values can be explained by lateral input from the coastline or islands (e.g. southernmost Yenisei station 1999) or resuspension and water column mixing due to strong winds (e.g. southernmost Ob stations in 2000). Average TSM concentration in bottom waters (range: 0,4-94,8 mg/l) exceeds that in surface waters. This can be attributed to the resuspension of sediments.

According to literature data the suspended matter concentration of Ob decreases downstream (Smith and Alsdorf, 1998) and reaches approximately 34 mg/l near Salekhard (Telang et al., 1991). This is consistent with our TSM-data at Salekhard during June 2000. For the Yenisei River lower values of 26-30 mg/l were reported (Telang et al., 1991, Lobbes et al., 2000). The estuaries of both rivers, however, are

characterized by much lower concentrations (this study, Shevchenko et al., 1996, Lukashin et al., 1999) indicating substantial particle sedimentation in the upstream area of both rivers.

The content of organic carbon in the suspended material in surface waters varied between 2,6-30,1 % (BP 1999) and 2,5-23,8 % (BP 2000), respectively (Fig. 7-8). Highest values were found in offshore waters, lowest ones in the river mouths. Compared to surface water samples, the suspended material from bottom waters can be characterized by reduced POC-contents (2,4-9,3 during BP 1999 and 2,2-13,3 during BP 2000). Generally, increasing TSM-concentrations are coupled to an exponential decrease in POC-content (Fig. 7-9). The suspended material collected from the Ob river at Salekhard during the high discharge period plots at the lower end of this regression (Fig. 7-9). This hints to the diluting character of relatively POC-poor riverine and sedimentary particulate matter on the one hand and the increased importance of *in-situ* produced organic matter at low TSM concentrations on the other hand. Despite the high contribution of POC to TSM in the distal part of the study area, absolute content of organic carbon in the surface waters is highest in the estuaries. Maximum values here are related to the elevated TSM concentration or to high biological productivity (e.g. Ob Estuary in 1999).

C/N values of the suspended matter in surface waters vary between 6,1 and 8,8 and may indicate a strong influence of algal material. Only 3 samples which seem to be influenced by lateral input of terrestrial material from the coastline show higher values of 9,3-11,2.

During BP 1999 the contribution of POC to TSM was higher in the Ob than in the Yenisei Estuary. This reflects the observed productivity pattern with higher abundance of algae in the Ob region. The elevated contribution of freshly produced algal organic matter is further corroborated by our amino acid data which reveal an elevated contribution of these labile organic compounds to the POC in the inner Ob Estuary surface samples as compared to the suspended material collected during the same cruise in the inner Yenisei Estuary or material from the Ob River at Salekhard in June 2000. With decreasing fluvial influence in offshore direction the amino acid contribution to the POC increases (only BP 1999 samples analysed by now) indicating higher proportions of freshly produced marine organic matter.

Sediments

The content of POC in the surface sediments reveal distinct regional variability related to the fluvial input. In contrast to the POC-content of suspended material in the surface water (Fig. 7-8) the POC content of the sediments decreases in offshore direction from 2,2 and 2,8 % in the Ob and Yenisei Estuary, respectively, to 1,1 % in the most distal parts of the study area (Fig. 7-10). Sporadic values <1% are related to coarser sedimentary matter with contribution of sandy material (see core description, Stein and Stepanets, 2000). This observation shows that not only POC input but also grain size and thus particle surface area of the sediments affect the potential preservation of organic material in sediments (Mayer, 1994; Keil et al., 1994; 1998; Bergamaschi et al., 1997). The opposing trends in POC concentration observed for suspended material and surface sediments indicate a more intensive degradation of organic matter within the water column in the distal part of the working area. This observation hints at the refractory nature of riverine borne organic matter.

C/N-values of the surface sediments vary between 7,2 and 12,4 (one exception: 5,5). In contrast to the suspended material the C/N values of surface sediments show a distinct regional variation with highest values in the Yenisei Estuary and an overall decrease in offshore direction. This reflects the significant influence of riverine and terrestrial organic matter which is characterized by higher C/N values (e.g. Hedges et al., 1986), on the composition of the sediments.

Acknowledgements

We would like to express our thanks to the Captain and crew of R/V "Akademik Boris Petrov" for their excellent assistance and support during the work on sea. We would also like to thank all colleagues onboard Akademik Boris Petrov for their help and friendly cooperation during the cruises.

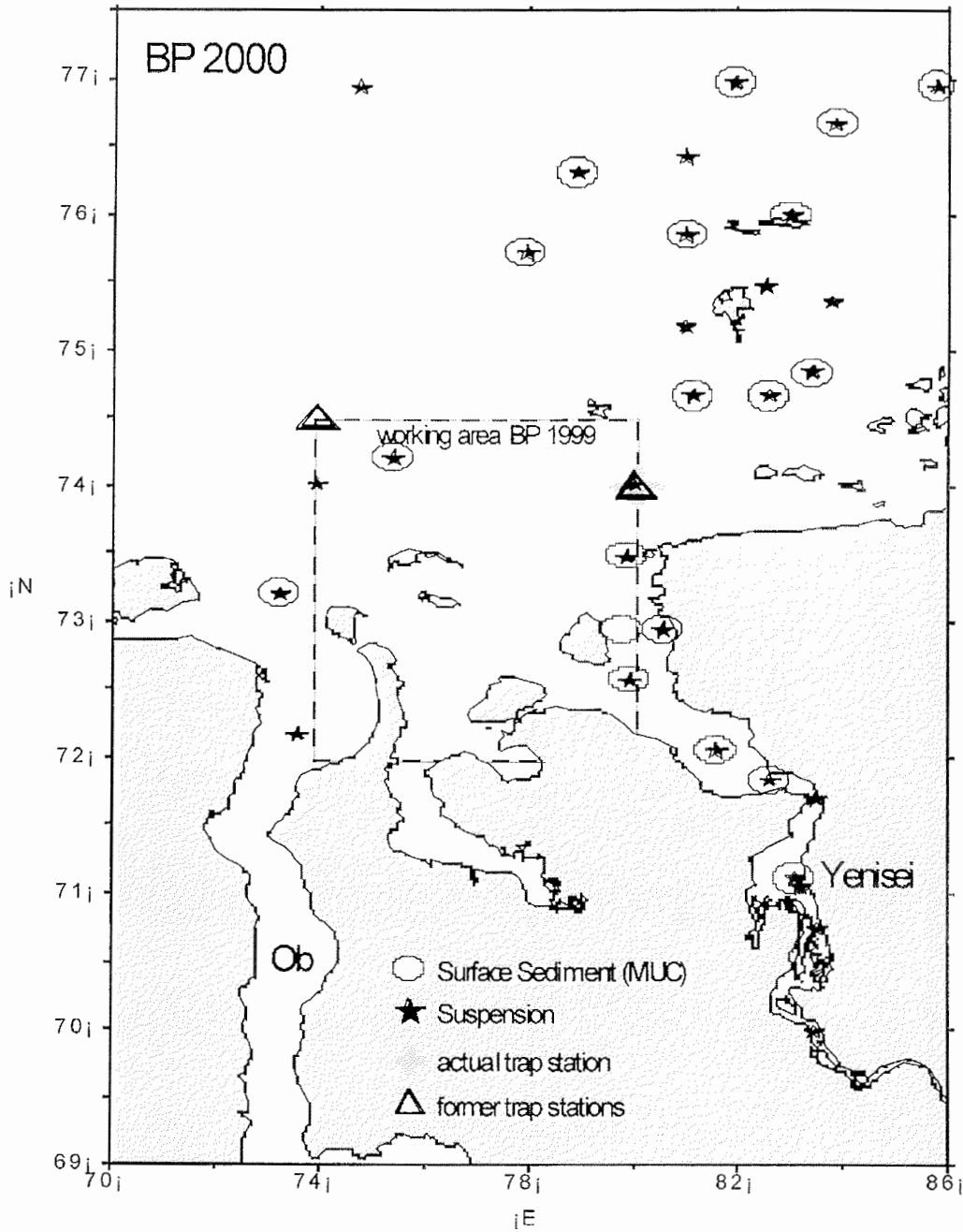


Fig. 7-6: Sites of suspended matter and surface sediment sampling and sediment trap recovery and deployment during BP 2000. The extension of the working area during BP 1999 is indicated by the stippled line.

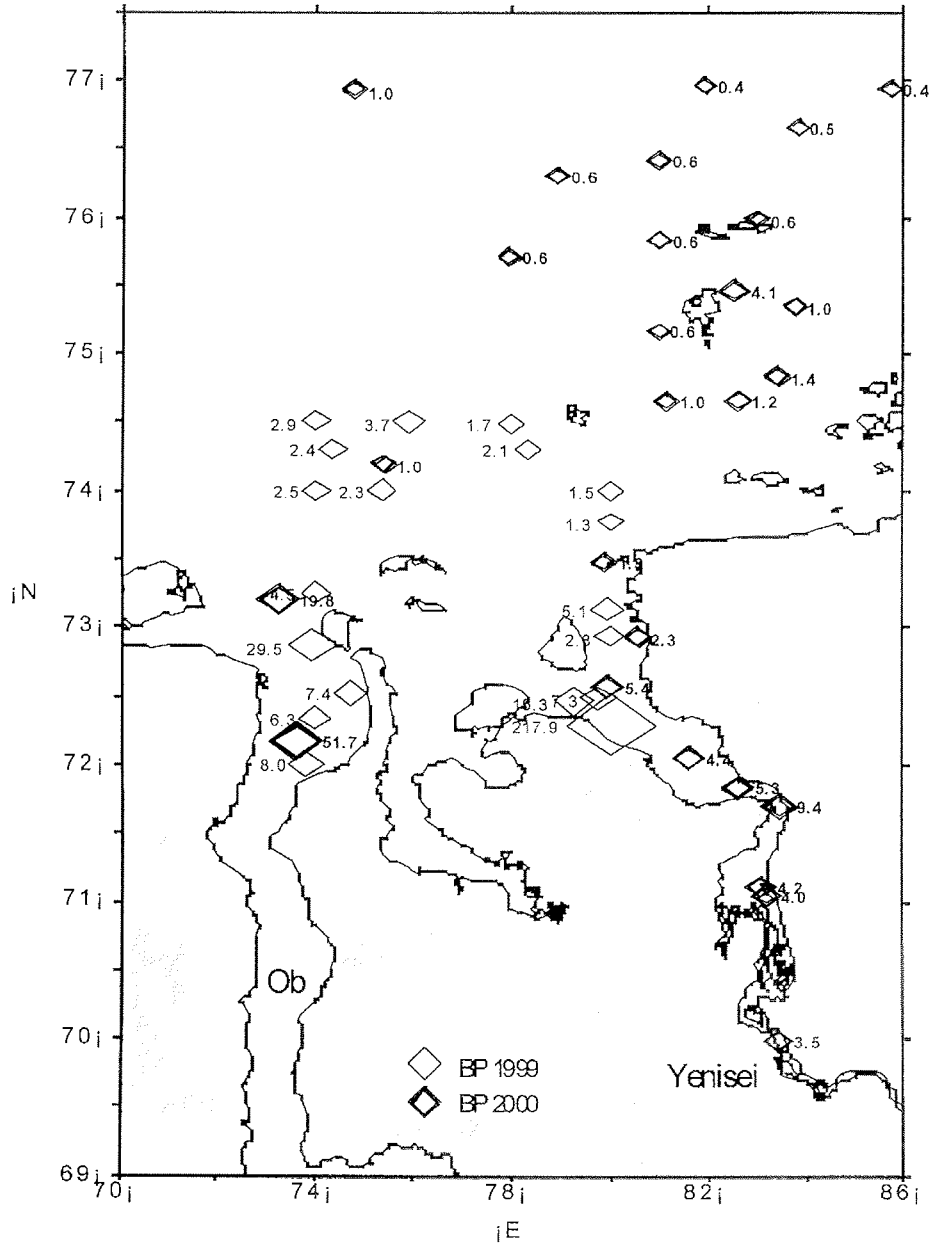


Fig. 7-7: Total suspended matter concentration [mg/l] in surface waters during BP99 and BP2000 (bold symbols and numbers).

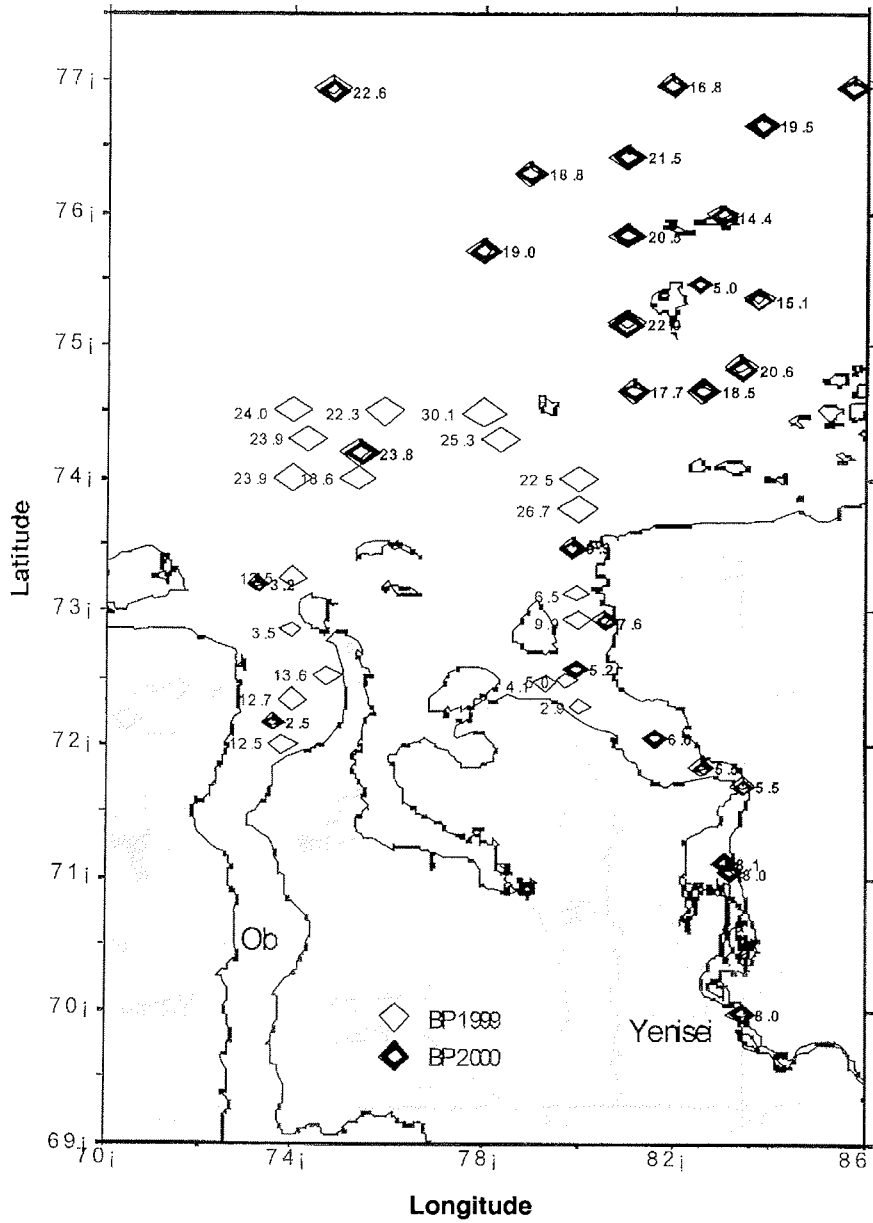


Fig. 7-8: Content of POC [%] in the total suspended material in surface waters in the Kara Sea during BP99 and BP2000 (bold symbols and numbers).

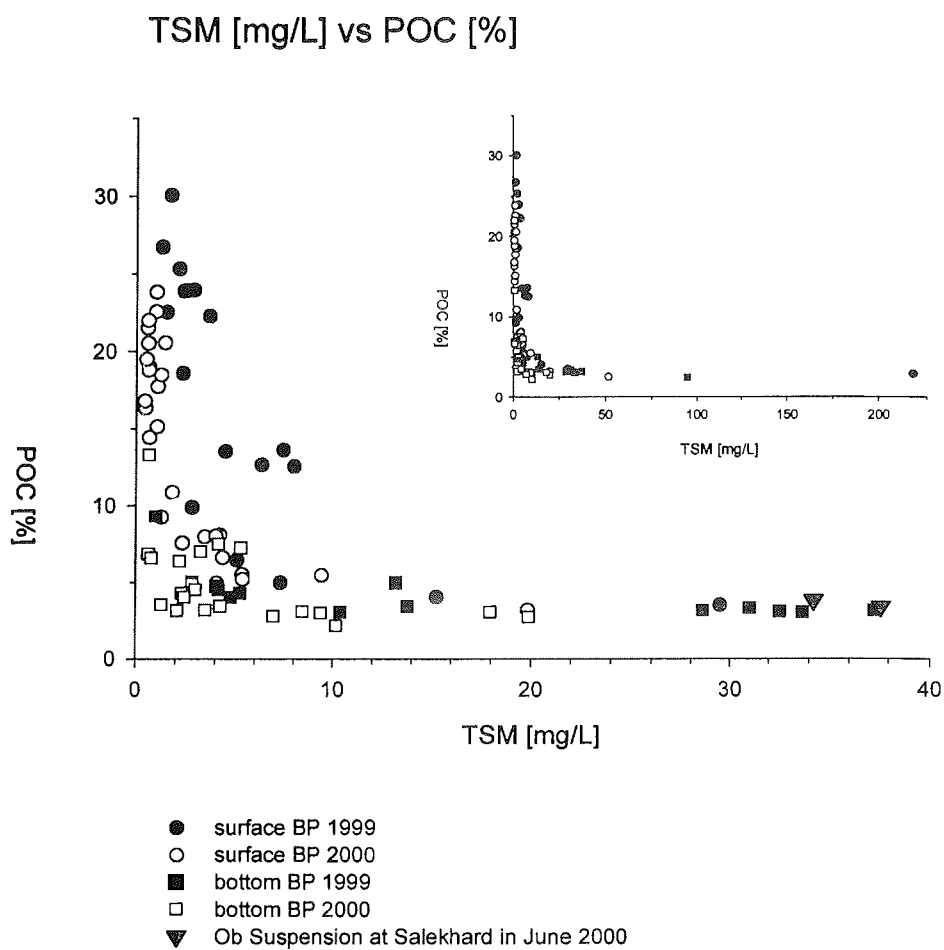


Fig. 7-9: The content of organic carbon decreases exponentially with increasing TSM concentrations. In the upper small graph, three samples with exceptional high TSM concentrations are included, in the lower big graph data from the Ob river at Salekhard are included.

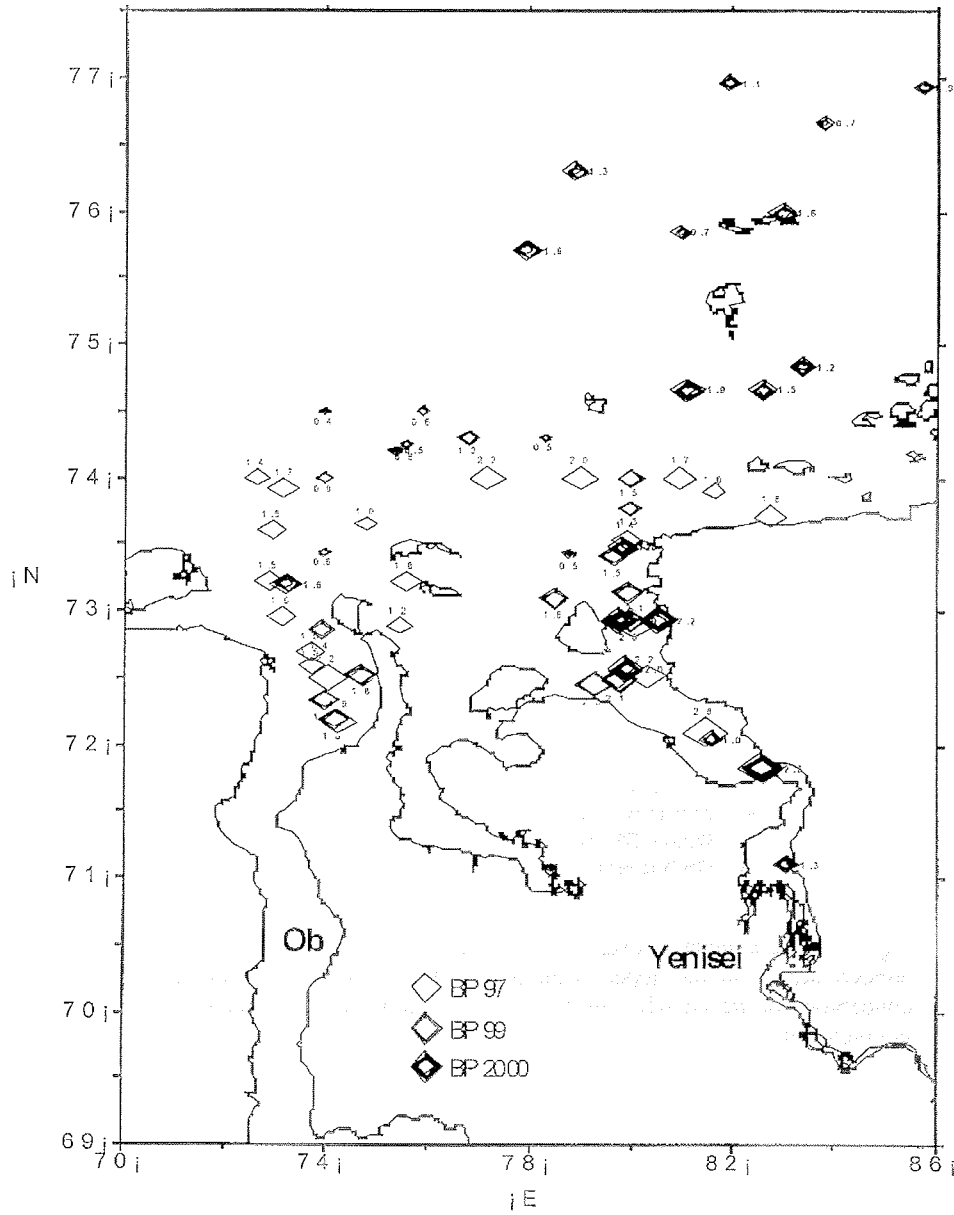


Fig. 7-10: Content of POC [%] in Kara Sea surface sediments taken during the cruises BP 97 (fine symbols and numbers), BP 99 and BP 2000 (bold symbols and numbers).

7.6. Geochemistry of particulate organic matter in the water column and sediments of the Yenisei River and inner Kara Sea

Fahl, K., Hollmann, B., and Stein, R.

Alfred Wegener Institute, Bremerhaven, Germany

Introduction

Major objectives are the characterization and quantification of particulate organic matter accumulated in the Ob and Yenisei estuaries and the adjacent Kara Sea. Information on the quantitative amounts of organic carbon derived from the respective sources (i.e. terrestrial/freshwater vs. marine) can be deduced from detailed organic-geochemical investigations of the suspended matter in the water column and the sedimentary organic carbon fraction. Both, bulk data (TOC, C/N-ratios, hydrogen index) as well as quantitative and qualitative biomarker distributions (*n*-alkanes, fatty acids, sterols, hopanoids, etc.) and $\delta^{13}\text{C}$ of biomarkers will be used to characterise and identify the different sources of the particulate and sedimentary organic carbon pool.

Sampling of particulate organic matter and sediments

67 water samples 27 stations were obtained either by use of a Niskin rosette water sampler, large volume sampler (Bathomat, 200 L) or a water bucket. Sample locations were selected according to the salinity gradient recorded by the CTD-system. Water sampling stations, depth of the subsamples and the respective salinity are given in Table 7-4. In general, three water depths were sampled at each of the selected stations: surface water, the pycnoclyne (mixed-water) layer and near-bottom water. The water samples were filtered through precombusted glas-fiber filters (Whatman GF/F, 47mm diameter). The particulate organic matter collected on these filters was pre-extracted onboard with a mixture of 10ml Dichlormethane/Methanol (1:1) and stored under light-protection at -20°C. The quantitative and qualitative distribution of individual biomarkers (*n*-alkanes, fatty acids, sterols, hopanoids) will be used to investigate the biological sources (marine vs. terrestrial) and the conversion of the particulate organic matter prior to sedimentation.

In addition to the water samples, at GKG and MUC stations (see station list, Annex 9.1) surface samples were taken for future organic-geochemical investigations. The sediment samples were stored frozen (-20°C) and under light-protection in precleaned 100 ml glass-bottles.

The studies of sediments will include surface sediments as well as samples from selected sediment cores. In all samples, the total organic carbon content (TOC) will be determined routinely. In Figure 7-11, the TOC content of surface sediment samples obtained during the "Akademik Boris Petrov" expeditions 1997, 1999, and 2000 are shown. The highest TOC values occur in the estuaries and the submarine channels towards the north. The shallower areas outside the channels are characterized by lower TOC values. In order to interpret the TOC data in terms of organic carbon sources and depositional processes, further data on the composition of the organic matter are

required (biomarkers, palynomorphs, etc.). This data will be produced within the "SIRRO" Project at AWI during the coming months.

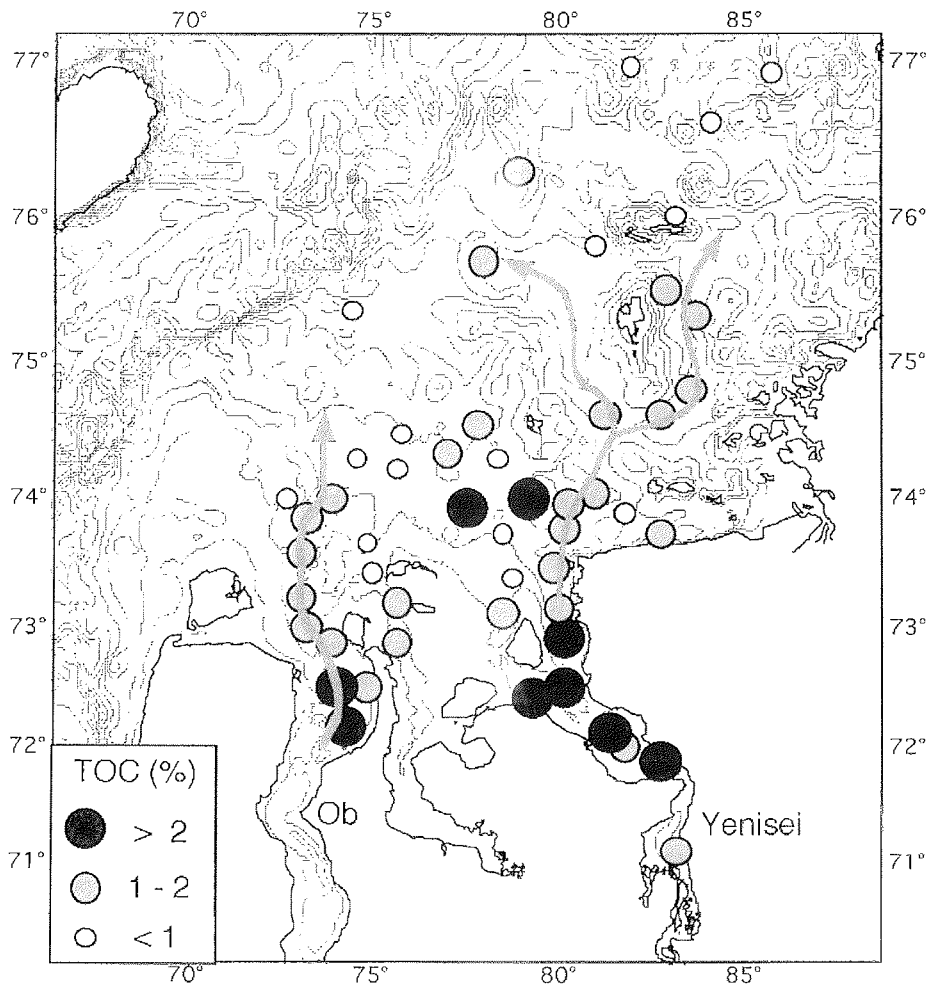


Fig. 7-11: Distribution of total organic carbon content in surface sediments.

Table 7-4: Stations used for sampling of particulate organic matter.

Station	sample-depth	Salinity(‰)	Volume(l)	sampler
BP00-02	0	17.6	10.5	bucket
	11.8	20.0	7.9	CTD/RS
	48	33.6	10.0	CTD/RS
BP00-03	0	21.3	21.5	bucket
BP00-04	0	25.7	10.2	bucket
	12	29.1	6.5	CTD/RS
	45-47	-	10.2	LVS
BP00-05	0	22.0	19.0	bucket
	10	22.1	15.0	LVS
	40	33.7	20.0	LVS
BP00-07	0	16.5	21.7	bucket
	11.5	25.5	9.9	CTD/RS
	35	32.8	18.0	LVS
BP00-08	0	20.9	21.8	bucket
	5.8	23.7	11.1	CTD/RS
	37	33.4	19.0	LVS
BP00-09	0	23.8	20.3	bucket
	15	28.5	10.0	CTD/RS
	43	33.5	15.6	LVS
BP00-13	0	21.6	16.0	bucket
	3.5	25.0	10.4	CTD/RS
	10.1	29.5	10.1	CTD/RS
BP00-15	0	6.7	10.5	bucket
	6.5	7.3	5.2	CTD/RS
BP00-16	0	2.3	10.1	bucket
	15.5	12.7	9.0	CTD/RS
	24	20.1	9.0	LVS
BP00-17	0	0	10.0	bucket
	18	0.6	9.8	LVS
BP00-19	0	0	10.6	bucket
	10	0	9.9	LVS
BP00-20	0	0	10.8	bucket
BP00-21	0	0.3	5.0	bucket
BP00-22	0	6.6	10.0	bucket
	3.7	19.6	9.7	CTD/RS
	10.7	30.4	9.9	CTD/RS
BP00-23	0	28.2	10.8	bucket
	9.2	30.3	9.8	CTD/RS
	32	33.1	18.0	LVS
BP00-24	0	23.8	22.1	bucket
	16	27.9	8.9	CTD/RS
	32	32.3	12.5	LVS
BP00-26	0	18.9	21.0	bucket
	17	25.6	10.5	CTD/RS
	63	33.7	19.8	LVS
BP00-27	0	23.2	21.7	bucket
	12.5	26.4	10.5	CTD/RS
	74	34.2	20.9	LVS
BP00-28	0	25.5	20.9	bucket
	16.2	29.5	10.0	CTD/RS
	50	34.1	20.8	LVS

Table 7-4: cont.

Station	sample-depth	Salinity(‰)	Volume(l)	sampler
BP00-29	0	27.2	21.7	bucket
	17.5	30.4	20.6	CTD/RS
	65	34.4	21.4	LVS
BP00-30	0	24.7	21.1	bucket
	28	29.6	20.2	LVS
	51	34	21.5	LVS
BP00-31	0	25.5	21.1	bucket
BP00-35	0	26.6	21.1	bucket
	13.7	30	20.0	CTD/RS
	46	33.3	20.3	LVS
BP00-36	0	27.1	20.5	bucket
	14.5	27.4	10.0	CTD/RS
	17.5	29.9-30.5	7.7	CTD/RS
	63	33.9	20.5	LVS
BP00-38	0	16.3	10.0	bucket
BP00-40	0	9.3	6.0	bucket

7.7 Preliminary results of geochemical investigations of sediment cores along the Yenisei Profile (Acoustic Units I - II)

Kodina, L.A., Tokarev, V.G., Sukhoruk, V.I., Vlasova, L.N., and Pribylova, T.N.

Vernadsky Institute of Geochemistry and Analytical Chemistry RAS, Moscow, Russia

Abstract

During the joint Russian-German expedition with R/V "Akademik Boris Petrov" in 2000, seven long cores were recovered along a longitudinal profile River Yenisei-Kara Sea for geochemical investigations of paleoenvironmental change in the Kara Sea, related to the sea level rise during the last deglaciation. The following parameters were determined: water content, wet bulk density, redox potential, and main nutrient concentration profiles. It is shown that some geochemical parameters of sediments might be useful tools for reconstructions of past depositional environments in the Kara Sea.

Introduction

Major objectives of our research are the geochemical characterization of sediments from some long cores taken along the longitudinal profile River Yenisei-Kara Sea in relation to the paleoenvironmental change in the Kara Sea, which is influenced by the sea level rise during the last deglaciation (Fairbanks, 1989; Polyak et al., 1997). In the glacial oceans, sea level was as much as 120m lower than at present, exposing most of the continental shelves.

The paleoenvironment of the Laptev Sea has been studied in detail within the framework of the Russian-German research project "System Laptev Sea" (Kassens et al., 1999). Organic geochemical studies of several ¹⁴C-dated long cores showed the increased content of isotopically light organic matter (OM) in the Holocene sediments as well as higher abundances of specific biomarkers. The supply of terrigenous organic matter increased sharply between 8 and 9 ka along the entire Kara Sea – Laptev Sea continental margin due to the large-scale sea level rise and increased river discharge (Stein and Fahl, 2000).

The Yenisei delta plain was shaped at about 5-7 ka when sea level reached its modern position (Harrison et al., 1981). Polyak et al. (in press) suggest that the transition from a freshwater to a normal marine environment in the Kara Sea began about 13 ka when sea-level started to rise. Fully marine conditions were reached at a site <100 km north of the Yenisei Estuary about 8,5 ka (Polyak et al., in press).

Recent sediments in the Laptev and Kara Sea have a similar lithological composition (Stein and Fahl, 2000). During the Russian-German Pilot Expedition to the Kara Sea in 1999 two acoustic units (I and II) were distinguished in the depocenter at shallow water in front of the Yenisei Estuary by a detailed sediment profiling survey (Stein and Stepanets, 2000). Acoustic Unit I is composed of thick undisturbed, soft, fine-grained siliciclastic sediments. The top of the acoustic Unit II is mainly represented by a strong

reflector (acoustic basement) with almost no penetration below. The boundary between both units is marked by a distinct change in magnetic susceptibility. The sediments of the Unit II might be formed during times of lowered sea level and represent fluvial deposits of pre-Holocene (Last Glacial?) age (Stein and Stepanets, 2000).

The goal of our study is to obtain geochemical records which might allow to characterize the boundary Unit I-Unit II, related to the postglacial sea-level rise.

Material and methods

During the joint Russian-German expedition on board R/V "Akademik Boris Petrov" in 2000 a sediment profiling survey was continued to the north and to the south from the Yenisei Estuary. Locations for coring have been selected according to the echosounding profiling. Seven cores were recovered (from 10 to 66 m water depth) with the gravity corer.

Locations of the cores and preliminary geological descriptions which have been completed onboard are presented in Chapter 6, Figures 6-2 and 6-16. In 4 cores the boundary of Unit I to Unit II is marked by a change of lithology, namely by sandy intercalations in the pre-Holocene sediments, while Holocene sediments are mostly silty, sometimes sandy-clayey. Based on the lithostratigraphy, Holocene sedimentation rates vary between 23 and > 66 cm/ky (see Chapters 6.6 and 6.7).

The cores were cut longitudinally before description. After the geological description both halves of each core section (1m length) were simultaneously described and sampled onboard in a cold room according to the following scheme:

The first core half:

- visual description;
- sampling for water content and wet bulk density (WBD) determination;
- collection of bivalves for ^{14}C -dating;
- measurements of redox potential (Eh-value) inside sediment along the section;
- subsampling for isotopic, elemental, pyrolytic analysis, lignin determination etc.;

The second core half:

- subsampling to extract pore water by squeezing under a nitrogen atmosphere onboard for hydrochemistry analysis (TAlk, NH_4^+ , SiO_4^{3-} , PO_4^{3-}) and isotope ratio $^{13}\text{C}/^{12}\text{C}$, $\text{C}^{37}/^{35}\text{Cl}$ measurement in the stationary lab;
- subsampling to separate hydrocarbon gases from sediment for molecular and isotope analysis;
- subsampling for collection of material (minerals) for absolute sediment dating.

Results

The results are presented in the Figures 7-12 and 7-13. These are sediment water content, wet bulk density, Eh-values, and some parameters of the pore water nutrients (TAlk, NH_4^+ , SiO_4^{3-} , PO_4^{3-}).

The clearly defined boundary Unit I-Unit II was detected on board in 4 (St.14, 22, 23, 37) of 7 cores (Fig. 7-12). Two parameters, namely water content and its mirror image WBD are the most lithology-sensitive indicators. These parameters denote changes of sedimentation conditions. The parameters are especially sensitive when Holocene sediments are homogenous, soft, wet clays (silty clays) of low WBD (organic-rich?) (Fig. 7-12, St.14).

Eh-values indicate reliably the change in oxidative-reductive regime at the boundary by the trend to more oxidative conditions. The most pronounced increase of Eh values (about 80 mV) is documented in the core from St. 22 (Fig. 7-12). This parameter shows a clear difference between the highly reduced (in total) Holocene sediments and less reduced (pre-Holocene?) sediments.

The hydrochemical parameters (TAlk, NH_4^+ , SiO_4^{3-} , PO_4^{3-}) show a similar trend. They are indicative of organic diagenetic transformations in sediments, which were effective in the cores with the largest thickness of the Holocene Unit I, as deduced from the high alkalinity (up to 35-45 mg-eq/l in cores 22 and 37 (Fig. 7-12) and in cores 7 and 36 (Fig. 7-13) and high concentrations of the other organic mineralization products (NH_4^+ , SiO_4^{3-} , PO_4^{3-}).

As seen in Figure 7-12 that the assumed boundary Unit I- Unit II is marked by modifications of the nutrient trend, in the majority of cases by a decline of concentrations.

Two long cores (St. 36, 7) are shown in Figure 7-13, which do not exhibit any visible changes in lithology at the core base. Cores 36 and 37 are more enriched in silty (sandy?) compounds throughout the profile as deduced from WBD data (Figs. 7-12 and 7-13). According to the onboard core description by Dr. R. Stein, small amounts of sand are present in the lower half of the core. We can point out, from interpretation of our data, that the bottom 15 cm of the differ from the Holocene interval by a more stable lithology (WBD data), by a small shift of Eh to less negative values and some changes of the trends in the nutrient curves. Therefore, we suggest that the boundary Unit I-II is probably also documented in these cores. As for St 7, we suppose that the gravity corer stopped close to the boundary Unit I-II.

Core St.15 located in the southern part of the Yenisei Bay is different to all described sediment cores (Fig. 7-13). The influence of river current is shown by numerous sandy intercalations typical of fluvial deposits (cf. Chapter 6.6 and 6.7). One can see that the curves of geochemical parameters run monotonously.

We emphasize that the pre-Holocene section is characterized by a distinct decrease in concentrations of main nutrients, corresponding with variations of Eh-values. The higher amounts of organic matter, starting at the Pleistocene-Holocene transition (Stein and Fahl, 2000), led to chemical changes in the interstitial waters of the sediments. The total organic carbon content comprise autochthonous aquatic plant material as well as allochthonous terrestrial plant debris. The Holocene shifts are well recorded by the hydrochemical data.

Alkalinity graphs demonstrate active diagenetic processes in sediments being mainly anaerobic sulphate reduction and uptake of organic matter. The occurrence of iron

sulfides is responsible for the black color in many parts of the Holocene deposits. Geochemical behavior of all nutrients throughout the Holocene characterize a substantial geochemical activity of organic matter. Station BP-00-37 demonstrates the most prominent example in this respect (Kodina et al., this vol.).

The top of the Unit II may represent fluvial deposits of pre-Holocene age (Stein and Stepanets, 2000), and is in all profiles characterized by distinctly decreasing nutrient concentrations, lower geochemical activity of organic matter, and by changes of sedimentation conditions, including variations in lithology.

The paper was prepared with financial support of the Russian Foundation of Basic Research, Grant 00-05-64575.

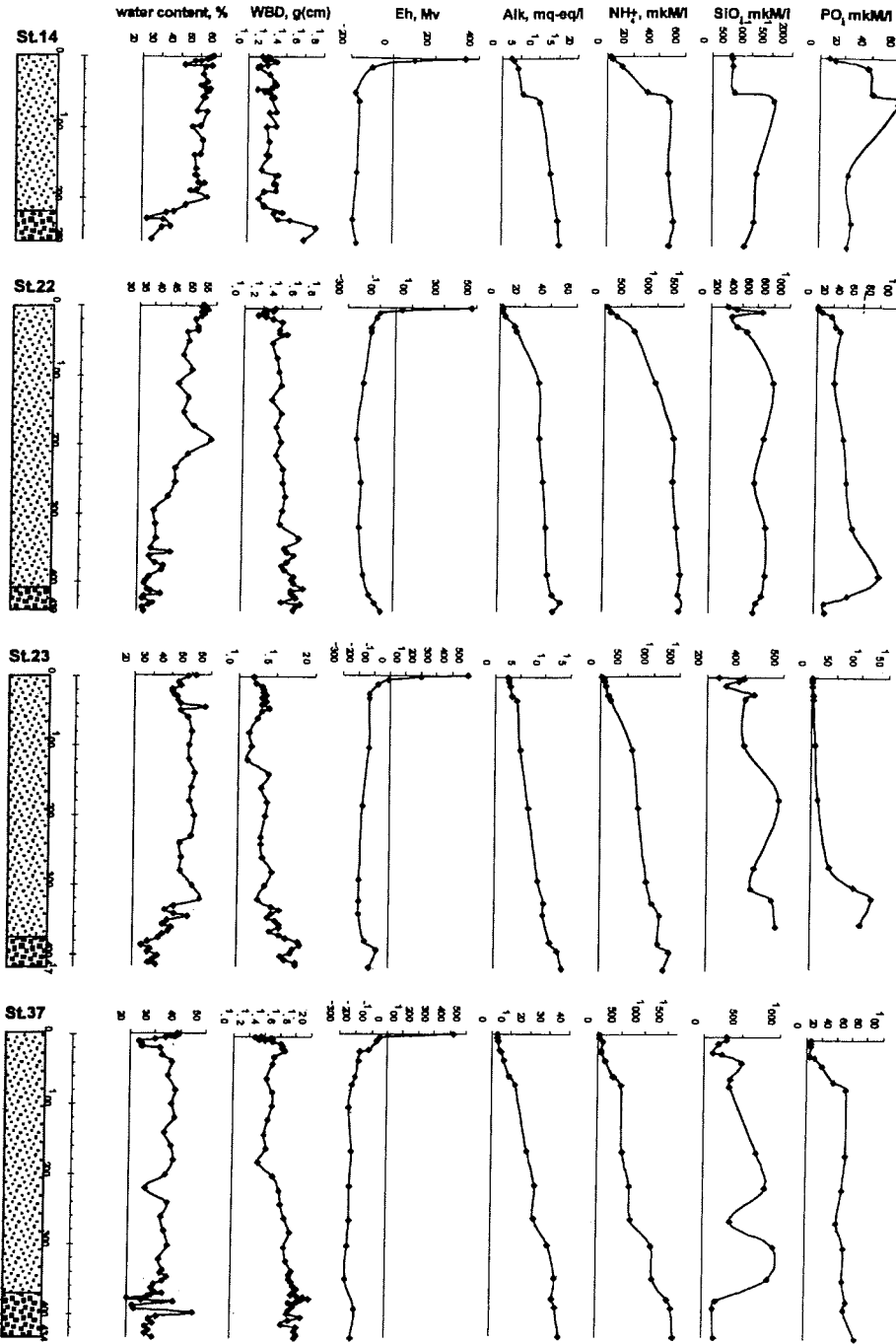


Fig. 7-12: Variations of some geochemical and physico-chemical parameters in sediments of acoustic Unit I and across the assumed lithological boundary Unit I- Unit II.

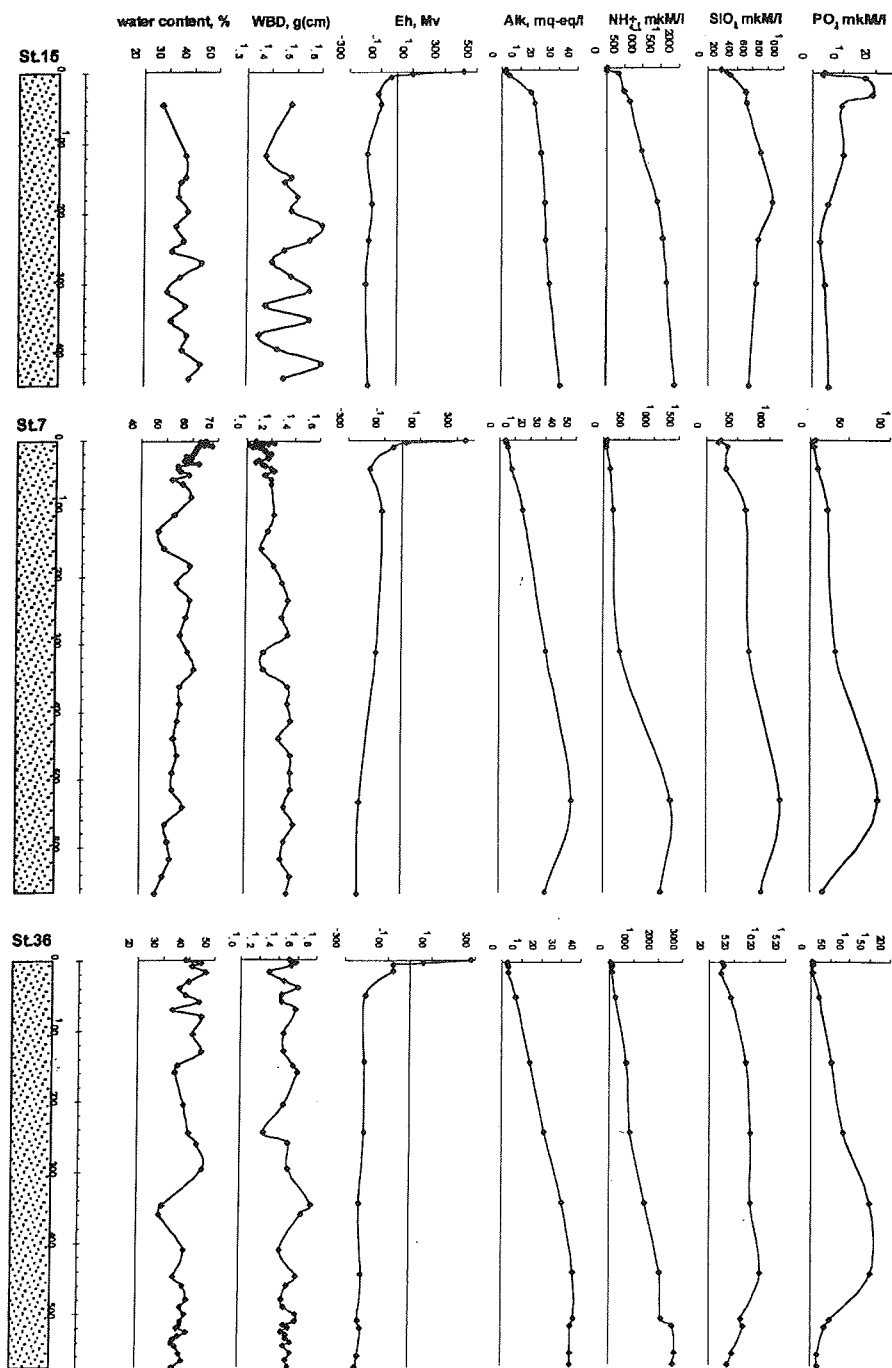


Fig. 7-13: Variation of some geochemical and physico-chemical parameters in sediments of acoustic Unit I.

7.8 Methane and other hydrocarbons in sediment cores along the Yenisei-Kara Sea profile

Korobeinik G.S., Tokarev V.G., Waisman T.I., and Kodina L.A.

V.I. Vernadsky Institute of Geochemistry and analytical Chemistry RAS, Moscow, Russia

Introduction

Most of past investigations on gas geochemistry in marine environments, including the Kara Sea, concentrated on the study of methane as the far abundant hydrocarbon gas, as well as the study of bacterial processes of methane generation (e.g., Bol'shakov and Egorov, 1995; Lein A. Yu., et al, 1996). In this short paper we present preliminary results on investigation of methane (C1), ethane (C2), ethylene (C2⁺), propane (C3), propylene (C3⁻), iso-butane (i-C4), n-butane (n-C4), butilene (C4⁻), iso-pentane (i-pentane), and n-pentane (n-C5) concentration and distribution pattern in sediment cores sampled during the expedition in the Kara Sea onboard R/V "Akademik Boris Petrov" in September-October 2000 (cruise 35). The sampling stations along the profile range from Yenisei mouth (72°N) northward to about 77°N (Stations BP00-15, 14, 23, 7, 37; for location of stations see Chapter 6, Fig. 6-2).

Methods

The «head-space» technique described previously (Bol'shakov and Egorov, 1995), was used as a basis in this work. The method was refined to evolve gases from sediment more completely and to concentrate them more. In our procedure sediment degassing was performed under the action of 3 following factors: vacuum, temperature, salt. Under this conditions hydrocarbons adsorbed by mineral or organic matter and dissolved in pore waters were evolved into gaseous phase. Hydrocarbons were analysed chromatographically by using flame-ionization and heat-conductivity detectors. The sensitivity of hydrocarbon detection is of 10⁻⁶ % (v/v). Concentration of the hydrocarbons is given in ml per litre of sediment (ml/l). The data obtained characterize essentially all gases, which might be present in sediments.

Results and Discussion

The data on methane concentration and distribution pattern through the depth of the sediment cores along the profile Yenisei-Kara Sea are summarized in the Table 7-5 and in Figure 7-14. C1 concentration at stations BP00-15, BP00-7 and BP00-37 varies within a wide range: from 18 x 10⁻⁴ ml/l in the subsurface core horizons to 47,2 ml/l at the core bottoms and increases down core with a great concentration gradient. We emphasize that the maximal methane concentrations with the steepest gradients were detected in the northernmost Core BP00-37, which is located most seaward in the northern part of the profile.

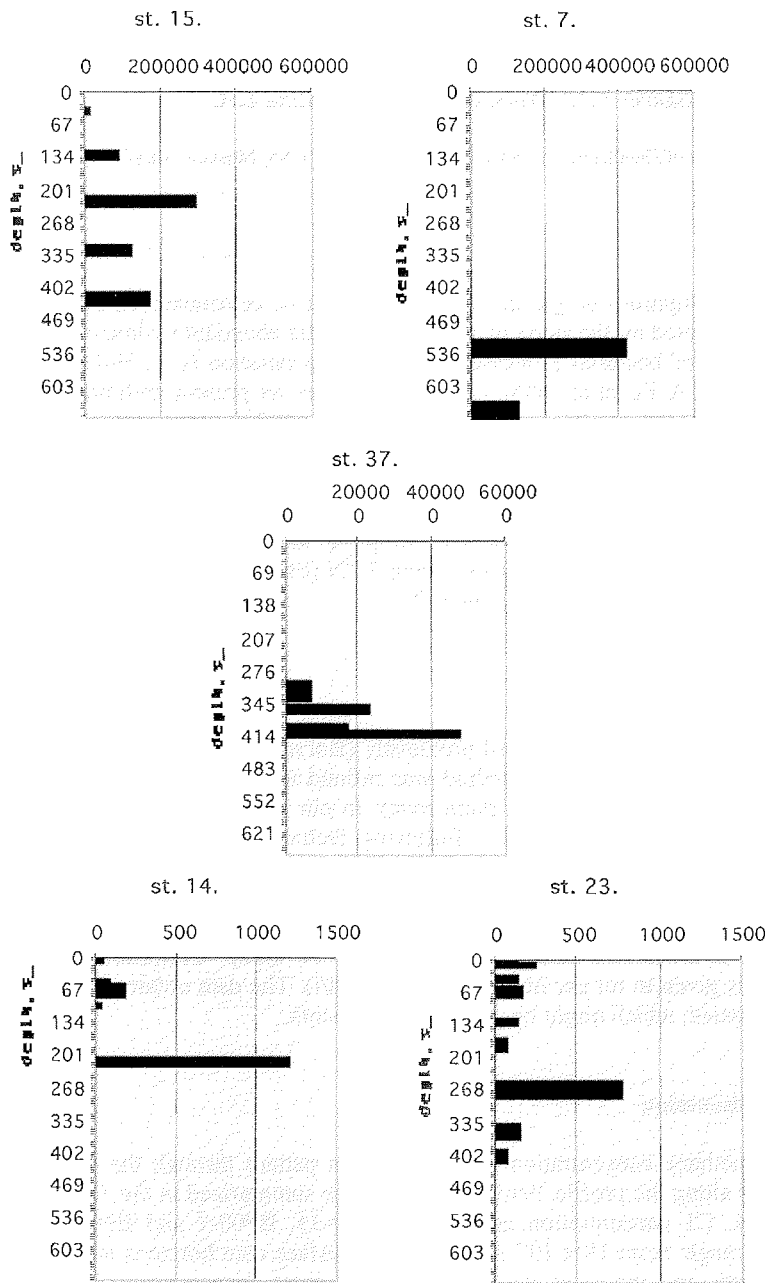


Fig.7-14: Methane (10^{-4} ml/l) in bottom sediment (Yenisei-Kara Sea). For location of stations see Figure 6-2.

At Core BP00-15 high C₁ concentration appeared even in the subsurface (10cm) sediment horizon. A steep concentration gradient might be indicative of the methane flow from the underlying sediments. Methane is practically completely oxidized aerobically in the surface sediment layer (2cm). Higher methane homologues including C₅ and C₄⁺ are present. The ratio C₂/C₂⁺ is about of 1.

High C₁ concentration in the bottom part of the cores and distribution pattern through the sediments at the st. 7 and 37 might be considered as a result from bacterial methanogenesis processes in the lowest part of the cores. It can be assumed that in the core bottom sediments where very steep concentration gradients were detected, intensive anaerobic methane oxidation occurred, and almost all methane was consumed in the sediment. Detected C₁ content is most properly viewed as a result of the balance between C₁ production and consumption (Kodina et al., this vol.). An anaerobic regime of sediments in the lower parts of the cores is favourable for methane generation. The absence of higher methane homologues and C₄⁺, as well as high C₂/C₂⁺ ratios support the idea of *in situ* biogenic methane origin at st.7 and 37.

C₁ concentration in sediments at stations BP00-14 and 23 is fairly low and varies slightly through the sediment depth. It ranges from 30 to 180x10⁻⁴ ml/l at st.14 and from 60 to 240x10⁻⁴ ml/L at st. 23. There are only separate sediment interlayers with an extremely high (n1000 x 10⁻⁴ ml/l) methane content. Hydrocarbon content and distribution pattern in sediments at these stations located in the zone of contact of the fresh and marine waters indicate another environment of sedimentation and organic matter diagenetic transformation in this part of the profile.

Sources of the higher methane homologues C₅ and C₄⁺ in sediments are uncertain. The fact, that these hydrocarbons are more frequent in surface sediments and have been revealed in the young recent sediments, enables us to assume that they did not migrate from deeper parts and might had arouse in some low-temperature chemical reactions or probably in biogeochemical processes and are the byproducts of organic diagenesis in sediments (Hunt, 1975, 1984; Claypool and Kvenvolden, 1983; Meyers and Brassell, 1985)

The work has been supported by the Russian Foundation for Basic Research, Grant 00-05-64575.

Table 7-5: Methane and other hydrocarbon gases in sediment cores along Yenisei- Kara Sea profile.

Stat.	Horizon, cm	C1	C2	C2=	C3	C3=	i-C4	n-C4	C4=	i-C5	n-C5	C2/C2=	C1/C2 +C3
15	0-2	38	5	2	5	0,2	3	3	0,3	7	3	2,5	4
	7-10	506	8	7	10	1	4	4	0,8	10	4	1,1	28
	30-40	10900	4	4	4	0,4	2	2	0,6	5	3	1	1362
	120-130	86600	9	7	14	1	9	7	-	18	9	1,3	3765
	210-230	288000	11	9	17	2	8	5	0,5	21	7	1,2	10285
	310-330	121600	6	5	8	0,5	4	2	0,8	22	9	1,2	8686
410-430	169600	10	6	12	1	8	6	1	18	6	1,7	7709	
14	0-2	34	8	2	10	0,4	2	2	0,6	15	5	4	2
	3-8	39	5	1	7	0,1	4	3	-	18	6	5	3
	45-50	79	3	0,5	0,7	0,1	2	1	0,6	7	2	6	21
	56-76	183	6	1	7	0,2	5	3	0,2	19	6	6	14
	96-100	31	1	10	-	0,2	-	-	0,2	-	-	0,1	52
206-220	1196	20	3	19	0,7	11	10	0,6	34	16	7	31	
23	0-2	131	19	17	25	7	15	15	9	37	15	1,1	3
	5-10	238	28	33	70	22	42	45	14	130	46	0,8	2
	30-40	136	4	6	8	0,9	3	3	2	7	2	0,7	11
	52-72	161	1	6	3	1	0,9	1	-	2	1	0,2	40
	120-130	138	2	3	4	0,4	1	1	-	3	1	0,7	23
	160-180	64	0,4	2	1	0,3	0,1	0,2	0,3	-	-	0,2	46
	250-280	759	4	38	3	1	0,1	0,3	0,7	-	-	0,1	108
	337-365	144	0,3	1	1	0,2	-	0,1	-	-	-	0,3	111
390-414	71	0,6	2	1	0,5	-	0,2	-	-	-	0,6	44	
7	0-2	127	14	10	17	5	11	10	14	27	14	1,4	4
	3-8	204	21	32	29	9	18	19	31	51	21	0,6	4
	10-18	179	17	10	21	0,1	12	10	0,5	27	4	1,7	5
	40-50	118	9	3	10	1	16	5	3	18	6	3	6
	98-127	243	5	0,9	6	0,3	4	4	0,5	12	4	5,5	22
	297-322	1099	13	1	12	0,7	4	3	0,9	13	4	13	44
	508-538	412900	22	2	24	3	16	14	4	40	20	11	8976
637-665	124900	5	1	6	0,4	4	3	0,3	10	4	5	11354	
37	0-2	18	2	1	2	1	0,9	0,9	-	4	4	2	4
	4-7	59	6	5	7	3	4	3	0,4	3	7	1,2	4
	9-14	43	4	4	5	2	3	3	0,3	10	5	1	5
	22-27	34	5	2	4	0,9	3	4	0,4	25	7	2,5	10
	45-55	374	5	2	7	1	2	2	-	15	5	2,5	31
	73-81	881	9	3	9	2	3	3	-	9	5	3	49
	90-103	1300	15	5	14	2	5	4	2	14	6	3	45
	113-130	730	14	4	14	2	3	3	-	27	9	3,5	26
	173-183	1400	14	3	15	1	1	3	2	5	-	4,7	48
	220-223	1800	16	3	13	1	1	2	3	3	1	5,3	62
	268-283	930	9	2	10	1	0,6	0,6	1	-	-	4,5	42
	298-333	68600	2	1	8	-	-	-	-	-	-	2	6860
	347-362	225200	6	1	6	-	0,3	0,3	-	-	-	6	18767
400-413	472000	5	3	8	2	0,6	0,8	-	-	-	1,7	36307	

7.9 Carbonate minerals ikaite and glendonite and carbonate nodules in Holocene Kara Sea sediments: Geochemical and isotopic evidences

Kodina, L.A., Tokarev, V.G., Vlasova, L.N., and Pribylova, T.N.

V.I. Vernadsky Institute of Geochemistry and Analytical Chemistry, RAS

Abstract

Numerous carbonate nodules and carbonate minerals identified as ikaite $\text{CaCO}_3 \cdot 6\text{H}_2\text{O}$ and its stable pseudomorph glendonite have been found in Holocene sediments of core BP00-37 at the subbottom depth from 25 to 230cm. Continuous modifications of ikaite structure to calcite at room temperature could be revealed by X-ray diffractometry. Pore fluids prepared from sediments showed high contents of nutrients (TALK , PO_4^{3-} , NH_4^+ , $\delta^{13}\text{C}_{\text{DIC}}$) through the sedimentary profile characteristic of intensive bacterial sulfate reduction. It is remarkably that extremely high contents of methane (16% v/v) have been determined in sediments (silty sandy clay) below the sulfate reduction zone (300-400cm), with a sharp decrease in the zone quickly declining to zero at the level of about 200cm subbottom depth. Anaerobic oxidation of methane coupled with sulfate reduction has been suggested as a driving process for the precipitation of extremely ^{13}C -depleted authigenic carbonate nodules ($\delta^{13}\text{C}_{\text{carb}} = -55$ to -60‰), minerals ikaite ($\delta^{13}\text{C}_{\text{carb}} = -49\text{‰}$) and its pseudomorph glendonite ($\delta^{13}\text{C}_{\text{carb}} = -36,5$ to $-37,5 \text{‰}$) in the polar environment. The actual range of $\delta^{13}\text{C}$ of the authigenic carbonates depends on the relative contributions of carbon from two sources: the methane and the isotopically depleted DIC pool of the pore fluids. The detection of ikaite and glendonite in the Kara Sea might be considered as an additional indication of high methane content in sediments.

Introduction

One of the objectives of the joint Russian-German Project studying the Kara Sea's recent and past environments was to gain insight into peculiarities of geochemical processes operating in the sedimentary cover of the shallow polar shelf sea characterized by large runoff. In this paper we present preliminary results of geochemical and isotopic study of the sediment core BP00-37 which is characterized by a high methane content and the presence of specific carbonate minerals and nodules embedded in the host sediment. This might be considered as a characteristic chemical phenomenon typical of the high latitude low-temperature areas of the Arctic Basin.

Material and methods

Location of Station BP-00-37 ($76^{\circ}57,99'\text{N}$; $82^{\circ}12,35'\text{E}$, see Fig. 6-2) was selected after an echosounder profiling survey on the gentle slope of a small basin in an area bordering an open floating ice. Water depth is about 65 m, bottom water salinity reached 34‰, temperature $-1,4^{\circ}\text{C}$. Surface water was influenced by floating ice, and its salinity was unstable (from 0 to 29‰ within the surface 1.5 m) The length of the core is 433cm. According to the geological description, two sedimentary units have been

distinguished in the core (see Stein and Levitan, this vol.). Unit I (from 0 to 373 cm) is represented mostly by soft Holocene silty clay with varying content of silt and sands, as also deduced from the wet bulk density data (Kodina et al., this vol.). The top of the Unit II is marked by a strong reflector, and sediments are characterized by the presence of sandy intercalations.

Three large and some small crystals of the highly hydrated calcium carbonate mineral ikaite $\text{CaCO}_3 \cdot 6\text{H}_2\text{O}$ were found in the dark gray silty clay at a subbottom depth of 103-113 cm. The size of the largest crystal is 6 x 4,4 x 3,5 cm and the color is yellowish-orange (Fig. 7-15). At subbottom depth of 213-233 cm a crystal cluster (diameter about 10cm) which looked like a rosette, was found inside the darker, viscous sediment, made up of dark-yellow relatively small crystals (2,5 x 1 x 1 cm) tightly connected with each other. This is a glendonite (Fig. 7-16). – a unique calcite pseudomorph after the metastable mineral ikaite (Suess et al., 1982; DeLurio and Frakes, 1999).

Besides the calcite minerals carbonate nodules of different shape (flat or looking like potato) and size (the largest one has a size of 10x6x4 cm) were found in the core. Almost all nodules contained shells of bivalves (in most cases *Yoldia hyperborea*, P. Lyubin, pers. comm.) (Fig. 7-15). Intact shells or shell fragments were widely distributed in the sediment especially in the upper part of the core. Nodules were found in the horizons 25-28 cm, 38-40 cm, and 58-68 cm. The largest accumulation of potato-shaped frozen solid nodules and cemented bivalves were found in the horizon 58-68 cm.

Eh-values were measured in the sediments along the core length, pore waters were squeezed out from the separated sediment sections (10-30 cm) along the core in a cold room and immediately analyzed for Alk, TAlk, PO_4^{3-} , NH_4^+ , SiO_4^{3-} , and dissolved inorganic carbon (DIC) was prepared as BaCO_3 onboard for $^{13}\text{C}_{\text{DIC}}$ measurement in the carbon geochemistry laboratory of the Vernadsky Institute. Classical hydrochemical methods were used. Gas samples were prepared by vacuum degassing of sediments onboard, and the hydrocarbon concentration distribution was studied throughout the core chromatographically at the Institute (Korobeinik et al., this vol.). Some gas samples were prepared for methane isotope analysis. Organic and inorganic carbon isotope composition of the carbonate minerals, nodules and host sediments was measured. X-ray phase study of minerals and nodules was performed by means of a DRON-3.0 diffractometer (graphite monochromator, CoK_{α} –radiation, scan speed – $1^\circ/\text{min}$) at the Vernadsky Institute RAS by Dr. Alexander Bychkov.

Results and discussion

Transformation of carbonate minerals (X-ray study)

Continuous phase transformations of the initial ikaite material was found. We measured different diffractograms which were scanned immediately after preparation of the sample (Fig. 7-17, curve 1) and 30 min after preparation (Fig. 7-17, curve 2). Thus, evidently phase transformations also occurred during scanning. Calcite was the final product of these transformations after one day (Fig. 7-17, curve 3). X-ray pattern of glendonite crystals is the same as for calcite (Fig. 7-17, curve 4). Crystal cement material (90%) of nodules consists of calcite and quartz approximately in equal parts (Fig. 7-17, curve 5). Small quantities of feldspars and clay material also were measured.

Pore fluids, geochemistry and carbon isotopic study

The processes of organic matter diagenetic remineralization are reflected in the distribution pattern of pore fluid nutrients through the depth of the sedimentary profile. The results of geochemical investigations of Core BP00-37 are summarized in Figure 7-18.

It is evident from the visual core description and the Eh-values along the core that sediments of Unit I (Holocene) are reduced except the thin surface and sub-surface core layers. The interval 205-340 cm with the lowest Eh-values and H₂S smell appeared to be the most reduced part of the core. Dark-gray color with black intercalations is indicative of the presence of iron sulfides in the sediment. These are indirect evidences of an anaerobic environment, with bacterial sulfate reduction operating in the sediment. The common trend of main nutrients supports the validity of the supposition.

Organic matter decomposition, primarily through activity of sulfate-reducing bacteria tends to increase alkalinity, phosphates, ammonium with increasing depth (Fig. 7-18). We emphasize that nutrients concentration in sediments of the water area was very high during the present study. Similar observations have been made by Suess et al. (1982) in the Bransfield Strait, a place where ikaite was found in deep water sediments (1950 m) at subbottom depths of 205 and 714 cm. High dissolved phosphate contents are known to inhibit calcite growth and allow ikaite precipitation (Burton and Walter, 1989).

A gently sloping cumulative curve of TAlk deviates sharply downcore at a depth of 220-233cm, marked by the presence of the calcite mineral glendonite (Fig. 7-18). A well-defined concave $\delta^{13}\text{C}_{\text{DIC}}$ -curve is in accordance with the behavior of the alkalinity curve related to the calcite deposition. Precipitation of single ikaite crystals at the depths range from 103 to 113 cm was also reflected in curves, however to a less degree.

Variations in the alkalinity and DIC isotope composition with depth indicate that ikaite and glendonite are authigenic carbonate minerals that precipitate from interstitial waters of sediments undergoing anaerobic diagenetic transformations, including remineralization of organic matter and formation of nutrient-rich pore fluids.

It is clearly seen (Fig. 7-18) that TAlk of the pore fluids continue to increase within sulfate reduction zone. At the same time, DIC is steadily enriched in the ¹³C isotopes. The contradictory behavior of the two indicators of the carbonate system might be explained by giving special attention to the extremely high (16%) methane content in the sediment.

A justified assumption on the genetic relation of ikaite with the methane cycle in Arctic sediments has been proposed repeatedly (Schubert et al., 1997; Kodina et al., 1997; Greinert et al., 1999). We report here preliminary results. What we suppose is the first presentation of the pore fluids hydrochemistry and methane distribution pattern in the sediment, coupled with the carbon isotopic analysis with relation to authigenic carbonate formation in anaerobic Arctic sediments.

When sulfate is exhausted from the interstitial water, methane formation properly takes place by methanogenic microflora that utilizes the pool of dissolved bicarbonate generated during sulfate reduction. We can see biogenic processes of methane

generation through steady pore water DIC enrichment in ^{13}C (Fig. 7-18). Isotope effect associated directly with ^{12}C consumption from the DIC pool, is obvious in the bottom part of the sulfate reduction zone and below it.

On the other side, an increase in alkalinity, steady state of the depleted DIC isotope composition throughout the sediment interval of 100-300 cm (range of $\delta^{13}\text{C}$ from -33 to -35‰), depleted isotope composition of sedimentary dispersed carbonate (range from -0,76 to -35‰) and extremely depleted $\delta^{13}\text{C}$ values of carbonate nodules (range from -55 to -60‰) as well as precipitation of the carbonate minerals ikaite (-49‰) and glendonite (-36,5 and -37,6‰) are attributed to anaerobic oxidation of methane coupled with sulfate reduction.

Geochemists have long suspected that methane oxidation also occurs in anoxic marine sediments, namely in a zone located between the sulfate reduction and methane production zones (Alperin and Reeburgh, 1984; Jørgensen, 1992; Harder, 1997). Methane-derived cementation of Holocene marine sediments is a well known phenomenon (Ivanov et al., 1991; Jørgensen, 1992). The actual range of $\delta^{13}\text{C}$ of the authigenic carbonates depends on the relative contributions of inorganic carbon from the methane and the DIC pool, as well as on the source of methane.

In the past years, it is becoming more and more clear that anaerobic methane oxidation results from intermicrobial metabolic interaction, termed "syntrophy" and is carried out by a consortium of archaeal methane consumers and bacterial sulphate reducers (Hinrichs et al., 1999; Delong, 2000). Sulfate reduction coupled with anaerobic oxidation of methane has been suggested as a driving process for the precipitation of isotopically depleted carbonates in the Arctic Basin. The detection of ikaite and glendonite in the Kara Sea might be considered as an additional indicator to the high methane content in sediments.

The work has been supported by the Russian Foundation for Basic Research, Grant 00-05-64575. Authors are indebted to Dr. A. Bychkov (Vernadsky Institute) for X-ray study of minerals, Dr. Carsten Eckert (AWI, Potsdam) for help with photographs and literature.

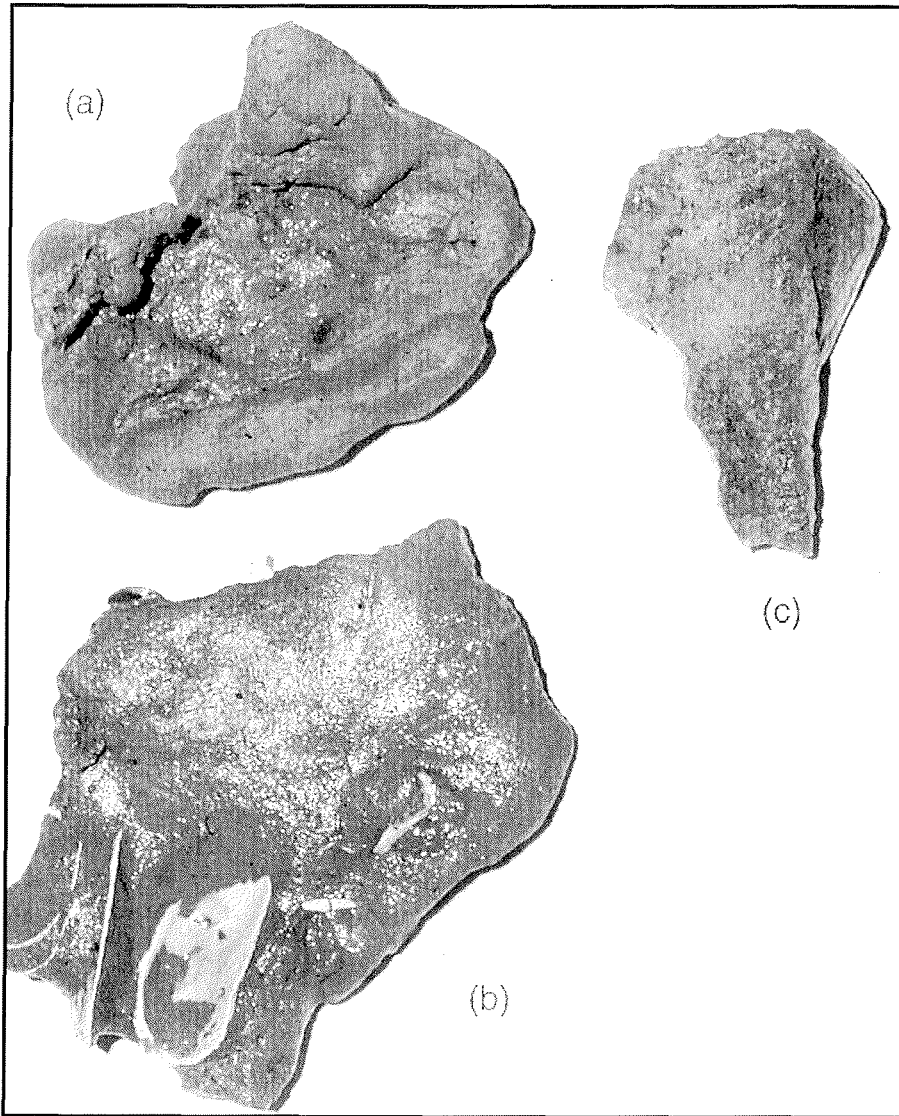


Fig.7-15: Carbonate inclusions in Holocene sediments, Station BP-00-37. (a) Nodule from horizon 25-28cm, (b) Nodule with cemented bivalve shells, horizon 38-40 cm, (c) Ikaite, horizon 103-113cm.



Fig. 7-16: Glendonite crystals and clusters. Two larger single ikaite crystals are present.

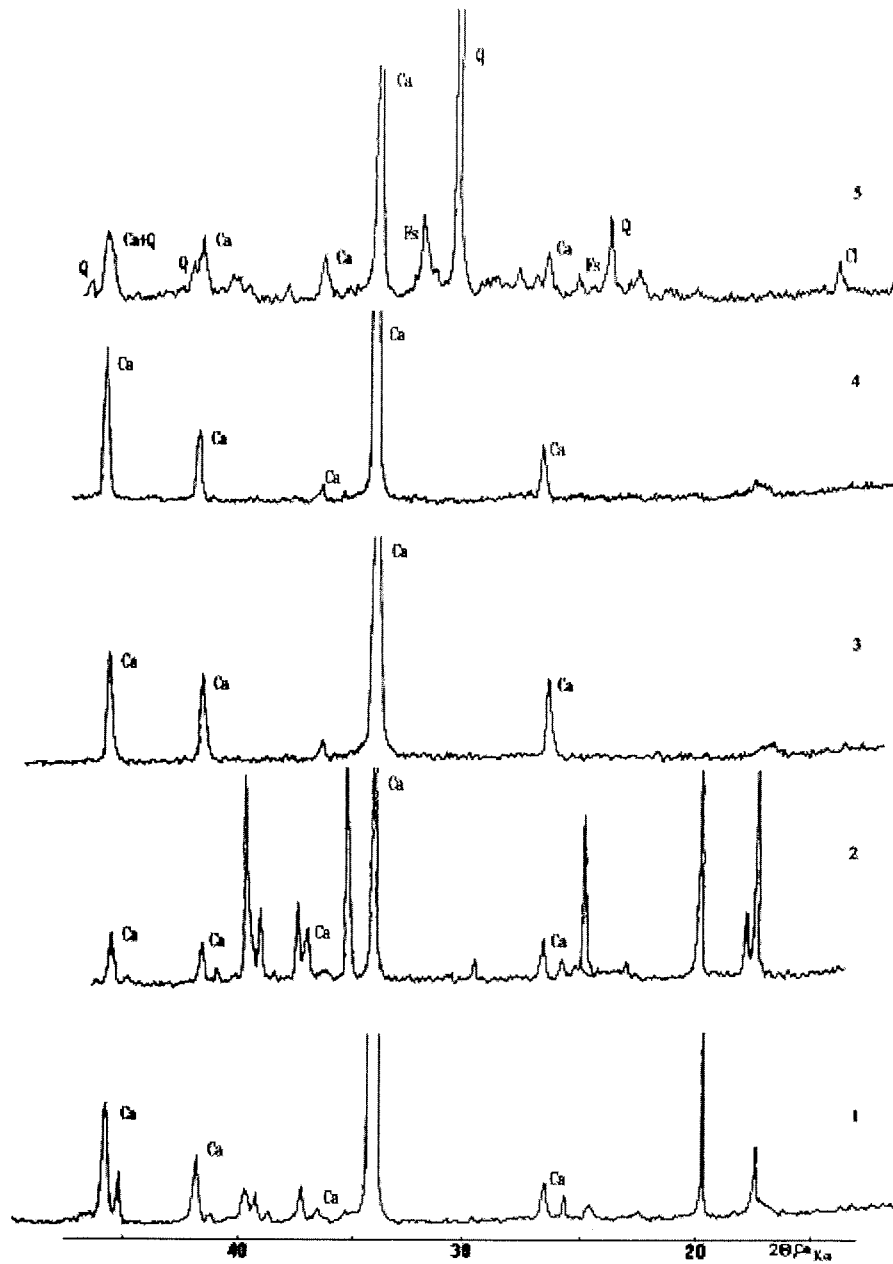


Fig. 7-17: X-ray diffractograms of the carbonate material and nodules at room temperature. 1. ikaite sample after careful keeping during 3 months in a freezer, and less 5 minutes of preparation; 2. ikaite sample in 30 min; 3. ikaite sample in one day; only calcite peaks are present; 4. glendonite; only calcite peaks are present; 5. nodule cement (native). Q - quartz, Ca - calcite, Fs - feldspar, Cl - clay material).

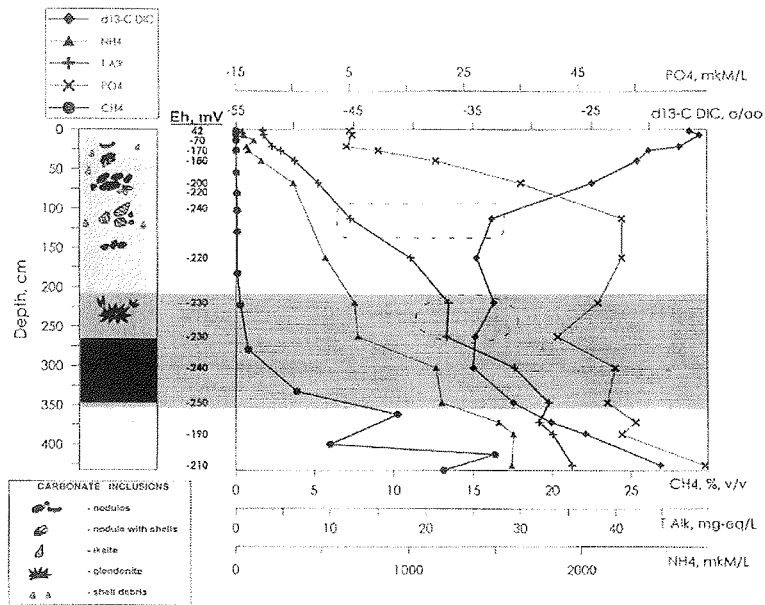


Fig. 7-18: Geochemical description of the environment of carbonate minerals and nodules precipitation of core BP00-37. The intensity of shading of the core section corresponds to the intensity of grey (to almost black) color of the sediment. The top layer (0-2 cm) has olive-gray color. The shading of the graph's area denotes a zone of the most intensive anaerobic geochemical transformations in the sediments (sulfate reduction).

7.10 Radioecological research in the Yenisei and Ob rivers and adjacent Kara Sea shelf.

O. Stepanets, A. Borisov, V. Komarevsky, A. Ligaev, E. Sisov, and G. Solovjeva

Vernadsky Institute of Geochemistry and Analytical Chemistry, RAS, Moscow, Russia

Introduction

One of the most important problems of anthropogenic pollution of the Arctic basin is the radioactive contamination of the water area. Several sources are contributing to the radioactive contamination of the Kara Sea:

- * fallout from nuclear weapons testing;
- * discharge of liquid and solid radioactive wastes in the Kara Sea;
- * transport of radionuclides discharged from European reprocessing plants;
- * transport of artificially produced radionuclides by rivers to the Arctic Seas.

On Novaya Zemlya, 83 air, 1 nearsurface, 3 underground, and 3 underwater nuclear explosions were performed in 1954-1962, releasing 13 million Curie of ^{137}Cs into the atmosphere. In 1965-1991, 48 underground nuclear explosions were performed, which caused a short-lived increase in the background values over limited land areas but virtually no such increase in the marine environment. Solid and liquid radioactive wastes disposed of in 1965-1968 within shallow-water bays of the Kara and Barents seas are potentially dangerous. From the 1950s to 1992, the Soviet Union submerged wastes with a total activity of 2.5 million Curie. The enterprises situated in Siberia and the Urals are pollution sources. The plutonium-producing radiochemical plant of PO Mayak stored up to 120 000 000 Curie of radioactive wastes in Lake Karachai. Through the system of rivers Techa-Iset'-Tobol-Ob, the radioactivity can reach the Kara Sea. The Siberian chemical plant is situated 30 km from the city of Tomsk. The liquid wastes of the plant were defected in the Tom' River, which enters the Ob River. The plutonium-producing Krasnoyarsk Mining and Chemical Work is located near the city of Krasnoyarsk. The pollution by the work's waste waters is observed in the Yenisei River, far away from the discharge sites.

A substantial amount of radionuclides is transferred from the Norwegian Sea, which contains wastes of reworked nuclear fuel from Sellafield (England) and from Ar Cape (France) to the Barents, White and Kara seas. In Great Britain, it was common practice for many years to pipe liquid radioactive wastes from nuclear plants into the Irish Sea. The amount of waste was so great (about 1 MCurie) that its influence is still perceptible in the Norwegian, Barents and Kara seas. The waters of the North and Baltic seas polluted by Chernobyl radioactivity, became a new source of anthropogenic radioactivity supply to the Arctic basins since 1986.

One of the sources of anthropogenic pollution in the Kara Sea are the catchment areas of the large Siberian rivers Yenisei and Ob, where radioactive wastes from reprocessing plants

can be discharged. The rivers Ob and Yenisei contribute to about 80% of run-off into the Kara Sea. The Yenisei carries the greatest water volume from the Siberian rivers. These rivers are the most important supplier of dissolved and suspended materials. In contact many dissolved elements precipitate and are fixed at the bottom. In this zone ("Marginal Filter"; Lisitzin, 1995) the maximal amount of suspended matter with mineral components and radioactive and chemical substances accumulate. A part of pollutants is born far in the sea, supplied by tidal currents.

From an ecological point of view the large Siberian rivers are potential sources of anthropogenic pollution of the Kara Sea and further of the Arctic basin. Therefore, the investigations connected with an assessment of levels of contents of radioactive and chemical admixing in high layer and on depth of core in samples of bottom sediments selected in fluvial medium, mixing zone and open part of the sea, help to estimate the modern ecological state of the local region and to reveal time intervals of massive fluvial input from radiochemical plants of Ural and Siberia into the marine area in the past.

The experimental investigations were carried out in the estuaries of the rivers Ob and Yenisei and the southern part of the Kara Sea (1999) and in the estuaries of the river Yenisei and the central part of the Kara Sea (2000). The main tasks of our radioecological research were to study the horizontal and vertical distribution of the artificial radionuclides (cesium, strontium and plutonium) in water and sediments. The map of sampling of sediments and water during the 2000 cruise is shown in Figure 7-19. The radiogeochemical research are important to estimate the influence of natural environmental parameters on laws governing the distribution and migration of radionuclides in the investigation area.

Sampling and Analytical Methods

Sediments were sampled with a box corer (50x50x60 cm), with subsequent subsampling with a plastic tube having an inner diameter of 10 cm. The cores were cut in 1-2 cm slices, and samples were dried at a temperature of 60-80°C.

Water was sampled with a large volume sampler (200 l Batomat) or taken by a pump through a plastic pipe system, and filled in storage tanks of 150 l volume. Before analysis some samples were filtered through a cartridge filter to remove suspended matter > 0.45µm.

The greatest amount of data was obtained for Cs-137 contents, and to a smaller extent for Sr-90 and Pu-239, 240. Cs-137, Sr-90 and Pu-239, 240 in water samples, and Sr-90 and Pu-239, 240 in sediment samples were determined with a radiochemical method. For the analysis of Cr-137 in sediments we used direct α -measurements without decomposition of the sample.

Measurement of the radioactivity of Cs-137 in sediment samples was carried out in a low-background installation with semiconductor Ge detector. Cs-137 was determined in water samples of 100 l volume using the sorption method under dynamic conditions with

subsequent γ -spectrometer measurements on concentrates. Co-ferrocyanid, fixed on an organic matrix, was used as quality sorbent for concentrating cesium.

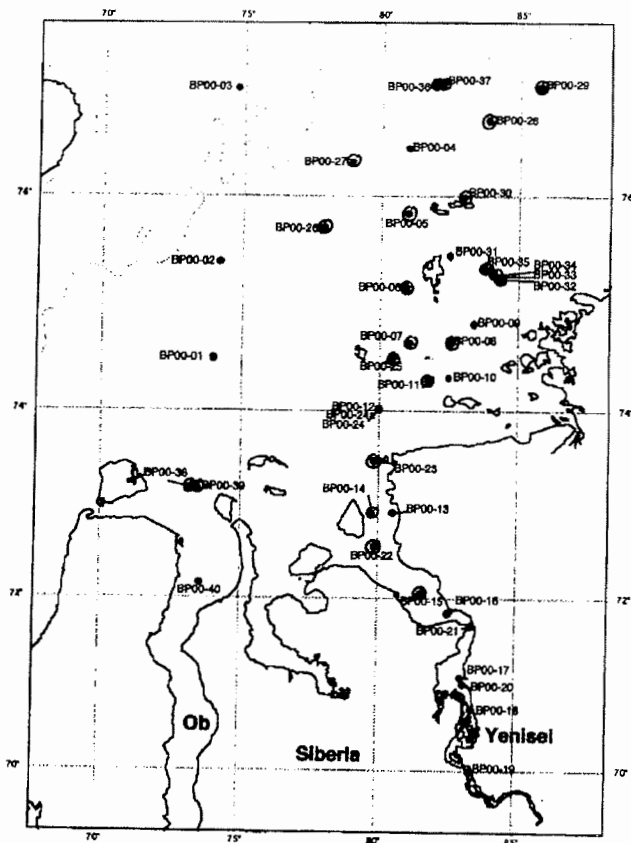


Fig.7-19: Stations of sampling for studies of radionuclides during the 2000 cruise.

The determination of Sr-90 in the water samples included precipitation of strontium carbonate. Then we use extraction chromatographic procedure with crown-ether dicyclohexano-18-crown-6 permitting to separate Sr-90 from other radionuclides. At passage 2μ of solution on hydrogen nitrate keeping radionuclides through column on a column remain strontium and lead. After unabsorption of strontium from the column by hot water, we carried out a final precipitation of Sr-90 as strontium oxalatum.

The analysis of plutonium in water samples consisted of precipitation of Pu with iron hydroxide (from a volume of 100 l), subsequent radiochemical cleaning and adsorption of

Pu on LaF₃. Precipitates were separated on a membrane filter and activity measured on α -spectrometer. For extraction of Pu from sediments samples were boiled in 7M HNO₃ with KBrO₃, and then were further processed as water samples Pu analysis.

Preliminary Results and Discussion

The distribution of Cs-137 in the surface sediments (0-2 cm) on the 2000 results of expedition is shown in Figure 7-20. The results confirm our previous interpretations about the significance of lithology of the surface sediments on the radioactivity level of Cs-137. In places, where the sediments are an ooze with a major content of a clay material, a rather high content of cesium-137 was observed. The conducted size analysis of sediments has allowed to receive a direct relation of a specific activity of cesium-137 in a sediment and the content of clay and sandy fractions in samples (Table 7-6).

During the investigation of the vertical distribution of Sr-90, some of the samples from Ob and Yenisei estuaries displayed significantly higher counts of this radionuclide (Figs. 7-21 and 7-22).

The investigation of the distribution of cesium and strontium radionuclides in water's samples provides additional evidence supporting our former results. The concentrations of water-soluble cesium species increase with increasing salinity, in opposite the concentrations of strontium decrease with increasing salinity (Table 7-7). The concentration of these two radionuclides are low in filtrated samples of water. This mean sthat the great Siberian rivers do not give a significant contribution to the summary level of radioactivity in this region.

Table 7-6: Results of lithological structure some surfuge sediments and activity of ¹³⁷Cs.

Stat.	Mineral composition, %				¹³⁷ Cs activity, Bq/kg
	Gravel	Sandy	Peryte	Clay	
11	2,7	73,6	17,8	5,9	6,4 ± 1,9
19	0,2	79,1	15,9	4,8	2,1 ± 0,7
22	0	2,5	14,8	82,7	40,0 ± 3,0
26	0	2,5	29,9	67,7	13,4 ± 2,5

Stat.	Fraction composition (mm), %							
	>1.0	1.0-0.5	0.5-0.25	0.25-0.125	0.125-0.1	0.1-0.063	0.063-0.001	<0.001
11	2,7	3,6	21,8	19,1	29,1	8,6	9,2	5,9
19	0,2	0,45	41,4	36,8	0,45	9,1	6,8	4,8
22	0	0,45	0,45	0,7	0,9	2	12,8	82,7
26	0	0	0	1,6	0,9	1,9	27,9	67,7
28	0,9	0,9	2,7	16,8	9,5	17,4	24,5	27,3

In order to estimate the retention in sediments of radionuclides released from nuclear wastes, sorption and desorption experiments with ^{134}Cs have been performed. The results of the sorption experiments (Fig. 7-23) show that Cs-134 is rapidly retained by the sediments and that one is well retained in sediments. The retention depends on contact time as well as on the sediment composition. Absorbtion isothermes (Fig. 7-24) illustrate that desorption of Cs-134 (Cs-137) follows a monomolecular model.

Thus, the horizontal distribution of Cs and Sr radionuclides is irregular and their concentrations depend on lithological and structure of sediments, which provides the necessity to carry out a combined investigations of radioactivity and geochemical parameters in the study area.

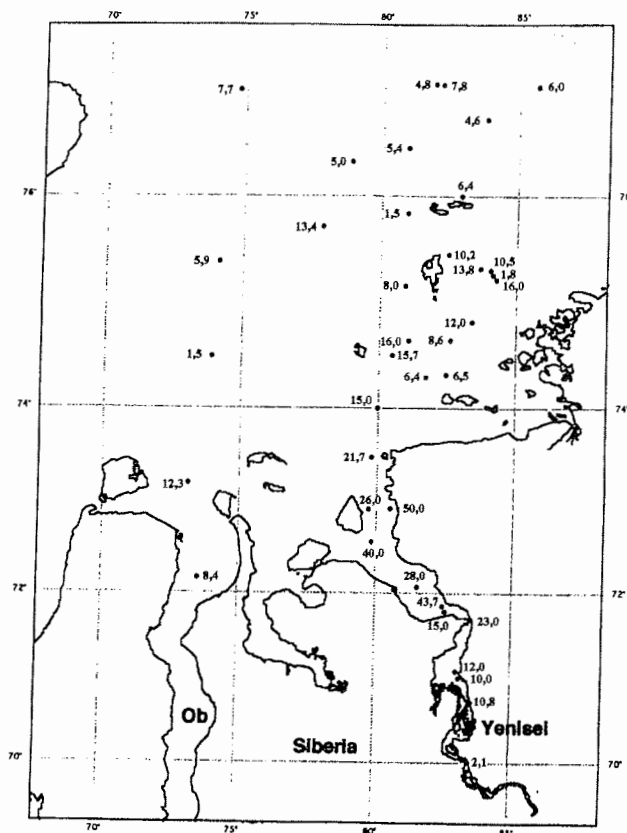


Fig. 7-20: Distribution of Cs-137 in surface sediments (Bq/kg).

Table 7-7: Results of measurement of ^{90}Sr in sea water.

Station	Depth, m	S, ppt	Activity ^{90}Sr , Bq/m ³
BP00-02	44	32	0.4 ± 0.1
BP00-05	42	33	0.9 ± 0.2
BP00-13	3	21	2.2 ± 0.4
BP00-15	2	6	4.2 ± 0.8
BP00-16	2	<0.1	4.4 ± 0.9
BP00-19	2	<0.1	4.2 ± 0.8
BP00-22	2	6	3.3 ± 0.7
BP00-26	2	18	2.3 ± 0.4
BP00-26	63	33	2.0 ± 0.1
BP00-36	2	28	0.4 ± 0.1
BP00-40	2	9.3	5.7 ± 1.1

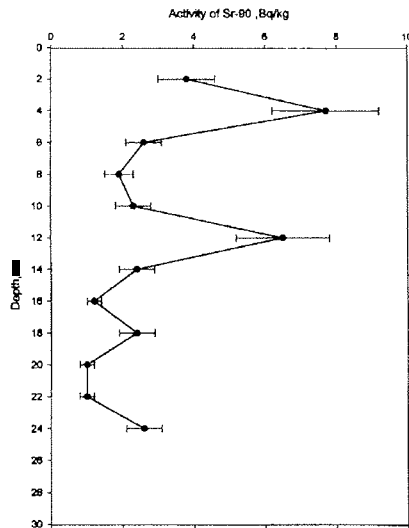


Fig. 7-21: Vertical distribution of Sr-90 in bottom sediments (St. BP99-06).

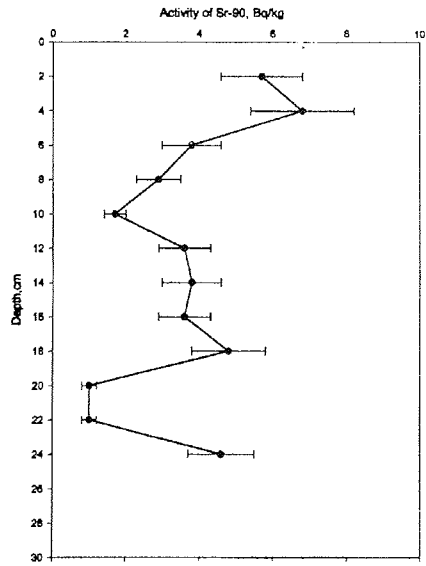


Fig. 7-22: Vertical distribution of Sr-90 in bottom sediments (St. BP99-19).

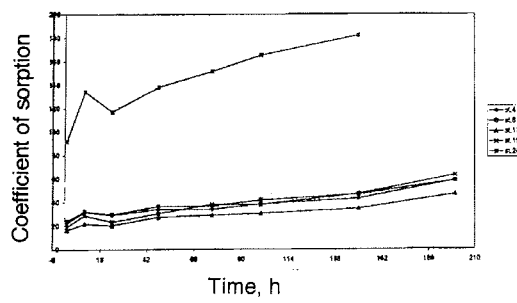


Fig. 7-23: Resulte of sorption experiments with Cs-134.

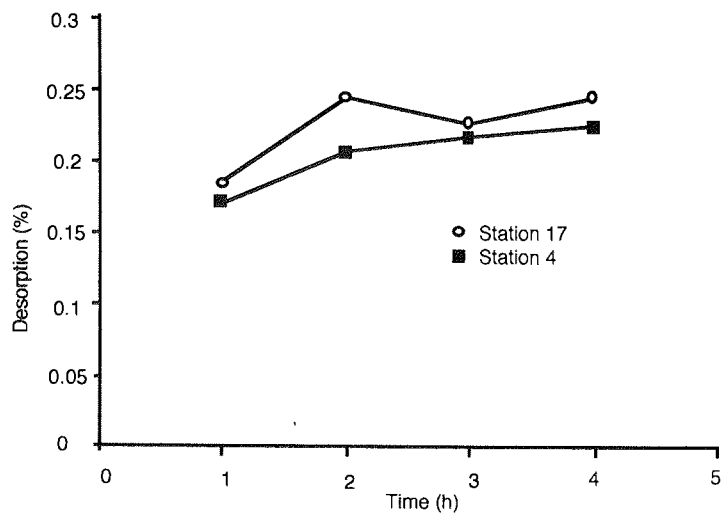


Fig. 7-24: Desorption of Cs-134 (Cs-137).

7.11 The investigation of sedimentation rate of the Kara Sea modern sediments using radioactive tracers

O. Stepanets, A. Borisov, A. Ligaev, and E. Galimov

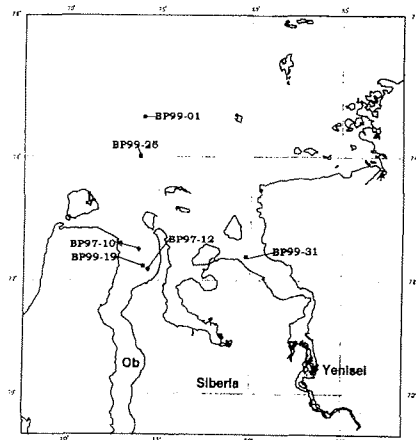
Vernadsky Institute of Geochemistry and Analytical Chemistry, RAS, Moscow, Russia

Introduction

In recent years the problems of sedimentation rate determination of modern deposits have a wide application for geochronological and paleogeological studies. Bottom sediments in lakes and estuaries may be not only a convenient and reliable resource for analysis of paleoenvironmental and climatic history, but it also appears to be useful for analysis of the influence of anthropogenic factors on sediments and, as a consequence, for ecological studies as a whole. With the help of such researches it is possible to study processes of different pollutants migration, including radio-isotopes in marine environment, and to determine sources and time domains of water area pollution in the past. The received geochronological information is useful for revealing concrete sources of industrial pollution of water environment. These investigations are very actual in the Kara Sea area, where the major Siberian rivers Ob and Yenisei may be the important pathways for long-distance transfer of pollutants.

The study of vertical distribution of artificial radionuclides (first of all of cesium-137) carried out before in the Kara Sea and the estuaries of the rivers Ob and Yenisei have shown, that several samples show significant variations of specific concentration of this radionuclide versus depth of a core. The comparison of the obtained data with geological descriptions of the vertical structure of sediments indicates that significant variations are not related to the structural heterogeneity in the vertical section, but more likely are connected with various rates of radioactivity input into the marine environment. This allows to identify the periods of massive inflow of radioactivity to the medium and to determine sources of such inflow under condition of correct interpretation of the obtained data for estimation of sedimentation rate in the investigated regions.

The use of sediment dating based on vertical distribution of cesium - 137 may lead to considerable errors at the expense of indefiniteness in "timing" of a core layer with maximal counting to the concrete historical period. Therefore, for more precise assessments of sedimentation rates, an optimum alternative is using several radioactive tracers, which presence in marine environment is conditioned by independent sources differing by geochemical nature and behavior. First of all it is possible to refer to tracers such as lead - 210 and cesium - 137 radionuclides.



Stations of the cores sampling for determination of the sedimentation rate.

Fig. 7-25: Stations of cores sampled for determination of sedimentation rate.

A major development in studies of sedimentation rate of modern sediments was recently gained by the plumbeous method on lead - 210, which at the beginning has successfully applied in glaciology for analysis of ice accumulation in Antarctica, and for analysis of sedimentation rate in intrinsic pools and adjacent seas. The radioactive lead is formed in the atmosphere due to the decay of radon - a rare gas incoming to the atmosphere at rocks emanating. In natural waters lead is unstable and rather easily floats to sediments. Measuring the decrease of lead - 210 activity versus depth of a core, it is possible to determine the time period over the range of 4-7 half-lives (about 100-150 years) and to estimate sedimentation rates in marine and river areas if a constant sedimentation rate during this period can be assumed. The plumbeous method (lead-210) is best to be used in rather quiet aqueous areas, such as lakes, embayments and quiet sites in rivers.

In the rivers Ob and Yenisei estuaries and the adjacent part of the Kara Sea complex sedimentation processes occur, conditions of predominant sedimentation, high hydrodynamic activity, partial fluid wash of ancient deposits, transportation and accumulation of matter. This means, that there is a number of hampering factors, such as bioturbation, influence of underwater currents, transformation of fluvial currents in different seasons etc., constructing jump-in sedimentation processes which may result in originating of trends on lead distribution curves in depth and distort the real picture of sedimentation processes. In this case, the results of sedimentation rates assessment based on

lead - 210, may be used for determination of average sedimentation rates only at larger time intervals.

On short time scales (about 50 years) it is convenient to use data on cesium-137 distribution in sediment cores, under condition of authentic "timing" of main peak with concrete historical events.

Method

In general, cesium method is a chronological method, using the effect of cesium-137 atmospheric fall-outs as a result of nuclear-weapons tests. This fission product appeared in atmosphere since the first days of nuclear-weapon tests and prolongs to precipitate in insignificant amounts on the earth and oceans surface even today. Cesium-137 distribution profiles in sediment cores demonstrate its deposition in time and may be used for estimation of timing dates. The first appearance of cesium-137 in sediments was fixed in 1954, when cesium-137 concentration achieved a level sufficient for its detection. Thus, the maximal depth of a core, at which the first increase of cesium-137 concentration is determined, may be referred to 1954. In some cases, when there are two peaks in a vertical distribution curve, the second one may be referred to the approximate period of 1963. It is explained by the increasing of nuclear-weapon tests at the end of 50 and the beginning 60 years. Knowing the depth in a core for the lower peak of cesium - 137 activity, it is possible to estimate the sedimentation rate for a time period of approximately 50 years, i.e. from the start time of nuclear testing.

To our opinion, simultaneous use of two radionuclides, analysis and comparison of the results of synchronic measurements in the same samples should give the most authentic results on real values of sedimentation rate. That is why our last investigations and interpretation of the obtained data on estimation of sedimentation rate in estuaries of the Siberian rivers and adjacent part of the Kara sea were performed using two methods: on lead-210 and on cesium-137).

For an assessment of sedimentation rate we selected samples from the Yenisei and Ob estuaries and from an open part of the Kara Sea. The location of all samples of bottom sediments taken during expedition in 2000 and earlier, and analyzed on radioactive tracers in depth of cores with cesium and plumbeous methods, are presented on Figure 7-25. Sediments were sampled with a box corer with subsequent subsampling with a plastic tube having an inner diameter of 10 cm. The cores were cut in 1-2 cm slices, and samples were dried at a temperature of 80°C.

Determination of cesium-137 was carried out without destruction of samples by measuring the gamma-activity of an aliquot subsample on low background installation with a semiconducting germanium detector.

For determination of lead-210 in samples of bottom sediments the extraction-chromatographic procedure, permitting to separate lead-210 and strontium-90 from one samples, was designed. The method is based on the ability of crown-aether-dicyclohexano-

18 crown-6 ($\text{DCH}_{18}\text{C}_6$) to selective extraction of different elements, including strontium and lead. At passage of 2M hydrogen nitrate solution keeping radioelements through the column with crown-aether, almost all radionuclides pass over. Strontium and lead remaining on the column, where then unabsorbed from the column by hot water.

Then, we carry out an electrolyte deposition of lead-210 and the subsequent deposition of strontium-90 as strontium oxalatum.

Results and discussion

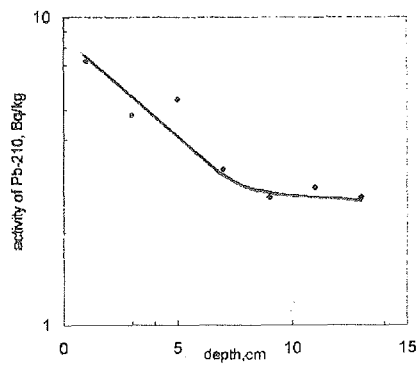


Fig. 7-26: Vertical distribution of Pb-210 in bottom sediments (St. BP99-10).

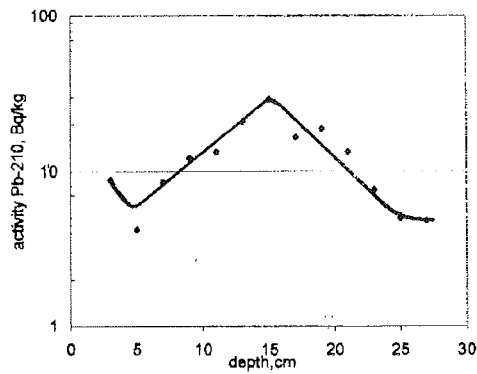


Fig. 7-27: Vertical distribution of Pb-210 in bottom sediments (St. BP99-19).

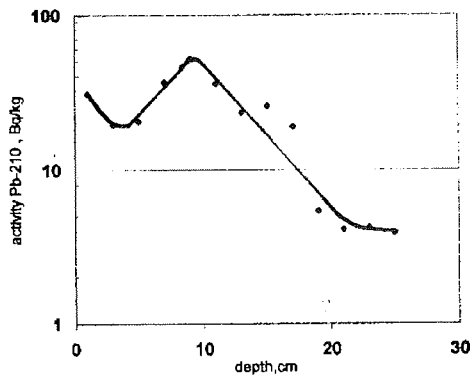


Fig. 7-28: Vertical distribution of Pb-210 in bottom sediments (St. BP99-06).

Data on counting lead-210 in length of the core (Figs. 7-26 to 7-28) demonstrate difficulties in interpretation of the obtained data. The first centimeters of sediments show the presence of abnormal trends in lead – 210 distribution, which are difficult to interpret. As a result we see on the profiles some trends with different characteristics. The analysis of these trends may result in different values of sedimentation rate (Fig. 7-29). It means, that in regions of intensive turbulence and possible local potent stirrings the plumbeous method has to be used in combination with the other method.

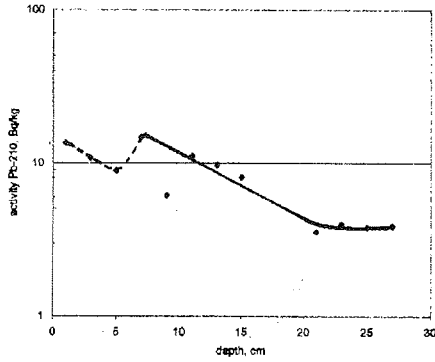


Fig. 7-29: Vertical distribution of Pb-210 in bottom sediments (St. BP99-25).

Examining the results of cesium distribution in the samples from the estuaries and the open part of the we may note, that despite of the differences in absolute activity of radionuclide for many cores, there are several significant peaks at different depth, the last of which, occurs at the horizon 17-18 cm (Figs. 7-30 to 7-32; stations 1, 19, and 31; for stations 10 and 12 see Berichte zur Polarforschung, 1999, vol. 300, p. 132).

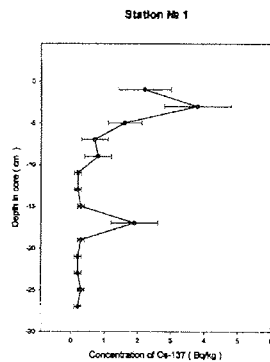


Fig. 7-30: Cs-137 profile at station BP99-01.

Examining the record of st. 19 (Fig. 7-31), it is obvious, that this wide peak consists of two separate peaks. In this case calculation of sedimentation rate using radioactive isotopes can be carried out as follows: for the lower spike 17cm depth\ 45 y (between 1954 and 1999) = 0,37cm/y, for the second spike 13 cm depth\36 y (between 1963 and 1999) = 0,36cm/y. For the open part of the Kara Sea (Fig. 7-30) the assessment of sedimentation rate gives similar values. The results of measuring sedimentation rate using cesium-137 for samples in the

Yenisei and Ob estuaries are very close to each other. Examining detail cesium-137 distribution curves in Cs-137 peak, it is possible to mark the presence of an intermediate at 8-9 cm for the samples from the Ob Estuary that should be related to the historical period of 1967, when there was one of the largest accident in the plant Majak. The influence of this accident is traced to a lesser degree in the Kara Sea, on route of Ob waters movement. In the cesium - 137 record in Core BP99-31 from the Yenisei Estuary (Fig. 7-32) there is a distinct variation at the horizon 12-13 cm, corresponding to the period 1950-1952. Its presence may be interpreted after acquaintance with the history of activity of the Krasnoyarsk radiochemical plant.

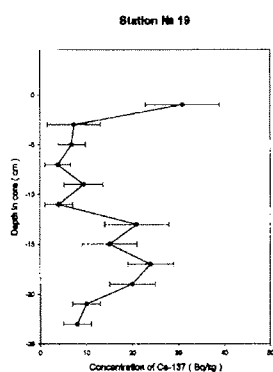


Fig. 7-31: Cs-137 profile at station BP99-19.

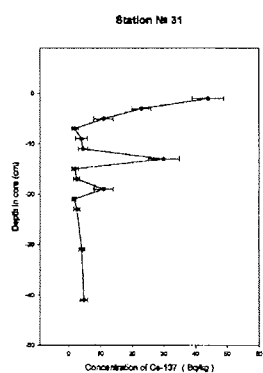


Fig. 7-32: Cs-137 profile at station BP99-31.

Differences in sedimentation rate values obtained by various methods can be explained by a sharp increase of sedimentation rates during the period 1953-1963, when powerful atomic explosions resulted in considerable stirrings of water environment and surface layer of bottom sediments more notably revealed in shallow-water regions. That is referred to the Ob and Yenisei estuaries. For the open part of the sea the data of assessments with both methods have rather close values. Another cause of different values may be explained by different average time interval chosen for assessments. The use of cesium method is suitable from the beginning of the mass nuclear-weapon tests, i.e., a time period till 50 years, while the plumbeous method is suitable for a period till 100-150 years. The comparison of the results of sedimentation rates obtained with the plumbeous method with available literature data for large time periods gives good agreement of results. Average late Quaternary sedimentation rates did not exceed 0,1 cm/y which -within the error of the used methods- coincides well with our data (0,12-0,14 cm / y).

7.12 The identification of chemical elements in bottom sediments using X-Ray fluorescence analysis.

E.Sizov, O.Stepanets, V.Komarevsky, and I.Roschina

Vernadsky Institute of Geochemistry and Analytical Chemistry, RAS, Moscow, Russia

Within the complex of methods for studying ecological conditions in shelf zones of the Arctic basin are important data on the chemical structure of heavy elements in water and in bottom sediments. Thus, the special task of this study is to obtain analytical information about the contents and distribution of heavy elements, including antropogeneous effect since a lot of sediments is transferred by currents from the rivers of Ob and Yenisei onto the shelf of the Kara Sea.

The contents of heavy elements were determined by a X-Ray-fluorescent method using X-ray spectrometer SPARK-1, which allows to determine chemical elements from Ti up to Sr on to - L-line and from Ba up to U on a L-line on fluorescent radiation. The power sanction in the central part of the spectrum (~ 30 Ev) allows to ensure high sensitivity of the analysis with minimum errors of measurements. The determination of the contents of elements was carried out by the method of external standards. Samples from 19 stations were taken and analyzed (12 stations in 1999 and 7 stations 2000 (Fig. 7-33).

We continued our investigation, that we began together with scientists from VNIIOkeangeologia during the Kara Sea Expedition 1997.

Preliminary results and discussion

The results of content of main elements in bottom sediments are presented in Table 7-8.

The analysis of the content of Fe and associated chemical elements revealed two different sediment groups: The first one with Fe > 5,83% and the second one with Fe < 5,88%. Each group is characterized by statistically significance of elements and correlation dependencies.

Two groups of elements can be distinguished because of the character of correlation with Fe. The first group includes Zn, Co, V, Ni, Ti, Mn and shows a high statistically significant correlation with Fe. The second group includes Cr, Cu, Sr and Pb and shows low insignificant or negative correlation to Fe. The first group of elements is positively correlated with sediments with low contents of Fe (<5,838%), whereas it is insignificantly correlated with sediments with high contents of Fe (>5,838%).

The regional distribution of the two sediment groups in the study area of the Ob and Yenisei estuaries is shown in Figure 7-34.

A well-defined zonation is observed: The inner zone presented mainly by sediments with high contents of Fe (>5,83%), is replaced northwestward by sediments with low contents of Fe (<5,83%). The observed zonation corresponds to the distribution of river waters.

Thus, the preliminary results show to significant differences of the contents of different elements in the sediment of estuaries of the rivers of Ob and Yenisei, that can be explained by a various geochemical nature of bottom sediments of these rivers. The consequent X-ray-fluorescent analysis of samples in stationary conditions of laboratory together with the use of the ratio of various elements to a "reference" element will allow in more detail to evaluate influences of a geological nature of the rivers to the element structure of deposits of a mixing zone, where the experimental researches in 1999 and 2000 were conducted, and to reveal the possible contribution of antropogeneous effect of heavy elements in this area.

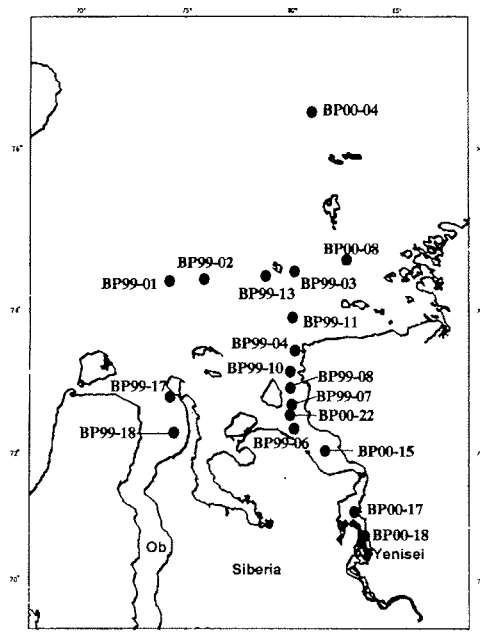


Fig. 7-33: Map of sampling of bottom sediments during the RV "Akademik Boris Petrov" cruise 1999 and 2000.

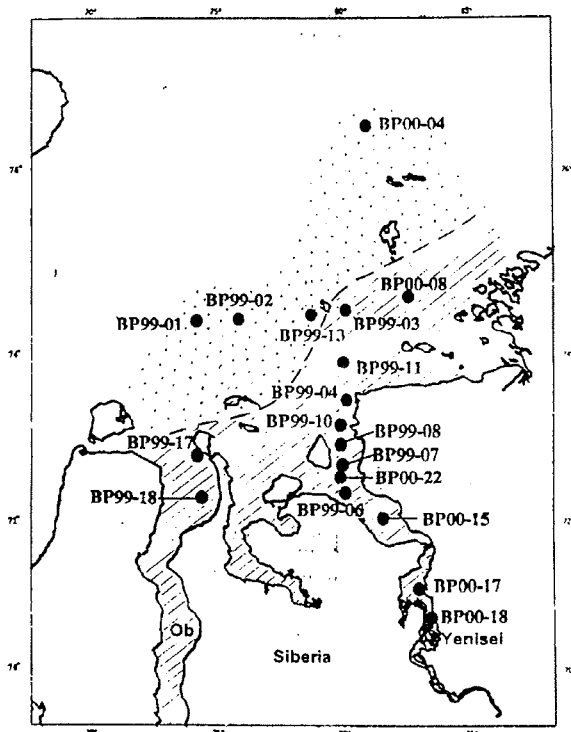


Fig. 7-34: Map of sampling of bottom sediments during the RV "Akademik Boris Petrov" cruise 1999 and 2000.

Table 7-8: The content of heavy elements in the bottom sediments.

Element Station	Rb (ppm)	Th (ppm)	Pb (ppm)	Zn (ppm)	Cu (ppm)	Ni (ppm)	Co (ppm)	Fe (%)	Mn (%)	Cr (ppm)	V (ppm)	Ba (%)	Ti (%)
BP99-01	152	<10	<10	24	130	24	16	1.8	0.14	50	64	0.07	0.23
BP 99-02	181	54	63	92	186	32	23	3.1	0.19	98	111	0.063	0.39
BP 99-03	131	16	<10	138	112	54	44	6.9	0.32	162	172	0.02	0.44
BP 99-04	<10	22	<10	128	140	78	47	7.8	0.37	77	144	<0.002	0.51
BP 99-06	48	12	<10	132	64	80	39	6.0	0.28	82	111	<0.002	0.50
BP 99-07		<10	<10	144	92	88	46	8.5	0.88	112	142	0.02	0.56
BP 99-08	62	<10	<10	127	48	69	46	8.7	0.71	106	160	0.01	0.57
BP 99-10		<10	<10	125	70	72	45	8.6	0.93	104	151	~0.002	0.58
BP 99-11		<10	<10	116	64	51	39	7.3	0.37	128	191	~0.002	0.54
BP 99-13		<10	<10	93	9	34	27	5.2	0.27	55	91	<0.002	0.38
BP 99-17		<10	<10	109	44	42	34	6.9	0.61	67	108	<0.002	0.47
BP 99-18		<10	<10	117	31	53	47	9.3	0.46	127	154	<0.002	0.59
BP 00-04	<15	11	59	70	95	40	25	3.6	0.88	62	116	0.02	0.41
BP 00-08	<15	<10	35	88	<30	45	42	6.1	3.0	94	130	0.02	0.38
BP 00-15	23	32	<20	95	90	62	40	5.4	0.62	112	134	0.05	0.49
BP 00-17	<15	38	<20	105	115	70	57	6.5	0.81	133	145	0.06	0.52
BP 00-18	26	<10	<20	112	130	80	55	7.2	0.46	118	155	0.02	0.58
BP 00-22	29	<10	<20	75	<30	37	36	4.9	0.58	68	112	0.01	0.42
BP 00-23	-	-	80	115	157	63	43	6.8	-	201	227	0.02	

7.13 The determination of heavy metals in water samples using sorption method for preconcentration of elements.

O.Stepanets, G.Solovjeva, S.Prijmak, N.Starshinova, and E.Sedjich

Vernadsky Institute of Geochemistry and analytical Chemistry RAS, Moscow, Russia

During the last years the interest in studies of microelement geochemistry in the Kara Sea in the light of its key position in transport processes of sea ice and water into the Arctic Basin, distinctly increased. This shallow shelf sea is characterized by a huge volume of fresh supply by the major rivers together with different technogenic pollution from the vast Siberian watershed area. A problem of chemical equilibrium in the Kara Sea attracts the particular attention in this context.

Sampling of surface waters was carried out in the Yenisei Estuary and open part of the Kara Sea onboard R/V "Academic Boris Petrov" during cruise-2000 (Fig. 7-35). One of the main tasks of the expedition was to study horizontal and vertical distributions of dissolved forms of heavy metals in sea and river water. It allows to estimate the flow of heavy metals to the sea with Siberian river run-off. Most part of the elements settle down to the bottom sediments within the estuaries. Some part of elements, however, enter to the open sea.

For determination of heavy metals in sea water samples we used the dynamic preconcentration of elements and subsequent - ICP – AES and ETAAS measurement. DATATA sorbent, based on polystyrene with conformational flexible amino-carboxylic groups, was used for preconcentration of the heavy metal group and removing of sea water macroelements.

Onboard analytical procedure of heavy metals determination in sea waters consisted of several operations: sampling, sample preparation and sorption preconcentration. The elements were desorbed with HNO_3 . Analysis of eluates by atomic emission method with inductively coupled plasma by using CP- spectrometer ICAP9000 was performed under laboratory conditions. Sea water samples were filtered through a membrane filter 0,45 μm . Filtered water samples (500-1000 ml) were brought to pH~5-6 and pumped through the microcolumn with DATATA sorbent, placed in the flow injection device BP1-1. The correctness of the method was examined by "standard addition" technique. The relative standard deviation of sorption ICP-AES determination of heavy metals is 0,06 at the 1 $\mu\text{g/l}$ level and 0,02 at 10 $\mu\text{g/l}$.

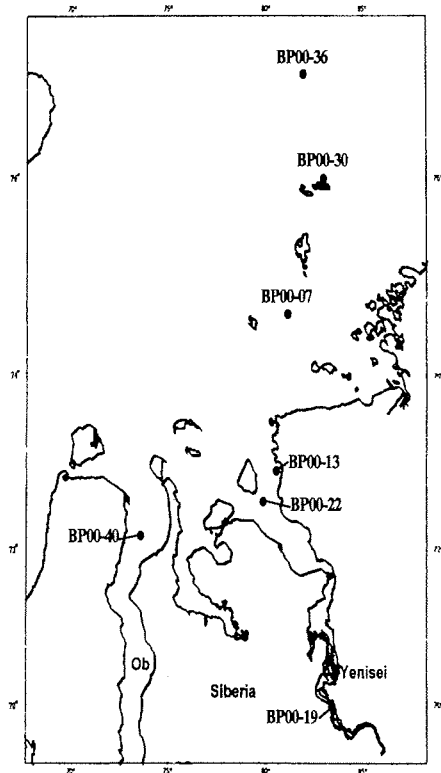


Fig. 7-35: Map of water sampling during the 35-cruise of RV "Akademik Boris Petrov" for determination of heavy metals.

Our preliminary results are summarized in Table 7-9. Anomalously high concentrations of Cd, Pb, Zn were found in Yenisei and Ob Bay in the mixing zone of fresh and saline waters. Concentrations of many elements increase with water depth. It evidences the feasible flow of elements out of the pore water. Concentrations of Fe, Mn, Co, and Cd increase in the pycnocline zone. Possibility, this effect can be related to a lot of particular matter being present in the boundary layer.

According to our results, a considerable increase of different metals in the estuaries was found. Concentration levels decrease to background in the open part of sea.

Table 7-9: Results of sea water samples analyses.

	Cd	Co	Cu	Fe	Mn	Ni	Pb	Ti	V	Zn	Cr
	mkg/ml	mkg/ml	mkg/ml	mkg/ml	mkg/ml	mkg/ml	mkg/ml	mkg/ml	mkg/ml	mkg/ml	mkg/ml
BP00-07 h=37m	$1,0 \cdot 10^{-4}$	$2,0 \cdot 10^{-4}$	$1,6 \cdot 10^{-3}$	$1,4 \cdot 10^{-2}$	$2,8 \cdot 10^{-3}$	$1,2 \cdot 10^{-3}$	$3,4 \cdot 10^{-4}$	$1,1 \cdot 10^{-3}$	$<2,0 \cdot 10^{-5}$	$4,0 \cdot 10^{-2}$	$<3,0 \cdot 10^{-5}$
BP00-07 h=37m	$1,0 \cdot 10^{-4}$	$2,0 \cdot 10^{-4}$	$4,0 \cdot 10^{-3}$	$1,9 \cdot 10^{-2}$	$3,1 \cdot 10^{-3}$	$1,5 \cdot 10^{-3}$	$4,2 \cdot 10^{-4}$	$1,8 \cdot 10^{-3}$	$1,2 \cdot 10^{-4}$	$4,1 \cdot 10^{-2}$	$<3,0 \cdot 10^{-5}$
BP00-13 h=0m	$4,0 \cdot 10^{-5}$	$5,0 \cdot 10^{-5}$	$1,3 \cdot 10^{-3}$	$1,3 \cdot 10^{-2}$	$4,5 \cdot 10^{-3}$	$1,0 \cdot 10^{-3}$	$5,2 \cdot 10^{-4}$	$1,9 \cdot 10^{-3}$	$7,3 \cdot 10^{-5}$	$1,3 \cdot 10^{-3}$	$<3,0 \cdot 10^{-5}$
BP00-13 h=0m	$4,0 \cdot 10^{-5}$	$5,0 \cdot 10^{-5}$	$1,2 \cdot 10^{-3}$	$1,6 \cdot 10^{-2}$	$4,2 \cdot 10^{-3}$	$9,2 \cdot 10^{-4}$	$5,4 \cdot 10^{-4}$	$2,5 \cdot 10^{-3}$	$6,9 \cdot 10^{-5}$	$8,9 \cdot 10^{-3}$	$<3,0 \cdot 10^{-5}$
BP00-19 h=0m	$7,0 \cdot 10^{-5}$	$1,6 \cdot 10^{-4}$	$1,2 \cdot 10^{-3}$	$1,9 \cdot 10^{-2}$	$2,5 \cdot 10^{-3}$	$5,8 \cdot 10^{-4}$	$5,0 \cdot 10^{-4}$	$4,5 \cdot 10^{-3}$	$1,1 \cdot 10^{-4}$	$8,2 \cdot 10^{-3}$	$<3,0 \cdot 10^{-5}$
BP00-22 h=0	$3,0 \cdot 10^{-5}$	$1,0 \cdot 10^{-4}$	$8,4 \cdot 10^{-4}$	$3,1 \cdot 10^{-2}$	$1,9 \cdot 10^{-2}$	$6,2 \cdot 10^{-4}$	$3,0 \cdot 10^{-4}$	$8,7 \cdot 10^{-3}$	$1,5 \cdot 10^{-4}$	$7,2 \cdot 10^{-3}$	$<3,0 \cdot 10^{-5}$
BP00-30 h=0m	$1,7 \cdot 10^{-4}$	$5,0 \cdot 10^{-5}$	$2,2 \cdot 10^{-4}$	$4,7 \cdot 10^{-3}$	$1,2 \cdot 10^{-3}$	$2,5 \cdot 10^{-4}$	$1,8 \cdot 10^{-4}$	$1,9 \cdot 10^{-3}$	$4,0 \cdot 10^{-5}$	$4,3 \cdot 10^{-3}$	$<3,0 \cdot 10^{-5}$
BP00-30 h=26m	$4,0 \cdot 10^{-4}$	$1,6 \cdot 10^{-4}$	$2,3 \cdot 10^{-3}$	$1,4 \cdot 10^{-2}$	$2,4 \cdot 10^{-3}$	$7,7 \cdot 10^{-4}$	$4,0 \cdot 10^{-4}$	$3,6 \cdot 10^{-3}$	$8,7 \cdot 10^{-5}$	$1,2 \cdot 10^{-2}$	$<3,0 \cdot 10^{-5}$
BP00-30 h=51m	$2,0 \cdot 10^{-4}$	$1,9 \cdot 10^{-4}$	$4,3 \cdot 10^{-4}$	$2,5 \cdot 10^{-2}$	$1,3 \cdot 10^{-3}$	$5,3 \cdot 10^{-4}$	$4,0 \cdot 10^{-4}$	$3,4 \cdot 10^{-3}$	$1,1 \cdot 10^{-4}$	$3,2 \cdot 10^{-3}$	$9,0 \cdot 10^{-5}$
BP00-36 h=0m	$4,0 \cdot 10^{-5}$	$1,0 \cdot 10^{-5}$	$1,8 \cdot 10^{-4}$	$7,6 \cdot 10^{-3}$	$1,0 \cdot 10^{-3}$	$1,7 \cdot 10^{-4}$	$9,0 \cdot 10^{-5}$	$1,9 \cdot 10^{-3}$	$4,5 \cdot 10^{-5}$	$1,3 \cdot 10^{-3}$	$<3,0 \cdot 10^{-5}$
BP36 h=28m	$5,0 \cdot 10^{-5}$	$8,0 \cdot 10^{-5}$	$1,7 \cdot 10^{-4}$	$1,6 \cdot 10^{-2}$	$6,3 \cdot 10^{-3}$	$2,5 \cdot 10^{-4}$	$1,8 \cdot 10^{-4}$	$3,3 \cdot 10^{-3}$	$6,5 \cdot 10^{-5}$	$4,0 \cdot 10^{-3}$	$<3,0 \cdot 10^{-5}$
BP00-40 h=0m	$6,0 \cdot 10^{-5}$	$9,0 \cdot 10^{-5}$	$2,8 \cdot 10^{-3}$	$4,3 \cdot 10^{-3}$	$3,8 \cdot 10^{-2}$	$5,5 \cdot 10^{-4}$	$1,1 \cdot 10^{-4}$	$2,1 \cdot 10^{-3}$	$5,0 \cdot 10^{-5}$	$3,9 \cdot 10^{-3}$	$<3,0 \cdot 10^{-5}$

7.14 Major and minor elements in suspended matter and sediments from the Yenisei River and the southern Kara Sea

Schoster, F.¹ and Beeskow, B.²

¹Alfred Wegener Institute, Bremerhaven, Germany

²Alfred Wegener Institute, Potsdam, Germany

Introduction

The Kara Sea is mainly supplied with water and particulate material by the Yenisei and Ob rivers. Both rivers have large, but different catchment areas. The Ob River drains the Siberian Lowlands and the Altai Mountains far south, the Yenisei River mainly drains the Putoran Mountains. These Putoran Mountains consist of Triassic Trap basalts, which show a significant chemical and mineralogical composition (Churkin et al. 1981, Lightfoot et al. 1989). Therefore, the surface sediments of the Kara Sea show a high smectite content and enhanced Ti/Al-, Mg/Al-, Fe/Al-, Cr/Al- and Ni/Al-ratios compared to the continental crust composition (Taylor and McLennan 1985, Schoster et al. 2000; Table 7-10). These elements are concentrated in the basalts of the Putoran Mountains, and smectite is formed by weathering of basalts (Lightfoot et al. 1989). This weathered basaltic material is distributed by currents and sediment-laden sea-ice into the Arctic Ocean, which is, for example, shown by the distribution of Ni/Al-ratios in surface sediments (Fig. 7-36, Wahsner et al. 1999, Schoster et al. 2000). Therefore, recent pathways of the material can be determined. Variations in the chemical and mineralogical composition of sediment cores are used to identify transport pathways in the late Quaternary and allow to reconstruct paleoenvironmental changes in the eastern Arctic Ocean (Müller 1999, Müller and Stein 2000, Schoster 2001). Due to the importance of material from the Putoran Mountains for the paleoenvironmental reconstruction of the eastern Arctic Ocean the investigations will be focussed on the Yenisei River and the southern Kara Sea. There are two main goals of our investigations: (1) Understanding of the distribution of the elements due to exchange reactions between water, suspended matter (SPM), and surface sediments, and determining of the variations of elemental concentrations in sediments of the southern Kara Sea during the time from the last deglaciation until present time.

Major and minor element distribution in water, suspended matter and surface sediments of the Yenisei Estuary

To characterize the recent material supply and its behavior in the estuarine mixing zone of the Yenisei River, the distribution of major and minor elements in the different components, water, SPM, and surface sediments, will be investigated. A comprehensive pattern of the composition of the Yenisei River run-off will be established. The focus of the examination is to understand the chemical processes in the estuarine environment of the Yenisei River. Variation in element ratios, which are caused by the exchange between dissolved and particulate phases in the transition zone between fresh-water and seawater, will be studied and interpreted. These data will provide characteristic signatures for the estuarine mixing zone, which will serve as a basis for paleoenvironmental reconstructions.

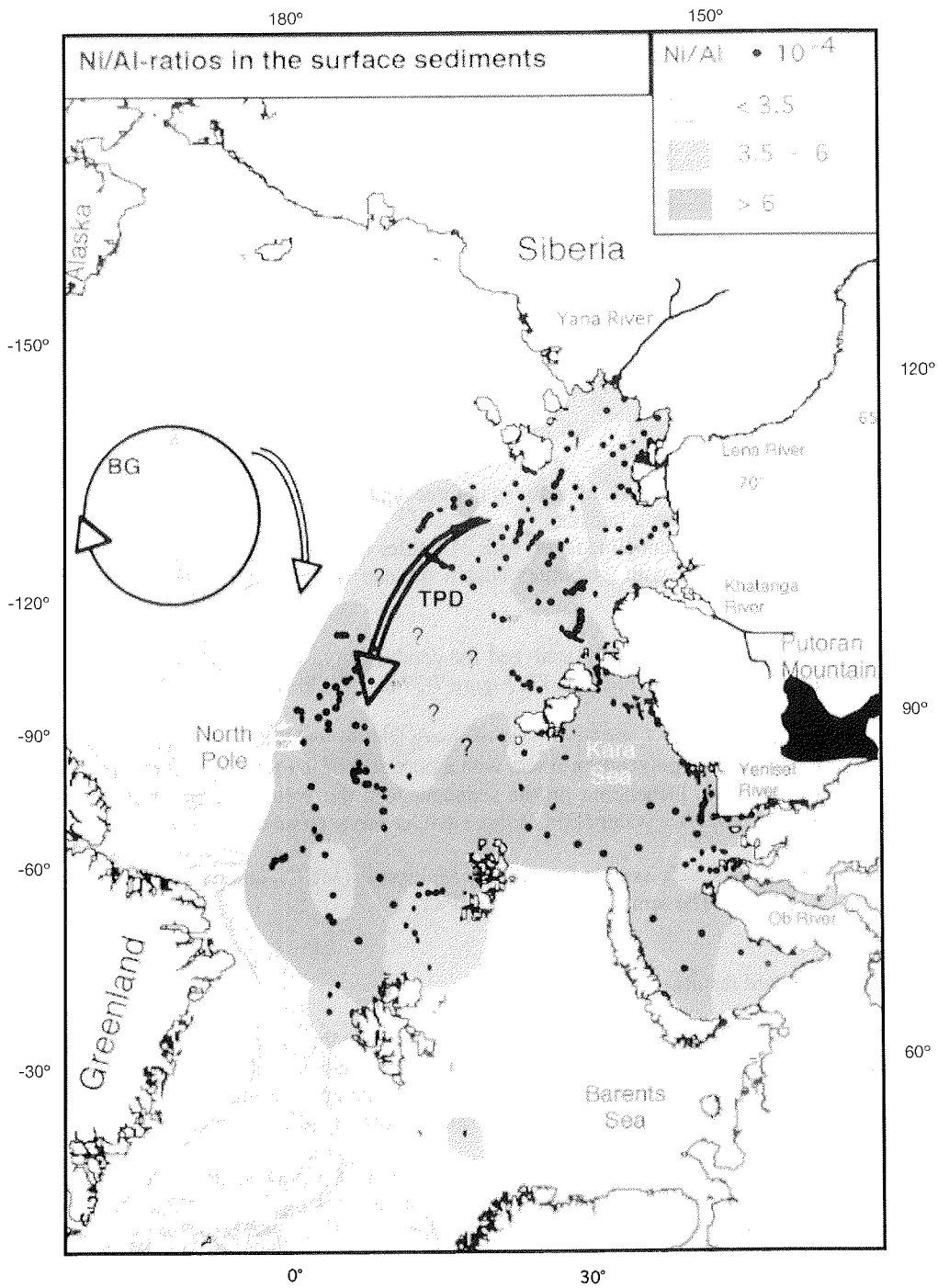


Fig. 7-36: Distribution of Ni/Al-ratios in the surface sediments of the eastern Arctic Ocean.

Table 7-10: Mean values of clay mineral contents and element/Al-ratios in suspended matter of the Yenisei and Ob rivers (Lukashin et al. 1999, Müller and Stein 1999).

	Yenisei	Ob
Illite	23	28
Smectite	44	43
Chlorite	18	15
Kaolinite	15	14
Ti/Al	0.07	0.03
K/Al	n.d.	n.d.
Ca/Al	0.13	0.05
Cr/Al*10 ⁻⁴	23.5	12.9
Ni/Al*10 ⁻⁴	26	23

Sampling program

Water samples were taken on all stations in three depths:

- surface water, with bucket;
- water of the pycnocline layer, with 24-bottles Niskin rosette sampler;
- bottom water, with 24-bottles Niskin rosette sampler and additional Multicorer-water.

All samples were immediately analyzed for conductivity, salinity, pH-value at 20°C and alkalinity. The results are presented in Figure 7-37 and Table 7-11.

To obtain the river SPM, surface water of every station was filtrated under slight vacuum through preweighted polycarbon filters with a pore size of 0.4 µm. The filters were dried at 40°C for two days. Depending on the sediment load the volume of filtered water varied from 5 to 20 l. For river water SPM of three depths was separated.

Surface sediments were sampled mainly by Multicorer (MUC), otherwise by Okeangrab or Large Box Corer. The samples are stored at 4°C.

First shipboard results

The values of conductivity and salinity increase towards the north, the alkalinity is lower in the river area than in the Kara Sea regions. Measured pH-values show no significant variance. In all regions depth profiles of the water column are mainly characterized by a decrease in temperature and an increase in salinity, conductivity and alkalinity.

The SPM concentrations strongly decrease as a function of the distance to the river mouth. In the freshwater SPM concentrations of approximately 4 mg/l were observed, while the average content at the northernmost stations is less than 0.5 mg/l. The SPM input by the Ob River is significantly higher. At station BP00-40 SPM content amounts to 45 mg/l.

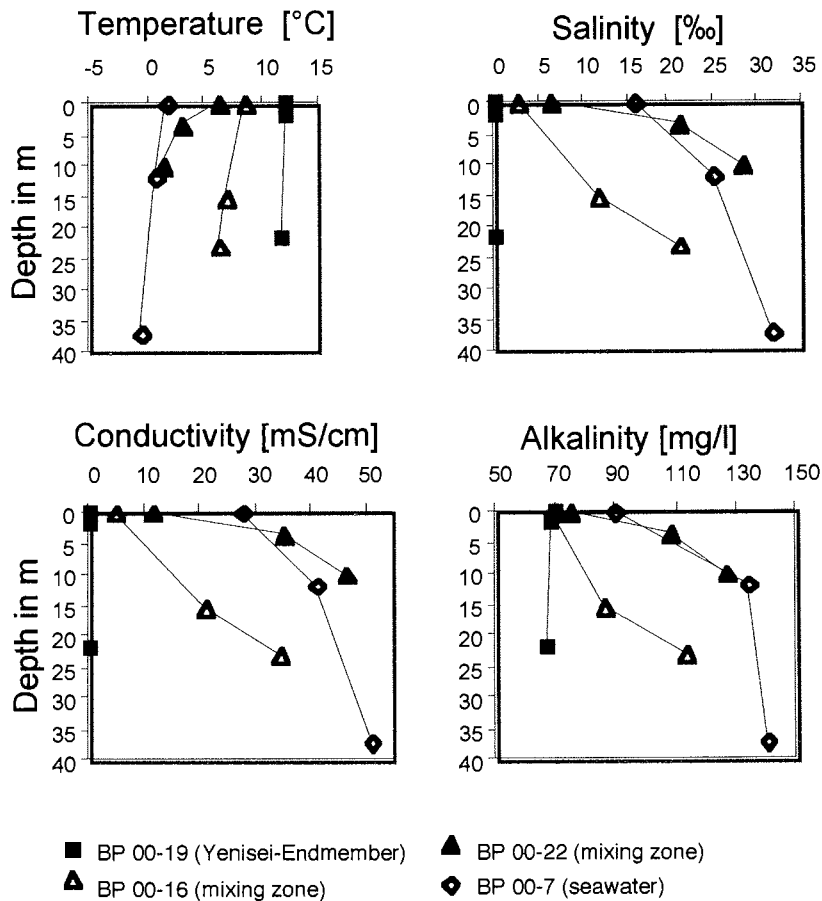


Fig. 7-37: Hydrochemical parameter of the Yenisei Estuary.

Analytical program

Analytical program for shore-based studies

In the laboratory detailed geochemical analyses will be performed. The concentrations of major and minor elements in all components (water, SPM and surface sediments) will be analyzed by Inductive-coupled plasma atom emission spectrometer (ICP-AES), Inductive-

Coupled Plasma Mass Spectrometer (ICP-MS), Ionic Chromatograph (IC) and additional for sediments by X-ray Fluorescence Spectrometer (XRF).

Table 7-11: Hydrochemical data (A: surface water, B: pycnocline water, C: bottom near water, D: Bottom-near water, MUC).

Station, BP 00-	depth in m	Temperature in °C	Salinity in ‰	Conductivity in mS/cm	pH at 20°C	HCO ₃ in mg/l
2A	0	4.3	17.1	28.9	7.68	96.45
2B	11.8	3.1	19.6	32.8	7.65	101.03
2C	48	-0.5	33	52.8	7.53	141.44
2D	49.6	-0.5	32.5	51.6	7.69	141.44
3A	0	4.2	21	34.5	7.87	121.62
4A	0	2.7	25.1	40.1	7.82	121.24
4B	12	2	28.3	44.9	7.78	129.24
4C	50	0.4	33.8	52.4	7.6	141.44
5A	0	2	21.5	35.3	7.7	106.75
5B	10	1.9	23.2	37.6	7.76	115.14
5C	40	0	32.8	51.5	7.69	141.06
5D	50	-0.7	32.7	51.6	7.61	144.11
7A	0	1.9	16	27.2	7.72	89.98
7B	11.5	0.7	24.8	40.7	7.49	134.2
7C	37	-0.6	31.8	50.8	7.53	139.92
7D	38	-0.2	31.5	49.1	7.52	139.54
8A	0	1.4	20.1	34.7	7.74	104.46
8B	5.8	0.6	21.6	35.4	7.76	104.46
8C	35.5	0.1	32.4	51.3	7.65	139.16
8D	41	-1.4	32.7	51	7.61	142.97
9A	0	0.4	22.8	37.2	7.82	112.47
9B	15	-0.2	27.7	44	7.82	132.29
9C	40	-0.2	32.6	50.8	7.61	144.49
9D	44.5	-1.1	32	50.1	7.69	141.06
13A	0	3.6	22.7	31.1	7.64	109.8
13B	3.5	2.3	25	40	7.41	119.71
13C	10	1.2	25	39.7	7.46	123.53
13D	13	0	29.3	45.1	7.53	136.49
15A	0	7.3	7	12.35	7.64	74.73
15C	6.5	6.4	7.5	13.18	7.33	75.49
15D	5.8	5.5	17.1	28.3	7.14	99.13
16A	0	8.4	2.4	4.64	7.65	68.63
16B	15.5	7	11.9	20.5	7.19	86.16
16C	23	6.2	21	34.3	7.06	112.85
16D	26	5.5	22.3	36.4	7.46	115.9
17A	0	10.9	0	0.182	7.88	70.15
17C	17.5	9.8	0.5	1.424	7.67	71.68
17D	18	8.2	12.2	20.7	7.38	86.93

Table 7-11: cont.

Station, BP 00-	depth in m	Temperature in °C	Salinity in ‰	Conductivity in mS/cm	pH at 20°C	HCO ₃ in mg/l
19A	0	12.2	0	0.158	7.29	70.15
19B	1.5	12.2	0	0.157	7.67	68.63
19C	21.5	11.7	0	0.156	7.25	67.1
20A	0	9.8	0	0.173	7.92	64.81
20C	19.5	8	16.3	21.3	7.17	97.6
21A	0	7.2	0.3	1.015	7.95	70.15
21B	12	7.4	6.4	11.47	7.56	81.59
21C	25	5.2	23.2	37.6	7.37	115.9
22A	0	6.4	6.4	11.54	7.78	74.73
22B	3.7	3	21.1	34.8	7.63	107.51
22C	10	1.3	28.1	46.1	7.56	126.57
22D	11	0.1	26.3	42.5	7.66	121.24
23A	0	0.6	26.3	42.1	7.75	126.57
23B	9.2	0.1	29.2	46.9	7.66	128.1
23C	32.1	-0.8	31.1	49.6	7.62	134.2
23D	33	-0.9	31.7	50.3	7.62	137.25
24A	0	1.4	22.8	37.4	7.76	111.33
24B	16	0.2	27	43.5	7.7	125.81
24C	31	0.1	31	49.8	7.59	134.2
26A	0	4.2	18.7	31	7.56	99.13
26B	17	3.5	25.3	41	7.82	123.53
26C	62	0.8	32.7	51.6	7.65	138.78
26D	68	-0.4	33	52.2	7.67	130.39
27A	0	2.5	22.4	36.5	7.83	112.85
27B	12.5	2.4	25.4	41.1	7.82	119.71
27C	74	0.8	33	51.4	7.68	138.77
27D	78	-0.5	33.4	52.2	7.71	139.54
28A	0	1.8	24.6	39.9	7.8	117.43
28B	16.2	1	28.4	45.2	7.78	128.86
28C	45	0.6	32.9	51.5	7.71	138.78
28D	50	-0.8	32.9	51.2	7.7	140.3
29A	0	1.9	25.7	42.7	7.84	118.9
29B	17.5	1.2	28.3	45	7.84	127.34
29C	62	-0.3	33.4	52.3	7.68	140.3
29D	68	-0.6	33.4	52.4	7.72	138.78
30A	0	1.2	24.1	39.3	7.79	116.66
30B	28	0	28.9	46.9	7.78	127.34
30C	49	-0.2	33.1	52.5	7.61	138.78
31A	0	0.7	23.8	39.2	7.82	118.19
35A	0	0.8	25.5	41.6	7.79	120.48
35B	13.7	-0.1	29.3	46.9	7.74	134.2
35C	44.5	-0.5	32.7	51	7.64	138.78
35D	46	-0.6	32.7	52.2	7.65	140.3
36A	0	2.2	26.5	43.1	7.83	122
36B1	14.5	1.5	26.6	43.2	7.86	122
36B2	17.5	0.3	28.8	46.3	7.83	126.58
36C	63	0.3	33.4	52.5	7.69	141.06
36D	66	-0.9	33.5	53.4	7.73	131.15
38A	0	2.5	16.1	27.3	7.69	96.08
40A	0	3	8.4	14.74	7.72	74.73

Major and minor elements in sediments of the southern Kara Sea from the last deglaciation until present

In order to get information about the quality and amounts of input of material into the Kara Sea from the last deglaciation until the present time sediment cores from the shelf area will be studied. Major and minor element concentrations and mineralogy are used to characterize the sediments. The surface sediments of the Kara Sea show high contents of smectite and enhanced Ni/Al-, Ti/Al-, Fe/Al-, and Cr/Al-ratios compared to the continental crust composition (Taylor and McLennan 1985). The K/Al- and Rb/Al-ratios are rather low in the Yenisei Estuary. In comparison with the sediment compositions of the Yenisei Estuary in the Ob Estuary K/Al- and Rb/Al-ratios are increased, the other mentioned element/Al-ratios are reduced (Schoster and Stein 1999). Therefore, it should be possible to distinguish between major input from one river or from the other at a given location in the southern Kara Sea.

Sampling program

The sediment cores were taken with a 3 to 8 m long gravity corer and divided in one meter long segments. They were stored on board at ca. 5°C. At the Alfred-Wegner-Institute the cores will be measured for the magnetic susceptibility. According to this data samples for the determination of major and minor elements and the mineralogy will be taken.

Analytical program for shore-based studies

After drying and grinding the samples will be analysed by XRF to get the major and minor element concentrations.

To determine the clay mineral composition the samples will be divided into sand, silt and clay fractions by sieving and grain-size fractionating after Atterberg (1912). In the clay fraction the contents of clay minerals will be determined by XRD.

8 References

- Alekseeva, T.N. and Svalnov, V.N., 2000. To the technics of grain-size analysis. *Oceanology*, 2: 304-311 (in Russian).
- Alperin M.J. and Reeburgh W.S., 1984. Geochemical observations supporting anaerobic methane oxidation. In: *Microbial growth on C-1 compounds*. Crawford R., Hanson R (Eds.), pp.282-289.
- Amon, R. and G.-H. Köhler, 1999: Distribution of surface salinity in the southern Kara Sea, Russia. *Ber. Polarforsch.*, 300, 20-27.
- Amon, R.M.W. and Spitzzy, A., 1999: Distribution of dissolved organic carbon during estuarine mixing in the southern Kara Sea. In Matthiessen, J. et al (eds.), *The Kara Sea Expedition of RV "Akademic Boris Petrov" 1997: First Results of a Joint Russian-German Pilot Study*. *Ber. Polarforsch.*, 300: 102-109.
- Benner, R., 1998. Cycling of Dissolved organic matter in the ocean. In: Hessen, D.O. and Tranvik, L.J. (eds.) *Aquatic humic substances; Ecology studies 133*: 317-330.
- Benner, R.; Biddanka, B.; Black, B. and McCarthy, M., 1997. Abundance, size distribution and stable carbon and nitrogen isotopic compositions of marine organic matter isolated by tangential-flow ultrafiltration. *Mar. Chem.* 57 (3-4): 243-263.
- Bergamaschi, B.A., Tsamakis, E., Keil, R.G., Eglinton, T.I., Montluçon, D.B. and Hedges, J.I., 1997: The effect of grain size and surface area on organic matter, lignin and carbohydrate concentration, and molecular compositions in Peru margin sediments. *Geochim.Cosmochim.Acta*, 61, 1247-1260.
- Bezrukov, P.L. and Lisitsin, A.P. 1960. Classification of sediments of modern sea basins. M., *Transactions of Shirshov Inst. Oceanol.*, 32: 3-14 (in Russian)
- Bol'shakov A.M. and Egorov A.V., 1995. Results of gasometric study in the Kara Sea. *Okeanologija*, v.35, No 3, pp. 399-304 (in Russian).
- Bol'shakov A.M. and Egorov A.V., 1998. Method of investigation of gas samples from water and bottom sediments. In: *Chemical analysis of sea sediments*. M., Nauka, pp. 248-251 (in Russian).
- Boucsein, B., Fahl, K., Siebold, M. and Stein, R., 1999: Quantity and quality of organic carbon in surface sediments of the Ob and Yenisei estuaries and adjacent coastal areas: Marine productivity vs. terrigenous input. *Ber. Polarforsch.*, 300, 116-126.
- Brodskii, K. A., 1950: Calanoida of the Far Eastern Seas and Polar Basin of the USSR. – *Key to the Fauna of the USSR*, No. 35: 78-117; 278-305; 314-321; 418-429.
- Burenkov, V.I. and Vasil'kov, A.P., 1995. The influence of runoff from land on the distribution of hydrologic characteristics of the Kara Sea. *Oceanology*, 34(5): 591-599 (English Translation)
- Burenkov, V.I., and Vasil'kov, A.P., 1994. The effect of continental runoff on the spatial distribution of hydrographic characteristics of the Kara Sea. *Oceanology*, 34(5): 652-661 (English Translation).
- Burkovsky, I. V. Udalov A. A. and Stoljarov A. P., 1997, The importance of juveniles structuring a littoral macrobenthic community, *Hydrobiologia* 355: 1-9
- Burton E. and Walter L.M., 1989. The role of pH in phosphate inhibition of calcite and aragonite precipitation rates in seawater//. *Geochim. Cosmochim. Acta*, v.54, pp.797-808.

- Butman, C.A., 1987. Larval settlement of soft - sediment invertebrates: the spatial scales of pattern explained by active habitat selection and emerging role of hydrodynamical processes. *Oceanogr. Mar. Biol. A. Rev.*, 25: 113-165.
- Churun, V. and Ivanov, B., 1998. Investigations of the hydrophysical structure in the mixing zone between fresh and saline waters. In Matthiessen, J. and Stepanets, O.V. (eds.), *Scientific Cruise Report of the Kara Sea Expedition of RV "Akademik Boris Petrov" in 1997*. Ber. Polarforsch., 266: 11-18.
- Claypool G.E. and Kvenvolden K.A., 1983. Methane and other hydrocarbon gases in marine sediment. *Ann.Rev. Earth Planet. Sci.*, v.11, pp.299 – 327.
- Cochrane, S., Kjeldrup, L., Palerud, R. and Dahle, S., 1997, Preliminary studies of benthic faunal communities in the estuaries of Ob and Yenisei. In Volkov, V. et al. (eds.) *Natural conditions of the Kara Sea and Barents Seas*. Norsk Polarinstittutt Rapport 97:64-65
- Corliss, B.H., 1991. Morphology and microhabitat preferences of benthic foraminifera from the northwest Atlantic Ocean. *Mar. Micropal.*, 17: 195-236.
- De Lurio J.L. and Frakes L.A., 1999. Glendonites as a paleoenvironmental tool: Implications for early Cretaceous high latitude climates in Australia. *Geochim.Cosmochim. Acta*, v.63,No 7/8, pp.1039-1048.
- Delong E.F., 2000. Resolving a methane mystery. *Nature*, v. 407, No 6804, pp.677-679.
- Descolas-Gros C. and Fontugne M., 1990. Stable carbon isotopes fractionation by marine phytoplankton during photosynthesis. *Plant Cell Environm.*, v.13, pp.207-218.
- Dobrovolsky, A.D., and Zalogin, V.S., 1982. *The seas of the USSR*. Moscow, Moscow State Univ. Publ.: 192 pp.
- Duplessy, J.C., Ivanova, E.V., Murdmaa, I.O., Paterne, M., and Labeyrie, L., 2001. Holocene paleoceanography of the Northern Barents Sea and variations of the northward heat transport by the Atlantic Ocean. *Boreas* (in press).
- Dussart B. and D. Defaye, 1995. *Copepoda. Introduction to the Copepoda*. SPB Academic Publishing BV 1995, pp.1-277
- Fairbanks, R.G., 1989. A 17000-year glacio eustatic sea level record: influence of glacial melting rates on the Younger Dryas event and deep-ocean circulation. *Nature*, v.342, pp.637-642.
- Fernandes, M.B. and Sicre, M.-A., 2000: The importance of terrestrial organic carbon inputs on Kara Sea shelves as revealed by n-alkanes, OC and $\delta^{13}\text{C}$ values. *Org. Geochem.*, 31, 363-374.
- Fetzer, I. and C. Arndt, 2000: The Distribution of Zooplankton in the Kara Sea. – *Berichte zur Polarforschung* 360: 37-45.
- Fischer, G., 1991. Stable carbon isotope ratios of plankton carbon and sinking organic matter from the Atlantic sector of the Southern Ocean. *Mar. Chem.*,v.35, pp.581-596.
- Fomin, O.K.,1989. Some characteristic structures of the zooplankton ('Nekatorije strukturnije kharakteristiki zooplanktona'). In: Matishov GG (Ed) *The ecology and bioresources of the Kara Sea ('Ekologia i Bioresurci Karskovo Moria')* Murmansk Marine Biological Institute, Akademia Nauk SSSR, Apatiti, Russia, pp 65-85
- Freeman K. and Hayes J.M., 1992. Fractionation of carbon isotopes by phytoplankton and estimates of ancient CO₂ levels. *Global Biogeochem.Cycles*, v.6, No 2, pp. 185-198.
- Frolov, V.T. 1995. *Lithology. M., MSU, pt. I, 345 pp.* (in Russian)

- Fry B. and Wainright S.C., 1991. Diatom sources of ^{13}C -rich carbon in marine food webs// *Mar.Ecol.Prog.Ser.*, v.76, pp.149–157.
- Gordeev, V.V., J.M. Martin, I.S. Sodorov, M.V. Sidorova, 1996: A reassessment of the Eurasian river input of water, sediment, major elements and nutrients to the Arctic Ocean.- *American Journal of Science* 296: 664-691.
- Greinert J., Suess E., Derkachev A.N., Obzhirov A., Baranov B., Winckler G., 1999. Gas venting, biota and carbonate mineralization along the Sakhalin shear zone, sea of Okhotsk. *AAPG Bull.*, v.83, No 4, pp 689-690.
- Gurevich, V.I., 1995. Recent sedimentogenesis and environment of the Arctic shelf of Western Eurasia. Oslo, Meddelelser. NR. 131, 92 pp.
- Hald, M., and Steinsund, P.I., 1996. Benthic foraminifera and carbonate dissolution in the surface sediments of the Barents and Kara Seas. In Stein, R., Ivanov, G., Levitan, M. and Fahl, K (eds.), *Surface sediment composition and sedimentary processes in the central Arctic Ocean and along the Eurasian Continental Margin*. Ber. Polarforsch., 212: 285-307.
- Halsband, C. and H.-J. Hirche, 1999, The Role of Mesozooplankton for the Transformation of Organic Matter. – *Berichte zur Polarforschung* 300: 45-50.
- Halsband, C., 1998: *Marine Biology – Zooplankton*. – *Berichte zur Polarforschung* 266: 25-27.
- Harder J., 1997. Anaerobic methane oxidation by bacteria employing ^{14}C -methane uncontaminated with ^{14}C - carbon monoxide. *Mar.Geol.*, v.137,pp.13-23.
- Hargrave, B.T., von Bodungen, B., Stoffyn-Egli, P and Mudie, P.J., 1993: Seasonal variability in particle sedimentation under permanent ice cover in the Arctic Ocean. *Cont. Shelf Res.*, 14, 279-293.
- Harrison L.M., Korotaev V.N., and Sidorchuk A.Yu, 1981. Paleogeomorfological analysis of the river Yenisei delta plain. *Vestnik MGU,Ser.5 (Geography)*, No 6,pp.103-110 (in Russian).
- Hayes J.M., 1993. Factors controlling ^{13}C content of sedimentary organic compounds: principles and evidence. *Mar.Geol.*, v. 113, pp.111-125.
- Hayes J.M., Strauss H., and Kaufman A.J., 1999. The abundance of ^{13}C in marine organic matter and isotopic fractionation in the global biogeochemical cycle of carbon during the past 800Ma. *Chem.Geol., Isotope Geosci.*, v.161, pp.103-125.
- Head, M.J., Harland, R., and Matthiessen, J., 2001. New cold marine indicators of the late Quaternary: The dinoflagellate cyst *islandinium* new genus. *Journ. Paleont.*, subm.
- Hebbeln, D. and Wefer, G., 1991: Effects of ice coverage and ice-rafted material on sedimentation in the Fram Strait. *Nature*, 350, 409-411.
- Hedges, J.I. and Keil, R.G., 1999: Organic geochemical perspectives on estuarine processes: sorption reactions and consequences. *Mar. Chem.*, 65, 55-65.
- Hedges, J.I., Clark, W.A., Quay, P.D., Richey, J.E., Devol, A.H. and de M. Santos, U., 1986: Compositions and fluxes of particulate organic material in the Amazon River. *Limnol. Oceanogr.*, 31, 717-738.
- Hinrichs K., Hayes J.H., Sylva S.P., Brewer P., and Delong E.F, 1999. *Nature*, v. 398, pp.802-805.
- Honjo, S., 1996: Fluxes of particles to the interior of the open oceans. In: *Particle flux in the ocean*. V. Ittekkot, P. Schäfer, S. Honjo and P.J. Depetris (Eds.). SCOPE, Wiley and Sons, Chichester, 91-154.
- Hunt J.M., 1975. Origin of gasoline-range alkanes in the deep sea. *Nature*, v.254, pp. 411-413.

- Hunt J.M., 1984. Generation and migration of light hydrocarbons. *Science*, v. 226, No 4680, pp.1265-1270
- Ito T., 1998. Factors controlling the transformation of natural ikaite from Shiowakka, Japan. *Geochemical Journal*, v.32, No4, pp. 267-273.
- Ittekkot, V., 1996: Particle flux in the ocean: Introduction. In: Particle flux in the ocean. V. Ittekkot, P. Schäfer, S. Honjo and P.J. Depetris (Eds.). SCOPE, Wiley and Sons, Chichester, 1-6.
- Ivanov M.V., Polikarpov G.G., Lein A.Yu., Galchenko V.F., Egorov V.N., Gulin S.B., Gulin M.B., Rusanov V.V., Miller Yu.M., and Kuptsov V.I., 1991. Biogeochemistry of carbon cycle in a locality of methane emission in the Black Sea. *Dokl. Akad. Nauk SSSR*, v.320, No 5 pp.1235-1240
- Jorgensen N.O., 1992. Methane derived carbonate cementation of marine sediments from the Kattegat, Denmark: Geochemical and geological evidence. *Mar. Geol.*, v.103, pp.1-23..
- Kassens H., Bauch, Dmitrenko I.A., Eicken H., Hubberten H-W., Melles M., Thiede J., Timokhov L.A. (Eds.)/Land-Ocean Systems in the Siberian Arctic. Dynamics and History. Springer, 1999, 711p.
- Keil, R.G., Tsamakis, E., Fuh, C.B., Giddings, J.C., Hedges, J.H., 1994: Mineralogical and textural control on organic matter composition in coastal marine sediments: Hydrodynamic separation using SPLITT-fractionation. *Geochim. Cosmochim. Acta*, 58, 879-893.
- Keil, R.G., Tsamakis, E., Giddings, J.C. and Hedges, J.I., 1998: Biochemical distributions (amino acids, neutral sugars, and lignin phenols) among size-classes of modern marine sediments from the Washington coast. *Geochim. Cosmochim. Acta*, 62, 1347-1364.
- Khusid, T.A. and Korsun, S.A. 1996. Modern benthic foraminiferal assemblages in the Kara Sea. *Ber. Polarforsch.*, 212: 308-314
- Khusid, T.A., 1996. Recent Benthic Foraminiferal assemblages in the Kara Sea. *Oceanology*, 36(5): 716-722 (English Translation).
- Kleiber, H.P. and Niessen, F., 2000. Variations of continental discharge pattern in space and time: Implications from the Laptev Sea continental margin, Arctic Siberia. *Intern. Journ. Earth Sciences*, 89: 605-616.
- Kodina L.A., Bogacheva M.P., Vlasova L.N., and Galimov E.M., 1999. Water particulate organic matter in the Yenisei Estuary: isotope composition, concentration, and genesis. *Geokhimiya*, No 11, pp.1206 –1217 (in Russian).
- Kodina L.A., Ljutsarev S.V., and Bogacheva M.P., 2000. Sources of sedimentary material of the drifting ice in the Arctic Basin as deduced from the organic carbon isotope composition of the ice particulate organic matter. *Dokl. Ros. Akad. Nauk*, v.371, _ 4, pp.511-515.
- Kodina L.A., Tokarev V.G., Vlasova L.N., Pribylova T.N., and Shpigun L.K., 1997. Geochemistry of organic Matter and other elements of the carbon cycle in the southern Kara Sea and estuarine zone (Ob, Yenisey). *Berichte zur Polarforschung*, 266: 54-62.
- Kodina, L.A., Bogacheva, M.P., Vlasova, L.N., Meschanov, S.L. and Ljutsarev, S.V., 1999: Isotope geochemistry of particulate organic carbon in the Yenisei Estuary: Sources and regularities of distribution. *Ber. Polarforsch.*, 300, 91-101.
- Korsun, S., 1998. Benthic foraminifera in the Ob and Yenisei Estuaries. In Matthiessen, J. and Stepanets, O.V. (eds.), Scientific Cruise Report of the Kara Sea Expedition of RV "Akademik Boris Petrov" in 1997. *Ber. Polarforsch.*, 266: 29-31.

- Korsun, S., 1999. Benthic foraminifera in the Ob Estuary, West Siberia. In Matthiessen, J., Stepanets, O.V., Stein, R., Fütterer, D.K. and Galimov, E.M. (eds.), The Kara Sea Expedition of RV "Akademik Boris Petrov" in 1997: First Results of a Joint Russian-German Pilot Study. *Ber. Polarforsch.*, 300: 59-70.
- Korsun, S.A., Pogodina, I.A., Tarasov, G.A. and Matishov, G.G., 1994. Foraminifera of the Barents Sea: Hydrobiology and Paleoecology. Apatity, Kola Sci. Center Publ.: 140 pp. (in Russian with English Abstract).
- Krasnyuk, A.D., Vanshteyn, B.G., 1999. Heavy metals in bottom sediments from the estuaries of the rivers Ob and Yenisei. *Ber. Polarforsch.*, 300: 188-195
- Kuhn, G., 1995. Sedimentphysikalische Untersuchungen. In: Gersonde, R. (Ed.), Die Expedition ANTARKTIS-XI/2 mit FS "Polarstern" 1993/94.- Berichte zur Polarforschung 163, 66-74.
- Lastochkin, A.N., 1977. Bottom topography of the Kara Sea. *Geomorphology*, 2: 84-91 (in Russian)
- Lein A.Yu., Rusanov I.I., Savvichev A.S., Pimenov N.V., Miller Yu.M., Pavlova G.A., Ivanov M.V., 1996. Biogeochemical processes of the sulfur and carbon cycles in the Kara Sea. *Geokhimiya*, No 11, pp. 1027-1044 (in Russian).
- Levitan, M.A., Bourtman, M.V., Gorbunova, Z.N., Gurvich, E.G. 1998. Quartz and feldspars in the Kara Sea surface-layer bottom sediments. *Lithology and miner. deposits*, 2: 115-125 (in Russian)
- Levitan, M.A., Dekov, V.M., Gorbunova, Z.N., Gurvich, E.G., Muyakshin, S.I., N_rnberg, D., Pavlidis, M.A., Ruskova, N.P., Shelekhova, E.S., Vasilkov, A.V., Wahsner, M. 1996. The Kara Sea: A reflection of modern environment in grain size, mineralogy, and chemical composition of the surface layer of bottom sediments. *Ber. Polarforsch.*, 212: 58-80
- Levitan, M.A., Ivanov, G.I., Bourtman, M.V., Ponomarenko, T.V., Krylov, A.V. 1999. Provenance of the Kara Sea surface sediments based on heavy mineral data. *Ber. Polarforsch.*, 342: 160-171
- Lisitzin A.P., 1994. Marginal filter of the oceans. *Okeanologija*, v.34, No 5, pp.735 – 747 (in Russian).
- Lisitzin, A.P. and Vinogradov, M.E., 1995. International high-latitude expedition in the Kara Sea (the 49th cruise of the R/V Dmitriy Mendeleev). *Oceanology*, 34 (5): 583-590.
- Lisitzin, A.P., 1995. The marginal filter of the ocean. – *Oceanology* 34(5): 671-682 (English Translation).
- Lisitzin, A.P., Kharin, G.S., Chernysheva, E.A. 2000. Coarse debris from the bottom sediments of the Arctic seas as an evidence of the ice transportation. 3-rd Workshop on LOIRA. M., IORAS, p. 81-83
- Ljutsarev S.V. and Chubarov V.V., 1994. Techniques for measuring the content of dissolved organic carbon in natural waters. *Optica Atmosphery I Oceana*, v.7 No 4, pp.479 – 491. (in Russian)
- Lobbes, J.M., Fitznar, H.P. and Kattner, G., 2000: Biogeochemical characteristics of dissolved and particulate organic matter in Russian rivers entering the Arctic Ocean. *Geochim. Cosmochim. Acta*, 64, 2973-2983.
- Lohse, L., Kloosterhuis, R.T., de Stigter, H.C., Helder, W., van Raaphorst, W. and van Weering, T.C.E., 2000: Carbonate removal by acidification causes loss of nitrogenous compounds in continental margin sediments. *Mar. Chem.*, 69, 193-201.

- Lukashin, V.N., Ljutsarev, S.V., Krasnyuk, A.D., Shevchenko, V.P. and Rusakov, V.Y., 1999: Suspended particulate matter in the Ob and Yenisei estuaries. *Ber. Polarforsch.*, 300, 155-178.
- Mackensen, A., Schumacher, S., Radke, J. and Schmidt, D.N. 2000. Microhabitat preferences and stable carbon isotopes of endobenthic foraminifera: Clue to quantitative reconstruction of oceanic new production? *Marine Micropaleontology* 40(3): 233-258.
- Makkaveev P.N., Stunzhas P.N., 1994. Hydrochemical characteristics of the Kara Sea based on results the 49 –th Cruise of R/V “Dmitry Mendeleev”. *Okeanologija*, v.34, No 5, p.662-667.
- Markhaseva, E.L., 1996. Calanoid Copepods of the Family Aetideidae of the World Ocean: Russian Academy of Science; Zoological Institute St. Petersburg
- Matthiessen, J. 1999. Distribution of palynomorphs in surface sediments from the Ob and Yenisei estuaries (Kara Sea, Arctic Ocean). *Ber. Polarforsch.*, 300: 222-235
- Matthiessen, J. and Boucsein, B., 1999: Palynomorphs in surface water of the Ob and Yenisei estuaries: Organic-walled tracers for riverine water. *Ber. Polarforsch.*, 300, 71-78.
- Matthiessen, J. and Kraus, M., 2001. Influence of river discharge on dinoflagellate cyst assemblages in the Ob and Yenisei Estuaries, Kara Sea, Arctic Ocean. *Journ. Quatern. Sci.*, *subm.*
- Matthiessen, J. and Stepanets, O., 1998. Scientific cruise report of the Kara Sea Expedition of RV "Akademik Boris Petrov" in 1997. *Berichte zur Polarforschung*, 266: 102pp.
- Matthiessen, J., Kunz-Pirring, M. and Mudie, P.J., 2000. Freshwater chlorophycean algae from the Beaufort, Laptev and Kara Seas (Arctic Ocean) as indicators of river runoff. *International Journal of Earth Sciences*, 89(3): 470-485.
- Mayer, L.M., 1994: Surface area control of organic carbon accumulation in continental shelf sediments. *Geochim. Cosmochim. Acta*, 58, 1271-1284.
- Methods of hydrochemical investigations in ocean. M., Nauka, 1978, 271 p
- Meyers P. A., Brassell. 1985. Biogenic gases in sediments deposited since Miocene times on the Walvis Ridge, South Atlantic Ocean. In: *Planetary Ecology*. Caldwell D.E., Brierly J.A., Caldwell C.L. (Eds), Wiley, N.-Y., pp.69 – 80.
- Mileikovskiy, S.A., 1971. Types of larval development in marine bottom invertebrates, their distribution and ecological significance: a re-evaluation. *Mar. Biol.*, 10: 193-213.
- Mook W.C., Bommerson J.C., and Staverman W.H., 1974. Carbon isotope fractionation between dissolved bicarbonate and gaseous carbon dioxide. *Earth Planet. Sci.Let.*, v.22, No 2, p.169-176.
- Mukhina, V.V. and Yushina, I.G. 1999. Diatoms in bottom sediments of the Laptev and Kara seas. *Ber. Polarforsch.*, 306: 110-119
- Müller, C. and Stein, R. 1999. Grain-size distribution and clay-mineral composition in surface sediments and suspended matter of the Ob and Yenisei rivers. *Ber. Polarforsch.*, 306: 179-187
- Musatov, E.E. 1989. Development of the Barents-Kara sea shelf in Cenozoic. *Geomorphology*, 3: 76-84 (in Russian)
- Nürnberg, D. 1996. Biogenic barium and opal in shallow Eurasian shelf sediments in relation to the pelagic Arctic Ocean environment. *Ber. Polarforsch.*, 212: 96-118

- Olafsson, E.B., Peterson, C.H. and Ambrose, Jr., 1994. Does recruitment limitation structure populations and communities of macro-invertebrates in marine soft sediments: the relative significance of pre- and post-settlement processes. *Oceanogr. Mar. Biol. A. Rev.*, 65-109.
- Opsahl, S., R. Benner and R. M.W. Amon. 1999. Major flux of terrigenous dissolved organic matter through the Arctic Ocean. *Limnol. Oceanogr.* 44: 2017-2023
- Pavlov, V.K. and Pfirman, S.L., 1995: Hydrographic structure and variability of the Kara Sea: Implications for pollutant distribution. *Deep Sea Res.*, 42, 1369-1390.
- Piepenburg, D. 1988, Zur Zusammensetzung der Bodenfauna der westlichen Fram-Straße, *Ber. z. Polarforschung* 52:1-172
- Piepenburg, D. and Juterzenka K.v., 1994, Abundance, biomass and spatial distribution pattern of brittle stars (Echinodermata: Ophiuroidea) on the Kobleinsey Ridge north of Iceland, *Polar Biol.* 14:185-194
- Piepenburg, D., Chernova, N.V., von Dorrien, C.F., Gutt J., Neyelov, A.V., Racher E., Saldanha L. and Schmid M.K., 1996, Megabenthic communities in the waters around Svalbard, *Polar Biol.* 16:431-446
- Polyak L., Forman S.L., Herlihy F.A. Ivanov G., Krinitsky P., 1997. Late Weichselian deglacial history of the Svyataya (Saint) Anna Trough, northern Kara Sea, Arctic Russia. *Mar.Geol.*, v.143, pp.169-187.
- Polyak L., Levitan M., Khusid T., Merklin L., Mukhina V., 2001. Variations in the influence of riverine discharge on the Kara Sea during the last deglaciation and the Holocene. *Global Planet. Change, Special Issue.* in press
- Polyak, L. and Solheim, A., 1994. Late- and postglacial environments in the northern Barents Sea west of Franz Josef Land. *Polar Res.* 13 (2): 197-207.
- Polyakova, Ye.I. 1999. New data on diatom distribution in surface sediments of the Kara Sea. *Ber. Polarforsch.*, 300: 209-221
- Romankevich, E.A., Danyushevskaya, A.I., Belyaeva, A.N. and Rusanov, V.P., 1982. Biogeochemistry of the organic matter in the Arctic seas. Moscow, Nauka: 240 pp. (in Russian).
- Rusanov V.P. and Vasil'ev A.N., 1976. Distribution of the river water in the Kara sea as deduced from the hydrochemical measurements. *Trudy AARII*, v.323, p.188-196.
- Sars, G.O., 1903. An Account of the Crustacea of Norway with short descriptions and figures of all species. – Vol. IV: Copepoda – Calanoida. Bergen.
- Scheltema, R.S., 1986. On dispersal and planktonic larvae of benthic invertebrates: an eclectic overview and summary of problems. *Bull. Mar. Sci.*, 39(2): 290-322.
- Schmidt-Nielsen, K., 1994, *Animal Physiology*, University Press, Cambridge, USA
- Schoster, F. and Stein, R. 1999. Major and minor elements in surface sediments of Ob and Yenisei estuaries and the adjacent Kara Sea. *Ber. Polarforsch.*, 300: 196-207
- Schoster, F., Behrends, M., Müller, C., Stein, R. and Wahsner, M., 2000. Modern river discharge in the Eurasian Arctic Ocean: Evidence from mineral assemblages and major and minor element distributions. *Int.ern. Journ. Earth Sci.*, 89/3, in press.
- Schubert C.J., Nürnberg, Scheele N., Pauer F., Kriews M., 1997. ¹³C isotope depletion in ikaite crystals: evidence for methane release from the Siberian shelves? *Geo-Marine Let.*, v.17, pp.169-174.
- Shevchenko V.P., Lein A.Yu., Zernova V.V., Ivanov G.I., Lisitzin A.P., 1996. Distribution and composition of suspended matter and phytoplankton in surface water of the Norvegy-Grenland Sea in the August 1996. *Dokl. Akademii Nauk*, v. 355, No 6, pp.805-807 (in Russian).

- Shevchenko, V.P., Lisitzin, A.P., Zernova, V.V., Lukashin, V.N., Politova, N.V., Rusakov, V.Yu., and Shanin, S.S., 1999. Vertical particle fluxes in seas of the western Russian Arctic. PACON 99 Proceedings, Symposium on "Humanity and the World Ocean: Interdependence at the Dawn of the New Millennium", Russian Academy of Sciences, Moscow, Russia, p. 239-249.
- Shevchenko, V.P., Severina, O.V., Maiorova, N.G. and Ivanov, G.V., 1996: Quantitative distribution and composition of suspended matter in Ob and Yenisei estuaries. *Vestnik Mosk. Univ., Geol.*, 3, 81-86, (in Russian).
- Smith, L.C. and Alsdorf, D.E., 1998: Control of sediment and organic carbon delivery to the Arctic Ocean revealed with space-borne synthetic aperture radar: Ob River, Siberia. *Geology*, 26, 395-398.
- Spitzzy, A. and Leenheer, J., 1991. Dissolved Organic Carbon in Rivers. In Degens, E.T. et al. (eds.) *Biogeochemistry of Major World Rivers*. J. Wiley and Sons, Chichester, SCOPE Rep. 43: 213-232.
- Spitzzy, A., S. Ertl and L. Eichinger, 2001. An improved method for the preparation of CO₂ from DOC in saline waters for isotope determination. *Anal. Chem.* (subm.)
- Stein R. and Fahl K., 2000. Holocene accumulation of organic carbon at the Laptev Sea continental margin (Arctic Ocean): sources, pathways, and links. *Geo-Marine Letters*, v.20, pp.27-36.
- Stein R., Boucsein B., Hefter J., Kraus M., Lau N., Schoster F., Simstich J., Weiel D., 2000. *Marine Geology. Ber. Polarforsch.*, v.360, pp.49-69.
- Stein R., Seung-II Nam, Schubert C., Vogt Christoph, Fütterer D., Heinemeier J., 1994. The last deglaciation event in the Eastern Central Arctic Ocean. *Science*, v.264, pp.692-696.
- Stein, R. (Ed.), 2000. Circum Arctic Paleo-River Discharge and Its Geological Record, *Intern. Journ. Earth Sci.*, 89/3, 447-616.
- Stein, R. and Stepanets, O., 2000. Scientific cruise report of the joint Russian-German Kara Sea expedition of RV "Boris Petrov" in 1999. *Berichte zur Polarforschung*, 360: 141pp.
- Stein, R., Boucsein, B., Fahl, K., Garcia de Oteyza, T., Knies, J., and Niessen, F., 2001. Accumulation of particulate organic carbon at the Eurasian continental margin during late Quaternary times: Controlling mechanisms and paleoenvironmental significance. *Glob. Plan. Change*, in press.
- Stephantsev L.A., Shmelkov B.M., 2000. Brief characteristics and results from measurements of hydrophysical structure of waters in the estuaries of Ob and Yenisei. *Ber. Polarforsch.*, v. 360, pp.8-19.
- Stephantsev, L. and Shmelkov, B., 1999: Brief characteristics and results from measurements of hydrophysical structures of waters in the estuaries of Ob and Yenisei. *Ber. Polarforsch.*, 300, 8-19.
- Stunzhas P.A., 1995. Dividing the Yenisei and Ob waters in the Kara Sea according to alkalinity and silicate data. *Okeanologija*, v.35, No2, p.215-219.
- Suess E., Balzer W., Hesse K.-F. Hesse, Müller P.J., Ungerer C.A., Wefer G., 1982. Calcium carbonate hexahydrate from organic-rich sediments of the Antarctic shelf: precursors of glendonites. *Science*, v.216, pp.1128-1130
- Sukhoruk V.I., Tokarev V.G., 2000. Sea water Hydrochemistry and nutrients. *Ber.Polarforsch.*, v. 360, p.22-27.

- Telang, S.A., Pocklington, R., Naidu, A.S., Romankevich, E.A., Gitelson, I.I. and Gladyshev, M.I., 1991. Carbon and mineral transport in major north American, Russian and Siberian rivers: the St. Lawrence, the Mackenzie, the Yukon, the Arctic basin rivers in the Soviet Union and the Yenisei. In: Biogeochemistry of major world rivers. E.T. Degens, S.Kempe and J.E. Richey (eds.), SCOPE, Wiley and Sons Ltd., 75-104.
- Thorson, G., 1946. Reproduction and larval development of Danish marine invertebrates, with special reference to the planktonic larvae in the sound (Øresund). Medd. K. Omm. Dan. Fisk. Havunder. Ser. Plankton, 4(1).
- Thorson, G., 1936. The larval development, growth and metabolism of Arctic marine bottom invertebrates compared with those of other seas. Medd. Grønland, 100(6): 1-155
- Thorson, G., 1950. Reproductive and larval ecology of marine bottom invertebrates. Biol. Rev., 25: 1-45
- Thurman, M and Malcolm, R., 1981. Preparative isolation of aquatic humic substances. Env. Sci. Technol., 15: 463-466.
- Tortell P.D, Reinfelder J.R., Morel F.M.M., 1997. Active uptake of bicarbonate by diatoms. Nature, v.390, pp. 243-244.
- Unger, D., Neumann, K. and Fetzer, I., 2000: Sediment trap investigations in the Kara Sea. Ber. Polarforsch., 360, 28-35.
- Weber, M.E., Niessen, F., Kuhn, G., and Wiedicke, M., 1997. Calibration and application of marine sedimentary physical properties using a multi-sensor core logger. Marine Geology, 136, 151-172.
- Whiticar M.J., Suess E., 1998. The cold carbonate connection between Mono Lake, California and the Bransfield Strait, Antarctica. Aquatic Geochem., v.4, pp. 429-454.

9. Annex

9.1 Station list

Abbreviations of activities:

- EBS-Epibenthos Sledge
- BD - Benthos Dredge
- CTD - Conductivity-Temperature-Depth probe for oceanography
- GC 500 - Gravity Corer with 500 cm core barrel
- GC 800 - Gravity Corer with 800 cm core barrel
- LBC - Large Box Corer (GKG)
- LVS - Large Volume Sampler (Batomat 200l)
- MUC - Multiple Corer
- PHN - Plankton Hand Net (10 μ m) (AWI, Geo)
- PN - Plankton Net (150 μ m) (AWI, Bio)
- Bucket - for surface water samples
- ST - Sediment Trap

Station	Date	Time (GMT)	Latitude ° N	Longitude ° E	Depth (m)	Gear No.	Activity	Recovery (cm)	Air Temp. (°C)	Water Temp. (°C) (ship/sample)
BP00-01	03.09.2000	17:05	74°321'	73°56.712'			ST-Recovery (no Recovery)			-/5
BP00-02	04.09.2000	5:53	75°24.114'	74° 11.82'	49.6		CTD/ RS/bucket PN		1.9	-/4.3
						/01	LBC			
						/02	MUC			
						/03	MUC			
						/04	GC 500 BD	68		
BP00-03	05.09.2000	4:38	76°55.537	74°46.502	193		bucket			-/4.2
		5:16	76°55.610	74°46.818	193	/01	LBC	34		
BP00-04	05.09.2000	16:22	76°24.989'	81°0.486'	54		CTD/ RS/bucket PN/LVS		2.7	3.1/2.7
						/01	LBC			
						/02	LBC	22		
		0:30				/03	GC 500	empty		
BP00-05	06.09.2000	4:20	75°50.22'	81°0.32'	50		CTD/ RS/bucket PN/ LVS		2.1	2.4/2.0
						/01	LBC			
						/02	LBC			

Station	Date	Time (GMT)	Latitude ° N	Longitude ° E	Depth (m)	Gear No.	Activity	Recovery (cm)	Air Temp. (°C)	Water Temp. (°C)
BP00-05	06.09.2000	4:20	75°50.22'	81°03.2'	50	/03	LBC	26		
						/04	MUC			
						/05	MUC			
						/06	GC 500	34		
							EBS			
BP00-06	06.09.2000	16:44	75°10.051'	80°59.748'	38	/01	bucket	288	2	1/1.8
							GC 500			
BP00-07	07.09.2000	6:22	74°39.456'	81°08.466'	38		CTD/RS/bucket		2.4	2.1/1.9
							PN/LVS			
						/01	LBC			
						/02	LBC			
						/03	LBC	40		
						/04	GC 500	503(-600)		
						/05	GC 800	632		
						/06	GC 800	665		
						/07	GC 800	723		
						/08	MUC	43		
						/09	MUC	43		
							BD			
							EBS			
BP00-08	08.09.2000	4:58	74°39.554'	82°38.553'	41		CTD/RS/bucket		-0.4	1.2/1.4
							PN/LVS			
						/01	LBC			

Station	Date	Time (GMT)	Latitude ° N	Longitude ° E	Depth (m)	Gear No.	Activity	Recovery (cm)	Air Temp. (°C)	Water Temp. (°C)
BP00-08	08.09.2000	4:58	74°39.554'	82°38.553'	41	/02 /03 /04	LBC MUC GC 500 EBS	30 28 191		(ship/sample)
BP00-09	08.09.2000	10:55	74°50.006	83°25.898	44.5		CTD/RS/bucket PN/ LVS		-0.4	1.2/0.4
						/01 /02 /03	LBC LBC MUC BD	27 40		
BP00-10	08.09.2000	17:17	74°19.09'	82°32.74'	29	/01	GC 500	empty	0.4	0.5/0.7
BP00-11	08.09.2000	19:45	74°17.536'	81°47.141'	42	/01	GC 800	322		-/-0.1
BP00-12	09.09.2000		74°00.284'	80°0.723'	31		ST-Recovery		-0.1	1.4/1.1
BP00-13	09.09.2000	12:38	72°56.018'	80°33.232'	13		CTD/RS/bucket PN		2.5	3.4/3.6
						/01 /02 /03	LBC LBC MUC	54 54		

Station	Date	Time (GMT)	Latitude ° N	Longitude ° E	Depth (m)	Gear No.	Activity	Recovery (cm)	Air Temp. (°C)	Water Temp. (°C) (ship/sample)
BP00-13	09.09.2000	12:38	72°56.018'	80°33.232'	13	/04	MUC EBS	54		
BP00-14	09.09.2000	17:48	72°55.853'	79°47.381'	19.2	/01 /02 /03 /04	LBC MUC GC 500 GC 500	51 45 243 256	2.1	5.2/4.7
BP00-15	10.09.2000	8:05	72°2.992'	81°36.157'	5.8		CTD/RS/bucket PN LBC LBC		4.0	6.7/7.3
BP00-16	10.09.2000	13:36	71°49.903'	82°36.991'	26	/01 /02 /03 /04	CTD/RS/bucket PN/LVS LBC LBC MUC MUC EBS		4.3	7.2/8.4
						/05 /06	GC 500 GC 500	369 438		

Station	Date	Time (GMT)	Latitude ° N	Longitude ° E	Depth (m)	Gear No.	Activity	Recovery (cm)	Air Temp. (°C)	Water Temp. (°C) (ship/sample)
BP00-17	11.09.2000	11:27	71°6.506'	83°5.533'	18		CTD/ RS/bucket PN/LVS		4.4	9.5/10.9
						/01	LBC	30		
						/02	MUC	20		
						/03	MUC	23		
							BD			
BP00-18	11.09.2000	17:37	70°44.023'	83°31.292'	15		CTD/ RS/bucket		4.1	10.6/10.3
BP00-19	12.09.2000	4:36	69°58.856'	83°27.192'	22		CTD/ RS/bucket LVS, PN		3.9	11.1/12.2
						/01	LBC	?		
BP00-20	12.09.2000	16:09	71°2.406'	83°11.786'	20		CTD/ RS/bucket		2.8	11.4/9.8
BP00-21	13.09.2000	6:48	71°41.489'	83°29.291'	24		CTD/ RS/bucket EBS		1.4	7.7/7.2
BP00-22	13.09.2000	17:36	72°33.990'	79°54.927'	11		CTD/ RS/bucket		3	6.4/6.4
						/01	LBC	41		
						/02	LBC	33		
						/03	MUC	30		
						/04	GC 500	438		
						/05	GC 500	436		
							EBS			

Station	Date	Time (GMT)	Latitude ° N	Longitude ° E	Depth (m)	Gear No.	Activity	Recovery (cm)	Air Temp. (°C)	Water Temp. (°C)
BP00-23	14.09.2000	4:36	73°28.542'	79°51.348'	33		CTD/RS/bucket PN/LVS		-1.6	(ship/sample) 2.3/0.6
						/01	LBC			
						/02	LBC	31/36		
						/03	LBC			
						/04	MUC	25-30		
						/05	MUC			
						/06	GC 500	417		
						/07	GC500	427		
							BD/EBS			
BP00-24	14.09.2000	14:01	74°0.505'	79°59.945'	31		CTD/RS/bucket PN/LVS		-0.6	1.7/1.4
BP00-24a	14.09.2000	13:32	74°0.275'	80°0.450'			ST-Deployment			
BP00-25	14.09.2000	14:01	74°30.324'	80°31.656'	59	/01	GC 800	332	-1.2	1.3/-
BP00-26	15.09.2000	7:20	75°42.512'	77°57.589'	68		CTD/RS/bucket PN/LVS		2.3	2.9/4.2
						/01	LBC	49		
						/02	LBC	42		
						/03	MUC	35		
						/04	GC 500	396		
							EBS			
							BD			

Station	Date	Time (GMT)	Latitude ° N	Longitude ° E	Depth (m)	Gear No.	Activity	Recovery (cm)	Air Temp. (°C)	Water Temp. (°C)
BP00-27	15.09.2000	15:28	76°18.045'	78°55.977'	78		CTD/RS/bucket		1.7	(ship/sample) 2.8/2.5
							PNLVS			
							MUC	35		
							MUC	25		
						/03	GC 800	670		
BP00-28	16.09.2000	3:40	76°39.33	83°52.61'	50		CTD/RS/bucket		1.8	1.3/1.8
							PNLVS			
							MUC	20		
							LBC	25		
							LBC			
						/04	LBC			
						/05	GC500	121		
							EBS			
BP00-29	16.09.2000	11:14	76°56.172'	85°45.793'	68		CTD/RS/bucket		2.2	1.6/1.9
							PNLVS			
							LBC	36		
							MUC	20		
						/03	MUC			
						/04	GC 500	329		
							EBS/BD			
BP00-30	17.09.2000	8:45	75°59.188'	89°2.174'	52		CTD/RS/bucket		1.7	0.9/1.2
							PNLVS			
						/01	LBC			

Station	Date	Time (GMT)	Latitude ° N	Longitude ° E	Depth (m)	Gear No.	Activity	Recovery (cm)	Air Temp. (°C)	Water Temp. (°C) (ship/sample)
BP00-30	17.09.2000	8:45	75°59.188'	83°2.174'	52	/02	LBC	35		
						/03	GC 800	732		
							BD			
BP00-31	17.09.2000	17:12	75°27.737'	82°32.817'	43		bucket		1.4	0.1/0.7
						/01	LBC			
						/02	LBC	40		
BP00-32	18.09.2000	5:01	75°15.392'	84°20.568'	32	/01	GC 800	574	0	0/-0.2
BP00-33	18.09.2000	6:05	75°16.760'	84°13.013'	22	/01	GC 300	53	-0.4	0
BP00-34	18.09.2000	7:11	75°17.638'	84°8.728'	39	/01	GC 500	452	-0.4	0.1/ -
BP00-35	18.09.2000	9:43	75°20.827'	83°48.086'	46		CTD/ RS/bucket		-0.5	0.2/0.8
							PN/LVS			
						/01	LBC	40		
						/02	LBC	38		
						/03	MUC	40		
						/04	MUC	40		
						/05	GC 500	261		
/06	GC 500	258								
						EBS				

Station List

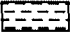





Station	Date	Time (GMT)	Latitude ° N	Longitude ° E	Depth (m)	Gear	Activity	Recovery (cm)	Air Temp. (°C)	Water Temp. (°C)	(ship/sample)
BP00-36	19.09.2000	3:35	76°57.707'	81°57.79'	66		CTD/RS/bucket		-2.6		2.3/2.2
							PN/LVS				
							GC 800	574			
							GC 800	573			
							GC 800	587			
							GC 800	563			
							LBC	33			
							LBC				
							LBC				
							LBC				
							MUC	20			
							MUC	20			
							EBS				
BP00-37	19.09.2000	12:16	76°58.007'	82°12.291'	63		GC 800	433	-2.6		2.7/
							LBC				
							LBC				
BP00-38	20.09.2000	10:41	73°11.807'	73°14.308'	20		bucket		-0.3		4.4/2.5
							LBC	54			
							GC 800	652			
BP00-39	20.09.2000	13:42	73°11.423'	73°29.188'	14		GC 800	128	-0.3		4.1/
BP00-40	20.09.2000	19:58	72°9.994'	73°34.832'	9		bucket		0.2		5.2/3
							LVS				

9.2




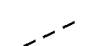
Geological Core Descriptions

Legend:

Lithology

-  clay
-  silty clay
-  sandy silty clay
-  sand
-  sandy clay
-  clayey sand

Structure

-  bioturbation
-  sharp boundary
-  gradational boundary
-  transition zone

BP00-02/4 (SL-5)

Southern Kara Sea

Boris Petrov 2000

Recovery: 0.68 m

75° 24.1' N, 74° 11.8' E

Water depth: 50 m

Depth in core (m)	Lithology	Texture Color		Description	Age
0		5Y 4/2		0 - 6 cm: olive gray (5Y 4/2) silty clay (3-5 cm brown, 10YR 4/3 lense) 6 - 22 cm: very dark gray (5Y 3/1) to black (5Y 2.5/1) silty clay, bioturbated 22 - 30 cm: very dark gray (5Y 3/1) and dark olive gray (5Y 3/2) silty clay, strongly bioturbated 30 - 68 cm: olive gray (5Y 4/2) silty clay with thin sandy laminae	
		5Y 3/1 to 2.5/1			
		5Y 3/1			
		5Y 4/2			
1					
2					
3					
4					
5					

Core description

BP00-05/6 (SL-5)

Southern Kara Sea

Boris Petrov 2000

Recovery: 0.34 m

75° 50.2' N, 81° 00.3' E

Water depth: 50 m

Lithology	Texture Color	Description	Age
0	5Y 3/2	0 - 1 cm: very dark grayish brown (2.5Y 3/2) silty (sandy) clay	
	5Y 3/2	1 - 8 cm: dark olive gray (5Y 3/2) silty clay, bioturbated polychaete tube at 6 - 8 cm	
	5Y 3/1-3/2	8 - 30 cm: dark olive gray (5Y 3/2) clayey silty sand	
		30 - 34 cm: dark olive gray (5Y 3/2) and very dark gray (5Y 3/1) clayey silty sand, bioturbated; small shell fragment at 31 cm	
1			
2			
3			
4			
5			

Core description

BP00-06/1 (SL-5)

Southern Kara Sea

Boris Petrov 2000

Recovery: 2.88 m

75° 10.1' N, 80° 59.7' E

Water depth: 38 m

Lithology	Texture Color	Description	Age
	<p>5Y 3/1 and 5Y 4/2</p> <p>2.5Y 3/2</p> <p>5Y 3/2</p> <p>5Y 3/1 to 3/2</p> <p>2.5Y 3/2</p>	<p>0-54 cm: very dark gray (5Y 3/1) and olive gray (5Y 4/2) silty clay; black spots, moderately bioturbated</p> <p>54-88 cm: very dark grayish brown (2.5Y 3/2) silty clay (at 60 and 67-69 cm olive gray lenses) thin sandy laminae</p> <p>88-188 cm: dark olive gray (5Y 3/2) silty clay; abundant thin more sandy laminae; at 92-94 and 129-132 cm large light crystals (pseudomorphs after ikaite?)</p> <p>188-220cm: dark olive gray (5Y 3/2) silty clay, occasionally more sandy; slightly bioturbated</p> <p>220-235cm: dark olive gray (5Y 3/2) to very dark gray (5Y 3/1) silty clay, bioturbated</p> <p>235-288cm: very dark grayish brown (2.5Y 3/2) silty clay, abundant more sandy layers</p> <p>shell debris at 6, 23, and 35 cm</p>	

Core description

BP00-07/6 (SL-8)

Southern Kara Sea

Boris Petrov 2000

Recovery: 6.65 m

74° 39,5' N, 81° 08,5' E

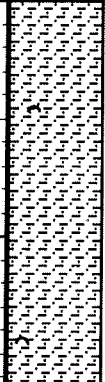

Water depth: 38 m

Lithology	Texture Color	Description	Age	
		0-3 cm: dark olive gray (5Y 3/2), homogenous, silty clay 3-65 cm: Dark olive gray, silty clay, bioturbated below 25 cm, occasionally to abundant black spots, black color dominates at 25-32 cm, few single more coarse-grained layers (1 mm thickness) at 8-12 cm 65-365 cm: Dark gray to dark olive gray, silty clay, moderately to strongly bioturbated (burrows preserved at 253-260 cm), abundant black spots, increasing downwards, black color (5y 2.5/1) dominates at 110-122, 195-198, 207-210, 225-235, 253-260, 287-289, and 289-291 cm, 365-500 cm: Very dark gray to black, (silty) clay, moderately to strongly bioturbated, black color dominates at 367-369, 378-383, 388-395, 411-417, 429-440, 454-465, 465-467, 474-482, and 494-498 cm 500-665 cm: Very dark gray to black, (silty) clay, moderately to strongly bioturbated, black color dominates at 503-514, 520-522, 526-542, 558-565, 565-570, 574-578, 582-587, 595-600, 605-608, 610-614, 620-622, 627-632, 645-653, and 660-665 cm, Bivalves at 237, 270, 544, and 644cm		
		5Y3/2		
		5Y 3/1 to 5Y 3/2		
		5Y 2.5/1 to 5Y 3/1		

BP00-07/6 (SL-8)

cont.

Boris Petrov 2000

	Lithology	Texture	Color	Description	Age
5			5Y 2.5/1 to 5Y3/1		
6					
7					
8					
9					
10					

BP00-07/7 (SL-8)

Southern Kara Sea

Boris Petrov 2000

Recovery: 7.23 m

74° 39,5' N, 81° 08,5' E

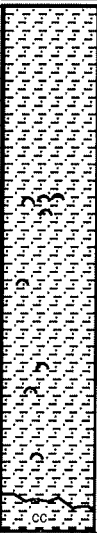
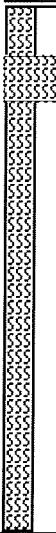
Water depth: 38 m

Lithology	Texture Color	Description	Age
	5Y 3/2	0-190cm: dark olive gray (5Y 3/2) silty clay (0-1 partly brown), black spots throughout, bioturbated 190-206cm: black (5Y 2.5/1) silty clay 206-223cm: dark olive gray (5Y 3/2) to very dark gray (5Y 3/1) silty clay,	
	5Y 2.5/1	black spots throughout, bioturbated 223-723cm: dark olive gray (5Y 3/2), very dark gray (5Y 3/1) and black	
	5Y 3/1 to 5Y 3/2	(5Y 2.5/1) silty clay, bioturbated Bivalves at 0-3 (plus two large gastropodes), 31, 125, 135, 254, 325, 335, 461, 581 (abundant), 586, 628, 652, 663, and 690cm	
	5Y 3/2 to 5Y 3/1 to 5Y 2.5/1		

BP00-07/6 (SL-8)

cont.

Boris Petrov 2000

	Lithology	Texture	Color	Description	Age
5			5Y 2.5/1 to 5Y 3/1 to 5Y 3/2		
6					
7					
8					
9					
10					

BP00-08/4 (SL-5)

Southern Kara Sea

Boris Petrov 2000

Recovery: 1.91 m

74° 39.6' N, 82° 38.6' E

Water depth: 41 m

Lithology	Texture Color	Description	Age
	5Y 4/2	0-1cm: olive brown (2.5Y 4/4) silty clay	
	5Y 3/2	1-9cm: olive gray (5Y 4/2) silty clay; pebble (quartz, 1cm diameter) at 7-8 cm	
	5Y 3/1	9-46cm: dark olive gray (5Y 3/2) silty clay, black spots, bioturbated	
	5Y 3/2	46-70cm: very dark gray (5Y 3/1) silty clay, moderately to strongly bioturbated	
	5Y 3/1	70-76cm: dark olive gray (5Y 3/2) silty clay, bioturbated	
	5Y 3/1	76-91cm: very dark gray (5Y 3/1) silty clay, bioturbated	
		91-191cm: dark olive gray (5Y 3/2) to very dark gray (5Y 3/1) silty clay, bioturbated	
		Bivalves at 12 and 80cm	
	5Y 3/2 to 5Y 3/1		
2			
3			
4			
5			

Core description

BP00-11/1 (SL-8)

Southern Kara Sea

Boris Petrov 2000

Recovery: 3.22 m

74° 17.5' N, 81° 47.1' E

Water depth: 42 m

Lithology	Texture	Color	Description	Age
		5Y 4/2	0-7cm: olive gray (5Y 4/2) silty clay 7-36cm: dark olive gray (5Y 3/2) to very dark gray (5Y 3/1) silty clay to silty sandy clay; polychaete tube at 18cm 36-43cm: dark olive gray (5Y 3/2) to very dark gray (5Y 3/1) silty clay 43-47cm: dark olive gray (5Y 3/2) to very dark gray (5Y 3/1) silty sandy clay 47-52cm: dark olive gray (5Y 3/2) to very dark gray (5Y 3/1) silty clay 52-70cm: dark olive gray (5Y 3/2) to very dark gray (5Y 3/1) silty sandy clay 70-88cm: dark olive gray (5Y 3/2) to very dark gray (5Y 3/1) silty clay polychaete tube at 69-73cm 88-122 cm: dark olive gray (5Y 3/2) to very dark gray (5Y 3/1) silty sandy clay 122-222cm: dark olive gray (5Y 3/2) to very dark gray (5Y 3/1) silty sandy clay to clayey silty sand	
		5Y 3/2 to 5Y 3/1	Bivalves at 18, 82, 104, 151, 184, 192, 205, 227, 240, 258, 289, 306, and 317cm	

BP00-14/3 (SL-5)

Yenisei Estuary

Boris Petrov 2000

Recovery: 2.43 m

72° 55.8' N, 79° 47.4' E

Water depth: 19 m

Lithology	Texture Color	Description	Age
	<p>2.5Y 4/2</p> <p>5Y 4/2 to 5Y 3/2</p> <p>5Y 4/2 to 5Y 3/2 to 5Y 3/1</p>	<p>0-4cm: dark grayish brown (2.5Y 4/2) silty clay, bioturbated</p> <p>4-43cm: olive gray (5Y 4/2) to dark olive gray (5Y 3/2) silty clay, bioturbated; worm tubes at 24 and 35cm</p> <p>43-213cm: dark olive gray (5Y 3/2) to very dark gray (5Y 3/1) silty clay, black spots, bioturbated; at 206-207cm more sandy horizon</p> <p>213-235cm: very dark gray (5Y 3/1) silty sandy clay</p> <p>235-243cm: void</p> <p>Bivalves at 56, 68, 183, and 223cm</p>	
<p>void</p>			

Core description

BP00-14/4 (SL-5)

Yenisei Estuary

Boris Petrov 2000

Recovery: 2.56 m

72° 55.8' N, 79° 47.4' E

Water depth: 19 m

Lithology	Texture Color	Description	Age
	2.5Y 3/2 5Y 4/2 to 5Y 3/2	0-3 cm: Very dark grayish brown (2.5Y 3/2), homogenous, silty clay 3-20 cm: Olive gray (5Y 4/2) to dark olive gray (5Y 3/2), silty clay, darker, more coarse grained, thin laminae 20-230 cm: Olive gray (5Y 4/2) to dark olive gray (5Y 3/2) to very dark gray (5Y 3/1) silty clay with occasionally silty laminae between 25 and 65 cm, moderately to strongly bioturbated, black spots, increasing below 125 cm, black color dominates between 156-198 and 215-230 cm, 230 cm - bottom: Olive gray (5Y 4/2) silty sandy clay with sand lense at 230-232 cm, last 5 cm = core catcher	
	5Y 4/2 to 5Y 3/2 to 5Y 3/1	Bivalves at 99, 205, 218 and 240 cm	
	5Y 4/2		

BP00-15/5 (SL-5)

Yenisei Estuary

Boris Petrov 2000

Recovery: 3.69 m

72° 03.0' N, 81° 36.2' E

Water depth: 6m

Lithology	Texture Color	Description	Age
	2.5Y 4/2 2.5Y 3/2	0-10 cm: dark grayish brown (2.5Y 4/2) sandy silty clay 10-14 cm: very dark grayish brown (2.5Y 3/2) sandy silty clay 14-369 cm: alternation of very dark grayish brown (2.5Y 3/2) and very dark gray (5Y 3/1) sandy silty clay; some bioturbation more sandy at 134-135, 152-160, 166-167, 184-187, and below 300 cm; at 274 cm large piece of wood (6 cm long); at 290 cm hard horizon (lithified?)	
	2.5Y 3/2 and 5Y 3/1		

Core description

BP00-15/6 (SL-5)

Yenisei Estuary

Boris Petrov 2000

Recovery: 4.38 m

72° 03.0' N, 81° 36.2' E

Water depth: 6m

Lithology	Texture	Color	Description	Age
0	[Lithology pattern]	2.5Y 4/2 and 5Y 3/1	0-23 cm: Very dark grayish brown (at 0-2, 5-9, and 11-19 cm), alternating with olive gray (at 2-5, 9-11, and 19-23 cm), sandy clayey silt, sandy layers at 5-9 and 19-23 cm, sandy lense at 13 cm	
		5Y 3/1 and 5Y 2.5/1	23-44 cm: Alternation of olive gray and very dark gray, clayey sandy silt and silty sand layers, interval of black, clayey silt at 35-38 cm	
1	[Lithology pattern]		44-250 cm: Alternation of black and dark olive gray intervals, dominantly sandy clayey silt with single thin, more sandy layers, moderately bioturbated, olive gray (5Y 4/2) interval at 112-115 cm with sharp contact to dark gray (5Y 4/1) layer at 115-121 cm	
			250-263 cm: Black, clayey sandy silt 263-274 cm: Olive gray, clayey silt 274-438 cm: Black, clayey sandy silt, occasionally thin more sandy layers, amount of sand increases downward, moderately bioturbated, thin dark olive gray (5Y 3/2) interval at 399-403 cm in contact to thin black (5Y 2.5/1) interval at 403-410 cm	
2	[Lithology pattern]	5Y 2.5/2 and 5Y 3/2		
3	[Lithology pattern]	5Y 2.5/2		
		5Y 4/2		
4	[Lithology pattern]	5Y 2.5/2		
5	[Lithology pattern]			

BP2000-22/4 (SL-5)

Yenisei Estuary

Boris Petrov 2000

Recovery: 4.38 m

72° 34.0' N, 79° 54.9' E

Water depth: 11 m

Lithology	Texture	Color	Description	Age
		10YR 3/2 5Y 3/1	0-2 cm: Very dark grayish brown, silty clay	
		5Y 4/2	2-17 cm: Very dark gray, silty clay, some black laminae	
		to 5Y 3/2	17-38 cm: Olive gray to dark olive gray, silty clay, moderately to strongly bioturbated (increasing downward)	
		5Y 4/2	38-51 cm: Olive gray, silty clay, some darker clouds	
			17-238 cm: Olive gray and dark olive gray to black, silty clay, black color dominates at 50-70, 95-97, 129-146, 164-166, and 185-190 cm, moderately to strongly bioturbated (bioturbation maxima at 85-92, 110-112, and 150-165 cm)	
			238-265 cm: Dark olive gray to black, silty clay, strongly bioturbated	
		5Y 4/2 to 5Y 3/2	265-268 cm olive gray interval (sharp contacts) 268-338 cm: Dark olive gray to black and olive gray, silty clay, strongly bioturbated, black spots	
			338-410 cm: Dark olive to very dark gray and dark olive gray, silty clay, strongly bioturbated, black spots throughout	
			410-438 cm: Olive gray to dark gray, sandy clayey silt, sand content increases towards the bottom	
			5Y 3/1 to 5Y 3/2 5Y 4/2	
		5Y 3/2 to 5Y 4/2		
		5Y 3/2 to 5Y 3/1		
		5Y 4/2 to 5Y 4/1		

Core description

BP2000-22/5 (SL-5)

Yenisei Estuary

Boris Petrov 2000

Recovery: 4.36 m

72° 34.0' N, 79° 54.9' E

Water depth: 11 m

Lithology	Texture Color	Description	Age
	<p>2.5Y 3/2 to 5Y 3/1</p> <p>5Y 3/2</p>	<p>0-1 cm: dark brown (10YR 3/3) silty clay</p> <p>1-297cm: very dark grayish brown (2.5Y 3/2) to very dark gray (5Y 3/1) silty clay bioturbated (maximum bioturbation at 78-100 cm) sharp boundary at 296-300 cm</p> <p>297-436cm: dark olive gray (5Y 3/2) sandy silty clay, black spots in the upper part</p>	

BP00-23/6 (SL-5)

Yenisei Estuary

Boris Petrov 2000

Recovery: 4.17 m

73° 28.5' N, 79° 51.3' E

Water depth: 33 m

Lithology	Texture	Color	Description	Age
		<p>5Y 3/2 to 5Y 4/2</p> <p>5Y 4/2 to 5Y 3/2 to 5Y 3/1</p> <p>5Y 3/2 to 5Y 3/1</p> <p>5Y 3/2</p>	<p>0-17 cm: olive gray (5Y 4/2) to dark olive gray (5Y 3/2) silty clay</p> <p>17-117 cm: olive gray (5Y 4/2) to dark olive gray (5Y 3/2) to very dark gray (5Y 3/1) silty clay; black spots, bioturbated</p> <p>117-340 cm: dark olive gray (5Y 3/2) to very dark gray (5Y 3/1) silty clay; black spots, bioturbated</p> <p>340-417 cm: alternation of dark olive gray (5Y 3/2) sandy silty clay and silty clayey sand (increasing sand content towards the bottom) at 369-370 cm large piece of wood (5 cm in length), at 397 cm small piece of wood</p> <p>Bivalves at 37, 44, 73, 88, 102, 107, 113.5, 133, 137, 143, 181, and 263 cm</p>	

BP00-23/7 (SL-5)

Yenisei Estuary

Boris Petrov 2000

Recovery: 4.27 m

73° 28.5' N, 79° 51.3' E

Water depth: 33 m

Lithology	Texture	Color	Description	Age
0	[diagonal lines]	5Y 3/2 to 5Y 4/2	0-25 cm: Dark olive gray to olive gray, silty clay 2 pieces of wood at 1-3 cm	
		5Y 3/2 to 5Y 2.5/1	25-53 cm: Black and dark olive gray, silty clay, black spots throughout, black color dominates at 40-43 cm, partly bioturbated	
1	[diagonal lines]	5Y 4/2 to 5Y 3/1	53-127 cm: Olive gray, dark olive gray to black, silty clay common to abundant black spots, moderately bioturbated 127-374 cm: Dark olive gray to black, silty clay, black intervals (2-4 cm thick) between 144-159, and 183-192 cm, moderately to (in the lower part) strongly bioturbated 374-427 cm: Olive gray, sandy clayey silt, thin more sandy layers throughout, material from core catcher below 414 cm	
			Shell debris (bivalve) at 24, 88, and 120 cm	
2	[diagonal lines]		void	
3	[diagonal lines]	5Y 3/2 to 5Y 2.5/1		
4	[diagonal lines]	5Y 4/2		
5				

BP00-25/1 (SL-8)

Southern Kara Sea

Boris Petrov 2000

Recovery: 3.32 m

74° 30.3' N, 80° 31.7' E

Water depth: 59 m

Lithology	Texture Color	Description	Age
	<p>5Y 3/2</p> <p>5Y 3/2 to 5Y 3/1</p>	<p>0-32 cm: dark olive gray (5Y 3/2) silty clay; below 13 cm black spots, bioturbated; 3 large manganese nodules near the sediment surface</p> <p>32-100 cm: dark olive gray (5Y 3/2) silty clay; more sandy intervals at 32-34, 40-41, 52-53, 69-71, 75-76, 80-82, and 86-88 cm; some bioturbation</p> <p>100-332 cm: alternation of dark olive gray (5Y 3/2) to very dark gray (5Y 3/1) silty clay and clayey silty sand (increasing sand content towards the bottom); large black clay-/siltstone at 109-111 cm (7 cm in length), small one at 122 cm</p> <p>Bivalves at 70 ("Schillhorizont"), 73, 77, 88, 114, 116, and 122 cm (occurrence of bivalves related to more sandy intervals)</p> <p>220-232 (= lowermost part of section) liner not totally filled with sediment; --> reduced mag. susceptibility values ?</p>	

BP00-26/4 (SL-5)


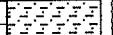
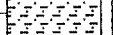
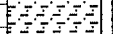
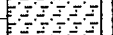
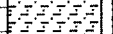
Southern Kara Sea

Boris Petrov 2000

Recovery: 3.96 m

75° 42.5' N, 77° 57.6' E

Water depth: 68 m

Depth in core (m)	Lithology	Texture Color	Description	Age
0			0-1 cm: dark brown (10YR 3/3) silty clay	
1		5Y 3/2	1-250 cm: dark olive gray (5Y 3/2) silty clay; black spots, bioturbated	
2			250-296 cm: alternation of dark olive gray (5Y 3/2) silty clay and clayey silty sand (increased sand content 250-280 cm)	
3			296-396 cm: dark olive gray (5Y 3/2) clayey silty sand	
4			Bivalves at 128, 173-174 (4 cm diameter), 187, 257 (debris), 276 (debris), 300-302, 325-330 ("Schillhorizont"), 341, 349, 356-358, and 375-376 cm ("Schillhorizont")	
5				

Core description

BP00-28/4 (SL-5)

Southern Kara Sea

Boris Petrov 2000

Recovery: 1.21 m

76° 39.3' N, 83° 52.6' E

Water depth: 50 m

Lithology	Texture	Color	Description	Age
		5Y 3/2	0-1 cm: dark brown (10YR 3/3) silty clay, bioturbated 1-5 cm: dark olive gray (5Y 3/2) silty clay, bioturbated 5-23 cm: dark olive gray (5Y 3/2) silty sandy clay 23-115 cm: dark olive gray (5Y 3/2) to very dark gray (5Y 3/1) silty clay, black spots, bioturbated; at 114-115 pebble (2 cm in diameter)	
		5Y 3/2 to 5Y 3/1	115-121 cm: dark olive gray (5Y 3/2) clayey silty sand Bivalves at 15, 44, 107, and 118 cm	
		5Y 3/2		
2				
3				
4				
5				

Core description

BP00-29/4 (SL-5)

Southern Kara Sea

Boris Petrov 2000

Recovery: 3.29 m

76° 56.2' N, 85° 45.8' E

Water depth: 68 m

Lithology	Texture Color	Description	Age
	5Y 3/2 5Y 3/2 to 5Y 3/1	<p>0-5 cm: dark olive gray (5Y 3/2) (sandy) silty clay, bioturbated</p> <p>5-23 cm: dark olive gray (5Y 3/2) to very dark gray (5Y 3/1) silty sandy clay; at 21 cm brown nodule</p> <p>23-29 cm: dark olive gray (5Y 3/2) to very dark gray (5Y 3/1) (sandy) silty clay</p> <p>29-84 cm: dark olive gray (5Y 3/2) to very dark gray (5Y 3/1) silty sandy clay to silty clayey sand (more sandy intervals at 47-53 and 59-60 cm)</p> <p>84-305 cm: dark olive gray (5Y 3/2) to very dark gray (5Y 3/1) (sandy) silty clay, bioturbated; at 200-205 cm and 258-260 cm light carbonate minerals (pseudomorphs after ikaite?)</p> <p>305-329 cm: dark olive gray (5Y 3/2) to very dark gray (5Y 3/1) silty sandy clay to silty clayey sand</p> <p>Bivalves at 65, 69.5, 72, 80-85, 88, 104, 121, 124, 138, 145.5, 150, 161, 162, 166, 306-307, and 313.5 cm</p>	

Core description

BP00-30/3 (SL-8)

Southern Kara Sea

Boris Petrov 2000

Recovery: 7.32 m

75° 59.2' N, 83° 02.2' E

Water depth: 52 m

Lithology	Texture Color	Description	Age
	<p>5Y 2.5/1 to 5Y 3/1 (to 5Y 3/2)</p> <p>5Y 3/1 to 5Y 3/2</p> <p>5Y 2.5/1 to 5Y 3/1 (to 5Y 3/2)</p>	<p>0-294 cm: dark olive gray (5Y 3/2) to very dark gray (5Y 3/1) to black (5Y 2.5/1)</p> <p>silty clay; bioturbated, black spots</p> <p>294-392 cm: dark olive gray (5Y 3/2) to very dark gray (5Y 3/1) silty clay,</p> <p>strongly bioturbated;</p> <p>at 317 cm black rounded pebble (1.5 cm in diameter);</p> <p>at 388-389 and 391 cm light nodules (carbonate mineral,</p> <p>pseudomorphs after ikaite?)</p> <p>392-631 cm: dark olive gray (5Y 3/2) to very dark gray (5Y 3/1) to black (5Y 2.5/1)</p> <p>silty clay; bioturbated</p> <p>631-639 cm: dark olive gray (5Y 3/2) silty clayey sand</p> <p>639-730 cm: dark olive gray (5Y 3/2) to very dark gray (5Y 3/1) to black (5Y 2.5/1)</p> <p>silty clay; bioturbated</p> <p>Bivalves at 67, 94, 104, 118.5, 125, 136, 140.5, 145, 153, 221, 536, 595, 627.5, and 651 cm</p>	

BP00-30/3 (SL-8)

cont.

Boris Petrov 2000

	Lithology	Texture	Color	Description	Age
5			5Y 2.5/1 to 5Y3/1 (to 5Y 3/2)		
6			5Y 3/2		
7			5Y 2.5/1 to 5Y3/1 (to 5Y 3/2)		
8					
9					
10					

Core description

BP00-32/1 (SL-8)

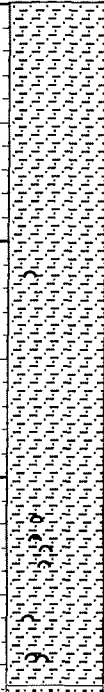
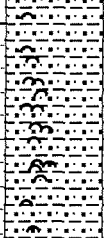
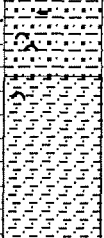



Southern Kara Sea

Boris Petrov 2000

Recovery: 5.74 m

75° 15.4' N, 84° 20.6' E

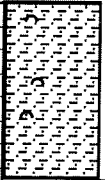

Water depth: 32 m

	Lithology	Texture Color	Description	Age
0			0-289 cm: dark olive gray (5Y 3/2) to very dark gray (5Y 3/1) to black (5Y 2.5/1) silty clay; bioturbated, black spots 289-374 cm: dark olive gray (5Y 3/2) to very dark gray (5Y 3/1) sandy silty clay, bioturbated; 374-424 cm: dark olive gray (5Y 3/2) sandy silty clay, bioturbated; 5Y 2.5/1 to 5Y 3/1 (to 5Y 3/2) at 397-398 cm pebble (2 cm in diameter) 424-574 cm: dark olive gray (5Y 3/2) to very dark gray (5Y 3/1) silty clay, bioturbated Bivalves at 114, 218, 226, 231, 238, 261, 276, 277, 298, 312, 317, 326, 327, 331, 337, 338, 346, 348, 350, 359, 361, 362, 367, 377, 388.5, 407.5, 412, 432, 506, 533, and 547 cm	
1				
2				
3		5Y 3/1 to 5Y 3/2		
4		5Y 3/2		
5		5Y 3/1 to 5Y 3/2		

BP00-32/1 (SL-8)

cont.

Boris Petrov 2000

5	Lithology	Texture	Color	Description	Age
5			5Y 3/1 to 5Y 3/2		
6					
10					

Core description

BP00-33/1 (SL-3)

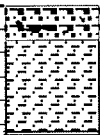
Southern Kara Sea

Boris Petrov 2000

Recovery: 0.53 m

75° 16.7' N, 84° 13.0' E

Water depth: 22 m

Depth in core (m)	Lithology	Texture Color		Description	Age
0		5Y 3/2		0-2 cm: dark brown (10YR 3/3) sand 2-13 cm: dark olive gray (5Y 3/2) silty sand with large not-rounded pebbles 13-53 cm: dark gray (5Y 4/1) (stiff) clay, thin olive gray (5Y 4/2) silty laminae, especially between 34 and 44 cm	
1		5Y 4/2 and 5Y 4/1			
2					
3					
4					
5					

Core description

BP00-34/1 (SL-5)

Southern Kara Sea

Boris Petrov 2000

Recovery: 4.52 m

75° 17.6' N, 84° 08.7' E

Water depth: 39 m

	Lithology	Texture Color	Description	Age
0 1 2 3 4 5 Depth in core (m)		5Y 3/2 to 5Y 3/1	<p>0-1 cm: dark brown (10YR 3/3) silty clay, bioturbated</p> <p>1-35cm: dark olive gray (5Y 3/2) to very dark gray (5Y 3/1) silty clay</p> <p>35-452 cm: dark olive gray (5Y 3/2) to very dark gray (5Y 3/1) (sandy) silty clay; black spots, bioturbated; more sandy intervals (silty sandy clay to silty clayey sand) at 256-258, 296-299, 306-310, 317-318, 321-322, 330-331, 369-371, 380-390, 395-404, 406-409, 411-416, and below 430 cm</p> <p>Bivalves at 44.5, 46.5, 61, 68.5, 81, 98, 103, 105, 107, 112, 115, 123.5, 127.5, 131, 135, 136, 141, 155.5, 168, 198, 207, 215, 222, 231, 243, 254, 258, 265, 270, 271.5, 275, 284.5, 292, 300, 304.5, 306, 310, 332, and 342 cm</p>	

BP2000-35/5 (SL-5)

Southern Kara Sea

Boris Petrov 2000

Recovery: 2.61 m

75° 20.8' N, 83° 48.1' E

Water depth: 46 m

	Lithology	Texture Color	Description	Age
0		2.5Y 4/4	0-3 cm: Olive brown, silty clay	
		5Y 4/2	3-27 cm: Olive gray, silty clay, olive brown (2.5Y 4/4) at 11-12 cm, thin black laminae between 3-6 cm	
			27-261 cm: Olive gray to dark olive gray and black, silty clay, black spots and laminae throughout, black color dominates at 75-78, 103-105, 136-148, 211-223, and 254-261 cm slightly to moderately bioturbated	
1				

Core description

BP00-35/6 (SL-5)

Southern Kara Sea

Boris Petrov 2000

Recovery: 2.58 m

75° 20.8' N, 83° 48.1' E

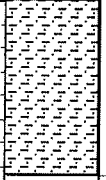

Water depth: 46 m

Lithology	Texture Color	Description	Age
	<p>5Y 3/2 to 5Y 3/1 to 5Y 2.5/1</p>	<p>0-1 cm: olive brown (2.5Y 4/4) silty clay 1-258 cm: dark olive gray (5Y 3/2) to very dark gray (5Y 3/1) to black (5Y 2.5/1) silty clay; black spots, bioturbated</p> <p>Bivalves at 15, 20, 63, 82.5, 125, 127.5, 130-133 ("Schillhorizont"), 145, 146, 171, 187, 203, 205.5, 218, 236, 237, 243, and 246 cm</p>	

BP00-36/1 (SL-8)

cont.

Boris Petrov 2000

Lithology	Texture	Color	Description	Age
		5Y 4/1 to 5Y 3/1		

Depth in core (m)

5

6

7

8

9

10

Core description

BP00-36/4 (SL-8)


Southern Kara Sea

Boris Petrov 2000

Recovery: 5.63 m

76° 57.7' N, 81° 57.8' E

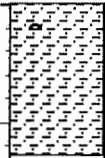

Water depth: 66 m

Depth in core (m)	Lithology	Texture Color	Description	Age
0		5Y 3/1 to 5Y 2.5/1	<p>0-1 cm: dark brown (10YR 4/3) silty clay</p> <p>1-563 cm: very dark gray (5Y 3/1) to black (5Y 2.5/1) silty clay,</p> <p>bioturbated</p> <p>Bivalves at 12.5, 23, 24.5, 27, 33, 42, 44, 59, 70, 73, 77, 82, 100, 120.5, 130, 131.5, 136, 139.5, 142.5, 150, 156.5, 159, 180, 187, 190, 197, 199, 212.5, 222, 240, 251, 261, 278.5, 297, 330, 365, 395.5, 397, 402, 408.5, and 509 cm</p>	
1				
2				
3				
4				
5				

BP00-36/4 (SL-8)

cont.

Boris Petrov 2000

	Lithology	Texture	Color	Description	Age
5			5Y 3/1 to 5Y 2.5/1		
6					
7					
8					
9					
10					

BP00-37/1 (SL-8)

Southern Kara Sea

Boris Petrov 2000

Recovery: 4.33 m

76° 58.0' N, 82° 12.3' E

Water depth: 63 m

Lithology	Texture Color	Description	Age
	<p>2.5Y 4/2</p> <p>5Y 4/1</p> <p>5y 4/1 to 5y 3/1</p> <p>5y 4/1</p> <p>5y 4/1</p>	<p>0-2 cm: dark grayish brown, (silty) clay</p> <p>2-248 cm: dark gray, (silty) clay, slightly bioturbated, concretions (lithified sediment, similar to the surrounding sediment) at 25-29, 38-39, 42-45, 60-69, and 166-169 cm lkaite at 109-111, 220, 225, and 228-232 cm</p> <p>248-346 cm: dark gray to black, (silty) clay black spots throughout, maximum between 248-284 slightly bioturbated</p> <p>346-375 cm: dark gray, (silty) clay</p> <p>375-433 cm: dark gray, (sandy) silty clay, common occurrence of sandy layers</p> <p>Bivalves/shell debris at 21, 125, 190, and 202 cm</p>	

Core description

BP00-38/2 (SL-8)

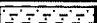
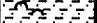
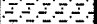
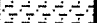
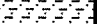
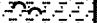
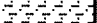
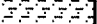
Ob Estuary

Boris Petrov 2000

Recovery: 6.52 m

73° 11.8' N, 73° 14.3' E

Water depth: 20 m

	Lithology	Texture Color	Description	Age
0			0-1 cm: dark brown (10YR 4/4) silty clay	
			1-630 cm: very dark gray (5Y 3/1) to black (5Y 2.5/1) silty clay, bioturbated; at 132 cm thin silty layer; at 351-352 cm silty sandy layer	
1			630-652 cm: very dark gray (5Y 3/1) sandy silty clay	
		5Y 3/1 to 5Y 2.5/1	Bivalves at 7, 10, 43.5, 45, 114, 160, 166.5, 179.5, 190, 213.5, 228, 250, 265, 287.5, 290, 296.5, 300, 309, 310, 321, 331, 349, 351, 355, 372, 381, 408-409, 457, 462, 481, 483, 495, 507, 510, 520, and 533 cm	
2				
3				
4				
5				

BP00-38/2 (SL-8)

cont.

Boris Petrov 2000

	Lithology	Texture	Color	Description	Age
5			5Y 3/1 to 5Y 2.5/1		
6					
7					
8					
9					
10					

Table 9-3: Summary of biological, geochemical, and geological studies performed at Russian and German institutes on water and sediment samples obtained during the "Akademik Boris Petrov" Kara Sea Expedition 2000.			
	Institute	Methods	Parameter
1. Water samples			
Sea (river) water	GEOKHI	Classical chemical analyses	Nutrients (PO ₄ , NO ₃ , NO ₂ , SiO ₂), alkalinity, pH, chlorinity
Sea water	GEOKHI	GC	Concentration and distribution of CH ₄ and C ₂ -C ₆ homologues
Dissolved organic matter	IFBM-AWI	HTC, HPLC, GC/MS, IRMS, CHN, NMR	DOC, DON; C, N; Amino acids, lignin phenols; structure
Carbon and silica cycle	IFBM	CN, HPLC, MS, Photometry	POC, PON, CaCO ₃ , Opal, aminoacids, carbohydrates; $\delta^{15}\text{N}$
Particulate organic matter	AWI	GC, GC/MS	Biomarkers (n-alkanes, fatty acids, sterols, hopanoids etc.)
Particulate organic matter	GEOKHI	CNS, MS	POC, PON; stable carbon and nitrogen isotopes
Particulate organic matter	GEOKHI	Radiochemistry	¹³⁷ Cs and other radionuclides
Geochemistry	GEOMAR	MS	Stable inorganic carbon and oxygen isotopes
Geochemistry	GEOKHI	MS	Stable inorganic carbon isotopes
Phytoplankton	GEOKHI	MS	Stable carbon and nitrogen isotopes
Phytoplankton	MMBI	Microscopy, statistical analysis	Abundances, species composition, community structure
Zooplankton	AWI	Microscopy, REM, statistical analysis	Abundances, biomass, species composition, community structure

	Institute	Methods	Parameter
2. Sediments			
Benthos ecology	AWI	Microscopy, statistical analysis	Abundances, biomass, species composition, community structure
Benthos	GEOKHI	Gamma-spectrometry	Total radioactivity
Sedimentology/Mineralogy	AWI	XRD	Bulk and clay mineralogy
Sedimentology/Mineralogy	IORAS	Microscopy	Heavy minerals; grain size
Organic geochemistry	AWI	CNS, Rock-Eval, GC, GC/MS; Microscopy	TOC, N, S; C/N, HI, OI; Biomarkers, $\delta^{13}C$ of biomarkers; Macerals
Organic geochemistry	IFBM	CN, HPLC, MS, Photometry	POC, PON, CaCO ₃ , Opal, aminoacids, carbohydrates; $\delta^{15}N$
Organic geochemistry	GEOKHI	CNS, Rock-Eval, GC, GC/MS	C, N, S; pyrolysis parameter; lignin; stable carbon and nitrogen isotopes
Hydrocarbon gases	GEOKHI	GC, GC/MS	Concentration and distribution of hydrocarbon gases; stable isotopes CH ₄
Pore-water chemistry	GEOKHI	classical chemistry analyses	Nutrients (PO ₄ , NO ₃ , NO ₂ , SiO ₂), alkalinity, pH, chlorinity
Radio-geochemistry	GEOKHI	Radiochemistry, gamma-spectrometry	¹³⁷ Cs, ⁹⁰ Sr, ²³⁹ Pu, ²⁴⁰ Pu, ²¹⁰ Pb
Radio-geochemistry	IGEM	Radiochemistry, gamma-spectrometry	¹³⁷ Cs, ⁹⁰ Sr, ²³⁹ Pu, ²⁴⁰ Pu, ²¹⁰ Pb
Micropaleontology	AWI	Microscopy	Palynomorphs, diatoms; pollen stratigraphy
Micropaleontology	IORAS	Microscopy	Benthic foraminifera
Geochemistry	GEOMAR	MS	Stable inorganic carbon and oxygen isotopes
Inorganic geochemistry	AWI	RFA	Major and minor elements
Inorganic geochemistry	GEOKHI	XRS	Heavy elements
Core logging	AWI	Multi-sensor core logging	Magnetic susceptibility, density, velocity
Dating of sediment cores	AWI	AMS ¹⁴ C	Chronology; flux rates
Sediment profiling	AWI	Sediment echograph, 3.5 khz profiling	sediment thickness, sediment structures

Research Participants

Name	Discipline	Institution
Stepanets, Oleg	Chief of Expedition	GEOKHI
Stein, Ruediger	Co-chief Scientist(Geology)	AWI
Beeskow, Bettina	Inorganic Geochemistry	AWI
Bogacheva, Margarita	Organik Geochemistry	GEOKHI
Borisov, Alexander	Radio-Geochemistry	GEOKHI
Dittmers, Klaus	Geology	AWI
Eckert, Carsten	Biology	AWI
Ivanova, Elena	Micropaleontology	IORAS
Fetzer, Ingo	Biology	AWI
Hollmann, Beate	Organic Geochemistry	AWI
Kodina, Lyudmila	Organic Geochemistry	GEOKHI
Köhler, Gert-Hayo	Organic Geochemistry	IFBM
Kriwanek, Sonja	Geology	GEOMAR
Larionov, Viktor	Biology	MMBI
Levitan, Michael	Geology	IORAS
Ligaev, Alexander	Radio-Geochemistry	GEOKHI
Lyubin, Pavel	Biology	MMBI
Neumann, Kirsten	Organic Geochemistry	IFBM
Osadchiy, Nikolay	Engineer	GEOKHI
Pribylova, Tatjana	Organic Geochemistry	GEOKHI
Schayen, Stephan	Organic Geochemistry	IFBM
Schoster, Frank	Inorganic Geochemistry	AWI
Simstich, Johannes	Geology	GEOMAR
Sizov, Yevgeniy	Engineer	GEOKHI
Solovjeva, Galina	Radio-Geochemistry	GEOKHI
Stefanzev, Leonid	Oceanography	GEOKHI
Steinke, Tatjana	Geology	AWI
Suchoruk, Vladimir	Marine Chemistry	IORAS
Suck, Inken	Biology	AWI
Testov, Stanislav	Radio-Geochemistry	GEOKHI
Tokarev, Viktor	Organic Geochemistry	GEOKHI
Unger, Daniela	Organic Geochemistry	IFBM
Vlasova, Lyudmila	Organic Geochemistry	GEOKHI